Green strategies for sample preconcentration and High performance liquid chromatographic determination of triazole fungicides

Rawikan Kachangoon

A Thesis Submitted in Partial Fulfillment of Requirements for
degree of Doctor of Philosophy in Chemistry
March 2025

วิธีการเพิ่มความเข้มข้นสีเขียวและการตรวจวัดสารกำจัดเชื้อรากลุ่มไตรอะโซลด้วยเครื่องโครมาโทกราฟีของเหลวสมรรถนะสูง

วิทยานิพนธ์

ของ

ระวิกานต์ คเชนกูล

เสนอต่อมหาวิทยาลัยมหาสารคาม เพื่อเป็นส่วนหนึ่งของการศึกษาตามหลักสูตร

ปริญญาปรัชญาดุษฎีบัณฑิต สาขาวิชาเคมี

มีนาคม 2568

Green strategies for sample preconcentration and High performance liquid chromatographic determination of triazole fungicides

Rawikan Kachangoon

A Thesis Submitted in Partial Fulfillment of Requirements

for Doctor of Philosophy (Chemistry)

March 2025

The examining committee has unanimously approved this Thesis, submitted by Miss Rawikan Kachangoon , as a partial fulfillment of the requirements for the Doctor of Philosophy Chemistry at Mahasarakham University

Examining Committee

.....Chairman
(Assoc. Prof. Rodjana Burakham , Ph.D.)

.....Advisor
(Assoc. Prof. Jitlada Vichapong , Ph.D.)

.....Co-advisor
(Assoc. Prof. Yanawath Santaladchaiyakit , Ph.D.)

.....Committee
(Asst. Prof. Kraingkrai Ponhong , Ph.D.)

.....External Committee
(Assoc. Prof. Nutthaya Butwong , Ph.D.)

.....External Committee
(Prof. Diana S. Aga , Ph.D.)

Mahasarakham University has granted approval to accept this Thesis as a partial fulfillment of the requirements for the Doctor of Philosophy Chemistry

.....
(Prof. Pairot Pramual , Ph.D.)
Dean of The Faculty of Science

.....
(Prof. Anongrit Kangrang , Ph.D.)
Acting Dean of Graduate School

TITLE Green strategies for sample preconcentration and High performance liquid chromatographic determination of triazole fungicides

AUTHOR Rawikan Kachangoon

ADVISORS Associate Professor Jitlada Vichapong , Ph.D.

Associate Professor Yanawath Santaladchaiyakit , Ph.D.

DEGREE Doctor of Philosophy **MAJOR** Chemistry

UNIVERSITY Mahasarakham University **YEAR** 2025

ABSTRACT

In this study, sample preparation methods for preconcentration of triazole fungicides have been developed. This study proposes novel sample preparation techniques for the preconcentration of triazole fungicides including myclobutanil (MCBT), triadimefon (TDF), tebuconazole (TBZ), hexaconazole (HCZ), and diniconazole (DCZ) from complex matrices, followed by high-performance liquid chromatography (HPLC) analysis. Five distinct approaches were developed and optimized as follows:

(i.) Micro-solid phase extraction (micro-SPE) using *Moringa oleifera* seeds (MO) was investigated as an efficient biosorbent for the determination of triazole fungicides. *Moringa oleifera* seeds were utilized as biodegradable biosorbent material, offering simplicity, rapidity, cost-effectiveness, and reduced solvent usage. Extraction parameters such as adsorbent amount, salt addition, sample volume, adsorption/desorption times, and elution solvent type and volume were systematically optimized. The method was successfully applied to environmental water, honey, and fruit juice samples. This is the first application of *Moringa oleifera* seeds in the preconcentration of triazole fungicides coupled with HPLC analysis.

(ii.) Micro-solid phase extraction (micro-SPE) using surfactant-modified coconut husk fiber (CHF) was developed as a green alternative sorbent. Coconut husk fiber was found to be a biodegradable, cost-effective, and environmentally friendly sorbent. Its high surface area and hydrophilicity were enhanced by surfactant coatings, forming hemimicelles that improved the adsorption of organic compounds. The method effectively extracted trace triazole fungicides from complex samples, demonstrating the potential of CHF in green analytical applications.

(iii.) Micro-solid phase extraction (micro-SPE) using a hydrophobic melamine sponge (MeS) incorporated with carbon dots was developed as a green sorbent. An in-situ synthesized melamine sponge, prepared by heating citric acid in a single step, exhibited hydrophobic properties and eliminated the need for centrifugation during phase separation. Various extraction factors were optimized using a univariate

experimental design. The method was applied to extract triazole fungicide residues from edible fungi, and its greenness was evaluated using the Analytical Eco-Scale and AGREE metrics.

(iv.) An in situ formation of ionic liquid as an extraction solvent based on liquid-liquid microextraction (LLME) was investigated. An ionic liquid ($[P_{44412}][PF_6]$) was generated in situ via metathesis of tributyl dodecyl phosphonium bromide ($[P_{44412}]Br$) with KPF_6. This process created a cloudy solution with fine microdroplets, significantly enhancing extraction efficiency without requiring dispersion solvents. The method was applied to water, honey, fruit juice, and egg samples. The in situ approach provided a short extraction time, ease of solvent recovery, and environmental friendliness.

(v.) Effervescence-assisted liquid-liquid microextraction using ternary deep eutectic solvents (TDESs) as an extraction solvent was investigated. A simple, selective, and green method was developed using effervescence-assisted LLME based on ternary DESs. Single- and double-chain fatty acids (e.g., octanoic acid, decanoic acid) were evaluated due to their low cost. Effervescence powder facilitated solvent dispersion without auxiliary devices. The method was optimized and applied to complex matrices, representing the first hyphenation of effervescence with DES-based LLME for triazole fungicide analysis.

Each method demonstrated good linearity with a coefficient for determination (R^2) greater than 0.99, and low limits of detection (LODs). The precisions were assessed from the relative standard deviations (RSDs) of retention time and peak area obtained from intra- (n=3) and inter-day (n=5×5) experiments, which were less than 10%. In addition, each proposed method shows high efficiency, environmental sustainability, and potential application for real samples. Comparisons with previously reported techniques highlighted their advantages, establishing these approaches as promising tools for the trace analysis of triazole fungicides.

Keyword : Micro-solid phase extraction, Liquid-liquid microextraction, Triazole fungicides, Moringa oleifera seed, Coconut husk fiber, Carbon dots, Ionic liquid, Ternary deep eutectic solvent, Sample preparation method

ACKNOWLEDGEMENTS

I would like to express my deepest and sincere gratitude to my advisor Assoc. Prof. Dr. Jitlada Vichapong for her unwavering kindness, which allowed me to be her advisee. Her invaluable supervision, insightful suggestions, continuous encouragement, constructive guidance, and criticism were instrumental throughout the study. I am equally grateful to my co-advisor Assoc. Prof. Dr. Yanawath Santaladchaiyakit from the Department of Chemistry, Faculty of Engineering, Rajamangala University of Technology Isan, Khon Kaen Campus, for his expert advice, generosity, and valuable comments and suggestions, which greatly enriched my research.

My sincere thanks and appreciation also go to my graduate committee members Assoc. Prof. Dr. Rodjana Burakham (Department of Chemistry, Faculty of Science, Khon Kaen University) Assoc. Prof. Dr. Nutthaya Butwong (Department of Applied Chemistry, Faculty of Sciences and Liberal Arts, Rajamangala University of Technology Isan, Nakhon Ratchasima) and Asst. Prof. Dr. Kraingkrai Ponhong (Department of Chemistry, Faculty of Science, Mahasarakham University) for their invaluable suggestions and constructive feedback.

I am profoundly grateful to the Department of Chemistry, Faculty of Science, Mahasarakham University for providing the necessary chemicals, instruments, and facilities that made this work possible. My heartfelt thanks also go to the National Research Council of Thailand (NRCT) (Project N41A640218) for the financial support provided during my study, as well as to Thailand Science Research and Innovation (TSRI), Mahasarakham University, and the Center of Excellence for Innovation in Chemistry (PERCH-CIC), Ministry of Higher Education, Research, and Innovation, for their partial support.

I would like to express my sincere gratitude to Prof. Dr. Diana S. Aga for giving me the opportunity to join Aga's Lab at Aga's lab, University at Buffalo, Buffalo, New York, USA. I truly appreciate the valuable knowledge and skills in analytical chemistry that I have gained under your guidance as well as your continuous support throughout my research abroad.

I would also like to extend my heartfelt thanks to all Aga's lab members for their kind assistance, guidance, and support during my time. Your generosity and

willingness to share your knowledge have made my experience truly enriching. I extend my appreciation to all the staff members of the Department of Chemistry, Faculty of Science, Mahasarakham University, for their assistance and support. My special thanks go to my friends and lab members in JV's lab for their encouragement and friendship and for making my academic journey enjoyable. For everyone who has contributed to this work, both directly and indirectly, your support means more than words can express. Above all, I would like to offer my deepest acknowledgment and heartfelt gratitude to my family, especially my parents and younger sister, for their unwavering love, constant care, boundless support, patience, and countless sacrifice throughout this extended period of study.

Thank you all.

Rawikan Kachangoon

TABLE OF CONTENTS

Page

LIST OF TABLES

Page

LIST OF FIGURES

Page

CHAPTER 1

INTRODUCTION

1.1 Background and rational

Pesticides are chemicals that control insects, fungi, warms, and weeds, affecting crops in agriculture [1]. Triazole fungicides (TFs) are a class of highly effective systemic fungicides containing a hydroxyl group, a substituted phenyl group, and a 1,2,4-triazole group in the main chain. They work by inhibiting the enzyme lanosterol 14α-demethylase, which is essential for fungal cell membrane synthesis. This disrupts fungal growth and reproduction, making triazoles highly effective against a broad spectrum of fungal pathogens [2]. TFs such as myclobutanil (MCBT), triadimefon (TDF), tebuconazole (TBZ), hexaconazole (HCZ), and diniconazole (DCZ) are heteroaromatic compounds which have been widely used in agriculture due to the satisfactory protective and curative effect against various crop diseases [3]. These chemicals have moderate lipophilicity, high chemical and photochemical stability and low biodegradability, they can easily remain in agricultural products and transport in environment [4,5]. To protect consumers, more pesticides action network organizations including Codex Alimentarius commission (CAC), Food and Agriculture Organization of the United Nation (FAO), World Health Organization (WHO), United States Environmental Protection Agency (US EPA) and Asian and Pacific Plant Protection Commission (APPPC) were stipulated maximum residue limits (MRL) of TFs in different food, fruits, vegetables and environment samples. For example, the MRL of hexaconazole, triadimefon and bitertanol is 0.01-0.02 mg kg^{-1}; the MRL of tebuconazole is 0.02-5.0 mg kg^{-1}; and the MRL of myclobutanil is 0.05-3.0 mg kg^{-1} [2]. Therefore, it is of great significance to develop a simple, sensitive, and reliable

method for the monitoring of triazole fungicide residues in agricultural products and environmental samples.

Various methods have been widely used to obtain the concentration data at trace contamination levels. High-performance liquid chromatography (HPLC) coupled with a variety of detection systems including UV [6] and diode array detector [7], fluorescence [8], chemiluminescence [9], and mass spectrometry [10], is the favored choice for triazole fungicides analysis. Gas chromatography (GC) has also been employed for triazole determination [11]; however, it necessitates specific conditions to minimize thermal decomposition. In contrast, spectrometric [10], [11] and chemiluminescence [9] techniques are typically simpler and more cost-effective than chromatographic methods. Nevertheless, these approaches lack the capability for multi-component analysis and often require derivatization to enhance sensitivity. Capillary electrophoresis (CE) has emerged as an appealing method for separating fungicide residues [12], [13]. However, its application is limited by low sensitivity, primarily due to the small sample volumes typically injected and the limited availability of compatible detection systems. Due to their typically low concentrations and the complexity of the matrix in which they occur, triazole fungicides are rarely detected without prior sample pretreatment.

Traditional sample preparation methods, such as liquid-liquid extraction (LLE) and solid-phase extraction (SPE), have been widely used. However, these techniques often require large volumes of hazardous organic solvents, resulting in significant waste and posing risks to both worker safety and the environment [14]. Recently, there has been increasing attention on green analytical chemistry, which emphasizes the use of low-toxicity solvents, reduced waste generation, and lower energy consumption [1].

Green analytical chemistry (GAC) was introduced to reduce the side effects of analytical methods on the environment or operators [15] and several principles have been declared from the point of view of GAC [16]. Therefore, developing an environmentally friendly and cost-effective solvent is of the most importance in chemical manufacturing. The demand for low-cost, environmentally friendly, less toxic, and biodegradable solvents has led to a gradual growth of new alternative solvents. Moreover, green solvents have been used in many applications, including extraction solvents [17]. Various types of solvents have been used such as ionic liquids (ILs), deep eutectic solvents (DESs), and supramolecular solvents (SUPARSs). Ionic liquids (ILs) and deep eutectic solvents (DES) have been integrated into LPME to improve selectivity, efficiency, and environmental compatibility. ILs, while thermally stable and hydrophobic, have raised concerns over their environment and aquatic toxicity [18]. DES has been explored as a greener alternative to address these limitations, offering advantages such as low toxicity, cost-effectiveness, easy synthesis, and sustainability. DES exhibits promising potential for the microextraction of fungicides, aligning with the principles of green chemistry.

In recent years, the development of green analytical chemistry (GAC) methods has gained significant attention due to the growing need for environmentally sustainable practices. These methods emphasize the use of materials that promote cleaner and healthier environments. Adsorbents, classified into natural, modified, synthetic, agricultural, and biosorbent categories, play a key role in various industrial and laboratory applications. Among biosorbents, plant-based materials such as *Moringa oleifera* and coconut husk are notable for their availability, biodegradability, cost-effectiveness, and high adsorptive potential. Additionally, advancements in

sorbent technology have led to the development of synthetic, polymer-based, and carbon-based materials, offering improved efficiency and stability in microextraction processes. However, natural sorbents remain attractive due to their lower environmental impact and cost. These advancements align with the principles of GAC, focusing on sustainable, efficient, and high-performance analytical methods. However, further studies on their toxicity and environmental impact are necessary to fully establish their "green" materials.

In this work, we proposed simple preconcentration methods for the sensitive determination of triazole fungicide residues. Five different simple microextraction methods for the enrichment of triazole were investigated including (i) micro solid phase extraction (μ-SPE) using *Moring Oleifera* seed as an efficient biosorbent (ii) micro solid phase extraction (μ-SPE) using surfactant-modified coconut husk fiber as a green sorbent (iii) micro solid phase extraction (μ-SPE) using hydrophobic melamine sponge incorporated with carbon dots as a green sorbent, (iv) liquid-liquid microextraction (LLME) using ionic liquid (IL) as an extraction solvent, and (v) liquid-liquid microextraction (LLME) using ternary deep eutectic solvent (TDES) as an extraction solvent. The experimental parameters affecting the extraction efficiency are evaluated systematically such as the kind and amount of sorbent, synthesis time, extraction time, and kind and volume of extraction solvent. The applicability of the proposed methodologies was investigated in various samples.

1.1 Purposes of the research

1. To apply two bio- (*Moringa oleifera* seed and Coconut husk fiber) and synthesis (Melamine sponge incorporated with carbon dots) adsorbents in the μ-SPE method for preconcentration of the selected triazole fungicide residues.

2. To develop the liquid-liquid microextraction method using ionic liquid (IL) and deep eutectic solvent (DES) for preconcentration of some triazole fungicide residues.

3. To explore the feasibility of the developed methodologies for application in real samples.

1.2 Scope of research

1. The method was validated by the following parameters: calibration curves, limits of detection (LOD), limits of quantitation (LOQ), and reproducibility.

2. The preconcentration method was studied for the determination of triazole fungicide residues in real samples.

3. A developed method was applied to the analysis of triazole fungicide residues in real samples.

1.3 Benefit of research

1. Enhances sensitivity for trace analysis

The proposed methods provide sensitive and efficient preconcentration techniques, enabling the accurate determination of trace-level triazole fungicide residues in complex matrices.

2. Introduces environmentally friendly approaches

By employing green solvents like deep eutectic solvents (DES) and ionic liquids (ILs), this study aligns with the principles of green chemistry, minimizing the use of hazardous chemicals and reducing the environmental impact.

3. Ensures cost-effectiveness

The use of bio-based sorbents and DES ensures lower material costs while maintaining excellent extraction performance, making the methods accessible and economically viable.

4. Demonstrates versatility across sample types

The proposed methodologies are adaptable and have demonstrated applicability in various sample types, including environmental and agricultural matrices, enhancing their practicality in real sample scenarios.

5. Improves extraction efficiency

The systematic optimization of parameters such as sorbent type, extraction time, and solvent concentration ensures high extraction efficiency and reproducibility.

6. Promotes sustainability

The integration of biodegradable sorbents and green solvents into microextraction techniques supports sustainable analytical practices and circular economy principles.

7. Advances in analytical techniques

By combining micro-solid-phase extraction (μ-SPE) with alternative materials, including bio- and synthetic sorbents, and liquid-liquid microextraction using alternative solvents like DES and ILs, this work contributes to the advancement of efficient and robust sample preparation methods.

8. Reduces waste and solvent use

The miniaturized extraction techniques used in this study consume minimal amounts of solvents and generate significantly less waste than traditional extraction methods, improving safety and sustainability.

CHAPTER 2

LITERATURES REVIEW

2.1 Triazole fungicides

Triazole fungicides (TFs) are a class of highly effective systemic fungicides that contain hydroxyl groups (ketone groups), substituted phenyl groups, and 1,2,4-triazole groups in the main chain. TFs have a wide fungicidal spectrum and can effectively control a variety of crop diseases. They are widely used in the cultivation of fruits, vegetables, grains, and other crops to prevent fungal diseases [19] such as powdery mildew and rust, in both pre- and post-harvest applications. Some of them are also used as plant growth regulators such as uniconazole, paclobutrazole, etc. [20], [21]. Triazole fungicides are also used in wood preservatives, textiles, leather, adhesives, antifouling agents, and paints [22]. Owing to their moderate lipophilicity, high stability, and long chemical and photochemical half-lives, they can be easily transported and accumulated in multiple environmental media. These residues have frequently been detected in food and environmental samples [23], [24]. TFs would interfere with endocrine activity in animals and humans by inhibiting enzymes involved in steroid hormone biosynthesis. They may disturb endocrine activity in animals and humans by inhibiting the enzymes involved in the biosynthesis of steroid hormones [22]. Notably, most triazole fungicides currently have one or two chiral centers (as shown in Table 1) and are agriculturally used as racemate products or mixtures of enantiomers and diastereomers [24], [25]. After a more in-depth study, enantiomeric differences in efficacy were gradually observed. For example, (−)-tebuconazole, (+)-flutriafol, (−)-hexaconazole, and (−)-diniconazole have strong fungicidal activity; the R-enantiomers of triadimenol, paclobutrazol, diniconazole, and

uniconazole have strong antibacterial activity; and their S-enantiomers have strong plant regulatory activity. Furthermore, enantiomers with different configurations usually behave differently, which may lead to diverse toxicology and degradation patterns [22], [25], [26]. Therefore, it is important to develop a simple, sensitive, and reliable method for monitoring triazole fungicide residues in agricultural products and environmental samples. To protect consumers, EU regulations stipulate maximum residue limits (MRL) for TFs in different fruits and vegetables. For example, the MRL of hexaconazole, triadimefon and bitertanol is 0.01-0.02 mg kg^{-1}; the MRL of tebuconazole is 0.02-5.0 mg kg^{-1}; and the MRL of myclobutanil is 0.05-3.0 mg kg^{-1}[22], [23]. Developing rapid, simple, and accurate methods for the quantification of residual TFs in environmental and food samples is of great significance in ensuring food and environmental safety.

The physical and chemical properties of triazole fungicides are shown in Table 1 [27] molecular weights range from 288.78 to 326.22 g mol^{-1}. Triazole fungicides have higher water solubility than other pesticides. The water solubility of triazole fungicides can also be altered using commercial pesticide formulations.

Table 1 Properties of the studied triazole fungicides from other chemical classes.

Triazole Fungicides	**Molecular Formula**	**Water Solubility (mg L^{-1}) at 20 ˚C**	**Log Kow**	**Structure**
Myclobutanil (MCBT)	$C_{15}H_{17}ClN_4$	142	2.94	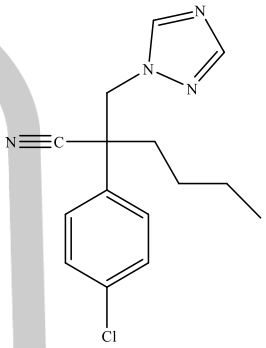
Triadimefon (TDF)	$C_{14}H_{16}ClN_3O_2$	70	2.77	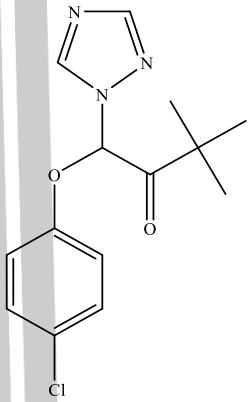
Tebuconazole (TBZ)	$C_{16}H_{22}ClN_3O$	36	3.7	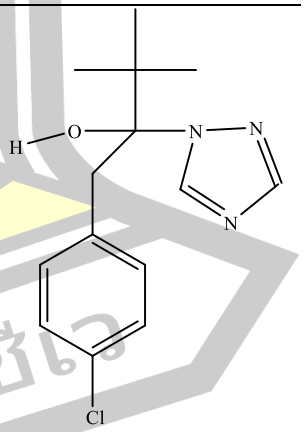

Table 1 Properties of the studied triazole fungicides from other chemical classes (cont.).

Triazole Fungicides	Molecular Formula	Water Solubility (mg L^{-1}) at 20 ˚C	Log Kow	Structure
Hexaconazole (HCZ)	$C_{14}H_{16}Cl_2N_3O$	17	3.9	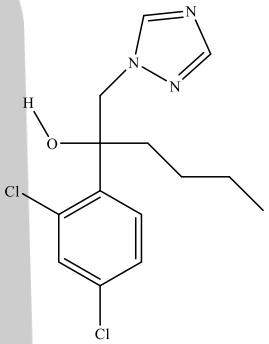
Diniconazole (DCZ)	$C_{15}H_{17}Cl_2N_3O$	4	4.3	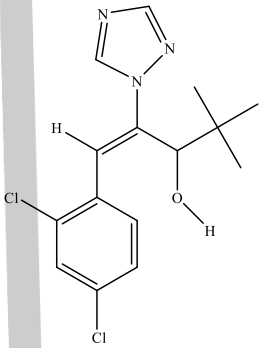

2.2 Biosorbents

Plant biomass (W) is the weight of living plant material above and below a unit of ground surface area at a given point in time. Production is the biomass or weight of organic matter assimilated by a community or species per unit of land area per unit time [28]. Plant biomass generally consists of wood and agricultural waste and is available worldwide in the form of seeds, leaves, roots, bark, and peel. Plant materials, such as guava seeds [29], neem leaves [30], and eucalyptus bark [31], have been proven to be potential materials for the removal of various analytes. In recent years, solid-phase microextraction (SPME) with biomass as a biosorbent has been used effectively because of its fast sorption and reversible desorption of various target analytes. Moreover, compared to conventional technologies, biosorption processes are advantageous because of their cost-effectiveness, high efficiency, and the absence of waste during the SPME procedure [32], [33].

Among these techniques, biosorption has been one of the most studied alternatives in recent years, mainly because of its economic conditions and rational application. The biosorption terminology consists of the combination of the “bio” prefix and the “sorption” suffix. From a technical perspective, the application of the adsorption method using materials from biological bias is often called biosorbents [33]. Biosorbents such as tobacco [34], rice husk [35], olive pomace [36], soybean straw [37], pine bark [36], oak bark [37], sugarcane pulp [38], corn straw [39], grapefruit peel, tangerine peel, banana peel [40], watermelon peel [41], Pinus brutia leaf [42], bamboo charcoal [43], *Moringa oleifera* leaf-seed-husk powder [44]and coconut husk-shell-fiber [45] have recently been successfully employed in adsorption processes.

Moringa oleifera Lam. is widely distributed in tropical and subtropical regions. It is an edible plant with great nutritional value and is rich in proteins, vitamins, mineral elements, and other nutrients. *Moringa oleifera* seeds (MO) have some nutritional benefits and medicinal properties It is considered to be a “Miracle tree” or “Tree of life” due to the substantial beneficial effects that it has on health, but also due to its potential use in water sanitation and environmental conservation [27], [42], [44]. The seeds of this plant have also been used for water purification. Anti-cancer [46], anti-inflammatory, and hepatoprotective activities [47] have also been reported in various tissues. However, even though it is the target of several studies, the identity of its active compounds remains poorly understood. As it is an excellent source of plant proteins, there is an enormous participation of protein compounds in the activities described for *Moringa oleifera* Leaves and seeds have the highest protein content (approximately 20 and 30%, respectively) and proteomic diversity and together account for a large portion of the research devoted to this species [48]. Cationic peptides and low-molecular-weight basic proteins have been purified from *Moringa oleifera* and are related to the activities described for this species (i.e., flocculant and antimicrobial activities) [46], [47], [48]. The identification and characterization of these molecules have been crucial in understanding their mechanisms of action, and an increasing number of studies have revealed the chemical identity of these active proteins because *Moringa oleifera* has already been highlighted as a source of powerful natural flocculating agents [49], and preliminary research from the 1990s has pointed out that cationic proteins and peptides ranging from 6 to 16 kDa are the main active components of *Moringa oleifera* involved in coagulation/flocculation properties [27], [50].

Cocos nucifera L. is the most widespread fruit on Earth and is present on almost every continent. Likewise, in Thailand, coconut (*Cocos nucifera*) was considered as one of the most important crops. Improvement of coconut product was very well known from the past decades. It has been developed for food and beverage (e.g., coconut oil and coconut milk) [51]. However, it was impressive to note that with the growth of edible components from coconut, coconut husk was finally generated. From the standpoint of waste management, the utilization of coconut husk [52] with higher efficiency was considered an extensive key for sustainable development. The adsorbents used in μ-SPE have a significant influence on the extraction efficiency of analytes. Currently, many studies are focused on improving the enrichment and extraction capacity of adsorbents for target analytes. Porous materials have drawn our attention owing to their inherent advantages, such as high surface area, satisfactory adsorption capacity, and good chemical stability [28]. Compared to the background, incorporating the advantages of modification of coconut husk fiber porous materials to construct an alternative adsorbent used in μ-SPE with improved extraction performance and adsorption capacity is enormously significant. On the other hand, the high surface area and large pore volume of coconut husk fiber porous materials play a key role in enhancing extraction efficiency, which not only provides for enhancing the contact area but also can increase active sites [52], [53]. Therefore, the coconut husk fiber powder was found to be a biodegradable green sorbent that reduces the use of solvents, and is a simple, rapid, and inexpensive adsorbent for μ-SPE. These potential advantages of coconut husk fiber biosorbents offer a perspective as adsorbents for the extraction of trace triazole fungicides from complex samples. Coconut husk fiber has high surface areas, is hydrophilic and shows

limited adsorption capacities for hydrophobic compounds. However, they can be modified by a coating surfactant to enhance their adsorptive tendency towards organic compounds. Only a few examples of this procedure can be found in the literature. Information involving *Moringa oleifera* (MO) applications and coconut husk fiber (CHF) as a biosorbent in the extraction process are summarized in Table 2 and Table 3, respectively.

Table 2 Literatures on extraction method using *Moringa oleifera* (MO) as a biosorbent.

Author (year)	**Analytes / Samples**	**Amount of sorbents**	**Extraction method**	**Detection**	**LODs**
Tomasin *et al.* (2021) [54]	Cu (II) ions/ hemodialysis water	10 mg	Disposable Pipette Extraction (DPX)	FAAS	50 $\mu g\ L^{-1}$
Sirajudheen *et al.* (2021) [55]	Organic pollutants/ waters	30 mg	Adsorption-desorption tests	-	-
Aldakheel *et al.* (2020) [56]	Ca, Mg, Mn, Cu, P, S and Zn/ traditional herbal medicine	100 mg	-	Laser-induced breakdown spectroscopy (LIBS) X-ray photoelectron spectroscopy (XPS) ICP-OES	-

Table 2 Literatures on extraction method using *Moringa oleifera* (MO) as a biosorbent (cont.).

Author (year)	**Analytes / Samples**	**Amount of sorbents**	**Extraction method**	**Detection**	**LODs**
Adenuga *et al.* (2020) [57]	Phthalate esters/ breast-milk and urine samples	200 mg	QuEChERS-d-SPE	GC-FID	0.012-0.020 µg L^{-1}
Çelekli *et al.* (2019) [58]	Synthetic dyes/ reactive red 120	250 mg	Adsorption experiments	- Adsorption kinetics - Activation - Energy - Thermodynamic	-
Kgatitsoe *et al.* (2019) [59]	Nitroaromatic explosive compounds/ polluted water	2500 mg	SPE	GC-TOF/MS	0.4-4.5 mg L^{-1}
Shirani *et al.* (2018) [60]	metal and dye pollutants/ wastewater	250-1500 mg	Adsorption experiments	- Adsorption kinetics - Isotherm modeling	-
Araujo *et al.* (2018) [61]	Pharmaceuticals/ water	25 mg	Chemisorption	- Adsorption kinetics - Equilibrium thermodynamic	-

Table 3 Literatures on extraction method using coconut husk fiber (CHF) as a biosorbent.

Author (year)	**Analytes / Samples**	**Amount of sorbents (g)**	**Extraction method/ Detection**	**LODs (ng L^{-1})**	**LOQs (ng L^{-1})**	**%Recovery**
Ma *et al.* (2023) [62]	Triazine herbicides/ Environmental and food samples	0.3	SALLE/ UPLC-MS/MS	6.99-11.00	23.33-36.68	69-124.72
Kodail *et al.* (2021) [63]	Organophosphorus pesticide/ Waters	0.2	Adsorption/ LC-MS/MS	70	200	96
Baharum *et al.* (2020) [64]	Diazinon pesticide/ aqueous solutions	2.0	SPE/ HPLC-DAD	2.5×10^{5}	-	-
Aguiar Jr. *et al.* (2019) [65]	5 pesticides/ waters	4.0	SPE/ GC-MS	-	1.0×10^{4}	89-98
Kumrić *et al.* (2019) [66]	Pesticides/ waters	0.05	SPE/ HPLC-DAD	25-39	83-129	58.2-105.3
Liang *et al.* (2018) [67]	12 pesticides/ vegetables	0.05	SPME/ GC-MS	0.01-0.10	-	76-104

2.3 Synthesis sorbents

Among other features of SPE, significant attempts have been dedicated to the development and characterization of new, advanced sorbent materials to aspiring to improve selectivity or specificity about target analytes, higher sportive capacity (with successive better sensitivities and detectability), and enhanced chemical or physical-mechanical stability [68]. Of course, it is not feasible to focus concurrently on achieving all these goals, and, among them, it is possible to perceive some clear trends. According to Poole *et al.* [69], sorbents for SPE can be divided into three groups: inorganic oxides, low-specific sorbents, and compound-specific and class-specific sorbents. Sorbents for SPE can be divided into three groups: inorganic oxides, low-specific sorbents, and compound-specific and class-specific sorbents [70], [71], [72]. The aperture for new developments in the first-class adsorptive inorganic oxides [e.g., silica, alumina, and Florisil (magnesium silicate)] is limited by the nature of such materials and the analyte-adsorbent interactions. Non-specific sorbents (severally most employed as SPE media) adopt surface-modified silicas and porous polymers (e.g., polystyrene-divinylbenzene resins and carbon-based materials) [69], [73]. Among them, surface-modified silicas have a wide range of applications but receive from several limitations, including limited stability when raised to aqueous samples with low or high pH; research work on this class of sorbents is typically activated by the investigation of materials with enhanced stability under intrusive conditions and/or higher offensive for polar analytes [74]. Despite the limitations of silica-based non-selective sorbents, their use in extracting analytes with low or medium polarity from such samples is excessive and, apart from more complex matrixes or differently problematic samples, is usually straightforward [75]. However, for issues related to

the desolation of highly-polar species or macromolecules from aqueous samples, where for most traditional non-selective sorbents the partition coefficients either do not support the transfer of the target compounds to the sorbent stinted or where there is irreversible sorption and for complex samples containing a great deal of interfering species, the use of compound-specific and class-specific sorbents may be important [76].

The synthesis sorbent materials used in adsorption and catalysis generally have a wide pore size and shape distribution. The ordered structure of mesopores promotes uniform diffusion of molecules in the sorbent and catalyst, which significantly increases the prospects for using these materials [73]. In addition, on homogeneous surfaces, a more uniform distribution of modifiers is observed during the modification process to synthesize materials with the required characteristics. Nowadays, several commercial materials or synthetic nano-materials such as functionalized silica [77], multi-walled carbon nanotubes [78], graphene, graphene oxide, modified magnetic nanoparticles [79], and polymer-based sorbents [69]. These nanomaterials can be used for the speciation, enrichment, and separation of various analytes from different matrices. The larger surface area of nanomaterials (that enhances the extraction kinetic) and the variety of different chemical interactions (that makes wider the applicability to different problems) can be treated among the main reasons. The compositions of different types of nanomaterials (hybrid nano-materials), as well as the combination of nanomaterials with micrometric systems (composites), have expanded the potential application in analytical sciences.

Carbon-based materials play an important role in the development of material science. Carbon nanodots (CDs), discovered in the mid-2000s [80], are one of the

protagonists of carbon nanoscience. CDs are nanoparticles smaller than ~10 nm commonly composed by carbon, oxygen, nitrogen, and hydrogen. From the conventional industrial carbon (e.g., activated carbon, carbon black) to new industrial carbon (e.g., carbon fibers, graphite) and new carbon nanomaterials such as graphene and carbon nanotubes (CNTs), principal research and applications of carbon-based materials are always famous in the fields of chemistry, materials, and other inter disciplines due to their environmental friendliness. However, macroscopic carbon material absences the relevant band gap, making it difficult to act as an impressive fluorescent material [73]. Recently, the carbon-based materials family, also known as carbon dots (CDs), have received fabulous consideration due to exceptional advantages such as low toxicity, high chemical stability, superlative biocompatibility, and high-fluorescence [81], [82]. Considering these unique physical-chemical characteristics, C-QDs have been applied widely in the fields of catalysis, printing ink, biological sensors, bioimaging, and drug delivery [83].

The use of sponge or sponge-like materials is a promising concept in liquid sample preparation techniques. Although their recruitment in passive various sampling is well known, sponge-like materials are scarcely employed for the extraction of analytes from aqueous matrices, due to their low extraction potential. One of the most widely exploited materials for such purposes is polyurethane foam. In the last five years, there have been an increasing number of articles that attempt to modify the surface of polyurethane foam in an effort to enhance its extraction capability [84]. The melamine sponge (MeS) has stimulated attention as an SPE sorbent material because of its fascinating attributes. In summary, MeS is a low-cost, low-density, high-porosity (> 99%) foam-like material with an open cell foam-hole

structure, high suction capacity, good elasticity, high thermal and mechanical stability, and chemical conversion ability. MeS consists One of the most widely exploited materials for such purposes is polyurethane foam. In the last five years, there have been an increasing number of articles that attempt to modify the surface of polyurethane foam in an effort to enhance its extraction capability of a formaldehyde-melamine-sodium bisulfite copolymer [85] and displays high sorption capacity for water due to its hydrophilic groups, such as hydroxyl, aldehyde groups, and ether bonds, introduced during synthesis. Due to the presence of functional groups, the MeS can be modified to exhibit a superhydrophobic behavior. These modifications have been utilized for oil-water separation applications and analytical purposes [86], inter alia, for the microextraction of triazole fungicides from various sample matrices. However, their potential to be used in microextraction procedures is yet to be explored. Recently, we proposed a modification of MeS with carbon dot using citric acid precursor in a one-step, fast procedure and utilized. The affinity of melamine with citric is well known and has been employed to detect the one in the presence of the other or even to prepare complexes, interchangeably [85]. Due to the presence of melamine in the building blocks of MeS, a high affinity for CA-CD is anticipated. a carbon dot using citric acid as a precursor coated MeS might exhibit hydrophobic properties that make it suitable for microextraction. Only a few examples of that procedure can be found in the literatures. Information involving applications of carbon dot as a sorbent in extraction process are summarized in Table 4.

Table 4 Literatures on extraction method using a synthesis sorbent.

Author (year)	Type of sorbents	Amount of sorbents	Analytes / Samples	Extraction method/ Detection	LODs
Dourado *et al.* (2022) [87]	MIP/NIP	200 mg	Saccharin/diet tea samples	MISPE/ HPLC-UV	2.47-3.38 mg/100 mL
Shirani *et al.* (2021) [88]	GO-LaNPs@ Ni foam	size of sorbent: 0.5 × 0.5 cm^2	Sulfonamides/ animal-based food products	RFS-SPME/ HPLC-PDA	0.08-0.14 μg L^{-1}
Huang *et al.* (2021) [89]	Co-MOF /CoO@C	10 mg	9 PAHs	MSPE/ HPLC-UV	0.06-1.30 μg L^{-1}
Yadeghari *et al.* (2021) [90]	Fe_3O_4@poly-phenols MNPs	125 mg	Different pesticides/ water, fruit, and vegetable	MSPE-DLLME/ GC-MS/MS	0.27-4.13 ng L^{-1}
Yang *et al.* (2020) [91]	Zr-based MOF	15 mg	Organic mercury/ fish and *Dendrobium officinale*	Miniaturized SPE/ CE-DAD	0.022-0.067 ng mL^{-1}
Ghorbani et al. (2020) [92]	ZIF-8/ZIF-67 core-shell	20 mg	Cr(III), Pb(II)/ water samples	SPE/ FAAS	0.21 μg L^{-1} Cr(III) and 0.40 μg L^{-1} Pb(II)

Table 4 Literatures on extraction method using a synthesis sorbent (cont.).

Author (year)	Type of sorbents	Amount of sorbents	Analytes / Samples	Extraction method/ Detection	LODs
Toudeshki *et al.* (2019) [93]	MIPs@MMWCNT	10 mg	Metformin/ biological fluids	Adsorption isotherm experiments/ Chemiluminescence	0.13 mg L^{-1}
Ruiz *et al.* (2019) [94]	AC and GO	10 g	Elemental analysis/ aqueous samples	D-µSPE/ Laser-induced breakdown spectroscopy	Activated carbon: below 100 µg kg-1 Graphene oxide: 50 µg kg^{-1}
Wang *et al.* (2018) [95]	PEI-modified hybrid SiO_2	18 mg	Thyreostat/ animal tissues	HILIC-SPE/ HPLC-PDA	0.5-2.2 µg kg^{-1}
Farajzadeh *et al.* (2018) [96]	Magnetic sorbent (toner powder)	200 mg	Some pesticides /fruit juices	MDSPE-DLLME/ GC-FID	0.15-0.36 µg L^{-1}

2.4 Ionic liquid and Deep eutectic solvent

In the present day, analytical chemistry explores the methods and practices that encourage green chemistry. Solvents are mentioned in the fifth principle of green chemistry: “safer solvents and auxiliaries: use of auxiliary substances (solvents and separation agents) where available, should be averted and, when used, these substances should be harmless”. In addition, the appellation is indirect in other principles such as the third principle explores to synthesis of less dangerous products: “Where feasible, the synthesis of a product should use and generate substances that have little or no toxicity to human health and the environment”. The fourth principle, one at a time, attracts the development of safe compounds: “Chemicals must be developed to perform the convenient function and at the same time low toxicity” [97]. These principles envelope many problems interesting minimizing waste generation, energy consumption, and volatile organic solvents. The substances used in many traditional extraction methods and separation techniques are solvents, typically used in large quantities and characterized by their high volatility, flammability, and toxicity. The search for environmentally friendly solvents and biodegradable raw materials is expanding [98]. Green solvents must have a variety of environmental, health, and safety characteristics that distinguish them from traditional solvents. Ionic liquids (ILs) are a new class of organic salts composed of organic cations and organic or inorganic anions, found to be liquid at or near room temperature with a melting point below 100 ˚C [99]. Likewise, ILs display a very low vapor pressure (ranging from 10-11 to 10-10 mbar) and acquire excellent thermal stability, with deterioration following within the temperature range of 250 ˚C to 450 ˚C. ILs vary from inorganic salts in terms of the symmetricity of both cations and anions. The high symmetric structure of

cations and anions of inorganic salts leads to the system crystallizing because of ionic interactions that bring about strong charge ordering [100]. Further, an absence of symmetry in the structure of each ion of the IL as they consist of organic moieties in appellations of cations, and occasionally anions can dilute their charge density localization. This asymmetricity causes weaker coulombic interactions and cohesive energies, which thereby induce a low melting point of ILs to be liquid at room temperature. The ionic composition of ILs makes the electrostatic interactions extensive in creating columbic bond sites. In addition, the organic moieties afford to dispersion forces sites and constantly hydrogen bonding sites. The existence of these disparate bond sites accordingly makes the ILs show a dual (polar/non-polar) nature and causes in earning specific properties and phase behaviors, making them disparate from coulombic-dominated inorganic salt. They can be used as polar/ nonpolar stationary phases to separate polar/nonpolar compounds [101]. The prevalent anions in ILs are hexafluorophosphate, tetrafluoroborate, halides, alkylsulfate, alkylsulfonate, trifluoromethylsulfonate, and bis [(trifluoromethyl)sulfonyl] amide; while the cations are based on imidazolium, phosphonium, ammonium, pyrrolidinium, and pyridinium. Hence, combinations of these cations and anions can provide many ILs and make specially tailored synthesis possible. There are several ways of synthesizing new ILs. Metathesis processes, acid-base neutralization, direct combination, microwave or ultrasonic irradiation, and synthesis using supercritical CO_2 or other bio-renewable sources are some examples [100], [102]. Correlating upon the traditional organic solvents, ILs have several advantages. Most important is the potentiality to be able to develop their physical characteristics based on the aspiration of the applications likewise the application field. As a consequence, they have usually been referred to as

“designer solvents”. There are more than 800 commercially available ILs. In general, more than 1500 ILs are known and this number continues to increase [99]. However, most ILs suffer from some limitations including non-environment friendly and relatively expensive. Therefore, further development of sample extraction procedures using a safe, cheap, renewable, and biodegradable organic compound is of great interest [103].

Development in deep eutectic solvents (DESs) describes an important advancement in green chemistry. DESs are generally identified as binary or ternary combinations of substances that can accomplished predominately through hydrogen bonds. DESs are broadly used around the world due to their unique characteristics. The expression of DESs was coined by Abbott *et al.*, in 2003 [104]. Ascribed to their significance and exciting potential, these solvents have developed as a dynamic, novel, and interesting “green chemistry” subfield. DESs are an encouraged class of ILs; their synthesis is as basic as just combining two or more substances made up of hydrogen bond donors (HBDs) and hydrogen bond acceptors (HBAs). HBAs are quartet phosphonium, ammonium, and mineral salts. HBDs are alcohols, organic acids, amides, and sucrose. DESs are molten and prepared from eutectic mixture of two or more harmless constituents that play a significant role as HBAs or HBDs-based new-generation solvents. In general, DES contains large asymmetrical ions with lower lattice energy. The decrease in the mixture's melting point relative to each component's melting point is caused by the charge delocalization of the hydrogen bond between the hydrogen bond donor moiety and halide ion. DESs have some distinguishing characteristics, including simple and green synthetic processes, cost-effectiveness, environmentally friendly, with high efficiency, making them suitable for large-scale

production. According to Abbott *et al.*, the strategy and preparation of DESs are quietly in their untimely stages, and more research is required. DESs is a trendy research generation in disparate workplaces with novel and emerging applications, mainly in chemistry, separation sciences, biomaterials, metals, electrochemistry, organo-catalysis, and photosynthesis. DESs have tunable properties with distinguish polarities ascribed to their agreement available hydrophobic or hydrophilic integrates. Additionally, DESs prepared from renewable sources have low toxicity with higher biodegradability. The ammonium-based quaternary salt has many preferences pending the preparation of DESs, such as low raw material cost, chemical stability with water, simple synthesis process, biodegradability, biocompatible, and low-toxic or non-toxicity. The advantages listed above all commit to DESs environmental friendliness. Since accomplishing the potential for applicable chemical methodologies, in the last decade, researchers have focused on DESs [104], [105], [106]. Some express DESs types have also earned much consideration, including natural-DESs (NADESs) [[107]], hydrophobic-DESs (HDESs), and ternary-DESs (TDESs) [[108]] were proposed. The eutectic mixtures are created by fundamental biological components, including alcohols, carboxylic acid, sugar, and amino acids. DESs have particular physicochemical characteristics (e.g., thermal stability, negligible vapor pressure, low cost, non-flammability, and a stronger hydrogen bond network. Compelling, DESs have another feature: they play a crucial role in nature's game. Despite the similarities between DESs and water, when tested severally in specific reactions, these “solvents” in nature sometimes attempt complimentary achievement on organic reactivity [109]. This review assists in studying the DES-based extraction techniques for the preconcentration of target analytes from various samples. This review focuses on the

new development in DESs-based extraction techniques, specifically in the synthesis, characterization, and applications. It is more integrative and attempts new ideas in different fields, including analytical chemistry, environmental, pharmaceutical, and biological. The applications of ionic liquids (ILs) and deep eutectic solvents (DESs) as an extraction solvent in the microextraction method are summarized in Tables 5 and 6, respectively.

Table 5 Literatures on ionic liquids (ILs) as an extraction solvent for microextraction method.

Author (year)	**Analytes / Samples**	**Extraction method/ Detection**	**LODs**	**%Recovery**
Xu *et al.* (2024) [110]	Phenyl urea herbicides/ food and environmental samples	ILs@CNTs-MSPE/ HPLC	0.02-0.03 μg L^{-1}	85.0-107.7
Wang *et al.* (2023) [111]	Six herbicides/ water samples	IL@COF-SPE/ HPLC	14.5-37.1 μg L^{-1}	85.3-122.9
Zeger *et al.* (2022) [112]	Pesticides and cannabinoids/ cannabis samples - 20 pesticides - 6 cannabinoids	PIL-SPME/ HPLC-UV	< 1 μg L^{-1}	95-141
Xu *et al.* (2021) [113]	Triazine and phenyl urea pesticide/ vegetable protein drinks	In-syringe TC-LLME-SFIL/ HPLC-DAD	0.25-2.59 μg L^{-1}	81.26-118.42

Table 6 Literatures on deep eutectic solvents (DESs) as an extraction solvent for microextraction method.

Author (year)	Analytes / Samples	Extraction method/ Detection	LODs	%Recovery
Sereshti *et al.* (2023) [114]	Multiclass pesticides/ fruit juice samples	TPDES-DLLME/ GC-μECD	-	67.9-108.4
Jing *et al.* (2022) [115]	Chiral mefentrifluconazole/ cereal samples	MDES-DLLME/ UPLC-DAD	0.003 μg g^{-1}	82.9-95.0
Monajemzadeh *et al.* (2021) [116]	Some pesticides and their metabolite/ egg samples	dSPE-DES-DLLME/ GC-MS	0.03-0.24 ng g^{-1}	73-92
Li *et al.* (2020) [117]	Pyrethroid pesticides/ urine samples Flumethrin Bifenthrin Silafluofen	In-situ IL-DLLME/ HPLC-UV	108-125 μg L^{-1}	88.0-101.1
Heidari *et al.* (2020) [118]	Organophosphorus pesticides/ fruit juice samples	DES-UALLME/ HPLC-UV	0.070-0.096 ng mL^{-1}	87.3-116.7
Jing *et al.* (2019)	Triazole fungicides/ water samples Myclobutanil Epoxiconazole Tebuconazole	EVA-DLLME-IL-SFO/ HPLC-DAD	0.0051-0.0090 g mL^{-1}	77.6-104.4

2.5 Solid phase (SPE) and Micro solid phase extraction (μSPE)

Extraction technology is especially suitable for the separation of target substances in large-scale complex systems due to its good selectivity and ease of large-scale continuous production. However, the extractant amount used for many low-concentration target substances isolation is very small, which causes difficulty in mix and dispersion, leading to low separation efficiency. Moreover, intense stirring usually causes emulsification and loss of organic solvents [119] with high energy consumption. Solid phase extraction (SPE) is currently being used as an enrichment technique when low-concentration analytes have to be recovered. The basic principle of SPE is the transfer of targets from the aqueous phase to the active sites of the adjacent solid phase [120]. SPE for both high enrichment factor and operation flexibility, has some processing advantages such as quick absorption kinetics, extractant can be reused, organic reagent consumption, produce less waste, failure material easy curing. It is widely used in the separation some key species analysis, concentration and environment water pollution treatment processes due to its selectivity and suitability for targets isolation from low concentration and trace system [121]. A sensitive, selective, and good pre-concentration technique is required to detect triazole fungicides in various matrices. Conventional sample preparation techniques, namely liquid-liquid extraction (LLE) and solid phase extraction (SPE) are considered time-consuming and require a large number of organic solvents [122]. So, miniaturized sorbent-based methods such as solid-phase microextraction (SPME), solid-liquid-liquid microextraction (SLLME) [123], liquid-phase microextraction (LPME) [119], magnetically assisted matrix solid-phase dispersion (MA-MSPD), and micro solid phase extraction (μSPE) using a sorbent [123] have been noticed. μSPE is

one of the effective methods due to its amazing properties. It's a miniaturized SPE method in which a little amount of packed sorbent is applied for the extraction of target analytes, especially in volume-limited biological fluids. This method has several advantages of simplicity, low sample, and organic solvent consumption, rapidity, and high reusability[119], [123], [124]. Moreover, due to some fascinating features of μ-SPE, like their unique potential for integration of on-site sampling and extraction, automation and utilization as the simplified methods in routine laboratory tasks, innovative geometries have been developed by the researchers. These geometries make μ-SPE more user-friendly and impressive for different types of sample matrices. The most promising geometries of the sorbent-based miniaturized sample preparation methods, have considerable advantages over other similar techniques, such as efficiency, simplicity, rapidity, and ease of automation with the chromatographic techniques [125]. These sorbents have also been used in the fields of SPE and μ-SPE. For example, *Moringa oleifera* seed and peanut shell an efficient biosorbent for selective enrichment of triazole fungicides [139-141]. NTD devices packed with nanoporous silica aerogel (NPSA) and superhydrophobic silica aerogel separately extracted volatile aldehyde compounds [129], carbon-based materials and graphene aerogels (GAs) demonstrated excellent extraction effects and durability in the SPE of pesticides such as pyrethroids and organophosphorus pesticides [123], [124], [130]. Moreover, there are many more adsorbent that are commonly used as an effective sorbent for μ-SPE and MSPE to extract the target analytes in various samples. According to these studies, it is evident including biosorbent and synthesis sorbent are excellent sorbents for SPE and μ-SPE.

This review primarily focuses on developing of biosorbent and synthesis sorbents for SPE and μ-SPE from 2018-2023. The sorbent materials SPE and SPME techniques have been successfully applied to extract and enrich various analytes in real samples such as environmental, biological, and food samples. Modification strategies for inorganic, organic, and hybrid sorbents and extraction techniques and performance for the targets are thoroughly reviewed. The applications of solid phase extraction (SPE) and micro solid phase extraction (μ-SPE) method are summarized in Table 7.

Table 7 Literatures on solid phase extraction (SPE) and micro solid phase extraction (μ-SPE) method.

Author (year)	**Analytes/ Samples**	**Extraction conditions**	**Detection**	**LODs**
Amini *et al.* (2021) [131]	Polyacrylonitrile/ water, soil and food	Sorbent: Zn-MOF-74@CO Amount of sorbent: 5 mg Sample volume: 5 mL Desorption solvent: acetonitrile (300 μL)	HPLC-DAD	0.08-1.10 ng L^{-1}
Rozaini *et al.* (2021) [132]	Mixed triclosan, triclocarban, 2-phenylphenol, bisphenol A and 4-*tert*-ocylphenol/ wastewater and lake water	Sorbent: MXene encapsulated sorbent Amount of sorbent: 2 mg Sample volume: 10 mL Desorption solvent: isopropanol (150 μL) Extraction time: 30 min	HPLC	0.37-0.58 μg L^{-1}

.

Table 7 Literatures on solid phase extraction (SPE) and micro solid phase extraction (μ-SPE) method (cont.).

Author (year)	Analytes/ Samples	Extraction conditions	Detection	LODs
Tsai *et al.* (2021) [133]	Emerging environmental pollution/ waters	Sorbent: graphene nanosheets (GNSs) Amount of sorbent: 10 mg Sample volume: 10 mL Desorption solvent: Acetone (500 μL)	HPLC-UV	0.5 ng L^{-1}
Nazir *et al.* (2020) [134]	Polycyclic aromatic hydrocarbons (PHAs)/ water and food	Sorbent: Spent tea leaves (STL) Amount of sorbent: 5 mg Sample volume: 10 mL Desorption solvent: Hexane (500 μL) Extraction time: 12 min	GC-FID	2.98-55.96 ng mL^{-1}
Manouchehri *et al.* (2020) [135]	Parabens/ breast milk	Sorbent: Mg-Al double layered hydroxide functionalized graphene oxide Amount of sorbent: 16 mg Sample volume: 500 μL Desorption solvent: acetonitrile (150 μL)	HPLC-UV	3.0-5.0 μg L^{-1}

Table 7 Literatures on solid phase extraction (SPE) and micro solid phase extraction (μ-SPE) method (cont.).

Author (year)	Analytes/ Samples	Extraction conditions	Detection	LODs
Sun *et al.* (2020) [136]	Benzodiazepines/ dietary supplements	Sorbent: poly(stryrene-co-divinylbenzene) Amount of sorbent: 6 mg Sample volume: 5 mL Desorption solvent: acetonitrile (100 μL)	CD-IMS (Corona discharge ionization-ion mobility spectrometry)	5-15 ng mL^{-1}
Xia *et al.* (2019) [137]	Aliphatic aldehydes/ cosmetics and food	Sorbent: NH_2-β-CD-Poly (St-DVB-MAA) Amount of sorbent: 10 mg Sample volume: 4 mL Desorption solvent: ethanol (200 μL) Extraction time: 5 min	HPLC-DAD	0.024-2.5 μg L^{-1}
Alhooshani *et al.* (2019) [138]	N-nitrosamine/ water resources	Sorbent: Al-activated carbon Amount of sorbent: 10 mg Sample volume: 10 mL Desorption solvent: methanol (200 μL) Extraction time: 15 min	GC-MS	0.8-3.3 ng mL^{-1}
Sammani *et al.* (2019) [139]	Flavonoids/ citrus juices	Sorbent: C18 Amount of sorbent: 30 mg Sample volume: 4 mL Desorption solvent: acetonitrile (500 μL) Extraction time: 25 min	HPLC-DAD	0.021-0.100 μg mL^{-1}

Table 7 Literatures on solid phase extraction (SPE) and micro solid phase extraction (μ-SPE) method (cont.).

Author (year)	**Analytes/ Samples**	**Extraction conditions**	**Detection**	**LODs**
Arabsorkhi *et al.* (2018) [140]	Tetracycline and cefotaxime/ honeys	Sorbent: GO-PET Amount of sorbent: 40 mg Sample volume: 100 mL Desorption solvent: MeOH (400 μL) Extraction time: 11 min	HPLC-UV	3.00 μg kg^{-1}
Zhu *et al.* (2018) [141]	Petroleum acids/ crude oils	Sorbent: chitosan fiber Amount of sorbent: 15 mg Sample volume: 500 μL Desorption solvent: TFA/EtAc (100 μL) Extraction time: 5 min	GC-MS	0.7-5.4 ng g^{-1}
Yao *et al.* (2018) [142], [143]	Cd and Pb/ edible vegetable oils	Sorbent: magnetic ionic liquid (MIL) Amount of sorbent: 60 mg Sample volume: 10 g Desorption solvent: HNO_3 (300 μL) Extraction time: 1.5 min	GFAAS	0.002 (Cd) ng g^{-1} and 0.02 (Pb) ng g^{-1}

2.6 Liquid phase microextraction

Major advancements have been assembled in the miniaturization of sample preparation in trace analysis of target analytes, contributing to the development of greener analytical chemistry practices[142],[143]. This comprises the reduction in sample volumes and sizes of organic solvents, ensuring in fewer hazardous waste materials and applicable. As a consequence, different microextraction techniques, based on either solid-phase or liquid-phase chemistry, have obtained more regard as environmentally friendly alternatives to traditional sample preparation.

LPME have already been imposed using in-house equipment, leading to variations in the extraction pattern traverse particular research laboratories. This comprises some in-house built semi- or fully automated systems [144]. LPME has shown promising results in various analytical applications, and they are efficient and reliable sample treatment techniques for the extraction and preconcentration of analytes from complex matrices [143]. In the last decade, the miniaturization of sample preparation techniques has offered several advantages such as low cost, simplicity, low sample volume required and high extraction efficiency. The liquid extracting phase of LPME is limited to microliter scale and many approaches have been performed thus far to stabilize the extracting phase, make separated phases and increase the extraction efficiency. There are two-phase and three-phase LPME approaches [142], [143]. In two-phase LPME, the extracting phase is an immediately contact with the sample solution, which may simplify the extraction procedure, while discounting the selectivity and sample cleanup and restraining the extracting solvent to water immiscible organic liquids are its disadvantages. However, in three-phase LPME, the sample solution and the final acceptor phase were separated via a third

solvent, which is immiscible with both phases. This composition certainly enlarges the method selectivity and makes using the aqueous acceptor phase possible. One of the main problems in LPME is the stabilization of the liquid extracting phase. Reference to this problem, some holders were introduced to house this phase. Moreover, some LPME setups and procedures were devised to increase the contact surface of the phases and raise the extraction driving force for improve the process speed and efficiency [142],[143].

The present, modern materials have the ability to enrich recovery in LPME methods via compensation of analytes phase transportation, replace the extracting phase characteristics, or form distinct interactions with the analyte. In addition, innovative extracting solvents have been synthesized, performing different interactions for extraction of an extensive range of analytes. These new materials may be used as additives in each of the extraction phases or may be merely used for the formation of the extracting solvent such as surfactant, ionic liquids, and deep eutectic solvents. All of these lead to the introduction of LPME patterns to defeat the drawbacks and offer unique advantages. The present review aims to list the existing LPME methods, considering their different principles and configurations that make each technique convenient for some cases and a novel reply to other method limitations. The applications of the liquid-phase microextraction procedure are summarized in Table 8.

Table 8 Literatures on liquid-phase microextraction method.

Author (year)	Analytes/ Samples	Extraction conditions	Detection	LODs
Rodríguez-Ramos *et al.* (2024) [145]	Xenobiotic contaminants/ tropical beverages	Sample volume: 10 mL Adjusted to pH 6 using NaOH or HCl solutions Extraction solvent: 300 µL of NAHDES Extraction time: 12 min	UHPLC-MS/MS	-
Ago *et al.* (2023) [146]	Organochlorine pesticides/ waters	Sample volume: 10 mL + effervescent precursors ratio (CO_2 source: proton donor): 2-3 min Extraction time: 4 min	GC-MS	0.03-0.27 µg L^{-1}
Yadav *et al.* (2022) [147]	Multi-residue pesticides/ soil, sugarcane and jaggery samples	Amount of sample: 1 mg + 1 mL ACN + 1 mL Ultrapure water Extraction solvent: 50 µL of 1-Dodecanol Extraction solvent: 42 min	GC-µECD	0.815-2.533 ng g^{-1}
Gallo *et al.* (2021) [148]	Pesticides/ urine samples	Sample volume: 3 mL diluted with 2 mL of water + 250 mg of NaCl Extraction solvent: 100 µL of DES Dispersing solvent: 400 µL of ethyl acetate Extraction time: 10 min	HPLC-MS	-

Table 8 Literatures on liquid-phase microextraction method (cont.).

Author (year)	Analytes/ Samples	Extraction conditions	Detection	LODs
Heidari *et al.* (2020) [118]	Organophosphorus pesticides/ fruit juice samples	Sample volume: 10 mL Adjusted pH at 5.92 by adding NaOH or HCl solutions Extraction solvent: 408 µL DES Emulsifier agent: 560 µL THF Extraction time: 27 min	HPLC-UV	0.070-0.096 ng mL^{-1}
Machado *et al.* (2019) [149]	7 triazole fungicides/ urine	Sample volume: 1 mL β-glucuronidoase 100 µL internal standard (Tebuconazole-(tert-butyl-d9) 20 µL + 2 mL of buffer (1 mol L^{-1} phosphate buffer pH 7) + CAN 1 mL Extraction solvent: toluene 200 µL Extraction time: 6 min	GC/MS	-

2.7 Sample preparation and chromatographic determination of triazole fungicides

Some severe problems have arisen when determining trace amounts of triazole fungicides in complex matrices, such as various samples. Therefore, sample preparation methods play a vital role in overcoming these obstacles. This prerequisite step is accomplished with the aim of sample clean-up and pre-concentration. With this end, the development of a sensitive, fast, convenient, and economic sample pretreatment method for the simultaneous determination of triazole fungicides is required. There are several reports for the determination of triazole fungicide residues in different samples by various sample preparation and preconcentration techniques followed by instrumental analysis such as LC-MS, GC, and HPLC. After extraction, the desorption solution containing the target analytes can be directly introduced int liquid chromatography[150], gas chromatography [151] systems without extract pre-dilution. UV-Vis and spectrofluorimetric [152] detection can also be implemented. For trace analysis of TFs using the aforementioned methods, the sample preparation step is commonly required. The development of sample preparation techniques mainly focuses on simplification, miniaturization and also environmental friendliness. In recent years, many techniques have been developed to preconcentrate TFs in various samples, such as liquid-liquid microextraction (LLE) [153] or solid-phase extraction (SPE)[154]. However, employment of these techniques involves a tedious process and the consumption of potentially toxic organic solvents. As an alternative sample preparation method, sorbent-based extraction, generally known as solid-phase microextraction (SPME), has been employed for the preconcentration of TFs [155]. SPME as a solventless extraction is very popular technique in recent years that use

different fiber materials in various configurations for the extraction of a wide range of volatile analytes [156]. Different sorbent materials have been used including [157], polydimethylsiloxane/fiber [158], graphene-based magnetic nanocomposite[11] and poly (ionic liquid)-functionalized magnetic adsorbent. Recently, a new approach for the extraction of triazole fungicides using *Moringa oleifera* seed powder as a biosorbent from various target analytes has been proposed. The bio-adsorbent can be used for adsorption without any modification step, simplifying the extraction process and showing the adsorption capacity of the adsorbent merely. Only a few examples of that procedure can be found in the literature. Information on sample preparation and preconcentration techniques combined with various instruments are summarized in Table 9.

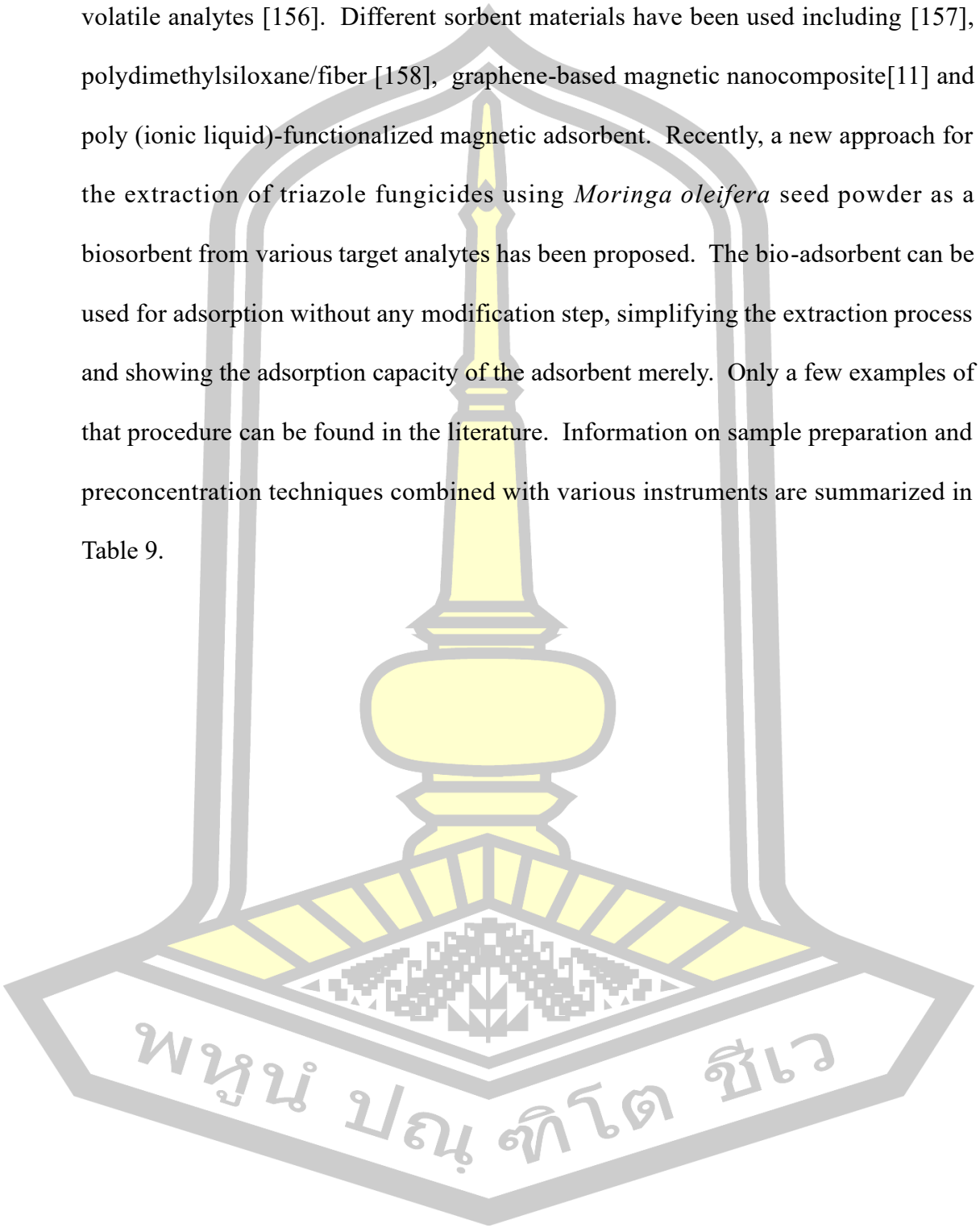

Table 9 Literatures on sample preparation and chromatographic determination of triazole fungicides.

Author (year)	Analytes / Samples	Chromatographic condition/ Preconcentration technique
Hergueta-Castillo *et al.* (2022) [159]	Triazole fungicides and their metabolites/ fruits and vegetables - Difenoconazole - Fenbuconazole - Tebuconazole - Cyproconazole - Myclobutanil - Penconazole - Propiconazole - Tetraconazole - Triadimenol - 1,2,4-triazole - Prothioconazole - Triticonazole - Bromuconazole - Epoxiconazole - Fluquinconazole - Flutriafol - Ipconazole - Metconazole - Paclobutrazole - Flusilazole	UHPLC-Q-Orbitrap-MS^2: Column: - Hypersil GOLD™ aQ (100 mm × 2.1 mm × 1.9 µm particle size) - Acclaim™ Trinity Q1 (100 mm × 2.1 mm × 3 µm particle size) - Acclaim™ Trinity P1 (100 mm × 2.1 mm × 3 µm particle size) - Hypercarb™ (100 mm × 2.1 mm × 5 µm particle size) Mobile phase: - (A) 4 mM ammonium formate and 0.1% formic acid - (B) acetonitrile Flow rate: 0.3 mL min^{-1} Injection volume: 10 µL Detector: Hybrid mass spectrometer Q-Exactive Orbitrap MS-ESI Run time: 10.5 min

Table 9 Literatures on sample preparation and chromatographic determination of triazole fungicides (cont.).

Author (year)	**Analytes / Samples**	**Chromatographic condition/ Preconcentration technique**
Gao *et al.* (2022) [160]	Triazole fungicides/human urine - Prothioconazole - Prothioconazole desthio	LC-MS/MS: Column: Phenomenex Kinetex XB-C18 reversed-phase column (2.1 × 50 mm, 1.7 µm) Mobile phase: - (A) water (with 5 mmol L^{-1} ammonium formate) - (B) methanol (with 5 mmol L^{-1} ammonium formate) Flow rate: 0.35 mL min^{-1} Injection volume: 1 µL Detector: Triple Quadrupole LC/MS Run time: 15 min SPE: Extraction device: Oasis HLB cartridges (3 mL/60 mg, 30 µm, Waters) Sample clean-up: - Conditioning: 2 mL dichloromethane, 2 mL methanol, dried with N_2, 2 mL water - Loading: 1 mL human urine (held for 30 min) - Washing: 1 mL water: methanol (95:5, v/v) Elution solvent: 60 mL methanol

Table 9 Literatures on sample preparation and chromatographic determination of triazole fungicides (cont.).

Author (year)	Analytes / Samples	Chromatographic condition/ Preconcentration technique
Yang *et al.* (2021) [161]	Triazole fungicides/Tobacco - Myclobutanil - Tebuconazole - Penconazole - Triadimefon	SFC-MS/MS: Column: - Chiralpak IG-3 [amylose-tris-(3-chloro5-methylphenylcarbamate)] (150 × 4.6mm, 3µm) - Chiralpak IC-3 [cellulose-tris (3, 5-dichlorophenylcarbamate)] (150 × 4.6mm, 3µm) - Trefoil AMY1 [amylose-tris-(3, 5-dimethylphenylcarbamate)] (150 × 3.0 mm, 2.5µm) - Trefoil: CEL1 [cellulose-tris-(3, 5-dimethylphenylcarbamate)] (150 × 3.0 mm, 2.5µm) - Trefoil CEL2 [cellulose tris-(3-chloro-4-methylphenylcarbamate)] (150 × 3.0 mm, 2.5 µm) Mobile phase: (A) CO_2:(B) ethanol, post-column additive: 0.1% formic acid:methanol (v/v) Flow rate: 0.2 mL min^{-1} Injection volume: 2 µL Detector: Triple Quadrupole-MS/ESI Extraction: - Sample volume: 3 mL - Transferred to the PRiME-SPE column and passed through the column under gravity

Table 9 Literatures on sample preparation and chromatographic determination of triazole fungicides (cont.).

Author (year)	Analytes / Samples	Chromatographic condition/ Preconcentration technique
Seebunrueng *et al.* (2021) [162]	Triazole fungicides/waters - Triadimefon - Flusilazole - Tebuconazole - Penconazole - Propiconazole	HPLC-DAD: Column: Zorbax Eclipse XDB-C18 (5 µm, 4.6 × 250 mm) Mobile phase: - (A) acetonitrile - (B) water Flow rate: 0.8 mL min^{-1} Injection volume: 20 µL Detector: Diode array detector (220 nm) SMMH-d-SPME: In-situ conditions: - Sample volume: 100 mL - 20 mg of Fe_3O_4@SiO_2 - 10 mg of SDS, - 0.738 g (5 mmol) of $Mg(NO_3)_2$, - 0.36 g (1.7 mmol) of $Al(NO_3)_3$, - 1 g NaCl - Adjusted to pH 10 using 0.1 mol L^{-1} NaOH Elution solvent: 6 mL acetonitrile (2 mL for 3 times) via ultrasonication for 2 min

Table 9 Literatures on sample preparation and chromatographic determination of triazole fungicides (cont.).

Author (year)	Analytes / Samples	Chromatographic condition/ Preconcentration technique
Belarbi *et al.* (2021) [163]	95 pesticide residues and 5 contaminants (PCB congeners) /complex food matrices	GC–MS/MS (triple-quadrupole): Column: Series (15 m long × 0.25 mm i.d., and 0.25 µm film thickness) Carrier gas: helium (high purity, 99.999%) Flow rates: 0.9- and 1.1-mL min^{-1} in the first and second columns Temperature program: - Initial temperature of 60 ˚C (1 min) to 170 ˚C at 35 ˚C min^{-1} and up to 310 ˚C at a rate of 10 ˚C min^{-1} with a hold time of 2 min at 310 ˚C Injection volume: 1 µL (splitless mode) GC-HRMS (Q-Orbitrap): Column: HP-5 MS UI (30 m × 250 µm × 0.25 µm film thickness) Carrier gas: helium (high purity, 99.999%) Flow rates: 1.0 mL min^{-1} Temperature program: - t_0: 60 ˚C, hold time of 0.2 min increased at 720 ˚C min^{-1} until reaching 310 ˚C with a hold time of 5 min Run time: 20 min QuEChERS d-SPE cleanup: - (a) d-SPE with PSA (300 mg) and $MgSO_4$ (900 mg) for purification of wheat extracts

Table 9 Literatures on sample preparation and chromatographic determination of triazole fungicides (cont.).

Author (year)	Analytes / Samples	Chromatographic condition/ Preconcentration technique
		- (b) d-SPE with PSA (150 mg), C18 (150 mg) and $MgSO_4$ (900 mg) for purification of rapeseed extracts - (c) d-SPE with Q-Carb® containing PSA (150 mg), graphitized carbon black GCB (150 mg) and $MgSO_4$ (855 mg) for purification of tea and cumin extracts
Han *et al.* (2020) [164]	Triazole fungicides/ river water, wheat flour and rice - Triadimefon - Tebuconazole - Hexaconazole - Diniconazole - Fluorene - Indomethacin - 2,4-dichloroaniline	HPLC-UV: Column: ZORBAX SB-C18 column (5 µm, 4.6 mm × 150 mm i.d.) at 30 ˚C Mobile phase: (A) methanol:(B) ultrapure water Flow rate: 1.0 mL min^{-1} Injection volume: 50 µL Detector: - 220 nm for TRI and TEB - 210 nm for HEX and DIN MSPE: Sample volume: 10 mL Amount of sorbent: 5 mg of Fe_3O_4@PC Desorption solvent: 200 µL of acidic methanol (19:1, $v_{methanol}/v_{acetic\ acid}$) - Fierce shaking for 1 min, magnetically isolated from the desorption solution

Table 9 Literatures on sample preparation and chromatographic determination of triazole fungicides (cont.).

Author (year)	Analytes / Samples	Chromatographic condition/ Preconcentration technique
Abolghasemi *et al.* (2020) [165]	Triazole fungicides/fruit juice and vegetable samples - Penconazole - Hexaconazole - Cyproconazole - Difenconazole - Propiconazole - Triticonazole - Diniconazole	GC-FID: Column: HP-5 MS (30 m × 0.25 mm with a thickness of 0.25µm film) Column temperature: - Kept for 2 min at 100 °C - Incremented to 200 °C at a rate of 20 °C min^{-1} Carrier gas: helium (99.999%) Flow rate: 1.1 mL min^{-1} Injection volume: 2 µL Injector temperature: 300 °C Detector: Flame Ionization detector Detector temperature: Adjust at 300 °C in H_2 flow rate 30 mL min^{-1} and air flow rate 300 mL min^{-1} DSE-HS-SDME: DES: ChCl: 4-chlorophenol (mole ratio 1:2) Sample temperature: 85 °C pH of aqueous phase: pH 6 Concentration of salt: 10% of NaCl Agitation: Stirring rate at 750 rpm - Extraction time: 30 min

Table 9 Literatures on sample preparation and chromatographic determination of triazole fungicides (cont.).

Author (year)	**Analytes / Samples**	**Chromatographic condition/ Preconcentration technique**
Senosy *et al.* (2020) [166]	Residual fungicides/ water, honey, and fruit juices - Epoxiconazole - Flusilazole - Tebuconazole - Triadimefon	HPLC-DAD: Column: Welch Ultimate® XB-C18 column (5 µm × 4.6 mm × 250 mm i.d.) at 30 ˚C Mobile phase - (A) methanol - (B) water Flow rate: 1 mL min^{-1} Injection volume: 20 µL Detector: Diode array detector (230 nm) MSPE: Sample volume: 30 mL pH of sample solution: pH 5 Concentration of salt: 1% NaCl Amount of sorbent: 16 mg Desorption solvent: 0.5 mL methanol Agitation: - Shaken (200 rpm min^{-1}) for 15 min - Vortex 1 min

Table 9 Literatures on sample preparation and chromatographic determination of triazole fungicides (cont.).

Author (year)	Analytes / Samples	Chromatographic condition/ Preconcentration technique
Zeng *et al.* (2019) [167]	Triazole fungicides/ vegetables and fruits	2D-LC-DAD: Model: Dionex UltiMate 3000 × 2 Dual UHPLC system 1st D Column: Kinetex XB-C18 (100 × 4.6 mm, 2.6 µm) at 25 °C Mobile phase: (A) acetonitrile: (B) water Flow rate: 0.4 mL min^{-1} Injection volume: 5 µL Detector: Diode array detector (230 nm) 2nd D Column: YMC CHIRALART Cellulose-SB column (5 µm, 250 mm × 4.6 mm) at 25 °C Mobile phase: (A) acetonitrile: (B) water Flow rate: 0.7 mL min^{-1} Detector: Diode array detector (220 nm) ATPE: Amount of sample: 2.0 g Amount of salt: 1.233 g K_2HPO_4 Extraction solvent: 2.3 mL of ethanol was diluted to 5 mL with water Agitation: - Vortex stirrer - Ultrasonicate at 60 °C for 21 min - Centrifuged at 5000 rpm for 5 min.

Table 9 Literatures on sample preparation and chromatographic determination of triazole fungicides (cont.).

Author (year)	**Analytes / Samples**	**Chromatographic condition/ Preconcentration technique**
Jabali *et al.* (2019) [168]	Pesticides/ waters - Myclobutanil - Penconazole - Tebuconazole	GC-MS: Column: Varian Factor Four VF-5MS capillary column (30 m × 0.25 mm i.d., 0.25 µm film thickness) Carrier gas: Helium (99.99%) Flow rate: 1 mL min^{-1} Oven temperature program - Initial temperature: 60 °C (hold 1 min) - Rate 30 °C min^{-1} to 180 °C (hold 3 min) - Rate 5 °C min^{-1} to 280 °C (hold 3 min) Total run time: 30 min Detector: Ion trap mass spectrometer (ITMS) in electron impact (EI) mode DI-SPME: Sample volume: 18 mL Adsorbent: Polyacrylate fiber (PA) Total immersed time: 45 min Agitation: Magnetic stirring of 500 rpm at 60 °C

Table 9 Literatures on sample preparation and chromatographic determination of triazole fungicides (cont.).

Author (year)	Analytes / Samples	Chromatographic condition/ Preconcentration technique
Ye *et al.* (2018) [169]	Triazole fungicides/ honey - Paclobutrazol - Myclobutanil - Diniconazole - Epoxiconazole	LC–MS/MS: Column: Chiralcel OD-RH column (150 mm × 4.6 mm, 5 μm) Mobile phase: - (A) 2 mM ammonium acetate aqueous - (B) acetonitrile Flow rate: 0.5 mL min^{-1} Total run time: 22 min MS conditions Capillary voltage: 3.00 kV Source temperature: 150 ˚C Desolvation temperature: 500 ˚C Desolvation gas flow: 1000 L h^{-1} SPE-DLLME: SPE conditions - Sample volume: 10 mL - PEP-2 cartridge previously activated with 3 mL of methanol and 3 mL of water at a flow rate of 5 mL min^{-1} - Elution solvent: 1 mL of acetone

CHAPTER 3

METHODOLOGY

3.1 Reagents and Standards

All reagents were analytical grade or higher. They were obtained from various suppliers, as summarized in Table 10. Aqueous solutions were prepared in deionized water with a resistivity of 18.2 MΩ.cm from a RiOs™ Type I Simplicity 185 (Millipore, USA).

Table 10 Chemicals and reagents used in this work.

Chemicals	Formula	Company	Country
Standard triazole fungicides			
Diniconazole (DCZ)	$C_{15}H_{17}Cl_2N_3O$	Dr. Ehren-storfer	Germany
Hexaconazole (HCZ)	$C_{14}H_{17}Cl_2N_3O$	Dr. Ehren-storfer	Germany
Myclobutanil (MCBT)	$C_{15}H_{17}ClN_4$	Dr. Ehren-storfer	Germany
Tebuconazole (TBZ)	$C_{16}H_{22}ClN_3O$	Dr. Ehren-storfer	Germany
Triadimefon (TDF)	$C_{14}H_{16}ClN_3O_2$	Dr. Ehren-storfer	Germany
Chemicals and reagents			
Acetic acid	CH_3COOH	Merck	Germany
Acetonitrile (ACN)	CH_3CN	Merck	Germany
Cetyltrimethylammonium bromide (CTAB)	$C_{19}H_{42}BrN$	Sigma Aldrich	Germany
Citric acid monohydrate	$C_6H_8O_7.H_2O$	Kemaus	Australia
Decanoic acid	$C_{10}H_{20}O_2$	Sigma Aldrich	Malaysia
Dodecanoic acid	$C_{12}H_{24}O_2$	Sigma Aldrich	Malaysia

Table 10 Chemicals and reagents used in this work (cont.).

Chemicals	Formula	Company	Country
Chemicals and reagents			
Ethanol	C_2H_5OH	Merck	Germany
Formic acid	HCOOH	QRëC®	New Zealand
Hydrochloric acid	HCl	Merck	Germany
Methanol	CH_3OH	Merck	Germany
n-hexane	C_6H_{14}	Leonid quality our forte	India
Octanoic acid	$C_8H_{16}O_2$	Sigma Aldric	China
Potassium hexafluorophosphate	KPF_6	Sigma Aldrich	China
Propanol	C_3H_7OH	Merck	Germany
Sodium dodecylbenzene sulfonate (SDBS)	$CH_3(CH_2)_{11}C_6H_4SO_3Na$	Sigma Aldrich	Germany
Sodium dodecyl sulfate (SDS)	$NaC_{12}H_{25}SO_4$	Merck Schuchardt OHG	Germany
Sulfuric acid	H_2SO_4	Merck	Germany
Sodium hydrogen carbonate	$NaHCO_3$	Kemaus	Australia

Table 10 Chemicals and reagents used in this work (cont.).

Chemicals	Formula	Company	Country
Chemicals and reagents			
Tributyldodecylphosphonium bromide ([P_{44412}]Br)	$C_{24}H_{52}BrP$	Sigma Aldrich	Switzerland
Material			
Melamine sponge	Purchased from an online vendor		

3.2 Instrumentation

The HPLC system consists of a Waters 1525 Binary HPLC pump (USA), and a Waters 2489 UV-Visible detector operated at 220 nm. Table 11 shows the chromatographic conditions used to separate triazole fungicide residues. The chromatographic separation conditions employed throughout this research are as follows:

Table 11 The chromatographic conditions used for separation of triazole fungicide residues.

Parameters	Conditions
Column	Purosphere® STAR RP-18 endcapped column (150 mm × 4.6 mm, 5.0 µm)
Mobile phase	50% acetonitrile in water
Flow rate (mL min^{-1})	1.0
Detector	UV-Visible detector
Wavelength (nm)	220
Injection volume (µL)	20

3.3 Real samples

3.3.1 Green fabrication of *Moringa oleifera* seed as efficient biosorbent for selective enrichment of triazole fungicides in environment water, honey, and fruit juice samples

3.3.1.1 Environmental water samples

Environmental waters were collected from the different natural locations near agriculture fields in Maha Sarakham province. These samples were filtered through a Whatman (no.1) filter paper and then passed through a 0.45 µm nylon membrane filter before extraction using the proposed method.

3.3.1.2 Honey samples

Honey samples were purchased from a supermarket in Maha Sarakham province. 5 g of sample was weighed into a 50-mL volumetric flask and diluted to the marker. The solution was filtered through a Whatman (no.1) filter paper to remove particulate matter and then passed through a 0.45 µm nylon membrane filter before extract using the proposed method.

3.3.1.3 Fruit juice samples

Commercial juice samples (orange and strawberry) were purchased from the supermarket in Maha Sarakham province. Before analysis, a 30.0 mL aliquot of fruit juice was centrifuged at 4000 rpm for 10 min and then filtered through a Whatman (no.1) filter paper. After that, the filtrate was passed through a 0.45 µm nylon membrane filter before extract using the proposed method.

3.3.2 Surfactant modified coconut husk fiber as a green alternative sorbent for micro-solid phase extraction of triazole fungicides at trace levels in environmental waters, soybean milk, fruit juice, and alcoholic beverage samples

3.3.2.1 Environmental water samples

The environmental waters were obtained from the different natural locations near agricultural fields in Maha Sarakham province, Northeast, Thailand. These samples were filtered through a Whatman (no.1) filter paper and passed through a 0.45 µm nylon membrane filter before extraction using the proposed method.

3.3.2.2 Fruit juice samples

Two kinds of commercial fruit juice samples, including an orange and pomegranate, were purchased from the supermarket in Maha Sarakham province, Northeast, Thailand. 10 g of all fruit juice were centrifuged at 4000 rpm for 10 min and the supernatant was collected. The supernatant was diluted with ultrapure water at ratio (1:2) [170].

3.3.2.3 Soybean milk samples

Two kinds of soybean milk samples were purchased from the local supermarket in Maha Sarakham province, Northeast, Thailand. 1 mL of sample was added into 15 mL centrifuge tube. After that, added 5 mL of acetonitrile and 1 mL of 0.1 mol L^{-1} trifluoroacetic acid before applying to vortex for 3 min. The solution was then centrifuged at 4500 rpm for 10 min. These samples were filtered through a Whatman (no.1) filter paper and passed through 0.45 µm nylon membrane filter before extract using the proposed method.

3.3.2.4 Alcoholic beverage samples

Alcoholic beverage samples including beers and wines (alcohol content as 5%) were purchased from different supermarkets in Maha Sarakham province, Northeast, Thailand. At initial, the selected alcoholic samples (10 mL) were degassed for 15 min in an ultrasonic bath, stored at room temperature, and then kept in clean, dry containers. After degassing, the samples were filtered through a 0.45 µm nylon membrane filter before analysis.

3.3.3 Hydrophobic melamine sponge incorporated with carbon dots as a green sorbent for micro-solid phase extraction of triazole fungicide residues in edible fungi samples

3.3.3.1 Edible fungi samples

Six edible fungi samples were obtained from a local market in Kalasin province, Northeast, Thailand. These samples were washed with tap water and rinsed with deionized water to remove substrates and foreign matter. After that, the edible fungi samples were blended using a mixer grinder. 2.0 g of sample was mixed with 2.00 mL of acetonitrile to extract the target analytes. The mixture was vortex for 30 s and centrifuged at 4500 rpm for 15 min. The supernatant was collected and diluted to 10.0 mL with water before it was subjected to the micro-SPE process.

3.3.4 An in situ formation of ionic liquid for enrichment of triazole fungicides in food applications followed by HPLC determination

3.3.4.1 Honey Samples

Honey samples were purchased from a supermarket in Maha Sarakham province. A total of 5 g of the sample was weighed into a 50 mL volumetric flask and diluted to the marker. The solution was filtered through a Whatman (no. 1)

filter paper. After that, the filtrate was passed through a 0.45 μm nylon membrane filter before extraction using the proposed method.

3.3.4.2. Fruit Juice Samples

Passion fruit juice and pomegranate juice (commercial juice samples) were bought from the supermarket in Maha Sarakham province. An aliquot of fruit juice (30.0 mL) was centrifuged at 4000 rpm for 10 min and then filtered through a Whatman (no. 1) filter paper. The solution was then passed through a 0.45 μm nylon membrane filter before extraction using the proposed method.

3.3.4.3. Egg Yolk Sample

Chicken eggs were purchased from local markets in Maha Sarakham province. The yolk was separated from the white to reduce interference, since in the analysis of egg collected from animals treated with anthelmintics, it is known that the interferences are greater in the yolk [171][172]. Fortification of the sample was performed directly in the yolk, and a period of about 12 h was allowed to elapse before continuing with any of the extraction processes to improve the interaction between the analytes and the matrix compounds [173]. A total of 10.00 g of egg yolk was mixed well with 0.2 g of anhydrous Na_2SO_4. After that, 1% (v/v) acetic acid in acetonitrile (2.00 mL) was added and shaken vigorously by hand for 1 min, and the homogenized eggs were centrifuged at 3500 rpm for 5 min for complete fat and protein precipitation. The supernatants were collected using a micro syringe. The solutions were diluted with deionized water to 10.00 mL, 100 μL of acetic acid was added, and the solutions were centrifuged to ensure the complete precipitation of fat and proteins [172]. The samples were spiked with the triazole fungicides at

different concentrations before fat and protein precipitation. The obtained clear solutions were then extracted using the proposed microextraction method.

3.3.5 Trace-level determination of triazole fungicides using effervescence-assisted liquid-liquid microextraction based ternary deep eutectic solvent prior to high-performance liquid chromatography

3.3.5.1 Environmental water samples

Environmental water samples were collected near an agricultural area in Kantharawichai District, Maha Sarakham Province, northeast Thailand. After the environmental water samples were taken to the laboratory, they were filtered by a 0.45 μm membrane filter and kept at 4 °C in a refrigerator until extraction.

3.3.5.2 Honey samples

Honey samples were bought from a supermarket in Kantharawichai District, Maha Sarakham Province, northeast Thailand. For the honey samples, 5 g of honey was diluted to 50 mL using water. The sample solution was mixed using hand shaking for 30 s and then filtered through Whatman (no.1) filter paper to remove particulate matter. The diluted honey was passed through a 0.45 μm nylon membrane filter and then extracted using the developed method.

3.3.5.3 Bean samples

Bean samples including soybean, red bean, and mung bean were bought from a local market in Maha Sarakham Province, northeast Thailand. Bean seeds were soaked in water for 10–15 min, rinsed again with DI water, and left to dry in the atmosphere. After that, the dried seeds were placed in an oven at 65 °C for 8.0 h before grinding into fine powder. The powdered bean sample was weighed (0.10 g) into centrifuge tubes and extracted with 5.0 mL of acetonitrile on a mechanical shaker

for 15 min. Then, the supernatant was adjusted to 10 mL with deionized water, passed through a 0.45 µm nylon membrane filter, and extracted using the developed method.

3.4 Experimental

3.4.1 Preparation of standard triazole fungicides in green fabrication of *Moringa oleifera* seed as efficient biosorbent for selective enrichment of triazole fungicides in environment water, honey, and fruit juice samples

The mixture of standard triazole fungicide solutions such as myclobutanil, triadimefon, tebuconazole, hexaconazole and diniconazole were prepared in methanol and working solution were diluted in deionization water before injected into HPLC with the optimum conditions. A calibration curve for each analyte was constructed by plotting between the peak areas versus the concentration of mixed standard triazole fungicides solution at seven different concentrations. The linearity range were evaluated by the calibration curve ($y = mx+ c$) and the correlation coefficient (R^2) value.

The sensitivity of the method were evaluated by limit of detection (LOD) calculated as three times the signal-to-noise ratio 3:1, and limit of quantitation (LOQ) calculated as ten times the signal-to-noise ratio 10:1. Precision of the method were determined by analyzing mixed standard triazole fungicides solution at a concentration of 100 µg L^{-1} in a same day and in three difference days, and the repeatability were evaluated in terms of %RSD.

3.4.2 Preparation of standard triazole fungicides in surfactant modified coconut husk fiber as a green alternative sorbent for micro-solid phase extraction of triazole fungicides at trace level in environmental water, soybean milk, fruit juices, and alcoholic beverages samples

The mixture of standard triazole fungicide solutions such as myclobutanil, triadimefon, tebuconazole, hexaconazole and diniconazole were prepared in methanol and working solution were diluted in deionization water before injected into HPLC with the optimum conditions. A calibration curve for each analyte was constructed by plotting between the peak areas versus the concentration of mixed standard triazole fungicides solution at seven different concentrations. The linearity range were evaluated by the calibration curve ($y = mx+ c$) and the correlation coefficient (R^2) value.

The sensitivity of the method was evaluated by limit of detection (LOD) calculated as three times the signal-to-noise ratio 3:1, and limit of quantitation (LOQ) calculated as ten times the signal-to-noise ratio 10:1. The Precision of the method were determined by analyzing mixed standard triazole fungicides solution at a concentration of 100 $\mu g\ L^{-1}$ in a same day and three difference days, and the repeatability were evaluated in terms of %RSD.

3.4.3 Preparation of standard triazole fungicides in hydrophobic melamine sponge incorporated with carbon dots as a green sorbent for micro-solid phase extraction of triazole fungicide residues in edible fungi samples

The mixture of standard triazole fungicide solutions such as myclobutanil, triadimefon, tebuconazole, hexaconazole, and diniconazole were prepared in methanol and working solution were diluted in deionization water before injected into HPLC

with the optimum conditions. A calibration curve for each analyte was constructed by plotting between the peak areas versus the concentration of mixed standard triazole fungicides solution at seven different concentrations. The linearity range were evaluated by the calibration curve ($y = mx + c$) and the correlation coefficient (R^2) value.

The sensitivity of the method were evaluated by limit of detection (LOD) calculated as three times the signal-to-noise ratio 3:1, and limit of quantitation (LOQ) calculated as ten times the signal-to-noise ratio 10:1. Precision of the method were determined by analyzing mixed standard triazole fungicides solution at a concentration of 100 µg L^{-1} in a same day and three difference days, and the repeatability were evaluated in terms of %RSD.

3.4.4 Preparation of standard triazole fungicides in an in situ formation of ionic liquid for enrichment of triazole fungicides in food applications followed by HPLC determination

The mixture of standard triazole fungicide solutions such as myclobutanil, triadimefon, tebuconazole, hexaconazole and diniconazole were prepared in methanol and working solution were diluted in deionization water before injected into HPLC with the optimum conditions. A calibration curve for each analyte was constructed by plotting between the peak areas versus the concentration of mixed standard triazole fungicides solution at seven different concentrations. The linearity range were evaluated by the calibration curve ($y = mx + c$) and the correlation coefficient (R^2) value.

The sensitivity of the method were evaluated by limit of detection (LOD) calculated as three times the signal-to-noise ratio 3:1, and limit of quantitation (LOQ)

calculated as ten times the signal-to-noise ratio 10:1. Precision of the method were determined by analyzing mixed standard triazole fungicides solution at a concentration of 100 µg L^{-1} in a same day and in three difference days, and the repeatability were evaluated in terms of %RSD.

3.4.5 Preparation of standard triazole fungicides in trace-level determination of triazole fungicides using effervescence-assisted liquid-liquid microextraction based ternary deep eutectic solvent prior to high-performance liquid chromatography

The mixture of standard triazole fungicide solutions such as myclobutanil, triadimefon, tebuconazole, hexaconazole and diniconazole were prepared in methanol and working solution were diluted in deionization water before injected into HPLC with the optimum conditions. A calibration curve for each analyte was constructed by plotting between the peak areas versus the concentration of mixed standard triazole fungicides solution at seven different concentrations. The linearity range were evaluated by the calibration curve ($y = mx + c$) and the correlation coefficient (R^2) value.

The sensitivity of the method were evaluated by limit of detection (LOD) calculated as three times the signal-to-noise ratio 3:1, and limit of quantitation (LOQ) calculated as ten times the signal-to-noise ratio 10:1. Precision of the method were determined by analyzing mixed standard triazole fungicides solution at a concentration of 100 µg L^{-1} in a same day and in three difference days, and the repeatability were evaluated in terms of %RSD.

3.5 Sample preconcentration

3.5.1 Green fabrication of *Moringa oleifera* seed as an efficient biosorbent for selective enrichment of triazole fungicides in environmental water, honey, and fruit juice samples procedure

Triazole fungicides were determined by green fabrication of *Moringa oleifera* seed as an efficient biosorbent followed by HPLC-UV. Figure 1 shows a schematic diagram of the proposed microextraction method.

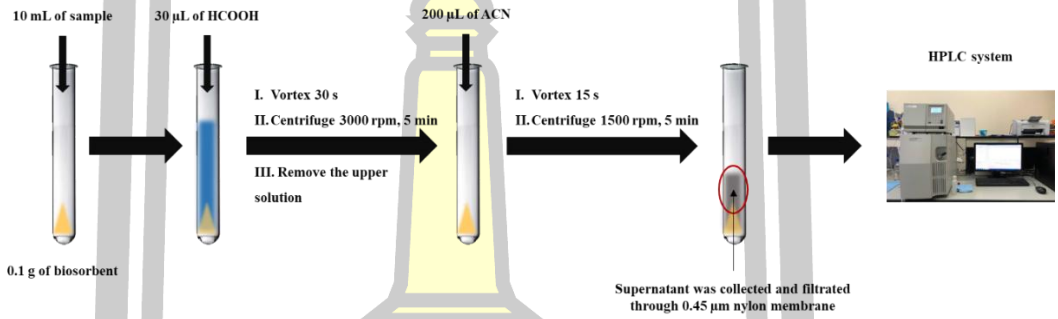

Figure 1 The schematic diagram of the proposed micro-solid phase extraction using *Moringa oleifera* seed and analysis by HPLC.

Micro solid phase extraction (µ-SPE) method

Schematic diagram of the µ-SPE method using *Moringa oleifera* seeds prior to HPLC analysis. Moringa oleifera seed powder (0.10 g) was added to a 15 mL conical centrifuge tube containing standard or sample solution (10.00 mL). Subsequently, 1 mol L^{-1} formic acid (300 µL) was added. Then, vortex adsorption was performed at 1500 rpm for 30 s and centrifuged at 3,000 rpm for 5 min to enhance the sorption of the target analytes. The supernatant was removed using a syringe. Acetonitrile (200 µL) was added to elute the target analytes. The mixture was vortexed for desorption at 1500 rpm for 2 min and centrifuged at 3,500 rpm for 5 min. The clear

supernatant was collected and then filtered through a 0.45 μm membrane filter before analysis by HPLC.

3.5.1.1 Optimization of microextraction procedure

3.5.1.1.1 Effect of amount of Moringa oleifera seed

The amount of *Moringa oleifera* seed is one of the critical parameters for extraction efficiency. To study the effect of the amount of biosorbent on the proposed extraction method, experiments were carried out by the addition of different amounts of *Moringa oleifera* seed was investigated.

The amount of *Moringa oleifera* seed was studied in the range of 0.05-1.0 g.

3.5.1.1.2 Effect of salt addition

The salt addition could potentially decrease the solubility of the analytes in the aqueous solution and enhance their partitioning into the adsorbent or organic phases. On the other hand, as the ionic strength of the medium increases, the viscosity and density of the aqueous solution are also enhanced, leading to a reduction of the mass transfer efficiency process. Salt addition often enhances the extraction of analytes in conventional microextraction due to the salting-out effect. To study the effect of ionic strength on the proposed extraction method, experiments were carried out by the addition of different salts such as NaCl, and Na_2SO_4 was investigated.

The concentration of selected salt was studied in the range of 0.3-3 g.

3.5.1.1.3 Effect of type and volume of acidic solution

The dissolution of biosorbent under acidic conditions (pH<4) is an outstanding advantage, improving extraction performance and reducing extraction time greatly. In this study, we investigated different types of acid such as formic acid (HCOOH), hydrochloric acid (HCl), acetic acid (CH_3COOH), and sulfuric acid (H_2SO_4).

The volume of acid was studied in the range of 30-300 µL.

3.5.1.1.4 Effect of vortex time (I), (II)

The vortex time was used for agitation during the extraction step to provide extraction efficiency as it increases the partition of the sample and the extraction solvent into an aqueous solution. The vortex agitation speed was fixed at 3500 rpm and different vortex times were evaluated in the range from 0-45 s.

3.5.1.1.5 Effect of centrifugation time (I), (II)

Centrifugation is another important step in a procedure to achieve phase separation, the process of mass transfer between two phases in the extraction procedure should be time dependent. This extraction method was divided into two parts of extraction, the round per minute (rpm) of centrifugation (I: loading) and (II: eluting) were studied in the range of 0-4500 rpm. The centrifugation time (I: loading) and centrifugation (II: eluting) time were studied in the range of 0-20 min at a fixed speed of 3000 rpm.

3.5.1.1.6 Effect of type and volume of elution solvent

To study the effect of different elution solvents, acetonitrile (ACN), methanol (MeOH), ethanol (EtOH), and propanol (PrOH) at 200 µL were investigated.

The volume of the elution solvent was in the range of 50-500 µL.

3.5.1.2 Analytical performance of the method

The 10.00 mL of sample solution was placed in a 15 mL centrifuge tube and spiked with each triazole fungicide (100 µg L^{-1}). The µSPE procedure was investigated under optimum conditions. The mixture of five triazole fungicide standards was prepared in deionized water. The linearity range, limits of detection (LODs), and limits of quantitation (LOQs) were defined as the concentrations of target analytes with S/N=3 and 10, respectively. The repeatability of the proposed method was performed at five different times on the same day (intra-day; n=5), and the reproducibility of the proposed method was performed at five different times and three different days (inter-day; n = 5×3 days) and calculated in terms of %RSDs at a concentration of 500 µg L^{-1}. The enrichment factor (EF), matrix effect, and extraction recovery were evaluated.

3.5.2 Surfactant modified coconut husk fiber as a green alternative sorbent for micro-solid phase extraction of triazole fungicides at trace levels in environmental water, soybean milk, fruit juices, and alcoholic beverages samples

Triazole fungicides were determined by surfactant modified coconut husk fiber as a green sorbent followed by HPLC-UV. Figure 2 shows a schematic diagram of the proposed microextraction method.

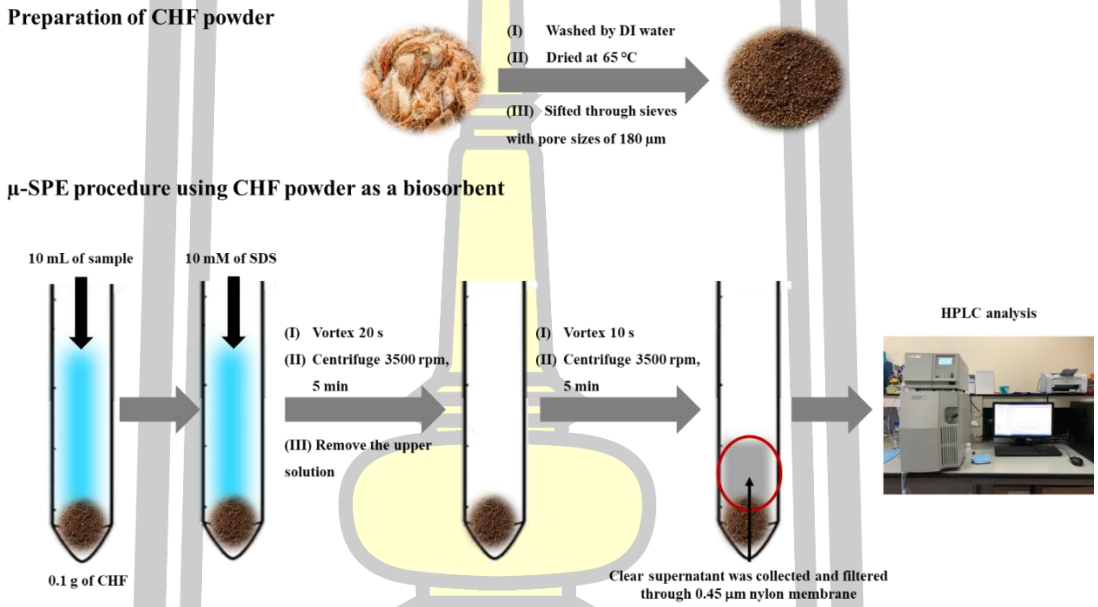

Figure 2 The schematic diagram of the proposed micro-solid phase extraction followed by HPLC-UV analysis.

Preparation of coconut husk fiber powder as a biosorbent

Coconut husk fiber (CHF) was obtained from Roi-Et province, Northeast, Thailand. The fibers were separated from the husks, washed with distilled water, and dried at 65 °C until the CHF material was dried. Subsequently, they were sifted through sieves with pore sizes of 180 µm. The powder was stored in a desiccator until use.

Micro solid phase extraction (m-SPE) procedure

Schematic of m-SPE method using coconut husk fiber powder prior to HPLC analysis. Coconut husk fiber (CHF) powder (0.1 g) was added into a 15 mL conical centrifuge tube containing standard or sample solution (10.00 mL). Subsequently, 150 µL of 10 mmol L^{-1} sodium dodecyl sulfate was added. The solution was then vortexed for 20 s and centrifuged at 3500 rpm for 5 min to enhance the sorption of the analytes onto the sorbent. The supernatant was then removed. Subsequently, 150 µL of methanol was added to elute the target analytes. The mixture was vortexed for desorption at 1500 rpm for 10 s and centrifuged at 3500 rpm for 5 min. The clear supernatant was collected and filtered through a 0.45 µm membrane filter before analysis by HPLC.

3.5.2.1 Optimization of microextraction procedure

3.5.2.1.1 Effect of amount of coconut husk fiber (CHF)

One of the most important parameters of the µ-SPE procedure is to determine the effective amount of the biosorbent. To study the effect of amount of biosorbent on the proposed extraction method, experiments were carried out by addition of different amount of biosorbent was investigated.

The amount of biosorbent was studied in the range of 30-1000 mg.

3.5.2.1.2 Effect of surfactant as modifier and pH on adsorption

Surfactant molecules have both polar and non-polar parts, which enables them to either dissolve in water as individual units (monomers) or to group with other molecules to form micelles. When surfactants are adsorbed onto the surface of a biosorbent, they interact through attractive electrostatic forces, leading

to the formation of monolayers known as hemimicelles. Following this, hydrophobic interactions between the hydrocarbon chains of the surfactant molecules promote the formation of micelles. The effects of different surfactants specifically the cationic CTAB, non-ionic Triton X-114, and anionic SDBS and SDS were studied at various concentrations to assess their role as modifiers in the adsorption process.

The surfactant concentration was studied in the range of 1-30 mmol L^{-1}.

3.5.2.1.3 Effect of kind and volume of desorption solvent

An effective desorption solvent should be selected to obtain the high desorption efficiency of triazole fungicides from CHF biosorbent. A reasonable desorption solvent is helpful to desorb the target TFs from the extraction biomaterial in a short time. To improve the accuracy of the experiment, four typical organic solvents, acetonitrile, methanol, ethanol, and isopropanol, were compared and investigated.

The volume of desorption solvent was studied in the range of 30-250 µL.

3.5.2.1.4 Effect of sample volume

In method development, demonstrating the capability of the system for the enrichment of analytes from a large sample volume is an important task. The sample volume affects the efficiency of the mass transfer; thus, it influences the extraction efficiency. The possibility of the extraction of trace amounts of analytes from the sample volume of the developed method was investigated.

The sample volume was studied in the range of 5-15 mL.

3.5.2.1.5 Effect of adsorption and desorption time

The µ-SPE procedure is a stable-based technique, and the institution of equilibrium invests the rate of mass transfer along with extraction time. The contribution of adequate contact time between the target analytes and the biosorbent to reach adsorption equilibrium is important. The vortex adsorption time, centrifugation rate, and time were investigated.

The vortex adsorption time was studied in the range of 0-30 s.

This extraction method is divided into two parts of extraction, the round per minute (rpm) of centrifugation. The centrifugation rate and time of the two parts were studied in the range of 1500-4500 rpm and 3-10 min, respectively.

3.5.2.2 Analytical performance of the method

The volume of 10.00 mL of sample solution was placed in 15 mL centrifuge tube and spiked of each triazole fungicides (100 µg L^{-1}). The µSPE procedure was investigated under the optimum conditions. The mixture of five triazole fungicide standards were prepared in deionized water. The linearity range, limits of detection (LODs), limits of quantitation (LOQs), were defined as the concentration of target analytes giving S/N=3 and 10, respectively. The repeatability of the proposed method was done on five different times in same day (intra-day; n=5), and the reproducibility of the proposed method was done on five different times and three different days (inter-day; n = 5×3 days) and calculated in term of %RSDs at two concentrations (50 and 100 µg L^{-1}). The enrichment factor (EF) and extraction recoveries were evaluated.

3.5.3 Hydrophobic melamine sponge incorporated with carbon dots as a green sorbent for micro-solid phase extraction of triazole fungicide residues in edible fungi samples

The determination of triazole fungicides was carried out by a hydrophobic melamine sponge incorporated with carbon dots as a green sorbent for micro-solid phase extraction of triazole fungicide residues in edible fungi samples followed by HPLC-UV. Figure 3 shows a schematic diagram of the proposed microextraction method.

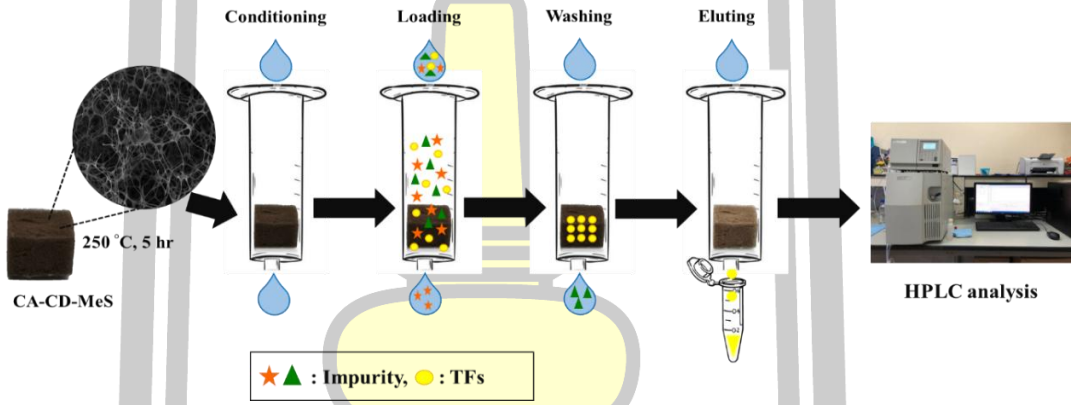

Figure 3 The schematic diagram of the synthesis and micro-SPE application of carbon dot embedded melamine sponge.

Fabrication of hydrophobic melamine sponge incorporated with carbon dots

A melamine sponge (MeS) was firstly cut into cubes of 1×1×1 cm^3, washed with DI water and ethanol, and then left to dry. Subsequently, MeS cube was immersed in an ethanolic solution containing citric acid 0.04 mol L^{-1}. The immersing/drying step was repeated until all the solution was soaked up. After that, MeS was immersed in citric acid overnight and then heated to remove solvent at

250 °C for 5 h. Finally, functionalized melamine sponges were characterized and kept in a desiccator until use.

Micro-solid phase extraction (micro-SPE) procedure

The synthesis material was placed into a syringe (5.00 mL) on cotton fabric and used as a SPE cartridge. After that, a representative aliquot of 10 mL of sample solution was loaded into the SPE cartridge by vacuum manifold. After that, the SPE cartridge was washed with 1.0 mL of n-hexane to remove interferences. Following this, the absorbent was eluted with 200 µL of acetonitrile. After filtration through a 0.45 µm nylon syringe filter, 20 µL of eluate were analyzed by HPLC-DAD.

3.5.3.1 Synthesis optimization *3.5.3.1.1 Size of melamine sponge (MeS)*

To achieve maximum loading of MeS with citric acid, the synthesis conditions were handled correctly and examined. The principle used to select the optimum synthesis conditions was the total adsorption capability of the resulting CA-CD-MeS, for a mixture of five TFs (100 µg L^{-1} each), and four sizes of MS were investigated.

The size of MeS was studied including 0.3×0.3×0.3, 0.5×0.5×0.5, 1×1×1, and 1.5×1.5×1.5 cm^3.

3.5.3.1.2 Effect of concentration of citric acid (as a precursor)

The citric acid precursor was prepared at different concentrations by dissolving citric acid (monohydrate) powder in ethanol. The effect of the concentration of citric acid on the extraction efficiency of triazole fungicides was investigated.

The concentration of citric acid was studied in the range of 0.01-0.1 mol L^{-1}.

3.5.3.1.3 Effect of soaking time

For the total adsorption capability of citric acid solution on MeS for synthesis, the soaking time was divided into two parts: part I, the soaking time in the range of 15-90 minutes was investigated, and part II, the soaking time in the range of 30-120 minutes was investigated.

3.5.3.1.4 Effect of oven temperature

Then, MeS-coated CA was heated to remove solvent and impurity substances, and the temperature of the oven in the range of 130-280 °C was investigated.

3.5.3.1.5 Optimization of micro-SPE conditions

To obtain the best extraction performance of CA-CD-MeS as a SPE sorbent in extracting TFs from mushroom samples, a single factor optimization was adopted to optimize several conditions that may affect such performance, such as kind and volume of solvent conditioning, kind and volume of washing solvent, kind and volume of eluting solvent. The standard concentration was 100 μg L^{-1}.

3.5.3.1.6 Effect of type and volume of elution solvent

The type of elution solvent is an essential parameter for SPE because it determines the accomplishment of analyte elution and, therefore, will result in sensitivity. In this work, the generally used HPLC-grade of methanol (MeOH), acetonitrile (ACN), and deionized water (DI) as the elution solvent were investigated for the elution of the five triazole fungicides.

The effect of the volume of the elution solvent acetonitrile was also studied in the range of 100-250 μL.

3.5.3.2 Analytical performance of the method

The 10.00 mL of sample solution was placed in a 15 mL centrifuge tube and spiked with each triazole fungicide (100 µg L^{-1}). The SPE procedure was investigated under optimum conditions. A mixture of the five triazole fungicide standards was prepared in deionized water. The linearity range, limits of detection (LODs), and limits of quantitation (LOQs) were defined as the concentrations of target analytes with S/N=3 and 10, respectively. The repeatability of the proposed method was evaluated five different times on the same day (intra-day; n=5), and the reproducibility of the proposed method was evaluated five different times and three different days (inter-day; n = 5×3 days) and calculated in terms of %RSDs at two concentrations (9 and 15 µg L^{-1}). Enrichment factor (EF) and extraction recovery were also evaluated.

3.5.4 An in situ formation of ionic liquid for enrichment of triazole fungicides in food applications followed by HPLC determination of triazole fungicides in environmental water, soybean milk, fruit juice, and alcoholic beverage samples

Triazole fungicides were determined by in situ formation of ionic liquid as extraction solvent followed by HPLC-UV. Figure 4 shows a schematic diagram of the proposed microextraction method.

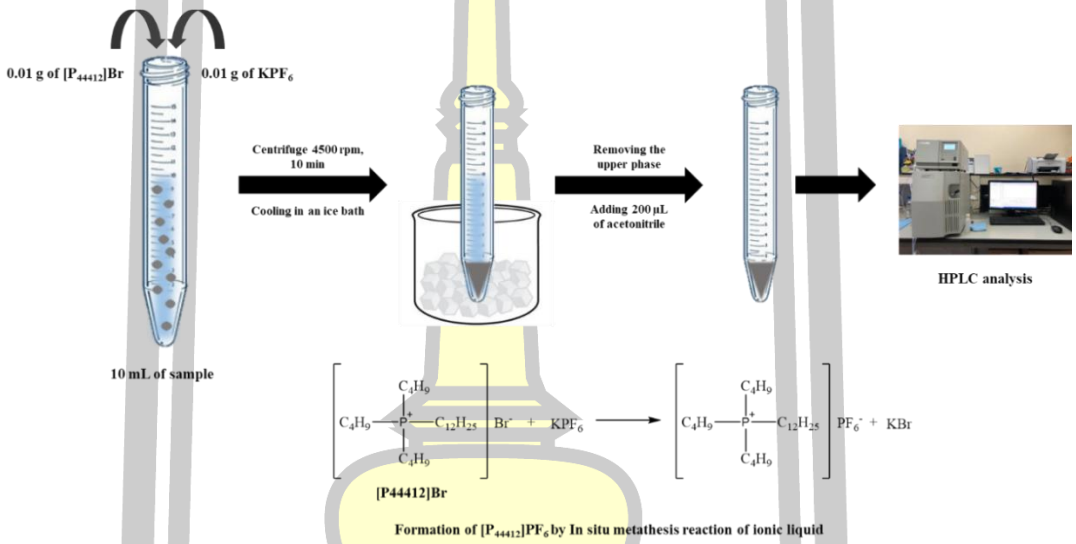

Figure 4 The schematic diagram of the microextraction proposed using in situ formation of the ionic liquid for triazole fungicides and HPLC analysis.

An in situ formation of ionic liquid based on liquid-liquid microextraction.

A schematic diagram of an in situ formation of ionic liquid based on a microextraction procedure. The mixed solution included the standard or sample solution (10.00 mL), 0.01 g of $[P_{44412}]Br$, and 0.01 g of KPF_6, which were added into a 15 mL conical centrifuge tube. The tube was shaken to dissolve $[P_{44412}]Br$ and KPF_6 and complete the in situ metathesis reaction. The solution was then centrifuged at 4500 rpm for 10 min. The centrifuge tube was then cooled in an ice bath until $[P_{44412}]PF_6$ was generated. The $[P_{44412}]PF_6$ phase (upper phase) was separated and

diluted with acetonitrile (200 µL) to decrease the viscosity before being injected into the HPLC system.

3.5.4.1 Optimization of in situ metathesis-generated ionic liquid combined with LLME

3.5.4.1.1 Effect of the amount of IL components

To form the ionic liquid ($[P_{44412}][PF_6]$), $[P_{44412}]Br$ and KPF_6 were selected because the starting extraction solvent could be completely dissolved in the aqueous solution, which promoted the analyte extraction in the absence of a dispersion solvent; the melting of this IL ($[P_{44412}][PF_6]$) was between 10 and 30 °C, and it could solidify at low temperatures [99]. Moreover, $[P_{44412}][PF_6]$ is denser than water, therefore it was easy to collect as the bottom layer after centrifugation.

The amount of $[P_{44412}]Br$ was studied in the range of 0.01-0.10 g.

The amount of KPF_6 varied in a range of 0.01-0.10 g.

3.5.4.1.2 Effect of extraction speed and time

Because the process of mass transfer and complete phase separation in an extraction procedure should be time-dependent, the effects of the extraction speed and time on the peak area were studied.

The effect of the centrifugation speed was evaluated in the range of 1500-5000 rpm.

The extraction times ranged from 3 to 15 min, whereas the other experimental conditions were kept constant.

3.5.4.1.3 Effect of dissolving solvent

Before HPLC analysis, acetonitrile (ACN) was added to dissolve the RTIL-rich phase due to its solubility property in the $[P_{44412}]PF_6$ phase and the compatibility with the mobile phase being used.

The ACN volume was investigated in the range of 30-250 µL.

3.5.4.2 Analytical performance of the method

The 10.00 mL of sample solution was placed in a 15 mL centrifuge tube and spiked with each triazole fungicide (100 µg L-1). The LLME procedure was investigated under optimum conditions. A mixture of the five triazole fungicide standards was prepared in deionized water. The linearity range, limits of detection (LODs), and limits of quantitation (LOQs) were defined as the concentrations of target analytes with S/N=3 and 10, respectively. The repeatability of the proposed method was done five different times on the same day (intra-day; n=5), the reproducibility of the proposed method was done on five different times and three different days (inter-day; n = 5×3 days) and calculated in terms of %RSDs at two concentrations (9 and 15 µg L^{-1}). The enrichment factor (EF) and extraction recoveries were evaluated.

3.5.5 Trace-level determination of triazole fungicides using effervescence-assisted liquid-liquid microextraction based ternary deep eutectic solvent followed by HPLC determination

The determination of triazole fungicides was carried out by effervescence-assisted liquid-liquid microextraction-based ternary deep eutectic solvent followed by HPLC-UV. Figure 5 and 6 shows a schematic diagram of the preparation of TDES and the proposed microextraction method, respectively.

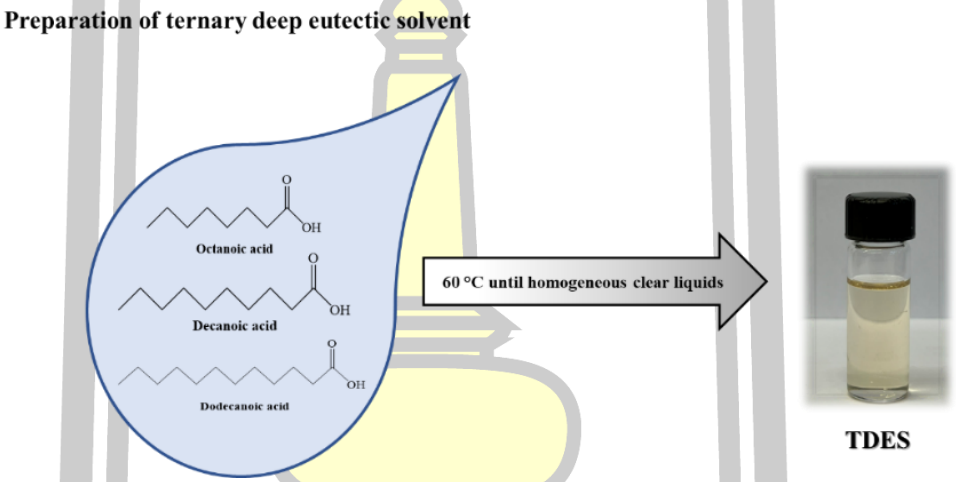

Figure 5 A schematic diagram of the preparation of TDES.

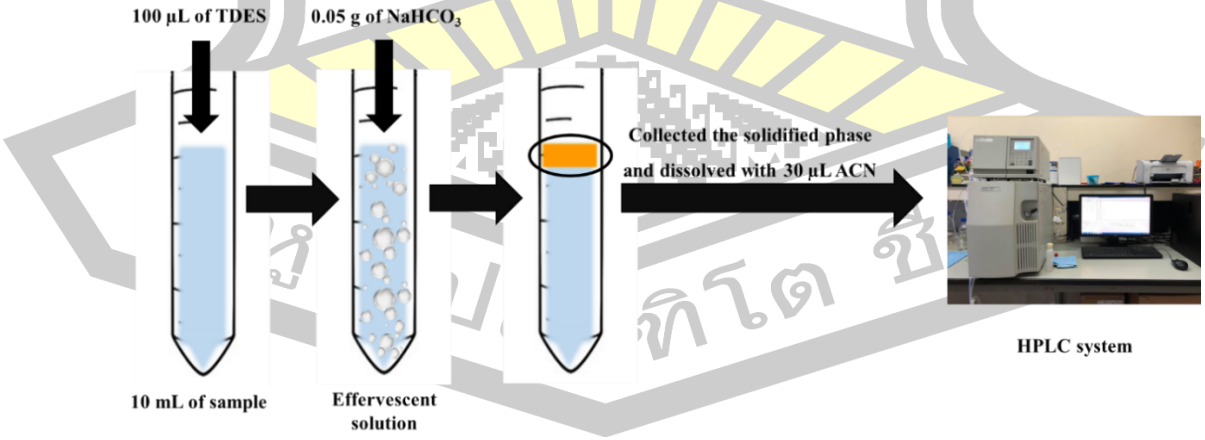

Figure 6 The schematic diagram of the proposed effervescence-assisted LLME based on the TDES method.

Effervescence-assisted liquid-liquid microextraction based on TDES.

A mixed standard/sample solution (10 mL) was transferred into a centrifuge tube. Then, 100 µL of TDES (extracting solvent) was added. After that, 0.05 g of sodium hydrogen carbonate (effervescence precursors) was added to the centrifuge tube. The dispersion of the organic phase by carbon dioxide bubbles and phase separation was observed (without agitators) within 20 s. The floating TDES droplets were collected and dissolved in 30 µL of acetonitrile to decrease viscosity before being injected into HPLC.

3.5.5.1 Optimization of effervescence-assisted LLME based on the TDES conditions

3.5.5.1.1 Effect of ratio and volume of TDESs

TDESs as extracting solvent were synthesized by mixing various molar ratios of the hydrogen bond donor (HBD) and hydrogen bond acceptor (HBA). The fatty acids with a shorter alkyl chain (octanoic acid or decanoic acid) act as HBA, while those with the longest one (dodecanoic acid) act as HBD. It is worth noting that the use of acids smaller than octanoic acid (hydrophilic acids) was not considered due to the chemical instability of the formed DES upon contact with water (acids leach to water).

TDES with the mole ratio including 1:1:1, 2:1:1, 3:1:1, 4:1:1, and 5:1:1 (octanoic acid: decanoic acid: dodecanoic acid) were investigated.

The volume of TDES was studied in the range of 50-200 µL.

3.5.5.1.2 Effect of effervescence agent

To induce the mass transfer (without another agitator), the main necessities of an effective effervescent process are an effervescency agent

(CO_2 source) and a proton donor agent, which can be less-alkali compounds (sodium carbonate, sodium bicarbonate, etc.). In this work, sodium bicarbonate ($NaHCO_3$) was used.

The amount of $NaHCO_3$ was investigated in the range of 0.02-0.3 g.

3.5.5.1.3 Effect of kind and volume of dissolving solvent

To reduce the viscosity of the extract before injecting it to the chromatographic system, different dissolving solvents including methanol, ethanol, isopropanol, and acetonitrile were studied.

The volume of dissolving solvent was investigated in the range of 25-200 µL.

3.5.5.2 Analytical performance of the method

The volume of 10.00 mL of sample solution was placed in 15 mL centrifuge tube and spiked of each triazole fungicides (100 µg L^{-1}). The LLME procedure was investigated under the optimum conditions. The mixture of five triazole fungicide standards was prepared in deionized water. The linearity range, limits of detection (LODs), and limits of quantitation (LOQs), were defined as the concentration of target analytes giving S/N=3 and 10, respectively. The repeatability of the proposed method was done five different times in the same day (intra-day; n=5), and the reproducibility of the proposed method was done on five different times and three different days (inter-day; n = 5×3 days) and calculated on terms of %RSDs at concentrations 10 µg L^{-1}. The enrichment factor (EF) and extraction recoveries were evaluated.

3.6 Data analysis

The average result (mean) was calculated by summing the individual result and dividing by the number (n) of individual values:

$$\bar{x} = \frac{x_1 + x_2 + x_3 + \cdots}{n}$$

The standard deviation was a measure of how precise the average is, that is, how well the individual numbers agree with each other. It is a measure of a type of error called random error. It is calculated as follows:

$$SD = \sqrt{\frac{(x_1 - \bar{x})^2 + (x_2 - \bar{x})^2 + (x_3 - \bar{x})^2 + \cdots}{n-1}}$$

The percentage relative standard deviations (%RSD) are calculated from the standard deviation and mean using the equation:

$$\%RSD = \frac{100 \times SD}{\bar{x}}$$

The percentage recovery (%Recovery) was calculated by concentration of sample and spiked sample using the equation:

$$\%Recovery = \frac{C_{spiked} - C_{unspiked}}{C_{added}} \times 100$$

Where C_{spiked} and $C_{unspiked}$ are the analyte concentration in the extraction phase and the initial analyte concentration in the aqueous samples, respectively. C_{added} is the concentration of spiked standard.

CHAPTER 4

Results and Discussion

4.1 Green fabrication of *Moringa oleifera* seed as efficient biosorbent for selective enrichment of triazole fungicides in environment water, honey, and fruit juice samples

This chapter presents the results obtained during the development of an extraction method for analyzing triazole fungicides, before high-performance liquid chromatography (HPLC). The studied fungicides including myclobutanil, triadimefon, tebuconazole, hexaconazole, and diniconazole were selected as model compounds. The second section evaluates the analytical performance of the proposed method. Finally, the method is applied to analyze triazole fungicide residues in environmental water, honey, and fruit juice samples. The findings are thoroughly discussed.

4.1.1 Scanning electron microscopy (SEM), Transmission electron microscope (TEM), and Fourier transform infrared spectroscopy (FTIR) analysis of biosorbent (*Moringa oleifera* seed)

Scanning electron microscopy (SEM) was used to investigate the morphology of the materials. As shown in Figure 7, the SEM micrographs represent the particle size and the porous structure of the adsorbent. The particle shape of the biosorbent (*Moringa oleifera* seed) is depicted in Figure 7(a). After adsorption of triazole fungicides (100 μg L^{-1} each), morphological changes in the biosorbent are observed in Figure 7(b). The biosorbent following the desorption process is shown in Figure 7(c). The particle size and surface area of the biosorbent significantly influence the adsorption rate. Smaller particle sizes provide a larger surface area, which enhances the adsorption capacity[176]. The adsorption process involves the diffusion

of triazole fungicide molecules from the aqueous solution to the biosorbent surface through its boundary layer [177]. This is followed by the migration of fungicide molecules from the surface to the inner pores of the adsorbent, where they are ultimately adsorbed onto the available active sites. The adsorption of triazole fungicides onto the biosorbent surface likely occurs via physical adsorption (physisorption), which involves the mechanical adhesion of the adsorbate to the adsorbent surface [178].

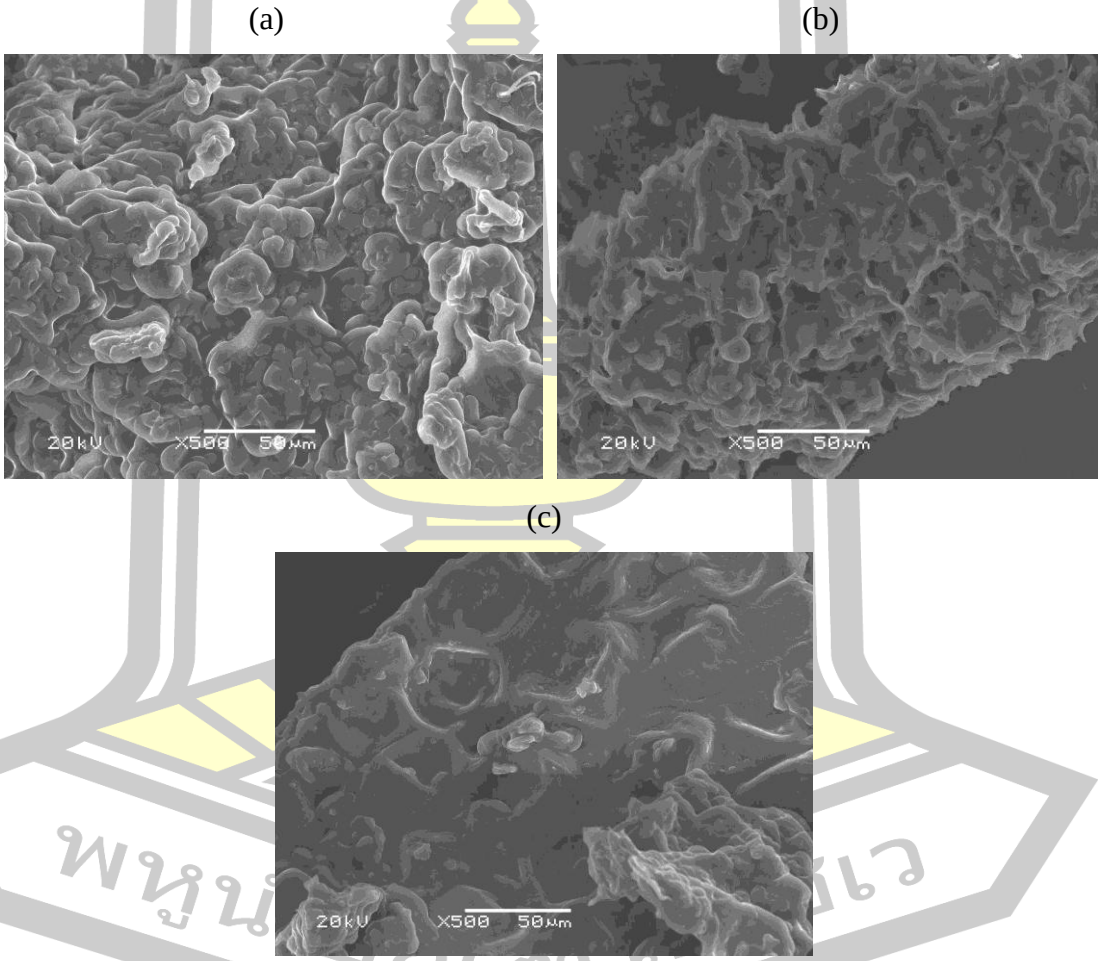

Figure 7 SEM images of (a) biosorbent (*Moringa oleifera* seed), (b) biosorbent (*Moringa oleifera* seed) after adsorption with triazole fungicides (100 µg L^{-1} each), and (c) biosorbent (*Moringa oleifera* seed) after desorption process.

Transmission electron microscopy (TEM) was performed to investigate the morphological features of the biosorbents. Figure 8(a) shows TEM images of untreated *Moringa oleifera* seed, while Figures 8(b) and 8(c) depict the seed after adsorption and desorption processes, respectively. The micrographs reveal an increase in particle size after adsorption (Figure 8(b)), likely due to the accumulation of target analytes on the seed surface. Following the desorption process, the particle size decreased, as shown in Figure 8(c).

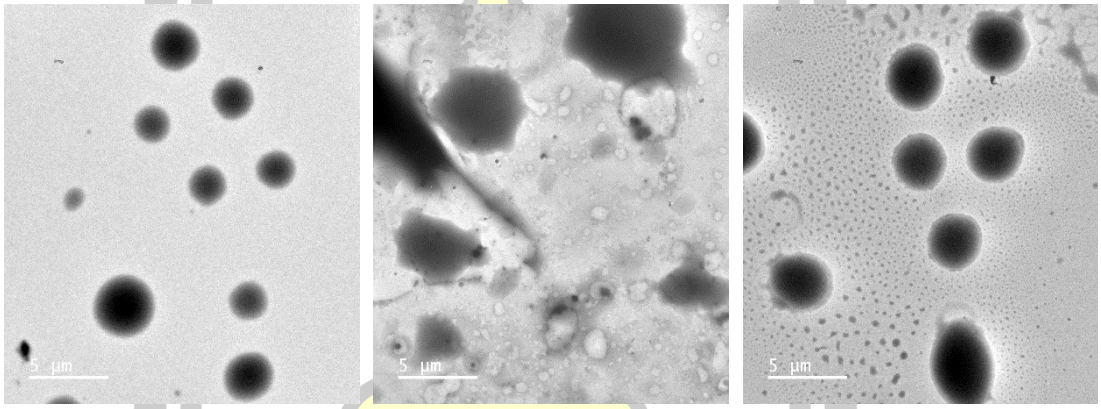

(a) (b) (c)

Figure 8 TEM images of (a) *Moringa oleifera* seed, (b) *Moringa oleifera* seed before adsorption, and (c) *Moringa oleifera* seed after adsorption.

Fourier-transform infrared (FTIR) spectroscopy was employed to identify the functional groups in the *Moringa oleifera* seed. FTIR spectra for untreated seed, seed after blank adsorption, and seed after adsorption of triazole fungicides (100 µg L^{-1} each) are presented in Figure 9. A strong peak at 3293 cm^{-1} indicates the presence of hydroxyl (-OH) groups, likely associated with proteins, fatty acids, carbohydrates, and phenolic compounds [179]. This region also shows contributions from N–H stretching in amide bonds, reflecting the seed's high protein content. Peaks at 2923 and 2853 cm^{-1} correspond to asymmetric and symmetric stretching of C-H bonds in the CH_2 group, characteristic of cellulose structure [180]. The peak at 1744 cm^{-1} is

attributed to carbonyl (C=O) groups, likely linked to fatty acids in lipids or amides (NH_2CO) in proteins [181]. The elongation of the peak at 1650 cm^{-1} is due to C=O stretching in carboxylic acids, while elongation at 1539 cm^{-1} is associated with N-O stretching in the functional group. A shift from 1412 cm^{-1} to 1457 cm^{-1} was observed, corresponding to C–O stretching. Peaks at 1056 and 721 cm^{-1} are attributed to C=C bending [182]. Additional peaks at 1159, 1094, 594, 570, and 515 cm^{-1} highlight changes in the natural composition of *Moringa oleifera* seed after adsorption.

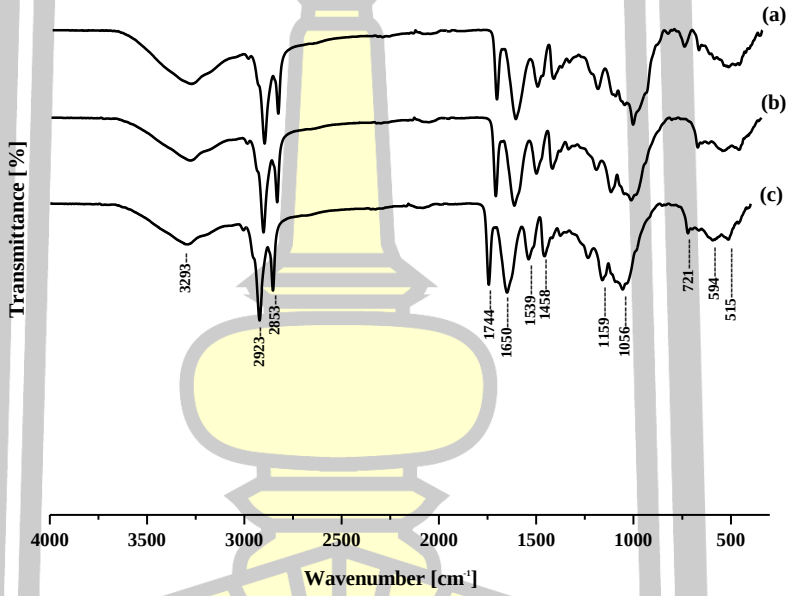

Figure 9 FTIR spectra of (a) *Moringa oleifera* seed, (b) *Moringa oleifera* seed after blank adsorption, and (c) *Moringa oleifera* seed after adsorption of triazole fungicides (100 µg L^{-1} each).

4.1.2 Optimization of the μ-SPE procedure

4.1.2.1 Effect of amount of Moringa oleifera seed

The effect of the amount of *Moringa oleifera* seed powder on extraction efficiency was evaluated by measuring the peak areas of triazole fungicides across a range of 0.05 to 1.0 g. The results showed that the peak areas of all triazole fungicides decreased as the amount of seed powder increased (Figure 10). The highest peak areas were observed with 0.1 g of biosorbent. This is likely because using more than 0.1 g of sorbent in a fixed sample volume reduces contact time during the elution process [183] and limits the availability of surface-binding sites [134]. Therefore, 0.1 g of biosorbent was selected as the optimum amount.

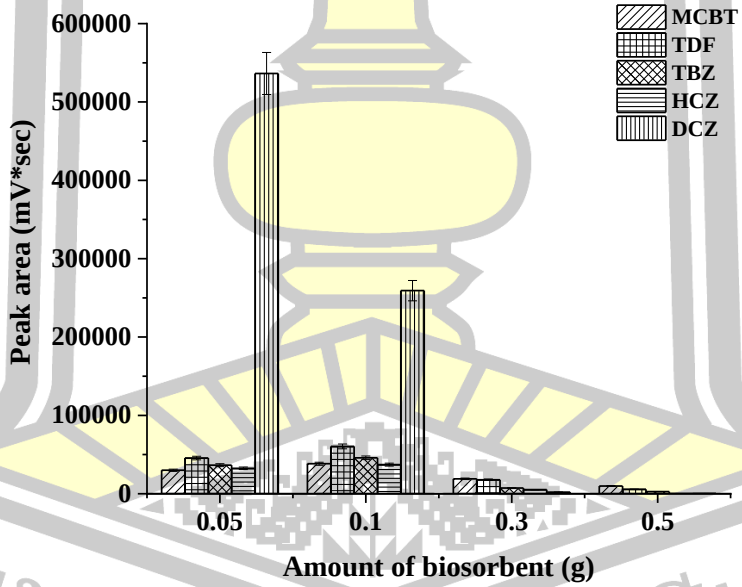

Figure 10 Effect of the amount of biosorbent (*Moringa oleifera*) seed. Conditions: 0.1 g of *Moringa oleifera* seed powder; without salt addition; 50 μL of 1M HCOOH; 500 μL of acetonitrile (desorption solvent); adsorption step-vortex (I) time 30 sec; centrifuge (I) at 3000 rpm for 5 min; desorption step-vortex (II) time 30 sec; centrifuge (II) at 3000 rpm for 5 min.

4.1.2.2 Effect of salt addition

In general, salt addition decreases the solubility of the analytes in the aqueous phase and enhances the extraction efficiency depending on the nature of the analytes. This forces the analytes to preferentially partition into the organic phase, enhancing extraction recovery. To investigate the influence of ionic strength on the performance of the proposed microextraction method, different electrolyte salts (e.g., NaCl, and Na_2SO_4) at 0.1 g were investigated and the results were compared with that obtained from the process without salt addition, the result was shown in Figure 11. It was found that salt addition was unnecessary for the proposed microextraction method of triazole fungicides.

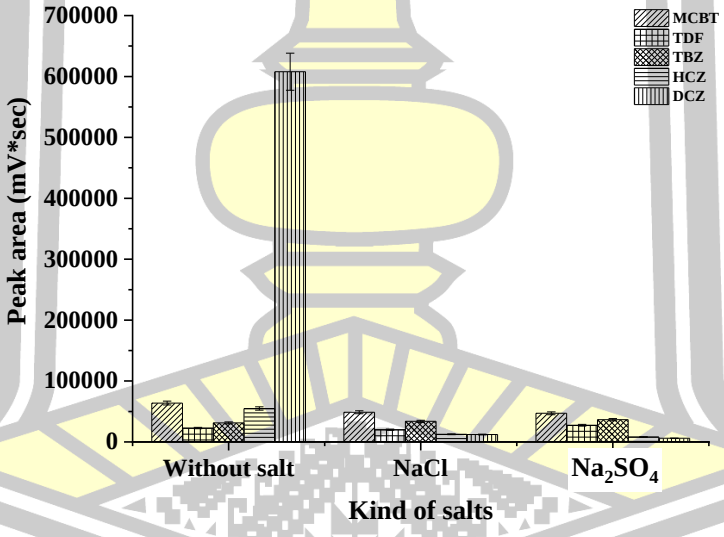

Figure 11 Effect of salt addition

Conditions: 0.1 g of *Moringa oleifera* seed powder; 50 µL of 1M HCOOH; 500 µL of acetonitrile (desorption solvent); adsorption step-vortex (I) time 30 sec; centrifuge (I) at 3000 rpm for 5 min; desorption step-vortex (II) time 30 sec; centrifuge (II) at 3000 rpm for 5 min.

4.1.2.3 Effect of type and volume of acidic solutions

The biosorbent surface is mainly composed of proteins, lipids, and carbohydrates, which are responsible for the surface charge of particles due to the dissociation of functional groups. This dissociation is pH-dependent. The pH of the solution is above the point of zero charge (PZC) of the biosorbent, and surface negative charges are present predominantly in dissociated carboxyl and hydroxyl. Thus, they display a cation exchange capacity, while the solution pH is below their PZC, the aforementioned functional groups are not dissociated, the amino groups of the amino acids are protonated, and the biomass attracts mainly anions. The surface of whole *Moringa oleifera* seeds is electrically neutral in the pH range of 5 to 6 [184]. Various kinds of acidic solutions for transforming the surface charge of biosorbent were studied, the result was shown in Figure 12. It was found that formic acid (HCOOH) provides high extraction efficiency in terms of peak area. Therefore, HCOOH was selected. Then various pH of HCOOH was studied (data not shown). Under acidic conditions (pH = 2), its strongly anionic characteristic from the N–H and O–H groups, is electrostatically attracted by the biosorbent's surface [185]. In this work, the functional groups at pH 2 was observed in the FTIR analysis (as shown in Section 4.1.1), such as hydroxyl and carboxyl groups on the biosorbent surface, and triazole fungicides that are negatively charged [186]. Other types of intermolecular interactions may act in the adsorption process (e.g. hydrogen bonds, van der Waals forces, hydrophobic-hydrophilic interactions) depending on the process conditions. Therefore, the operational conditions that provided the best performances of triazole fungicides adsorption when formic acid (HCOOH) at pH = 2 was chosen.

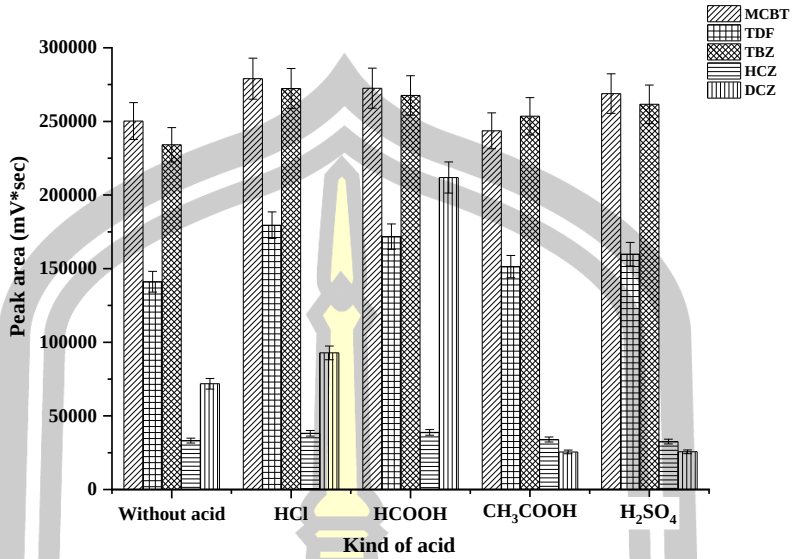

Figure 12 Effect of type of acidic solutions.

Conditions: 0.1 g of *Moringa oleifera* seed powder; without salt addition; 50 µL of each acidic solution (HCOOH, HCl, CH_3COOH, H_2SO_4); 500 µL of acetonitrile (desorption solvent); adsorption step-vortex (I) time 30 sec; centrifuge (I) at 3000 rpm for 5 min; desorption step-vortex (II) time 30 sec; centrifuge (II) at 3000 rpm for 5 min.

4.1.2.4 Effect of sample volume

Sample volume is one of the most important parameters to be studied because it determines the extraction efficiency of the method. The effect of sample volume on the extraction efficiency was varied in the range of 3.00-12.00 mL (Figure 13). The peak areas of the analytes increased with an increase of the sample volume from 3.00 to 10.00 mL, and then slightly decreased with further increase of sample volume. Therefore, the sample volume of 10.00 mL was used for further experiments.

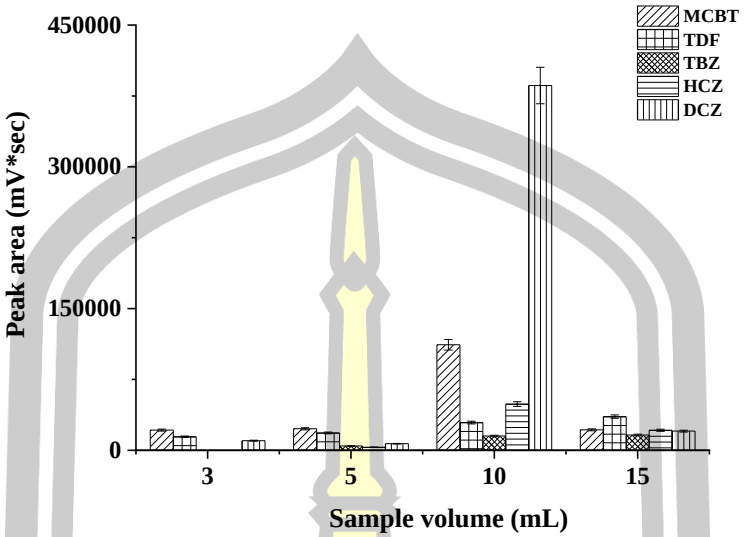

Figure 13 Effect of sample volume

Conditions: 0.1 g of *Moringa oleifera* seed powder; without salt addition; 50 µL of each acidic solution HCOOH; 500 µL of acetonitrile (desorption solvent); adsorption step-vortex (I) time 30 sec; centrifuge (I) at 3000 rpm for 5 min; desorption step-vortex (II) time 30 sec; centrifuge (II) at 3000 rpm for 5 min.

4.1.2.5 Effect of type and volume of desorption solvent

The desorption solvent also plays a crucial role in the microextraction process. Considering the solubility of target analytes and compatibility with the chromatographic system, methanol (MeOH), ethanol (EtOH), propanol (PrOH), and acetonitrile (ACN) were investigated as elution solvents (as shown in Figure 14). The highest efficiency was achieved when acetonitrile was employed. The choice of desorption solvent for triazole fungicides, including methanol, ethanol, propanol, or acetonitrile, depends on several factors, including solubility, polarity, elution strength, and interaction with the sorbent material. Acetonitrile with a cyanide group can easily enter the pores of biosorbent and replace the analytes, achieving

complete desorption. Therefore, acetonitrile was selected for further experiments. Different volumes (50-500 µL) of acetonitrile were varied. The results were shown in Figure 15. It was found that acetonitrile 200 µL was found to be sufficient to completely desorb the analytes. When the volume of desorption solvent more than 200 µL, the peak area of the target triazoles decreased due to the dilution effect. Therefore, 200 µL of acetonitrile was chosen as the optimum desorption volume.

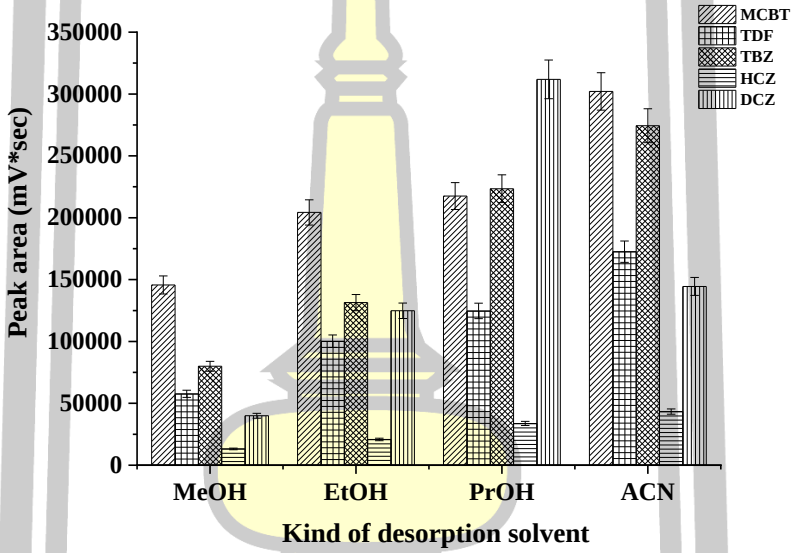

Figure 14 Effect of kind of desorption solvent

Conditions: 0.1 g of *Moringa oleifera* seed powder; without salt addition; 50 µL of each acidic solution HCOOH; 500 µL of acetonitrile (desorption solvent); adsorption step-vortex (I) time 30 sec; centrifuge (I) at 3000 rpm for 5 min; desorption step-vortex (II) time 30 sec; centrifuge (II) at 3000 rpm for 5 min.

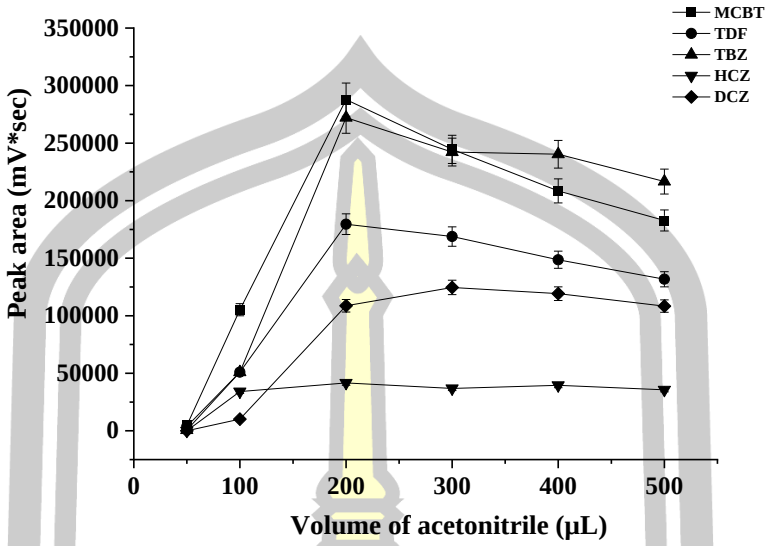

Figure 15 Effect of desorption volume (µL)

Conditions: 0.1 g of *Moringa oleifera* seed powder; without salt addition; 50 µL of each acidic solution HCOOH; 500 µL of acetonitrile (desorption solvent); adsorption step-vortex (I) time 30 sec; centrifuge (I) at 3000 rpm for 5 min; desorption step-vortex (II) time 30 sec; centrifuge (II) at 3000 rpm for 5 min.

4.1.2.6 Effect of adsorption time

To accelerate the µ-SPE process in the present work, vortex agitation was applied during the adsorption and desorption processes. The vortex adsorption time were studied in the range from 0 to 45 sec. It was found that the extraction efficiency slightly increased with increasing vortex adsorption time and reached a maximum of 30 sec (Figure 16.). Therefore, a vortex time of 30 sec was selected for analyte adsorption from the sorbent.

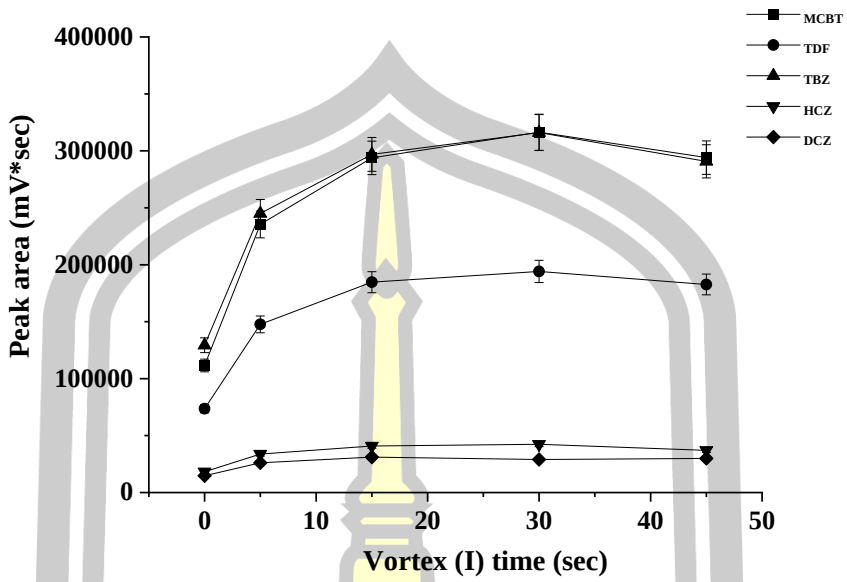

Figure 16 Effect of adsorption time (I)

Conditions: 0.1 g of *Moringa oleifera* seed powder; without salt addition; 50 µL of each acidic solution HCOOH; 500 µL of acetonitrile (desorption solvent); adsorption step-vortex (I) time 30 sec; centrifuge (I) at 3000 rpm for 5 min; desorption step-vortex (II) time 30 sec; centrifuge (II) at 3000 rpm for 5 min.

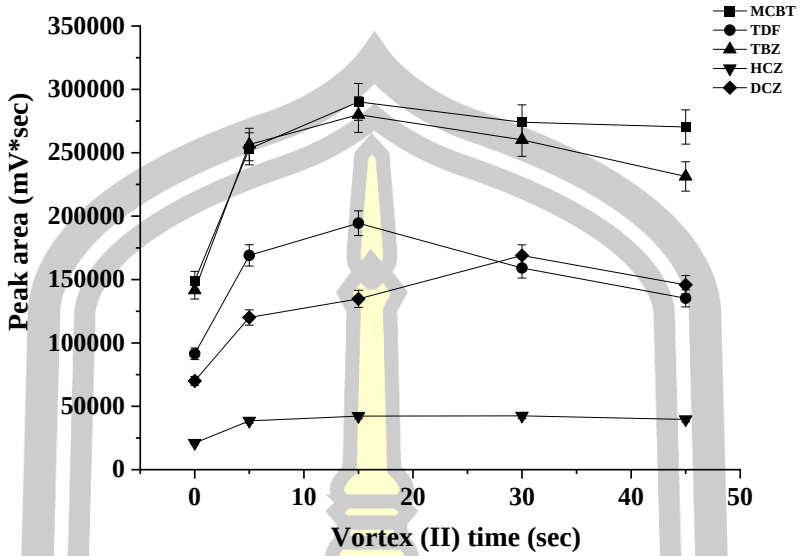

Figure 17 Effect of adsorption time (II)

Conditions: 0.1 g of *Moringa oleifera* seed powder; without salt addition; 50 µL of each acidic solution HCOOH; 500 µL of acetonitrile (desorption solvent); adsorption step-vortex (I) time 30 sec; centrifuge (I) at 3000 rpm for 5 min; desorption step-vortex (II) time 30 sec; centrifuge (II) at 3000 rpm for 5 min.

4.1.2.7 Effect of desorption time

The vortex desorption time was also an important parameter influencing the analyte contents desorbed from the sorbent. The vortex time during the desorption step was studied in the ranged from 0 to 45 sec. It was found that, the extraction efficiency slightly increased with increasing vortex desorption time and reached a maximum at 15 s (data not shown). Therefore, a vortex time of 15 s was selected for analyte adsorption from the sorbent.

4.1.3 Analytical performance of the μ-SPE procedure

The developed method was evaluated, and the analytical characteristic of the method have been summarized in Table 12. The linearity range was assessed by plotting the peak area against the concentration of the respective compounds for quantitative purposes. It was found that, the proposed method provides a good linearity in the range of 10-500 μg L^{-1} with the coefficient of determination (R^2) greater than 0.99. Method detection limit (MDL) and limit of quantification (LOQ) were evaluated by the analytes concentration giving the signal to noise ratio (S/N) of 3 and 10, respectively. MDL were in the range of 30-50 μg L^{-1} and LOQ were in the range of 90-150 μg L^{-1}, respectively. Intra-day (n = 5) and inter-day (n = 5 × 3 days) precisions are also evaluated and reported as the relative standard deviations (RSDs) at the concentration of 500 μg L^{-1}. Acceptable precisions with RSDs were less than 5.0%. Under the optimum conditions, the extraction performance of the developed method was evaluated in terms of enrichment factor (EF). EF can be calculated using the ratio of the extracted analyte concentration (C_{sed}) in the precipitate phase to its initial concentration (C_0) in the aqueous sample solution, according to the equation:

$$EF = C_{sed}/C_0$$

EF which ranged from 8 to 11 folds. It can be concluded that (as shown in Figure 18), the developed method provided significant enhancement of the signal for the target triazoles when compared to that without preconcentration (direct injection analysis). The standard addition method was used to investigate the matrix effect (ME) (as shown in Table 13). MEs (%) can be calculated using the ratio of the slopes obtained from calibration curves of each analyte spiked into the samples to

those obtained after extraction using the proposed method. MEs (%) were calculated from the following equation [187]:

ME (%) = (slope of spiked real sample/slope of standard solution) ×100

In the absence of ME, the slope of calibration curves from both standard solution and spiked real samples should be similar (ME (%) ≈100%) [188]. The result was shown in Table 3. It was found that, MEs (%) are in the range of 76.9-113.9%. This means that target compounds have experienced an enhancement (values up 100) or suppression (values below 100) in their responses. However, it is important to consider that in both cases the ratio of signal enhancement to signal suppression is not really relevant. Because the universally accepted tolerance is normally considered ± 5% [189]. The results confirmed that ME was practically non-existent and/or low in real samples. Standard addition method is usually required when the matrix of the real samples differs from that of the calibration standards and the analytical technique employed is sensitive to the matrix. A study of ME (%) show that the μ-SPE procedure using Moringa oleifera seed is not sensitive to the matrix. As the matrix effect was not significant, it was concluded that the external calibration method could be used instead of the standard addition method for the determination of triazole fungicides in real samples.

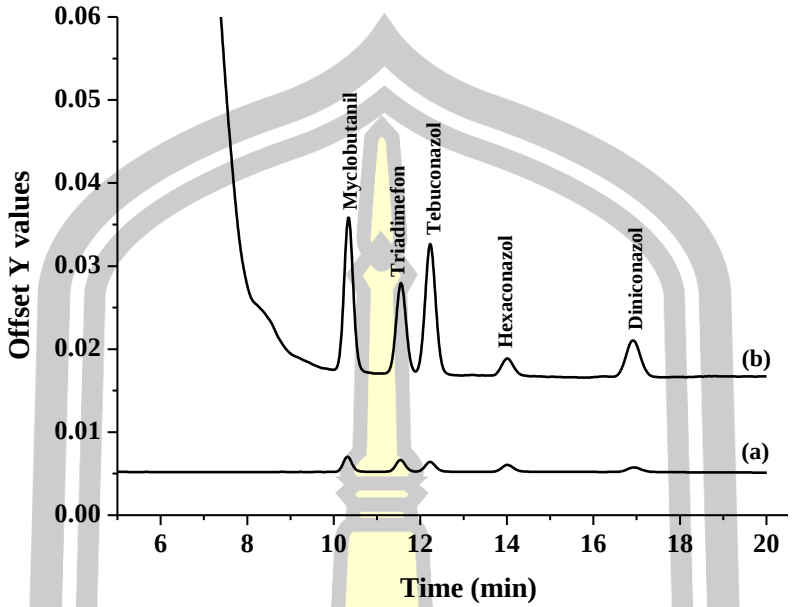

Figure 18 Chromatograms of standard triazole fungicides obtained by (a) without preconcentration and (b) with micro solid phase extraction using *Moringa oleifera* seed: concentration of all standards was 100 µg L^{-1}.

Table 12 Analytical characteristics of standard triazole fungicides.

Analyte	Linear range (µg L^{-1})	Linear equation	R^2	LOD (µg L^{-1})	LOQ (µg L^{-1})	Intra-day precision (n=5), RSD (%)		Inter-day precision (n=5), RSD (%)		EF (C_{ex}/C_o)[b]
						t_R	Peak area	t_R	Peak area	
Myclobutanil	90-500	y = 564166x + 178.82	0.9998	30	90	0.19	4.20	0.22	4.51	11.17
Triadimefon	90-500	y = 344559x + 3555.3	0.9976	30	90	0.20	2.36	0.26	2.36	10.03
Tebuconazole	90-500	y = 368997x – 1316.6	0.9985	30	90	0.07	4.03	0.20	4.13	10.56
Hexaconazole	90-500	y = 181068x – 2449.9	0.9986	50	150	0.90	2.39	0.97	3.70	11.55
Diniconazole	90-500	y = 84491x – 217.39	0.9971	30	90	0.16	3.60	0.19	4.25	8.49

[a] Precision were calculated at the concentration of 100 µg L^{-1} of each triazole.

[b] Ratio of the concentration of the target analytes in extraction phase to the initial concentration in the original sample solutions.

Table 13 Matrix effect (ME, %)

Sample	%ME				
	MCBT	**TDF**	**TBZ**	**HCZ**	**DCZ**
Water sample I	76.9	75.1	77.9	79.5	82.6
Water sample II	96.2	75.7	70.7	77.4	100.6
Honey sample I	94.0	79.5	93.2	107.0	99.1
Honey sample II	97.4	84.4	89.6	82.0	97.6
Orange juice sample I	91.5	81.9	74.5	91.3	107.7
Strawberry juice sample II	106.1	93.6	109.9	116.7	113.9

4.1.4 Analysis of real samples

The proposed method applicability was evaluated for determining triazole fungicides in environmental water, honey, and fruit juice samples. The relative recoveries of the proposed method were studied by spiking samples with triazole fungicides at two different concentrations of 300, and 500 μg L^{-1}. The results are summarized in Table 14. It was found that no residue of the studied fungicides was observed in all studied samples. The relative recoveries of the sample were in the range of 70.00-112%, with the relative standard deviations (RSDs) below 5.0%. At a confidence limit of 95%, there was no significant difference between the results and the data of the alternative analysis. Thus, the method proved to be reliable for the sample types examined. The overlaid chromatograms of water sample II, and honey sample II are shown in Figure 19 and Figure 20, respectively. The results show that no triazole fungicides were detected in the studied samples. Moreover, intra-day (n = 5) and inter-day (n = 5 × 3 days) precisions for detection of target analytes in real samples

analysis are also studied and reported as the relative standard deviations (RSDs) at the concentration of 100 and 300 µg L^{-1}. Acceptable precisions with RSDs were less than 5.0%. The present method is a simple, effective, sensitive, and reliable analytical method for screening triazole fungicides in various samples.

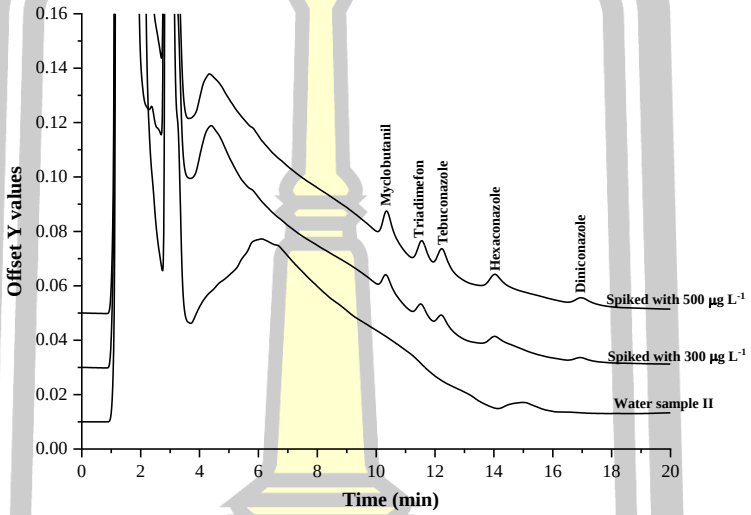

Figure 19 The overlaid chromatograms of water sample II.

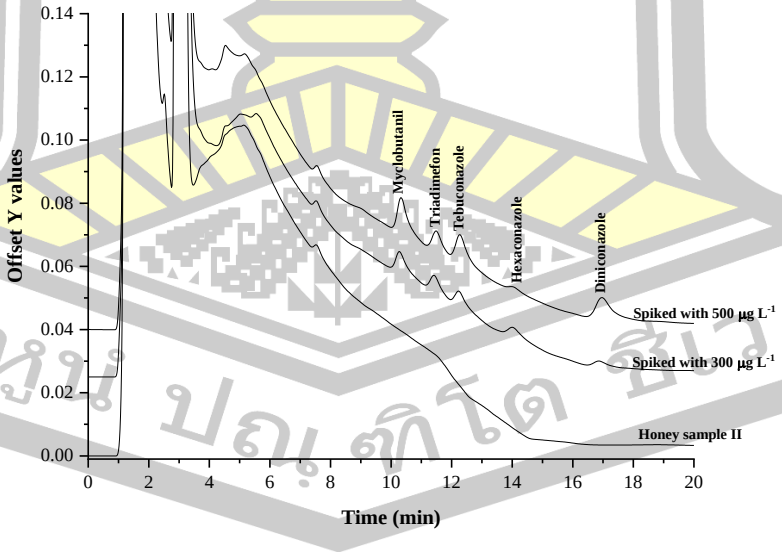

Figure 20 The overlaid chromatograms of honey sample II.

Table 14 Recovery obtained from the determination of studied triazoles in studied samples (n = 3).

Analyte	Spiked ($\mu g\ L^{-1}$)	Environmental water sample I			Environmental water sample II			Honey sample I			Honey sample II			Fruit juice sample I			Fruit juice sample II		
		Found ($\mu g\ L^{-1}$)	%RR[b]	%RSD	Found ($\mu g\ L^{-1}$)	%RR	%RSD	Found ($\mu g\ L^{-1}$)	%RR	%RSD	Found ($\mu g\ L^{-1}$)	%RR	%RSD	Found ($\mu g\ L^{-1}$)	%RR	%RSD	Found ($\mu g\ L^{-1}$)	%RR	%RSD
MCBT	0	ND[a]	-	-	ND*	-	-	ND*	-	-	ND*	-	-	ND*	-	-	ND*	-	-
	300	219.5	73.2	2.24	268.9	89.6	1.49	217.4	72.4	1.14	287.8	95.9	1.04	226.5	75.4	0.09	280.4	93.4	1.31
	500	407.8	81.5	2.02	475.6	95.1	1.91	466.2	93.2	3.10	473.6	94.7	1.06	433.5	86.7	1.13	510.4	102.0	0.15
TDF	0	ND*	-	-	ND*	-	-	ND*	-	-	ND*	-	-	ND*	-	-	ND*	-	-
	300	221.3	73.7	1.97	228.1	76.1	2.99	214.1	71.3	4.21	284.1	94.7	2.13	237.6	79.2	2.25	324.4	108.2	0.75
	500	379.2	75.8	0.86	390.8	78.2	0.88	407.5	81.5	3.72	402.0	80.4	0.73	419.6	83.9	1.98	461.5	92.3	0.73
TBZ	0	ND*	-	-	ND*	-	-	ND*	-	-	ND*	-	-	ND*	-	-	ND*	-	-
	300	225.5	75.2	4.36	228.6	76.2	2.84	225.2	75.1	1.70	239.6	79.8	2.46	201.7	76.2	2.00	254.3	84.7	1.76
	500	370.9	74.2	1.42	366.3	73.3	1.89	455.9	91.2	1.37	439.6	87.9	1.08	395.7	79.1	1.65	547.2	109.4	0.92
HCZ	0	ND*	-	-	ND*	-	-	ND*	-	-	ND*	-	-	ND*	-	-	ND*	-	-
	300	220.7	73.5	0.99	213.2	71.1	0.96	299.3	99.7	3.52	278.0	92.6	1.58	321.8	107.2	3.58	297.5	99.1	1.59
	500	414.9	82.9	2.26	401.7	80.3	0.59	502.4	100.4	1.27	400.3	80.0	3.48	426.7	85.3	1.56	559.0	111.8	1.05
DCZ	0	ND*	-	-	ND*	-	-	ND*	-	-	ND*	-	-	ND*	-	-	ND*	-	-
	300	244.8	81.6	4.15	332.3	110.7	4.31	325.5	108.5	3.87	307.9	102.6	3.78	213.4	71.1	1.29	262.4	87.4	3.24
	500	413.1	82.6	3.01	479.7	95.9	0.76	451.5	90.3	2.99	470.9	94.1	1.85	553.7	110.7	3.74	553.7	110.7	2.82

[a]ND: not detected. [b]: relative recovery.

4.1.5 Comparison of the proposed method to other relevant methods

Table 15 displays the performances of the proposed μ-SPE method using *Moringa oleifera* seed as biosorbent and other relevant methods for the analysis of triazole fungicides. The advantages of the present method are high analytical performance, short time analysis, environmentally friendly, and cost-effective method. The proposed method sensitivity in terms of method detection limit (MDL) is almost comparable to that obtained from other microextraction methods. The presented method achieves low MDL, which are below the MRLs established by the Codex Alimentarius Commission (CAC) for triazole fungicides. This proposed can be used as a powerful alternative miniaturized extraction and preconcentration method for the analysis of triazole fungicides in various samples.

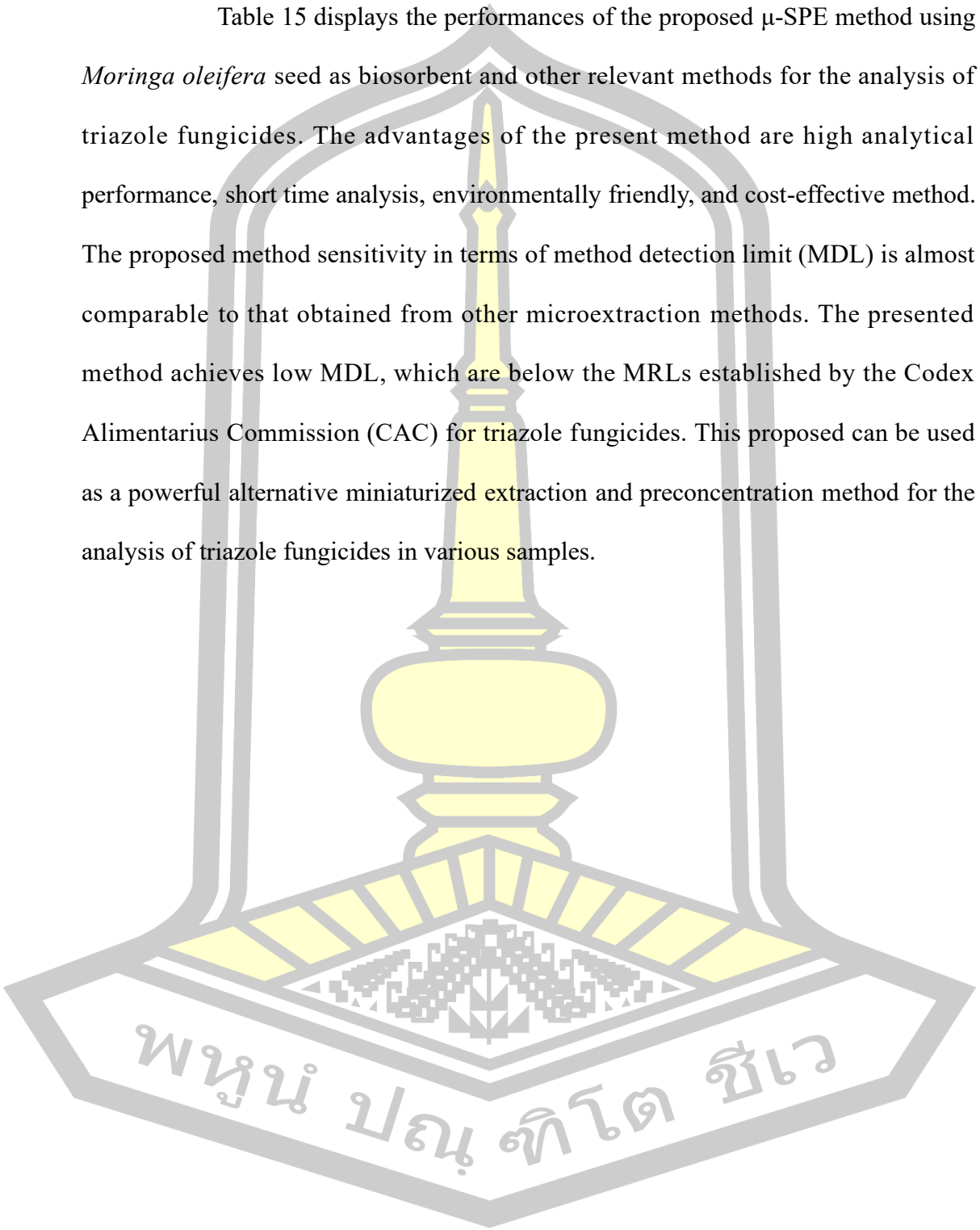

Table 15 Comparisons of the proposed method with other methods for the quantitation of triazole fungicides.

Extraction method	Sorbent	Amount of sorbent (g)	Extraction time (min)	Linear range (μg L^{-1})	Recovery (%)	LOD (μg L^{-1}or μg Kg^{-1})	EF	%RSD	Ref.
QuECHERS-LC-MS/MS	BCDP	NR	7	50-20000	76.1-103.4	0.05-0.1 μg Kg^{-1}	0.43-0.57	4.8-11.9	[190]
MSPE-HPLC-UV	Fe_3O_4@PC	0.05	6	1-1200	82.8-113.2	0.2-0.3	281-283	1.2-4.6	[191]
HS-SPME-GC-MS	PIL	2.00	95	5-1500 ng g^{-1}	83-114	0.06-2.00 ng g^{-1}	NR	NR	[192]
SBSE-HPLC-DAD	HC-POF	0.05	50	0.1-500	80.7-111	0.022-0.071	49-57	6.4-12.4	[193]
MSPE-GC-FID	MOPs	5.00	20	0.5-200	84.7-117	0.12-0.19	845-903	2.6-6.8	[194]
SB-μ-SPE-GC-MS	$10N_3$-Ph-SBA15	0.02	35	1-600	88.5-99.2	0.23-0.37	NR	2.3-7.5	[195]
SPME-HPLC-DAD	GO-poly-3-aminophenol	0.03	15	0.5–100	95.2-98.0	LOQ: 0.2-0.4	190-196	2.8-4.2	[196]
MSPE-LC-MS/MS	m-MWCNTs-NH_2	0.075	16	0.001-0.5	80.3-106.3	0.08-2.04 ng g^{-1}	0.45-0.60	2.1-13.4	[197]
μSPE- HPLC-PDA	Biosorbent (*Moringa oleifera*)	0.10	12	90-500	70 - 116	30-50	8-11	≤ 5	**This work**

*NR: Not Reported

** QuECHERS-LC-MS/MS; Quick, Easy, Cheap, Effective, Rugged, and Safe-Liquid chromatography tandem mass spectrometry, MSPE-HPLC-UV; Magnetic solid-phase extraction-high performance liquid chromatography-ultraviolet detector, HS-SPME-GC-MS; headspace solid-phase microextraction-gas chromatography, SBSE-HPLC-DAD; stir bar sorption extraction-high performance liquid chromatography-diode array detector, MSPE-GC-FID; Magnetic solid-phase extraction- gas chromatography-flame ionization detector, SB-μ-SPE-GC-MS; stir bar-supported micro-solid-phase- gas chromatography-mass spectrometry, SPME-HPLC-DAD; solid phase micro extraction-high performance liquid chromatography-diode array detector, MSPE-LC-MS/MS; Magnetic solid-phase extraction-Liquid chromatography tandem mass spectrometry, μSPE- HPLC-PDA; micro solid phase extraction-high performance liquid chromatography-photo diode array detector.

*** BCDP; Bridged bis(β-cyclodextrin)-bonded chiral stationary phase, Fe_3O_4@PC; Magnetic porous carbon, PIL; Polymeric ionic liquid, HC-POF; Hydroxyl-containing porous organic framework, MOPs; Magnetic porous organic polymers, $10N_3$-Ph-SBA15; 4-phenyl-1,2,3-triazole functionalized mesoporous silica SBA-15, GO-poly-3-aminophenol; Graphene oxide-poly 3-aminophenol, m-MWCNTs-NH_2; Magnetic amino modified multiwalled carbon nanotubes.

4.2 Surfactant modified coconut husk fiber as a green alternative sorbent for micro-solid phase extraction of triazole fungicides at trace level in environmental water, soybean milk, fruit juice, and alcoholic beverage samples

This chapter presents the results obtained and describes the development of the extraction method prior to its application in high-performance liquid chromatography (HPLC). The studied triazole fungicides including myclobutanil, triadimefon, tebuconazole, hexaconazole, and diniconazole were used as model compounds. The second section evaluates the analytical performance of the proposed method. Finally, the method is applied to analyze triazole fungicide residues in environmental water, soybean milk, fruit juices, and alcoholic beverage samples. The findings are thoroughly discussed.

4.2.1 Characterization of the biosorbent

Fourier-transformed infrared (FTIR) spectra were used to detect when the structure of cellulose, hemicellulose, and lignin of coconut husk fiber changed after the pretreatment method. The FTIR spectra of CHF, CHF-adsorption and CHF-desorption are illustrated in Figure 21 (a, b, and c), respectively. The similarities of cellulose fiber (as shown in Figure 21) indicated that there were no significant changes in the structure of the coconut husk fiber before and after pretreatment. The absorption bands are observed in two wave number regions of 3660-2900 cm^{-1} and 1630-900 cm^{-1}. The presence of peaks on the spectra of cellulose samples coming from CHF corresponds to bands of microcrystalline cellulose (as shown in Figure 21(a)). In contrast, differences in absorption band intensities and the appearance of new peaks in spectra of CHF-adsorption are observed. Identification of the absorption bands is ensured. The attended peaks in the wave number range of 3660-2900 cm^{-1} are

characteristic of the stretching vibration of O-H and C-H bonds in polysaccharides. The broad peak at 3331 cm^{-1} is characteristic of the stretching vibration of the hydroxyl group in polysaccharides [198]. This peak also includes inter- and intra-molecular hydrogen bond vibrations in cellulose [199]. The band at 2895 cm^{-1} is referred to CH stretching vibration of all hydrocarbon ingredients in polysaccharides [200]. But the peak of -CH stretching of hydrocarbon in polysaccharides does not appear in CHF-adsorption and CHF-desorption spectra because a biosorbent coated by surfactant when passing through the adsorption and desorption process interaction between functional group on CHF surface with target analytes have changed.

Typical bands entrusted to cellulose were inspected in the region of 1630-900 cm^{-1}. The peaks located at 1636.07 cm^{-1} correspond to the vibration of water molecules absorbed in cellulose [198]. The absorption bands at 1428, 1367, 1334, 1027 cm^{-1} and 896 cm^{-1} belong to stretching and bending vibrations of $-CH_2$ and -CH, -OH and C-O bonds in cellulose [201]. In the same way, CHF-adsorption, and CHF-desorption in this procedure show that the adsorption bands shifted at 987.68, 932.01, and 598.42 cm^{-1}. Desorption bands shifted at 1114.14, 1016.35, 931.91, and 596.25 cm^{-1} belong to stretching and bending vibrations of $-CH_2$ and -CH, -OH, and C-O bonds, respectively in cellulose due to the pretreatment, adsorption, and desorption process. The band at around 1420-1430 cm^{-1} is associated with the amount of the crystalline structure of the cellulose, while the band at 897 cm^{-1} is assigned to the amorphous region in cellulose [202]. The peak as mentioned above appeared in the corresponding FTIR results of CHF biosorbent, CHF-adsorption, and CHF desorption.

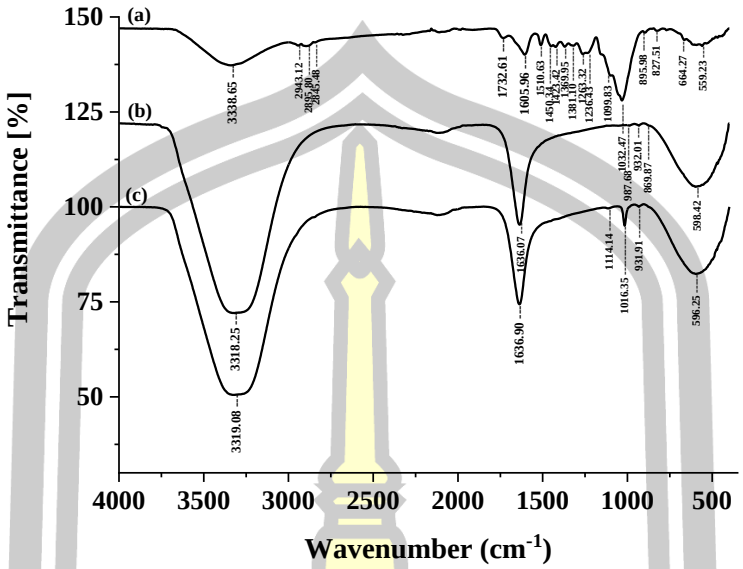

Figure 21 FTIR spectra of (a) coconut husk fiber (CHF), (b) SDS modified CHF after adsorption of triazole fungicide (100 µg L^{-1}), and (c) SDS modified CHF after desorption process.

SEM images of coconut husk fiber powder are shown in Figure 22. The SEM result presents the morphological properties of cellulose in CHF (Figure 22(a)) and after the adsorption process (Figure 22(b)). It exhibited that porosity can be observed along composite structure due to the µ-SPE procedure; the porosity can be formed by modification of the CHF-adsorption process. It was remarkable to note that the porous structure was affected by surfactant coated and adsorption of target analytes in microextraction procedure. The irregular size/shape and interconnected structure as channels were observed. It was important to note that the amount of pore and pore radius was reduced when they were replaced by triazoles in the adsorption procedure. In the desorption process as shown in Figure 22(c), it was found that the size, shape, and interconnected structure of CHF pores decreased.

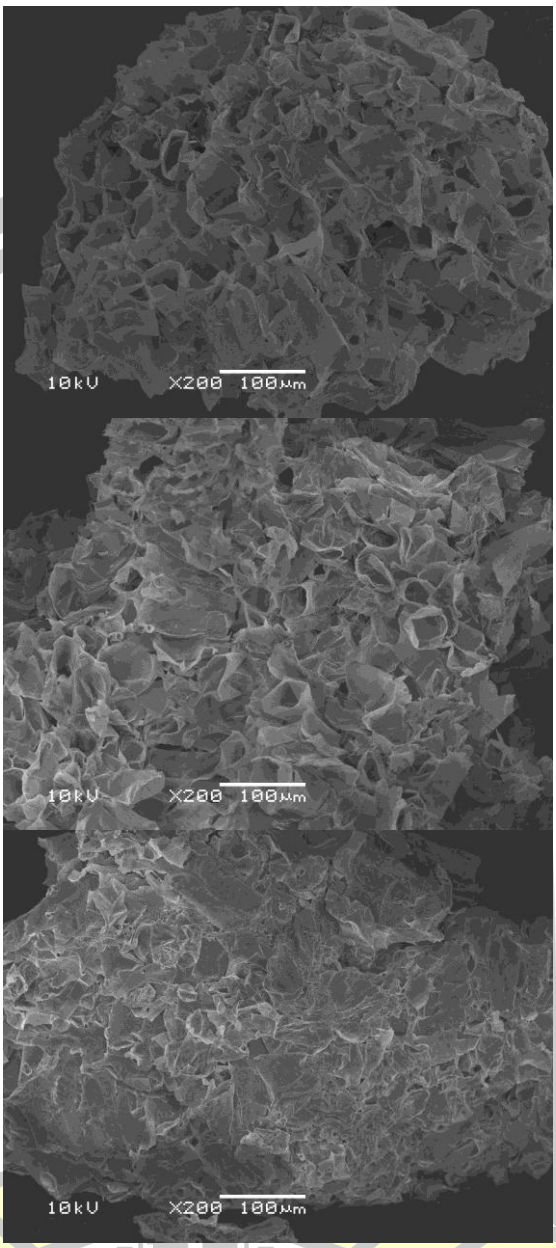

Figure 22 SEM images of (a) coconut husk fiber, (b) SDS modified CHF after adsorption with triazole fungicides (100 µg L^{-1} each) and (c) SDS modified CHF after the desorption process.

Transmission Electron Microscopy (TEM) are also studied. The TEM image for coconut husk fiber powder without adsorption procedure (as shown in Figure 23(a)) showed the microparticles of coconut husk fiber powder as sheet-shaped particles. The images of the TEM for coconut husk fiber powder after the adsorption procedure (Figure 23(b)) with triazole fungicides (100 µg L^{-1} each) are seen as tiny spherical particles clinging to the sheet-shaped particles of fiber structure in CHF. In the desorption procedure, some parts of CHF surface powder, and triazole particles disappeared due to the desorption effect as shown in Figure 23(c).

(a)

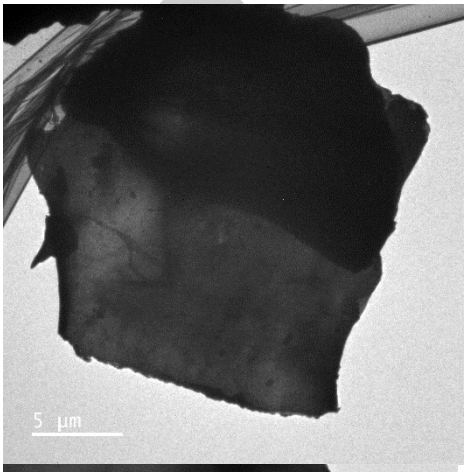

(b)

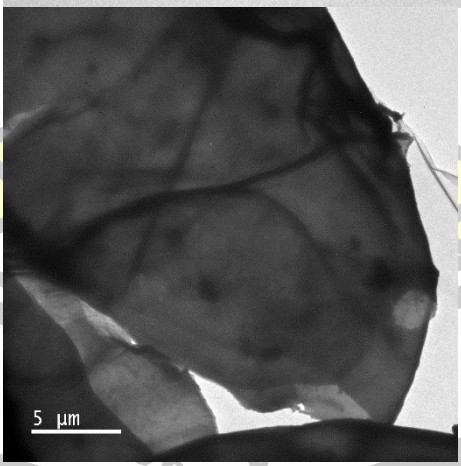

(c)

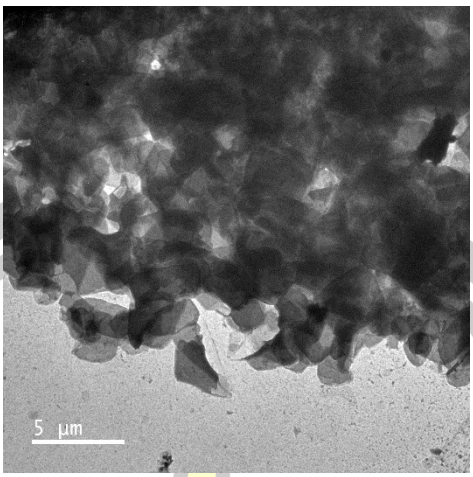

Figure 23 TEM images of (a) coconut husk fiber, (b) SDS modified CHF after adsorption with triazole fungicides (100 µg L^{-1} each) and (c) SDS modified CHF after desorption process.

4.2.2 Optimization of µ-SPE conditions

Some important parameters were investigated including the amount of biosorbent, kind and concentration of surfactant, kind and volume of desorption solvent and extraction time. Thus, the µ-SPE procedure required to optimize and obtain the optimal extraction conditions. In this section, the optimization was carried out on an aqueous solution containing 100 µg L^{-1} of each analyte. The parameters were modified by modifying one at a time while keeping the remaining constant.

4.2.2.1 Effect of amount of coconut husk fiber (CHF)

One of the most important parameters of the µ-SPE procedure is to determine the effective amount of the biosorbent. To obtain a high extraction efficiency, amounts of CHF (30-1000 mg) were investigated. As illustrated in Figure 24, when 30-300 mg the extraction efficiency in terms of the peak area of all triazoles increased with increasing CHF amount and reached the maximum at 100 mg. And then, the peak area of triazoles decreased. This might be that an increase in the amount

of biosorbent could be the absorbent trend to aggregation, which led to a negative effect on the binding site between the CHF and the target analytes. Therefore, 100 mg of CHF was employed in the further experiment.

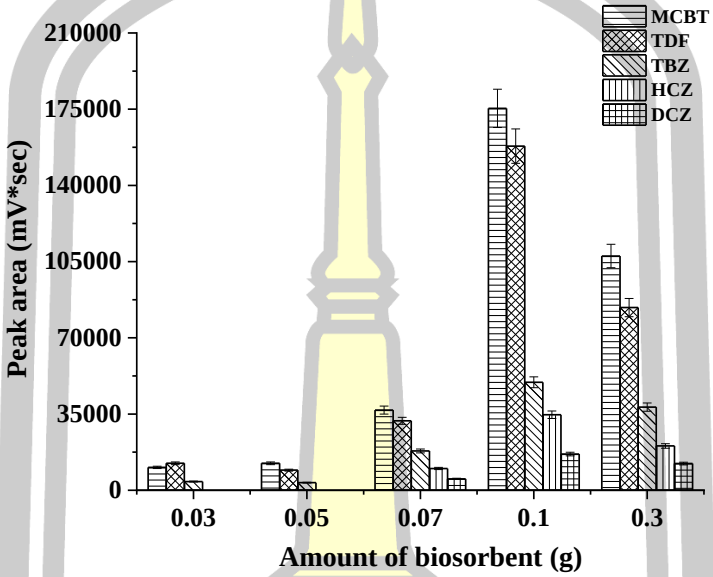

Figure 24 Effect of the amount of biosorbent (coconut husk fiber, g). Conditions: 0.1 g of CHF; 150 µL of 10 mM SDS, vortex adsorption time 20 sec and vortex desorption time 10 sec; centrifuge adsorption and desorption process at 3500 rpm for 5 min; 150 µL of methanol (sample volume 10 mL, 100 µg L^{-1} of each triazole fungicides).

4.2.2.2 Effect of surfactant as modifier and pH on adsorption

Surfactant molecules have a polar and non-polar moiety, so they can dissolve in water as monomers or be incorporated with other molecules to form a micelle [174]. The surfactants could be adsorbed to the surface of biosorbent through attractive electrostatic interactions resulting in the formation of monolayers of adsorbed surfactant termed hemimicelles. After that, hydrophobic interactions between hydrocarbon chains of surfactant molecules result in the formation of admicelles

[201]. In term of hemimicelles, the hydrophobic tails are exposed to aqueous solution, so the surfactant-coated biosorbent surface will become hydrophobic, which favors the adsorption of non-ionic organic compounds onto the sorbents. Since possessing larger special areas and more ion-exchangeable OH groups on surface, modified biosorbent are expected to have obvious advantage for the sorption of ionic surfactant, and behave remarkable adsorption capability to organic compounds correspondingly [202]. Various surfactants, the cationic CTAB, and non-ionic Triton X-114, apart from the anionic SDBS and SDS, were evaluated. The percentage of each surfactant used was calculated by considering their respective critical micelle concentrations (CMC). The CMC refers to the concentration above which a surfactant forms micelle [174], depends on various factors. In this case, the concentration chosen of SDS, CTAB, SDBS, and Triton X-114 as additives were slightly below their corresponding CMC values (8.2 mM, 1.0 mM, 0.61, and 0.24 mM, respectively). The results in Figure 25 shows that SDS was the most effective in enhancing the extraction performance of CHF biosorbent. SDS coated on CHF biosorbent, with its polar group protruding towards the aqueous phase [203], assisted to reduce the surface tension between the hydrophobic CHF biosorbent and the solution surface. Therefore, triazole molecules dissolved in the solution were effectively closer to the sorbent. Additionally, the zero point of charge (zpc) of CHF occurs at about pH 5-6. In other words, CHF surface is positively charged at acidic conditions (pH < 6), whereas it is negatively charged in a more alkaline media (pH > 6). CHF surface must be positively charged to adsorb any anionic surfactant through ionic interaction [204]. Which, all the cycle of the triazole is positively charged and the positive poles are the atoms of carbon and hydrogen causing a desirable electrostatic attraction between the SDS on the CHF surface and

protonated analytes resulting in improved extraction efficiency of the analytes. The other three surfactants did not share this advantage provided by SDS.

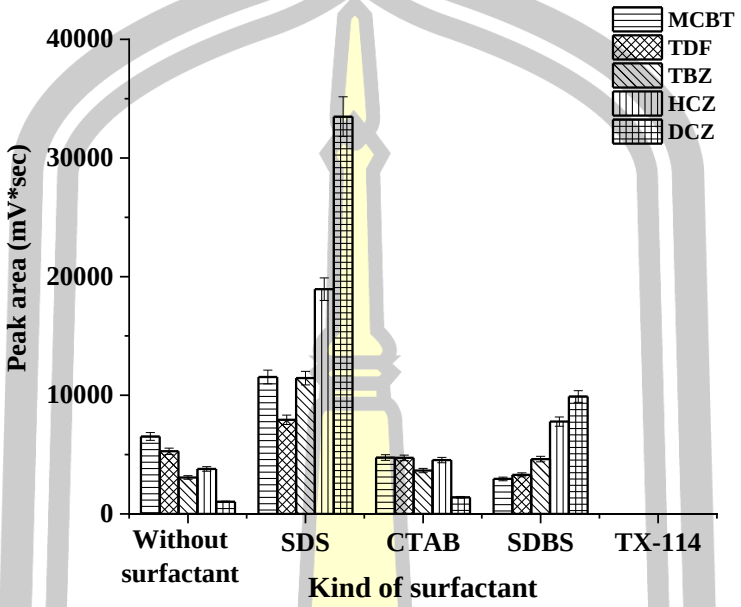

Figure 25 Effect of kind of surfactant.

Conditions: 0.1 g of CHF; 150 µL of 10 mM SDS, vortex adsorption time 20 sec and vortex desorption time 10 sec; centrifuge adsorption and desorption process at 3500 rpm for 5 min; 150 µL of methanol (sample volume 10 mL, 100 µg L^{-1} of each triazole fungicides).

The concentration of SDS functionalized on CHF was explored at concentrations below and above the CMC level (between 0.5 and 30 mmol L^{-1}) to determine the optimum interaction with CHF for the most suitable extraction performance. As illustrated in Figure 26, the extraction efficiencies of triazole fungicides generally increased when 1-10 mmol L^{-1} of SDS were used and decreased when the concentration of SDS was higher than 10 mmol L^{-1}. Thus, 10 mmol L^{-1} of SDS was the optimum concentration of surfactant required to functionalize the CHF

biosorbent. The reason for such trends to be observed was largely due to the change of interaction between SDS and the studied triazoles, as the concentration of SDS was increased. Below the CMC level (5 mmol L^{-1} of SDS), the extraction efficiency in terms of peak area decreased, mainly due to the slight electrostatic attraction. It was therefore estimated that 10.0 mmol L^{-1} of SDS was the most suitable concentration.

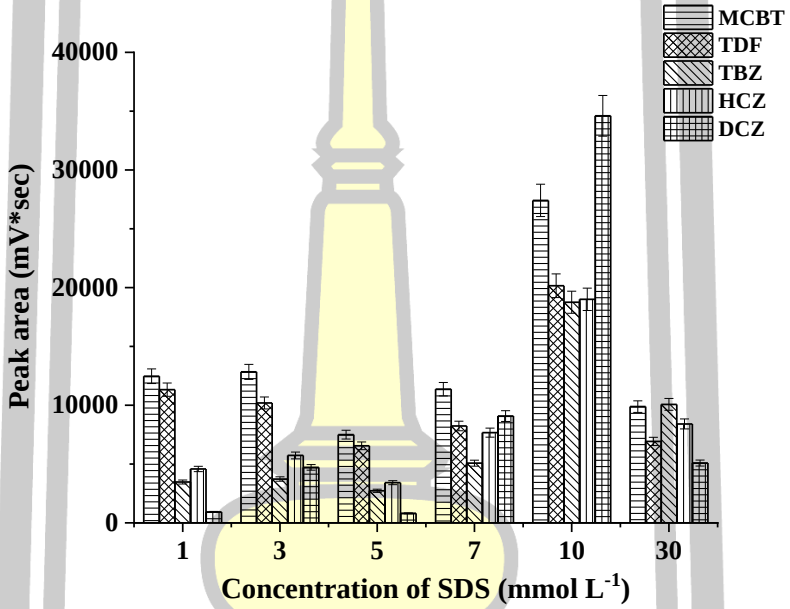

Figure 26 Effect of concentration of SDS (mmol L^{-1}).

Conditions: 0.1 g of CHF; 150 µL of 10 mmol L^{-1} SDS, vortex adsorption time 20 sec and vortex desorption time 10 sec; centrifuge adsorption and desorption process at 3500 rpm for 5 min; 150 µL of methanol (sample volume 10 mL, 100 µg L^{-1} of each triazole fungicides).

The effect of SDS volume was studied in the range of 30-250 µL using a concentration of 0.10 mmol L^{-1} of SDS. It was found that the highest peak area was obtained for all triazoles using an SDS volume of 150 µL (Figure 27). At higher volumes than 150 µL, the peak areas of all the analytes slightly decreased. Therefore, 150 µL of SDS was selected for further experiments.

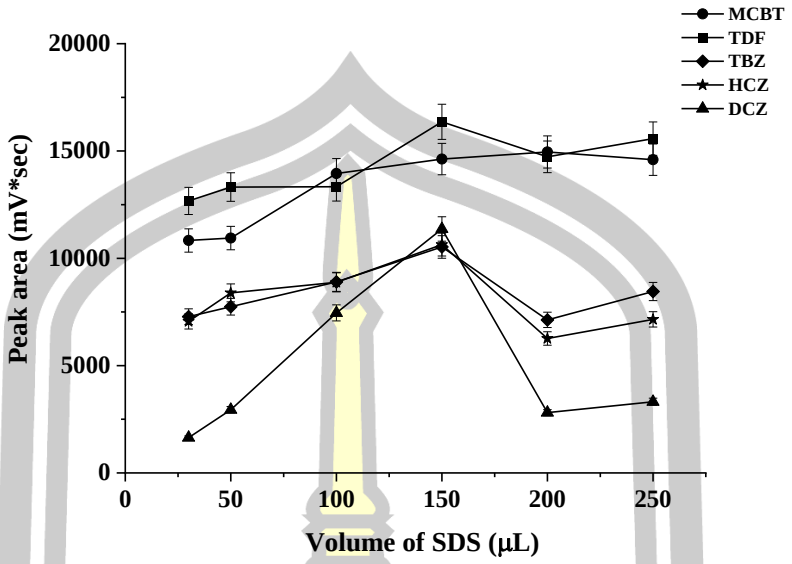

Figure 27 Effect of volume of SDS (µL).

Conditions: 0.1 g of CHF; 150 µL of 10 mmol L^{-1} SDS, vortex adsorption time 20 sec and vortex desorption time 10 sec; centrifuge adsorption and desorption process at 3500 rpm for 5 min; 150 µL of methanol (sample volume 10 mL, 100 µg L^{-1} of each triazole fungicides).

4.2.2.3 Effect of sample volume

Sample volume is one of the most important factors to be investigated because it determines the extraction efficiency of the method. The effect of sample volume on the extraction efficiency was varied in the range of 5.00-15.00 mL (data not shown). The peak areas of the analytes increased with an increase of the sample volume from 3.00 to 10.00 mL and then decreased with further increase of sample volume. Therefore, the sample volume of 10.00 mL was utilized in the subsequent experiments.

4.2.2.4 Effect of kind and volume of desorption solvent

To obtain high desorption efficiency of triazole fungicides from CHF biosorbent, an effective desorption solvent should be selected. Reasonable desorption solvent is helpful to desorb the target TFs from the extraction bio-material in a short time. To improve the accuracy of the experiment, four typical organic solvents such as acetonitrile, methanol, ethanol, and isopropanol were compared. The results in Figure 28 indicated that methanol achieved a higher desorption ability than other desorption solvents for the target triazole fungicides. Therefore, methanol was used as the desorption solvent for further experiments.

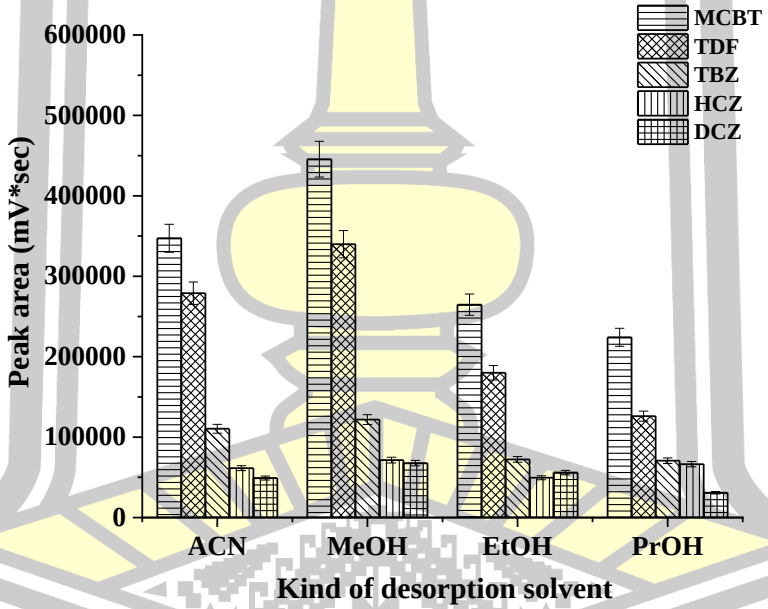

Figure 28 Effect of kind of desorption solvent.

Conditions: 0.1 g of CHF; 150 µL of 10 mmol L^{-1} SDS, vortex adsorption time 20 sec and vortex desorption time 10 sec; centrifuge adsorption and desorption process at 3500 rpm for 5 min; 150 µL of methanol (sample volume 10 mL, 100 µg L^{-1} of each triazole fungicides).

The volume of the desorption solvent should be attentively optimized as it can have a significant effect on the results of sensitivity and reproducibly in microextraction method. The desorption volume (30, 50, 100, 150, 200 and 250 µL) was also optimized (Figure 29) to ensure high desorption efficiency of studied fungicides. It was found that, low volume of methanol 30 µL wasn't sufficient for desorb of target fungicides. After that the peak area constantly increased with increasing the volume of desorption solvent, the full desorption of all target fungicides was achieved by 150 µL. When the volume of methanol more than 150 µL, the peak area of fungicides decreased due to the dilution effect. As a result, methanol 150 µL was selected.

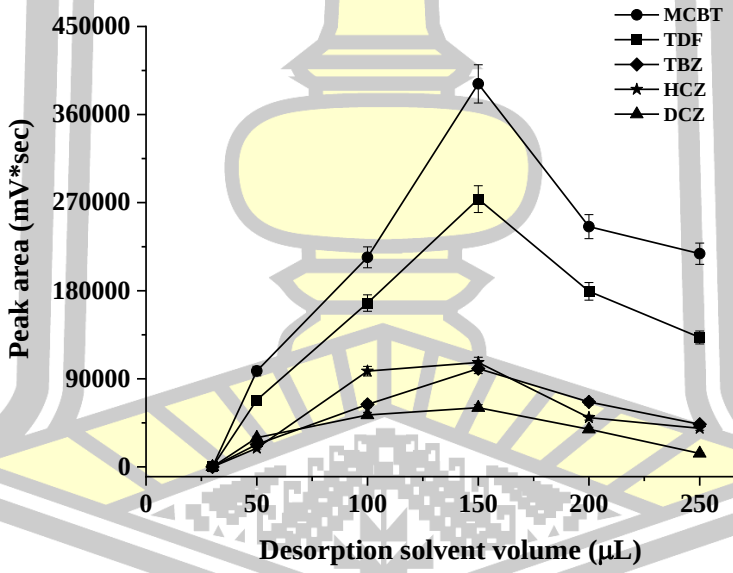

Figure 29 Effect of desorption volume (µL).

Conditions: 0.1 g of CHF; 150 µL of 10 mmol L^{-1} SDS, vortex adsorption time 20 sec and vortex desorption time 10 sec; centrifuge adsorption and desorption process at 3500 rpm for 5 min; 150 µL of methanol (sample volume 10 mL, 100 µg L^{-1} of each triazole fungicides).

4.2.2.5 Effect of adsorption time

In μ-SPE procedure is a stable-based technique, and the institution of equilibrium invests the rate of mass transfer along with the extraction time. Contributing an adequate contact time between the target analytes and biosorbent to reach an adsorption equilibrium is important. The rate of mass transfer can be increased by vortex, and equilibrium can be obtained in an approximately shorter time. Vortex and centrifuge were other important parameters that could affect the separation of TFs from biosorbent particles. The time of vortex adsorption was investigated between 0 and 30 sec. The results exhibited that when the vortex time was up to 20 sec, extraction efficiency in terms of peak area was improved after which it gradually decreased. As can be seen in Figure 30, 20 sec was selected as the optimal vortex time adsorption.

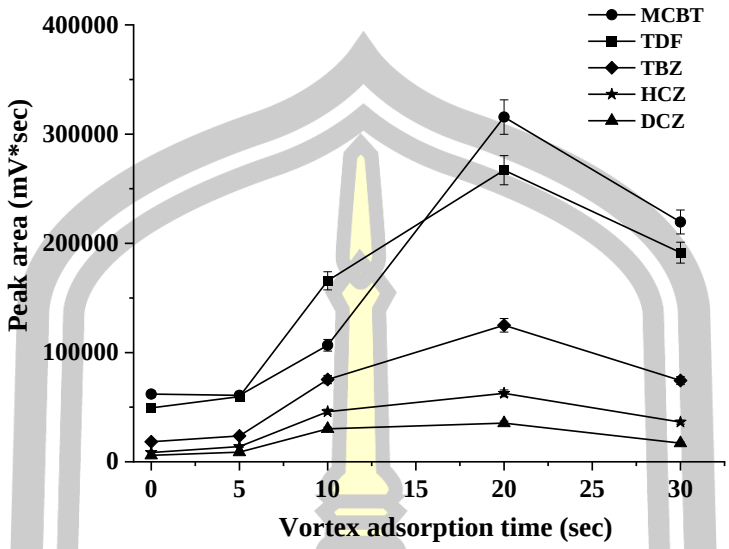

Figure 30 Effect of vortex time adsorption (sec).

Conditions: 0.1 g of CHF; 150 µL of 10 mmol L^{-1} SDS, vortex adsorption time 20 sec and vortex desorption time 10 sec; centrifuge adsorption and desorption process at 3500 rpm for 5 min; 150 µL of methanol (sample volume 10 mL, 100 µg L^{-1} of each triazole fungicides).

The centrifugation rate and time were varied in the range of 1500-4500 rpm and 3-10 min, respectively. It was found that these parameters were effective (data not shown) so 3500 rpm and 5 min were selected as centrifugation rate and time, respectively.

4.2.2.6 Effect of desorption time

The effect of desorption time on extraction efficiency was evaluated by varying the vortex time from 0 to 30 sec as shown in Figure 31. It was found that the extraction efficiency increases in terms of peak area with the increase of time from 0 to 10 sec. There was a slight change when vortex time desorption was over 10 sec. The centrifugation rate and time of desorption were varied in the range of

1500-4500 rpm and 3-10 min, respectively. It was found that these parameters were effective so 3500 rpm and 5 min were selected as centrifugation rate and time, respectively. Therefore, an optimum vortex time (10 sec), centrifugation rate (3500 rpm), and centrifugation time (5 min) of desorption was acceptable for further experiments.

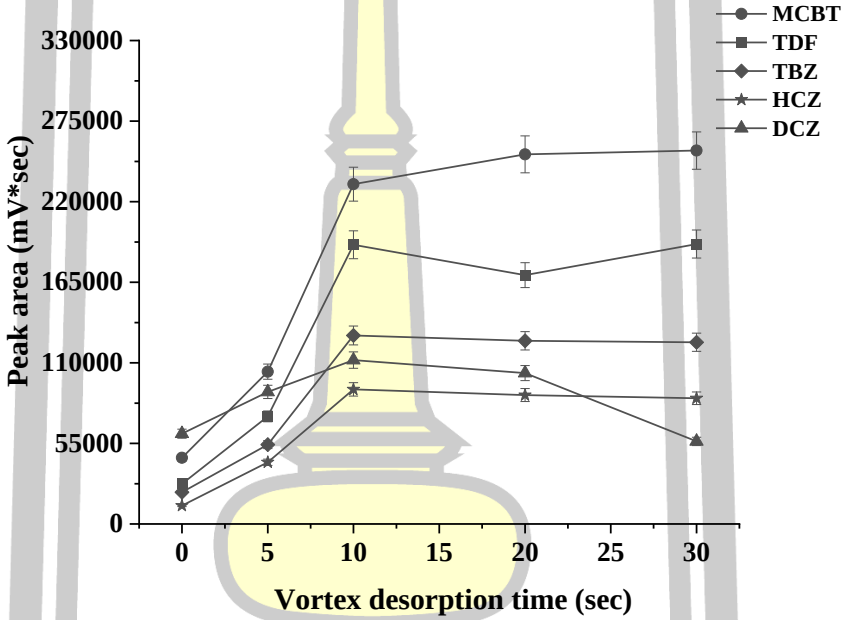

Figure 31 Effect of vortex time desorption (sec).

Conditions: 0.1 g of CHF; 150 µL of 10 mmol L^{-1} SDS, vortex adsorption time 20 sec and vortex desorption time 10 sec; centrifuge adsorption and desorption process at 3500 rpm for 5 min; 150 µL of methanol (sample volume 10 mL, 100 µg L^{-1} of each triazole fungicides).

4.2.2.7 Stability and reusability

To assess the stability of SDS on CHF which was evaluated in terms of reproducibility of the production procedures for eleven triazoles across six different batches. The percentage of RSD were calculated (data not shown), and the

findings show high accuracy, with RSDs less than 8.1%. These favorable results indicate that the suggested SDS on CHF sorbent can be used to extract all the triazoles under investigation.

The reusability of the prepared surfactant modified coconut husk fiber was studied by using an aqueous solution containing mixed TFs standard solution (each TF of 100 µg L^{-1}). The sorbent was washed by methanol 5 times between the cycles and then dried for the next SPE cycle (data not shown). It was found that the peak area of TFs had a significant decrease after 3 SPE cycles, indicating that the prepared sorbent could be reused at least 3 times (data do not show). Extraction efficiency in terms of peak area decreased thereafter because the sorbent was destroyed. This indicates that sorbent possesses excellent reusability as an efficient adsorbent.

4.2.2.8 Adsorption mechanism of CHF sorbent

The adsorption mechanism (as shown in Figure 32) was used to estimate the capability of the proposed method. Mechanisms appear as a function of the physicochemical properties of the lignocellulosic in CHF sorbent and the interaction in a sample aqueous solution. These properties can be estimated as a function of surface charge, solubility, hydrophobicity, chemical components, reactivity, and molecular size [205]. Individual properties are specified, and the sorption mechanism of interaction between CHF sorbent or while the appearance of struggle between the mechanisms targets TFs, which have different closeness with active sites of sorbents, thus it is essential to examine the entail mechanism. Important factors that influence the adsorption mechanism include (i.) types and amounts of lignocellulosic sorbent material, (ii.) the chemistry of target analytes solution, and

(iii.) environmental conditions [206]. Functional groups on CHF surfaces of lignocellulosic materials can cooperate with functional groups of TFs in several modes. The adsorption capacity of CHF can be ascribed to carboxylic, hydroxyl and phenolic functional groups exhibited in hemicellulose and lignin. However, the dominant adsorption mechanism in this study is hydrophobic interaction. Hydrophobicity plays a crucial role in the adsorption process, as nonpolar interactions between the CHF sorbent surface and target analytes facilitate the sorption process. The introduction of hydrophobic regions on the CHF surface enhances its affinity for nonpolar organic compounds, leading to increased adsorption efficiency.

Surfactants are amphiphilic compounds, which contain a nonpolar hydrocarbon chain bonded to a polar group (anionic, cationic, neutral, or zwitterionic) [207]. They are used in extraction methods including liquid-liquid extraction and solid-phase extraction. In the solid-phase extraction procedure, surfactants are used to increase the dispersion of sorbent particles in the bulk solution or to enhance the sorption ability on the surface of the solid material to increase the extraction properties of the sorbent. Overall, surfactants in extraction processes significantly improve the efficiency and selectivity of the procedures, as well as the solubility of the compounds, resulting in higher extraction recovery of the analytes and cost-effective sample preparation. Hydrophobic interactions primarily drive the adsorption of nonpolar TFs onto CHF sorbents. The introduction of surfactants, particularly nonionic surfactants, leads to an increase in the hydrophobicity of the CHF surface, thereby enhancing the sorption of nonpolar compounds. In this process, surfactants modify the surface properties of CHF, promoting the adsorption of hydrophobic molecules through van der Waals forces and hydrophobic attraction. The modified CHF surface creates an

environment that favors the partitioning of nonpolar TFs, increasing the extraction efficiency.

Moreover, the addition of the surfactant greatly influences the extraction efficiency by promoting the mass transfer of analytes into the organic phase [209]. Nonionic and ionic surfactants with different hydrophilic-lipophilic balance (HLB) values measure the degree of their hydrophilicity or lipophilicity. The surface of modified CHF becomes more hydrophobic, which enhances the adsorption of non-ionic organic compounds onto the sorbents. As a result, the extraction efficiency is significantly improved due to the strengthened hydrophobic interactions between the sorbent and the target analytes.

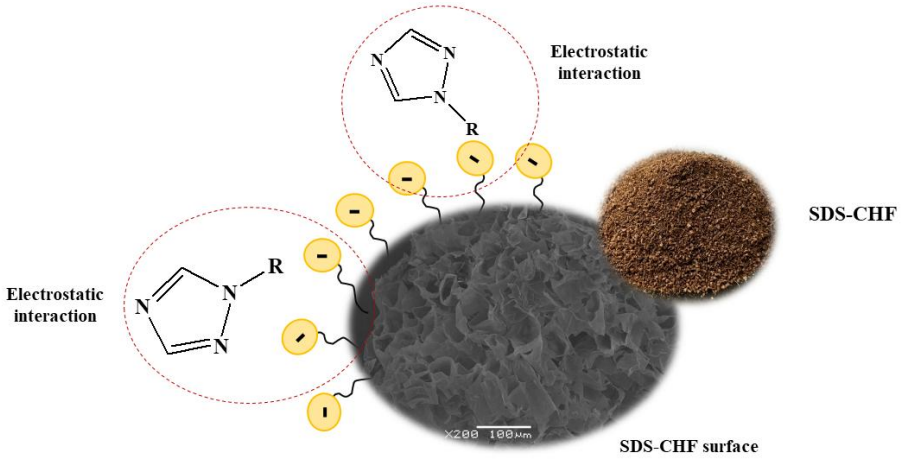

Figure 32 The modification process of SDS modified CHF involved the proposed reaction mechanism.

4.2.2 Evaluation of analytical method

To validate the analytical performance of the proposed method, the analytical aspects of the method consisting of linearity, correlation coefficients, extraction efficiency (EF), the limit of detection (LOD), and limit of quantification (LOQ) were evaluated under the optimum conditions. The results are summarized in Table 16. The proposed method provides a good linarite of the five triazole fungicides were observed in the range 9-300 μg L^{-1} for myclobutanil, triadimefon, tebuconazole, and 30-300 μg L^{-1} hexaconazole, diniconazole with a coefficient for determination of greater than 0.99. LODs and LOQs were calculated based on signal to noise (S/N) of 3, and 10, respectively. LODs and LOQs of five triazole fungicides were obtained in the range from 3.00 to 10.00 μg L^{-1} and from 9.00 to 30.00 μg L^{-1}, respectively. The precision of the proposed method was invented by testing inter-day and intra-day variations. The inter-day values were evaluated by five replicates at two concentrations (50 and 100 μg L^{-1}) in the same day, and the obtained relative standard deviation (RSD) values were in the range from 1.96 to 4.38%. The intra-day precision values were measured on three ensuring days with RSD values in the range from 0.63 to 4.25%. Good precision with RSDs were less than 5.0%. The enrichment factor (EF), defined as the concentration ratio of the analytes in the settled phase (C_{set}) later the sedimented phase is diluted with 150 μL of ethanol and in the aqueous sample (C_0), ranged from 2.7-34.9 folds. Chromatograms of the studied triazole fungicides obtained from direct HPLC and preconcentrated by the proposed microextraction method are shown in Figure 33.

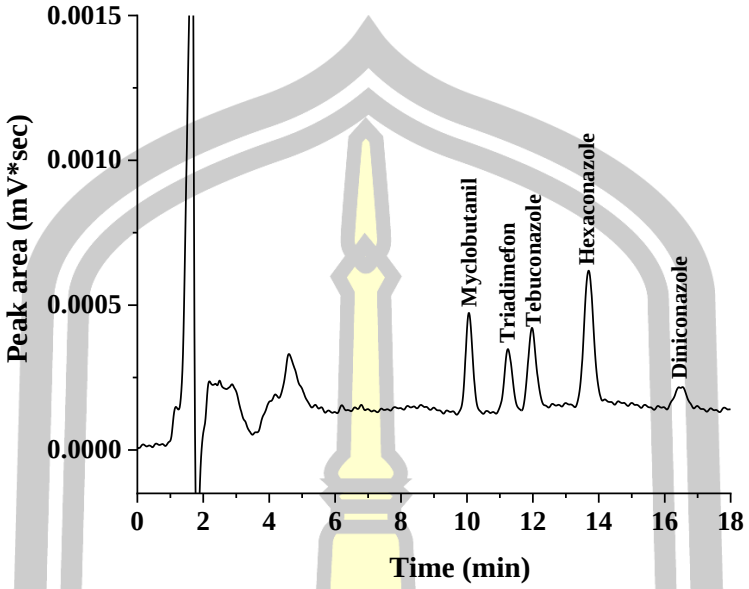
0.0015
0.0010
0.0005
0.0000
Peak area (mV*sec)
Myclobutanil
Triadimefon
Tebuconazole
Hexaconazole
Diniconazole
0
2
4
6
8
10
12
14
16
18
Time (min)

(a)

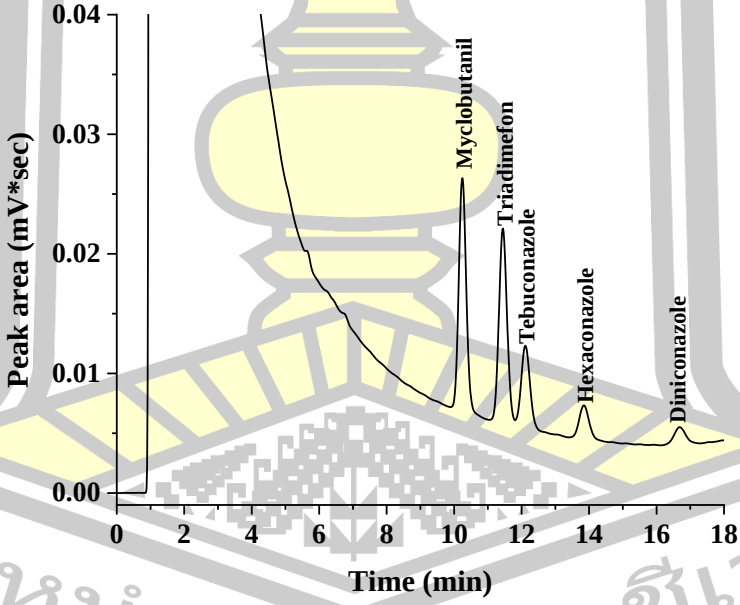
0.04
0.03
0.02
0.01
0.00
Peak area (mV*sec)
Myclobutanil
Triadimefon
Tebuconazole
Hexaconazole
Diniconazole
0
2
4
6
8
10
12
14
16
18
Time (min)

(b)

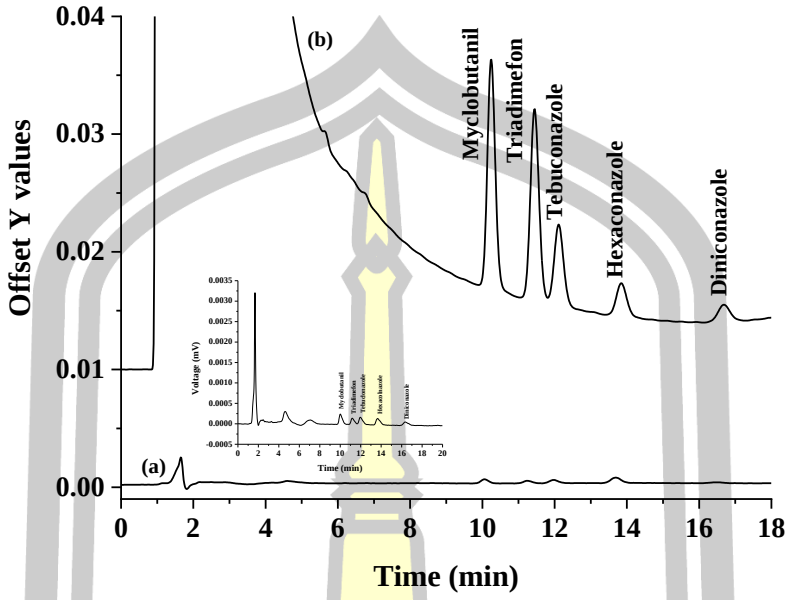

(c)

Figure 33 Chromatograms of standard triazole fungicides were obtained by (a) without preconcentration, (b) with micro solid phase extraction using SDS modified CHF, and (c) overlaid chromatograms of standard triazole fungicides: concentration of all standards was 100 µg L^{-1}.

Table 16 Analytical characteristics of the standards triazole fungicides (n=3).

Analyte	Linear range ($\mu g\ L^{-1}$)	Linear equation	R^2	LOD ($\mu g\ L^{-1}$)	LOQ ($\mu g\ L^{-1}$)	Intra-day precision[a] (n=5), RSD (%)		Inter-day precision[a] (n=5), RSD (%)		EF (C_{ex}/C_o)[b]
						t_R	Peak area	t_R	Peak area	
Myclobutanil	9-300	y = 389553x + 1864.5	0.9974	3	9	0.22	0.63	0.26	1.96	25.9
Triadimefon	9-300	y = 314270x + 1665.8	0.9964	3	9	0.25	0.99	0.28	2.30	34.9
Tebuconazole	9-300	y = 452574x + 105.21	0.9973	3	9	0.02	2.74	0.04	3.41	23.4
Hexaconazole	9-300	y = 387892x + 3273.1	0.9959	3	9	0.04	2.89	0.09	3.58	12.7
Diniconazole	9-300	y = 297186x + 6728.6	0.9973	3	9	0.16	4.25	0.20	4.38	2.7

[a] Precision were calculated at the concentration of 50 and 100 $\mu g\ L^{-1}$ of each triazole.
[b] Ratio of the concentration of the target analytes in extraction phase to the initial concentration in the original sample solutions.

4.2.3 Recovery studies and real sample analysis

The extraction of triazoles in different samples, including environmental water, fruit juice, soybean milk, and alcoholic beverage samples, was accomplished according to the developed μ-SPE method. A matrix-matched calibration approach was used to evaluate the matrix effect in real samples. A set of matrix-matched calibration curves was prepared using representative samples spiked with 9-30 μg L^{-1} of each triazole. The percentage of matrix effect (%ME) can be calculated by equation:

$$\%ME = (S_m/S_s) \times 100$$

where S_m and S_s are the slopes of the calibration curve in the matrix and solvent, respectively. Typically, a ME between 80 and 120% suggests that there are no matrix effects, a ME between 50 and 80% or 120 and 150% corresponds to minor matrix effects, and a ME less than 50% or greater than 150% involves major matrix effects [207]. It was found that minor MEs for environmental water and alcoholic beverage samples were observed, whereas major MEs were found in fruit juice, and soybean milk (data not shown).

To test the accuracy, samples spiked at three different concentration levels (9, 15, and 30 μg L^{-1}) were analyzed to determine the recoveries. The relative recoveries are summarized in Table 17. The acceptable relative recoveries (RR) were obtained in the 67.0-105% range with RSD in the range from 0.18 to 4.59%. Figure 34 and Figure 35 show the overlaid chromatograms of the beer sample and spike beer sample, soybean milk sample, and spiked soybean milk sample, respectively. The results demonstrated that the proposed method based on CHF-μ-SPE coupled with HPLC performances is accurate and dependable for the microextraction method and determination of triazole fungicides in real samples.

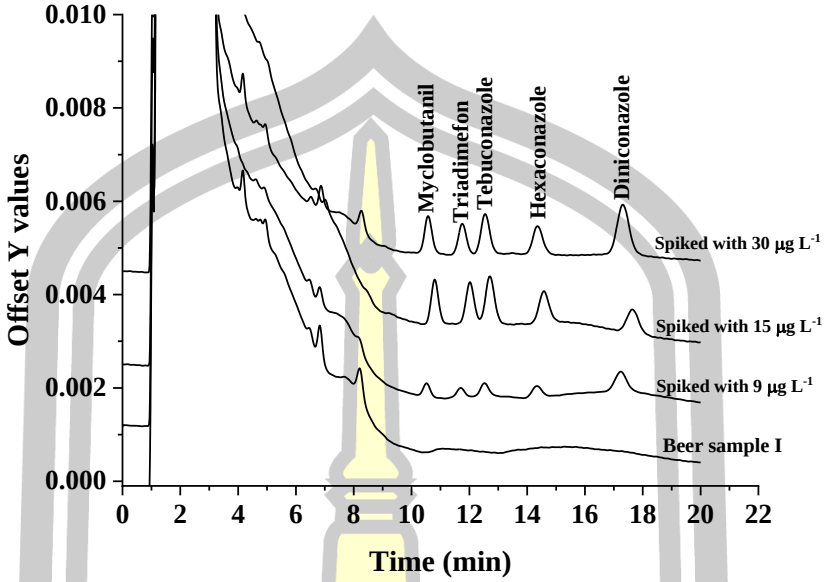

Figure 34 The overlaid chromatograms of the beer sample and spike beer sample.

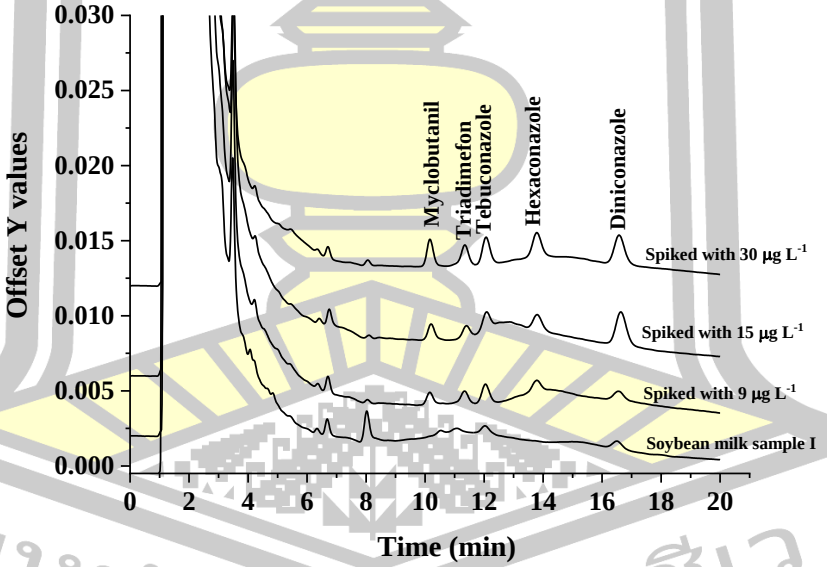

Figure 35 The overlaid chromatograms of the soybean milk sample and spiked soybean milk sample.

Table 17 Recovery obtained from the determination of studied triazoles in studied samples (n = 3).

Sample	Spiked ($\mu g\ L^{-1}$)	%Recovery at different spiked levels (%RSD, n=3)				
		MCBT	TDF	TBZ	HCZ	DCZ
Agricultural water I	9	91.6 (3.1)	71.5 (1.3)	86.9 (4.6)	73.1 (2.2)	73.2 (2.5)
	15	82.2 (1.5)	87.2 (2.5)	92.3 (1.4)	97.8 (1.0)	82.5 (1.3)
	30	86.2 (0.8)	90.9 (2.5)	80.1 (1.2)	76.1 (0.5)	72.1 (1.8)
Agricultural water II	9	72.5 (3.8)	81.9 (1.5)	83.2 (2.7)	73.2 (2.9)	97.1 (1.0)
	15	78.2 (2.8)	86.4 (2.4)	79.4 (3.7)	88.3 (1.9)	94.5 (1.6)
	30	96.3 (0.8)	94.2 (3.2)	92.5 (1.7)	94.6 (0.3)	97.5 (0.8)
Soybean milk I	9	76.9 (2.6)	97.5 (1.8)	78.7 (2.5)	72.6 (4.2)	79.9 (1.0)
	15	94.0 (2.6)	105.0 (1.3)	77.9 (0.2)	91.6 (2.2)	89.2 (2.0)
	30	100.2 (1.7)	105.7 (0.6)	86.1 (1.5)	80.9 (1.0)	87.7 (1.4)
Soybean milk II	9	71.7 (2.9)	66.6 (3.7)	67.0 (2.8)	76.7 (1.8)	81.8 (0.7)
	15	82.9 (2.0)	75.7 (3.1)	76.9 (0.8)	82.2 (1.6)	76.3 (0.9)
	30	84.4 (1.2)	83.9 (0.9)	89.4 (2.0)	92.8 (1.4)	91.4 (2.5)
Soybean milk III	9	70.1 (2.2)	68.9 (2.6)	67.8 (3.0)	70.5 (1.8)	95.8 (3.8)
	15	81.1 (2.8)	74.1 (3.1)	74.1 (3.4)	73.2 (2.4)	90.8 (1.1)
	30	89.4 (2.0)	92.8 (1.4)	91.4 (2.5)	93.2 (1.7)	80.9 (0.8)
Orange juice	9	81.9 (2.6)	80.4 (2.6)	90.9 (3.6)	81.5 (2.7)	90.2 (1.1)
	15	88.6 (2.9)	98.8 (2.8)	99.5 (1.5)	99.6 (1.9)	92.1 (0.6)
	30	91.2 (1.2)	101.7 (1.3)	99.8 (1.7)	92.2 (1.8)	99.2 (2.0)
Pomegranate juice	9	79.7 (4.1)	67.5 (3.1)	75.7 (4.0)	67.7 (1.6)	74.3 (3.7)
	15	84.8 (2.7)	86.4 (1.7)	88.9 (2.2)	83.9 (1.9)	83.9 (1.4)
	30	86.4 (0.5)	93.1 (1.9)	91.2 (1.6)	87.2 (0.8)	102.4 (1.7)
Beer I	9	82.3 (3.4)	70.8 (4.1)	76.0 (3.7)	73.1 (3.2)	74.4 (1.9)
	15	83.7 (2.0)	95.2 (2.2)	99.2 (2.7)	99.0 (1.0)	82.1 (0.3)
	30	91.9 (2.0)	96.2 (2.5)	95.1 (1.3)	97.5 (1.3)	102.9 (1.4)
Beer II	9	73.7 (1.8)	68.1 (2.2)	84.1 (3.8)	67.4 (0.9)	100.2 (2.3)
	15	99.5 (3.0)	86.2 (3.8)	92.7 (3.1)	101.2 (1.2)	98.8 (1.1)
	30	81.6 (2.5)	93.2 (1.0)	92.9 (0.6)	97.8 (1.4)	103.6 (1.3)
Red wine	9	68.9 (0.9)	68.1 (2.3)	71.8 (3.5)	68.9 (1.6)	73.2 (2.5)
	15	79.3 (2.2)	75.6 (3.6)	74.9 (4.5)	73.4 (2.7)	80.7 (0.8)
	30	81.3 (1.9)	78.2 (1.2)	75.9 (1.7)	71.4 (0.8)	102.4 (0.8)
White wine	9	68.6 (2.8)	68.9 (2.2)	67.8 (4.2)	67.8 (3.0)	72.5 (1.2)
	15	81.3 (2.0)	80.9 (3.1)	77.2 (3.6)	80.2 (2.3)	81.4 (1.5)
	30	88.0 (0.9)	90.1 (0.7)	90.2 (0.7)	76.9 (1.0)	101.7 (1.8)

4.2.4 Assessment of method greenness

To estimate the green standpoint of the proposed method, an analytical eco-scale evaluation tool was applied [210]. Briefly, the analytical eco-scale approach provides quantitative information regarding the greenness of the analytical method in terms of the type and number of reagents and solvents, instrument energy, occupational hazards, and waste generation. To determine the final eco-scale score, penalty points are allocated to each parameter, and the total penalty points are subtracted from 100. A set of penalty points (PPs) are used to assign the departure from ideal greenness. The PPs for hazardous chemicals can be determined by multiplying the sub-total PPs for a given quantity and the hazard. The ultimate AEC value can be calculated from "AEC = 100 − total PPs". The scores higher than >75 illustrate an ideal green, the scores between 50 and 75 are acceptable green, and the scores <50 are insufficient green method. The final score for this method is 74 and it can be acceptable as a green method [211]. The obtained results can be found in Table 18.

Table 18 The penalty points (PPs) for microextraction method for the determination of triazole fungicides in environmental water, soybean milk, fruit juice and alcoholic beverage samples.

Reagent	Penalty points (PPs)				
	Amount PP	**Hazard PP**	**Total PPs (Amount PP × Hazard PP)**	**Instrument**	**PPs**
ACN (<10 mL)	1	4	4	HPLC-UV	1
MeOH (<10 mL)	1	6	6	Occupational hazard	0
SDS (<10 mL)	1	6	6	Waste	5
TFA (<10 mL)	1	2	2	Centrifuge	1
				Vortex	1
Subtotal PP			18		8
Total PPs			26		
Analytical Eco-sale score (AEC)			74		

4.2.5 Comparison of the proposed method to other related methods

Table 19 exhibits the analytical performance of the established μ-SPE using surfactant modified coconut husk fiber as a biosorbent compared with other microextraction methods [212], [213], [214], [215], [216], [217] used to determine triazole fungicides in various samples when comparing the type of sorbent, amount of sorbent, kind and volume of desorption solvent, extraction time, instrument, limit of detection (LOD), and relative recovery (RR) values achieved. Another advantage of this preparation of CHF biosorbent in the proposed method is simple and rapid, there was no specific and expensive reagent involved in the reactions, while the previous study used some expensive, specific reagents which were difficult to synthesize. Some studies have used commercial sorbent that is easy to use but expensive. It is a good choice for the development of adsorbents under the principle of green analytical chemistry. In addition, the method provided favorable LOD and RR values. Consequently, the proposed μ-SPE using surfactant modified coconut husk fiber as a biosorbent was a simple, rapid, and efficient pretreatment method for the determination of triazole fungicides via HPLC-DAD.

Table 19 Comparisons of the proposed method with other methods for the quantitation of triazole fungicides.

Extraction method	Sorbent	Amount of sorbent (g)	Desorption solvent	Extraction time (min)	Linear range (µg L^{-1})	Recovery (%)	LOD	EF	%RSD	Ref.
SPME-HPLC-DAD	GO-poly-3-aminophenol	0.03	Methanol (5 mL)	15	0.5–100	95.2-98.0	LOQ: 0.2-0.4 µg L^{-1}	190-196	2.8-4.2	[206]
MSPE-GC-FID	MOPs	5.00	Ethyl acetate (400 µL)	30	0.5-200	84.7-117	0.12-0.19 µg L^{-1}	845-903	2.6-6.8	[151]
SBSE-HPLC-DAD	HC-POF	0.05	Acetonitrile (200 µL)	50	0.1-500	80.7-111	0.022-0.071 µg L^{-1}	49-57	6.4-12.4	[152]
QuECHERS-LC-MS/MS	BCDP	NR	Acetonitrile (20 mL)	7	50-20000	76.1-103.4	0.05-0.1 µg kg^{-1}	0.43-0.57	4.8-11.9	[218]
SPE-HPLC-MS/MS	Fe_3O_4-MWCNT@MOF-199	0.01	Acetonitrile: ammonium water (7:3 v/v, 4 mL)	20	5-500	63.1-90.3	0.25-1.83 µg L^{-1}	NR	0.06-6.1	[216]
PT-SPE-GC-FID	CAs	0.005	Acetonitrile (500 µL)	NR	0.24-200 mg kg^{-1}	81-119	0.08-16 mg kg^{-1}	NR	0.4-8.5	[215]
UA-dSPME-GC-FID	CMC/Zn (BDC)/GO	0.015	Ethanol (100 µL)	10	1-1000	83-86	0.3-1.5 ng mL^{-1}	419-426	3.4-7.3	[214]
µSPE-HPLC-DAD	Biosorbent (Coconut husk fiber)	0.1	Methanol (150 µL)	10	9-300	67-105	3.00-10.00 µg L^{-1}	2.7-25.9	<5	**This work**

*NR: Not Reported

** SPME-HPLC-DAD; solid phase micro extraction-high performance liquid chromatography-diode array detector, MSPE-GC-FID; Magnetic solid-phase extraction- gas chromatography-flame ionization detector, SBSE-HPLC-DAD; stir bar sorption extraction-high performance liquid chromatography-diode array detector, QuECHERS-LC-MS/MS; Quick, Easy, Cheap, Effective, Rugged, and Safe-Liquid chromatography tandem mass spectrometry, SPE-HPLC-MS/MS; Solid phase extraction- high performance liquid chromatography tandem mass spectrometry, PT-SPE-GC-FID; pipette-tip solid-phase extraction- gas chromatography-flame ionization detector, UA-dSPME-GC-FID; Ultrasonic assisted dispersive solid phase microextraction-gas chromatography-flame ionization detector.

*** GO-poly-3-aminophenol; Graphene oxide-poly 3-aminophenol, MOPs; Magnetic porous organic polymers, HC-POF; Hydroxyl-containing porous organic framework, BCDP; Bridged bis(β-cyclodextrin)-bonded chiral stationary phase, Fe_3O_4-MWCNT@MOF-199; Magnetic- multiwalled carbon nanotubes @metal organic framework-199, CAs; Carbon aerogels, CMC/Zn (BDC)/GO; Carboxymethylcellulose/Zn-based metal–organic framework/graphene oxide

4.3 Hydrophobic melamine sponge incorporated with carbon dots as a green sorbent for micro-solid phase extraction of triazole fungicide residues in edible fungi samples

This chapter presents the study results. The first section describes the development of the extraction method, which was optimized for subsequent analysis using high-performance liquid chromatography (HPLC). The study focused on triazole fungicides, including myclobutanil, triadimefon, tebuconazole, hexaconazole, and diniconazole. The second section evaluates the proposed method's analytical performance. Finally, the method is applied to determine triazole fungicide residues in edible fungi samples, and the findings are discussed.

4.3.1 Characterization of superhydrophobic melamine sponge incorporated with carbon dots

The as-prepared melamine sponge incorporated with carbon dots was characterized by Field emission scanning electron microscopy (FE-SEM), X-ray diffraction analysis (XRD), Fourier transform infrared spectroscopy (FTIR), nitrogen adsorption techniques, and the contact angle of a water droplet. The prepared melamine sponge incorporated with carbon dots was characterized by FE-SEM analysis (as shown in Figure 36). The results show that where the bare MeS (as shown in Figure 36(a)) had an interconnected 3D framework with large pores size ranging between 100 μm and 200 μm and the surface of framework was very smooth [219]. Due to the large pores size of this material, it could be induced the absorption capacity. After coating treatment-functionalization, the color of MeS changed from white to dark brown revealing the successful coating of carbon dot onto MeS due to the presence of carbon dot that was used in the modification. Figure 36(b) shows the FE-

SEM images of the decoration of carbon dot embedded melamine sponge, respectively. It was found that the MeS was thicker which proved that carbon dot was successfully coated on MeS. Figure 36 shows carbon dot embedded melamine sponge adsorbing triazole fungicides observed with a thicker sponge structure and a thin film-like coating between the sponge pores which shown that the successful adsorption of the target material. Figure 36(d) shows some pore damage, and the thin coating has disappeared. Since the targets are eluted by suitable elution solvents in the elution step.

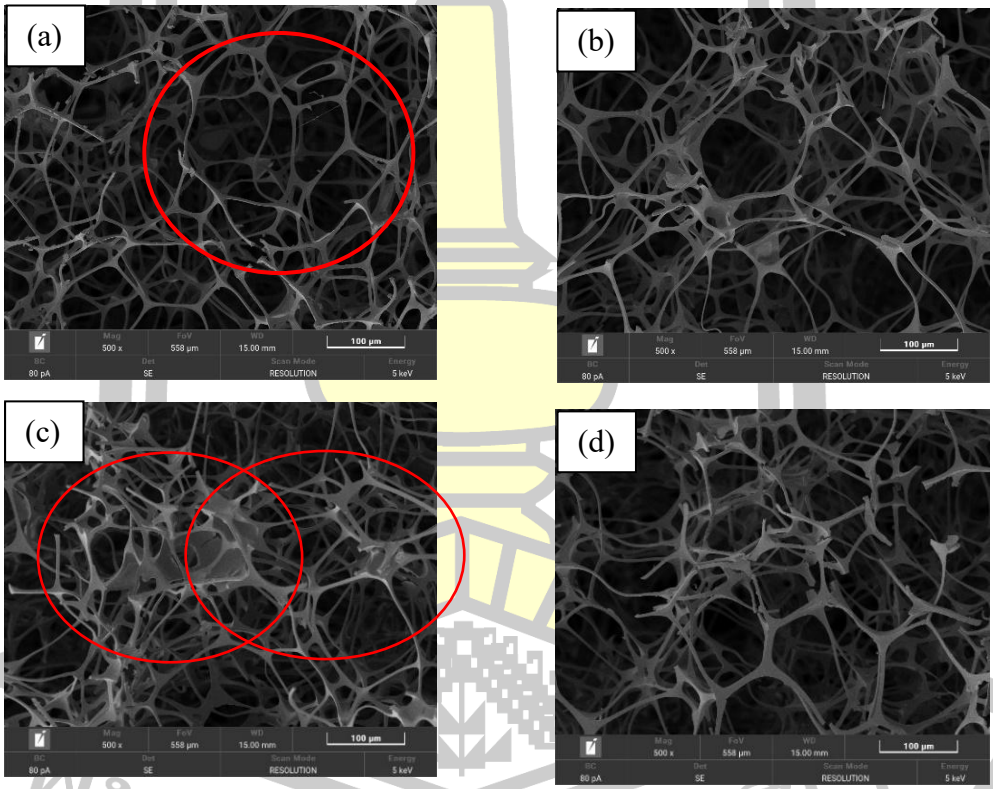

Figure 36 FE-SEM of (a) bare MeS, (b) carbon dot embedded melamine sponge, (c) carbon dot embedded melamine sponge after adsorption with triazole fungicides (100 µg L^{-1} of each), and (d) carbon dot embedded melamine sponge after desorption process.

The crystal structure of as-prepared synthesis sorbent is determined from XRD patterns as presented in Figure 37. There is a board diffraction peak centered at ca 26.5° (2θ) due to highly disordered carbon atoms. Reflexes (100) and (101), for which 2θ ≈ 42.4 and 44.6°, respectively, determine the longitudinal dimension La of the structural elements. The results show that reflexes in the diffraction pattern are asymmetric. That auxiliary indicates the possession of many carbon phases (substructures) with different degrees of order and structural characteristics [220].

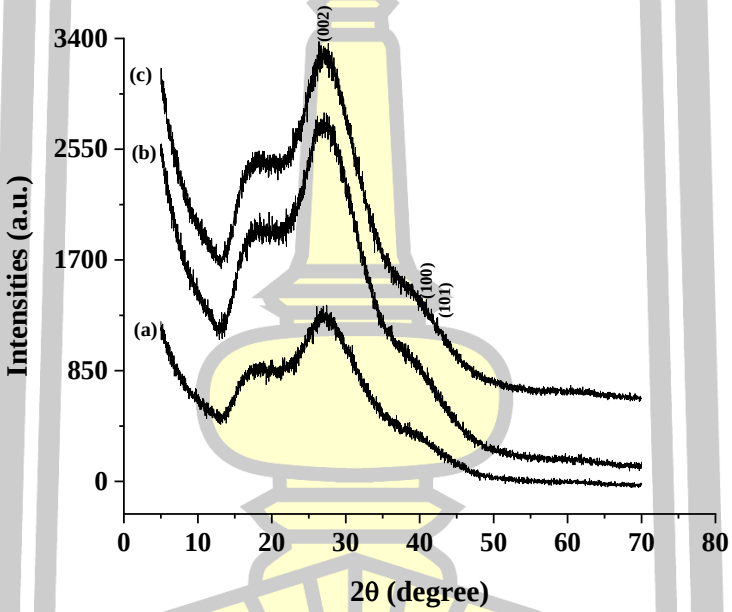

Figure 37 XRD pattern of (a) bare MeS, (b) carbon dot embedded melamine sponge after adsorption with triazole fungicides (100 μg L^{-1} of each), and (c) carbon dot embedded melamine sponge after desorption process.

The FTIR spectra presented in Figure 38 showed the characteristic peaks of the bare MeS (as shown in Figure 38(a)) and the carbon dot embeded MeS (as shown in Figure 38(b)). It was found that the carbon dot embedded MeS provide various absorption core, almost all are linked to the functional groups. The IR spectrum of the bare MeS, the peaks at 3727.44, 3703.90, 3626.68, 3599.09 and 3331.97 cm^{-1} represent the characteristic absorption peak of -OH stretching vibration in H_2O molecules, inner surface -OH, -OH covalent bond absorption at high frequencies and primary amine respectively, 1635.83 and 1580.12 cm^{-1} are ascribed to the absorption peak of triazinyl. It is apparent that the peak of 809.97 cm^{-1} occurs in total these three IR spectrums which is the characteristic peak of triazinyl [28, 29]. After thermal treatment, the carbon dot embedded melamine sponge composites consisted of these bands confirmed that melamine and formaldehyde are successfully cross-linked with carbon dot (as shown in Figure 38(c)). The band of 2900.93 and 2971.60 cm^{-1} were assigned to the stretching vibration of C-H. And the new peak at about 1327.12 cm^{-1} was related to the vibration of methane. For the spectra of bare MeS, the peak at 1079.88 cm^{-1} was attributed to the structure of the formation of C-O-C. Then, after aging this peak disappeared which confirmed the theoretical prediction.

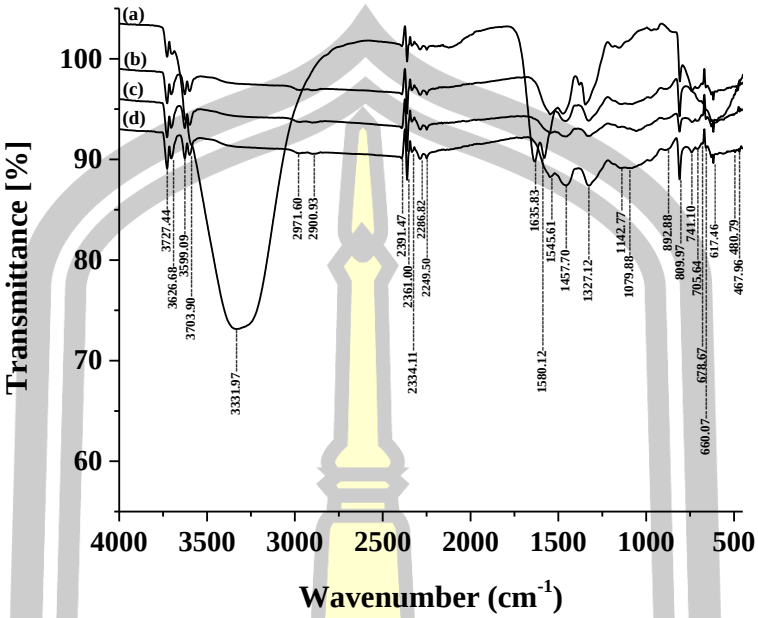

Figure 38 FTIR spectra of (a) bare MeS, (b) CA coated MeS, (c) carbon dot embedded melamine sponge after adsorption with triazole fungicides (100 µg L^{-1} of each), and (d) carbon dot embedded melamine sponge after desorption process.

The pore size of the bare MeS and MeS after modification was determined N_2 adsorption-desorption isotherms at 77 K. The capacity of the materials was investigated in term of surface area and porosity of the prepared materials. BET isotherm without modification and with modification are shown in Figure 39(a) and 39(b), respectively. After modification, MS showed Type-III adsorption in the IUPAC classification (as shown in Figure 39), illustrating that MS has a large pore size with weak interaction. The surface area of MS was up to 13.3773 m^2g^{-1} and the pore diameter was 85.298 Å. After modification, BET isotherm exhibited a reversible type I isotherm which confirmed that the prepared materials provide low micropores (≈1 nm). Because the low micropores could be associated with the MeS support preparation process. The lower porosity of carbon dot-MS results from the uneven

distribution of the carbon dot on the MS surface. The result indicated that carbon dot obstructed the pores of MS, resulting in a preconcentration of triazoles. The mechanism of carbon dot embedded melamine sponge with studied compounds occurred. The BET surface area and pore parameter (V_{pore}) of the as-prepared sorbent material were -23.5367 m^2/g and 0.001 cm^3/g, respectively. The results showed that the negative surface area and less pore size distribution due to the pores of MeS was filled with carbon dot as a result decreased the surface area and pore size. The mechanism of carbon dot embedded melamine sponge exhibits a hydrophobic behavior due to the conversion of hydroxyl groups to C-O-C in the CA-CD-MeS, which is illustrated in Figure 40. Two reactions occurred as follows (i) direct hydrogen bonding between the hydroxyl groups of citric acid precursor and the secondary amine groups on the melamine sponge skeleton's surface and (ii) citric acid-carbon dot-melamine sponge (CA-CD-MeS) binds to the target analytes at the active site via electrostatic interaction and hydrogen bonding, respectively. Finally, resulted in the self-assembled multilayer covalently bonded onto the surface of MeS after modification.

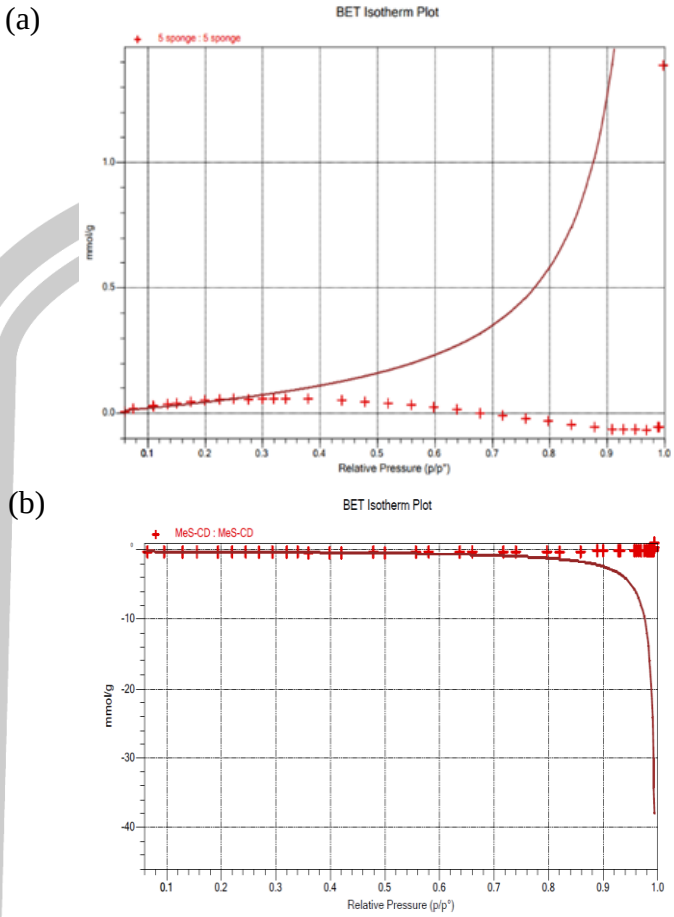

Figure 39 BET isotherm without modification (a) and with modification (b).

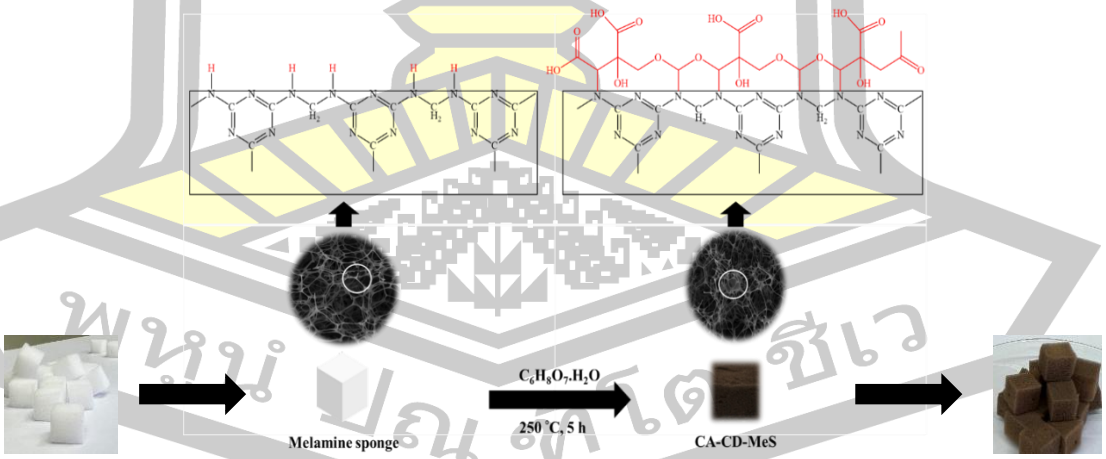

Figure 40 The mechanism for the functionalization of CD-MeS.

To characterize the hydrophobicity of the modified and unmodified MeS, the contact angle of a water droplet on their surfaces was measured (Figure 41). Based on the measured value of the water contact angle, θ, surfaces can be classified as superhydrophilic (θ ~ 0◦), hydrophilic (θ = 30˚~90˚), hydrophobic (θ = 90˚~150˚) and superhydrophobic (θ > 150˚). For the modified MeS surface, the average water contact angle was approximately 124˚, which is classified as hydrophobic (i.e., the water contact angle ≥ 90˚~150˚) [221]. In contrast, the water contact angle of the unmodified MeS surface could not be recorded because the water droplet was immediately absorbed by the material, indicating a highly hydrophilic nature. Thus, also this result confirms the successful introduction of the hydrophobic alkyl chains of the carbon dot coupling agent to the MeS surface.

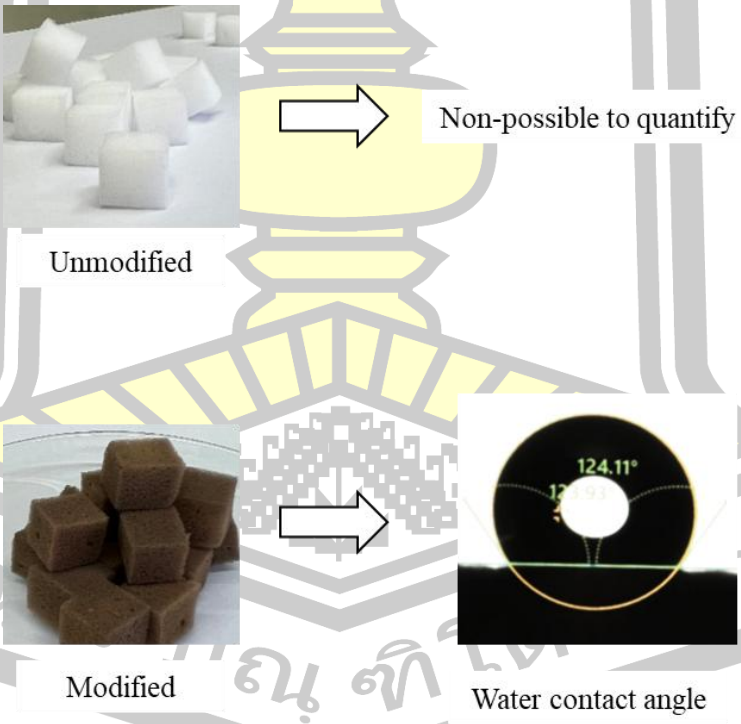

Figure 41 Comparison of water contact angle on modified and unmodified sponge surfaces.

4.3.2 Thermal and chemical stability

In addition, the thermal stabilities of the material which indicates the stability of the material under the thermal condition [222], were investigated by thermogravimetric (TGA) analysis. TGA curves of bare melamine sponge (MeS) and carbon dot embedded melamine sponge (MeS-CD) are shown in Figure 42. Three weight losses of bare MeS (as shown in Figure 42(a)) were shown at the following temperatures: 30-150, 350-410, and 410-650 °C. In the 30-150 °C range, the mass loss is derived from the evaporation of the water absorbed in the MeS [223], [224]. The weight of bare MeS is stable before 350 °C, confirming the stability of the sponges. A rapid weight loss in MeS was observed from 410 to 700 °C. The breakdown of the methylene bridge (HN–CH_2–NH) of the MeS structure contributes to the mass loss between 350 and 410 °C. At a temperature higher than 410 °C, the mass loss was attributed to the thermal decomposition of the triazine ring [225]. At 650 °C, less than 20% weight is left. A slight mass loss can also be observed by increasing the temperature above 650 °C, indicating still N, H, and C releasing at higher temperatures. The thermal decomposition of the MeS-CD (as shown in Figure 42(b)) mainly occurred in the temperature range of 122 to 400 °C, which is consistent with the thermal behavior of the reported typical critic acid [226]. The initial weight increases result from water vapor adsorption by the hydrophilic functional groups of citric acid [227]. The slight drop to 15-20 wt% which occurred from 120 °C until 225 °C, can be attributed to the citric acid as a carbon dot precursor. No significant weight loss was observed in both before 500 °C, due to the pre-carbonization processes. Thus, the MeS and MeS-CD show thermal stability.

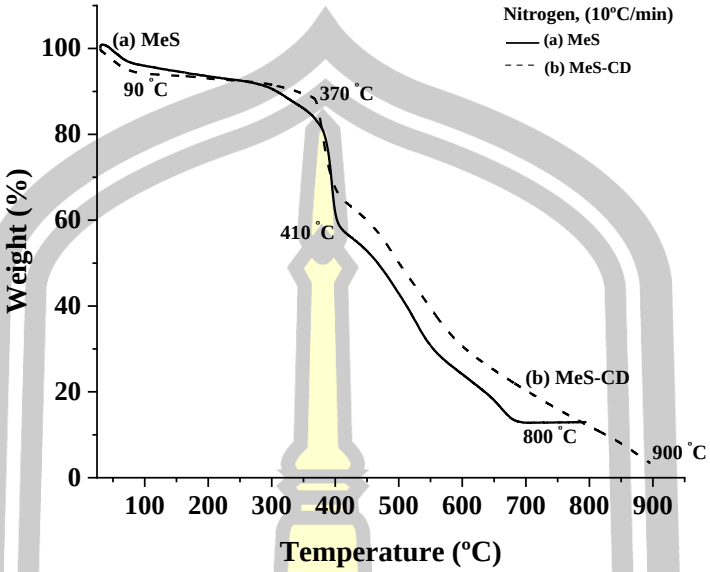

Figure 42 TGA curves of (a) bare melamine sponge (MeS) and (b) carbon dot embedded melamine sponge (MeS-CD).

Ideally, a good sorbent should be able to function in acidic, alkaline, and neutral solutions [228]. For the aforementioned reason, the stability of the as-prepared melamine sponge incorporated with carbon dots under these conditions was evaluated. The sorbent was immersed in acidic (pH of 3), alkaline (pH of 10), and neutral (pH of 7) solutions for 24 h, then washed and dried. After that, the as-prepared sorbent was then extracted of triazole fungicides prior to HPLC analysis. The result was shown in Figure 43. It was found that the peak areas were slightly different but the variation was not statistically significant after being immersed in three different solutions. The high chemical stability of the sponge could be a consequence of the cross-linked network and chemical inertness of carbon dots grafted on its surface.

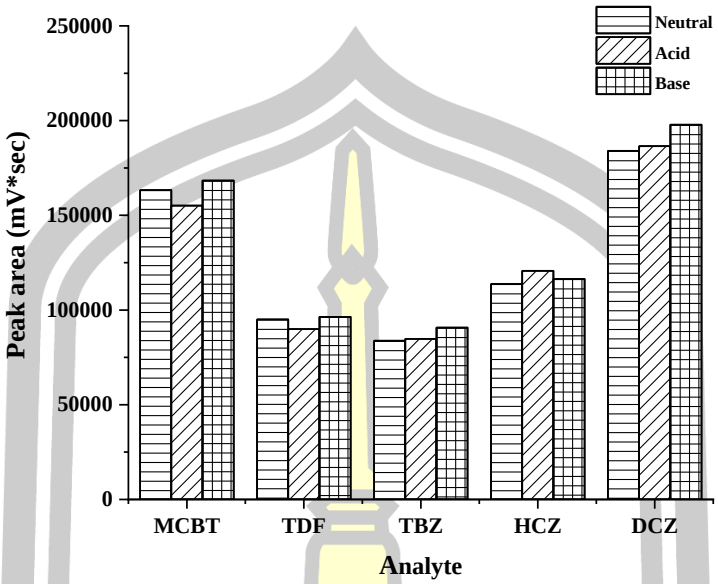

Figure 43 Chemical stability of the as-prepared sorbent.

4.3.3 Synthesis optimization

Various factors influencing the extraction efficiencies of the micro-SPE were studied. All experiments were examined in triplicate using standard solutions of triazoles 100 µg L^{-1}. The synthesis conditions were tested to obtain maximum loading of MeS with citric acid. The principle used to select the optimum synthesis conditions was the total adsorption capability of the resulting carbon dot embedded melamine sponge. However, the adsorption and desorption of each TFs also was considered.

4.3.3.1 Size of melamine sponge

To achieve maximum loading of MeS with citric acid, the synthesis conditions were handled correctly and examined. The principle used to select the optimum synthesis conditions was the total adsorption capability of the resulting CA-CD-MeS, for a mixture of five TFs (100 µg L^{-1} each). 4 sizes of MeS were investigated including 0.3×0.3×0.3 cm^3, 0.5×0.5×0.5 cm^3, 1×1×1 cm^3, and 1.5×1.5×1.5 cm^3. As shown in Figure 44, it indicated that the highest extraction

recoveries of most analytes were achieved using 1×1×1 cm^3 of MeS, except diniconazole. Unless otherwise stated, single MeS cubes (1×1×1 cm^3) were used as the optimal size to optimize the synthesis.

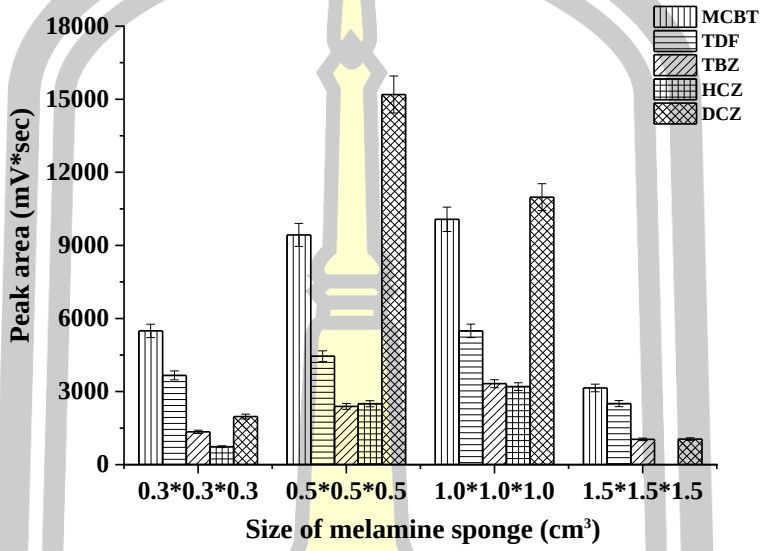

Figure 44 Effect of size of melamine sponge (cm^3).

Conditions: 1×1×1 cm^3 of melamine sponge material; MeS was immersed in an ethanolic solution containing citric acid 0.04 mol L^{-1}(as a precursor) overnight; heat at 250 °C for 5 h.; SPE-condition with 5 mL of n-hexane and eluted with 200 µL of acetonitrile (sample volume 10 mL, 100 µg L^{-1} of each triazole fungicide).

4.3.3.2 Effect of concentration of citric acid (as a precursor)

The citric acid (as a precursor) was produced at different concentrations of 0.01, 0.02, 0.04, and 0.1 mol L^{-1} by dissolving citric acid (monohydrate) powder in ethanol. The effect of the concentration of citric acid on the extraction efficiency of triazole fungicides was evaluated in the range of 0.01 to 0.1 mol L^{-1}. It was found that the extraction efficiency in terms of peak area of all triazole fungicides decreased with the increase in the concentration of citric acid up to 0.04

mol L^{-1} and decreased when the concentration of citric was higher than 0.04 mol L^{-1}. Thus, 0.04 mol L^{-1} of citric acid was selected for further experiments (as shown in Figure 45).

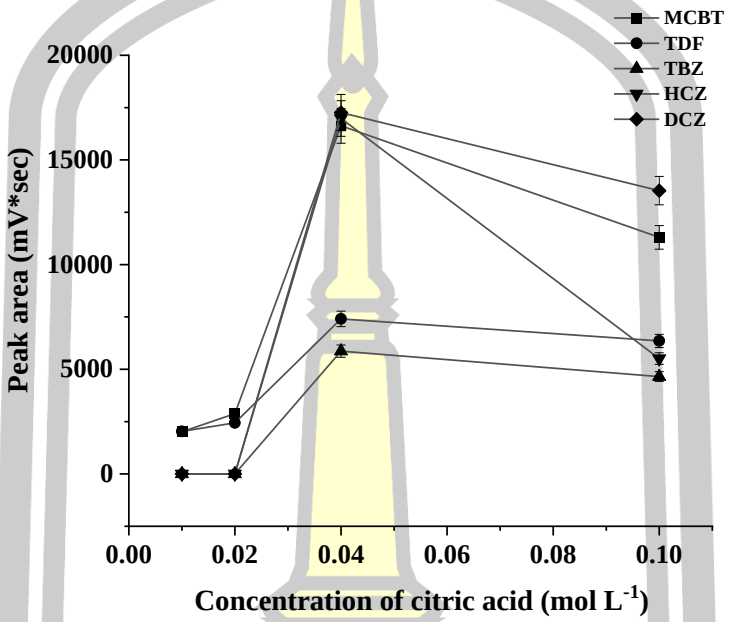

Figure 45 Effect of concentration of citric acid (mol L^{-1}) as a precursor. Conditions: 1×1×1 cm^3 of melamine sponge material; MeS was immersed in an ethanolic solution containing citric acid 0.04 mol L^{-1} (as a precursor) overnight; heat at 250 °C for 5 h.; SPE-condition with 5 mL of n-hexane and eluted with 200 µL of acetonitrile (sample volume 10 mL, 100 µg L^{-1} of each triazole fungicide).

4.3.3.3 Effect of synthesis temperature

Carbon dots are prepared by pyrolyzing citric acid at 200 °C [229]. The heating temperature studied here was less than 280 °C to avoid burning the sponge [230]. The heating temperature was studied between 130 and 280 °C, for 5 h (as shown in Figure 46). Due to, the melting point of anhydrous citric acid is 153 °C, therefore the extraction efficiency at 130 °C is very low. The extraction efficiency in

terms of the peak area of all triazoles increased when the temperature was up to 250 °C. While the temperature increased, the MeS was shrunk and impaired, therefore the extraction efficiency decreased. Consequently, the temperature was selected at 250 °C.

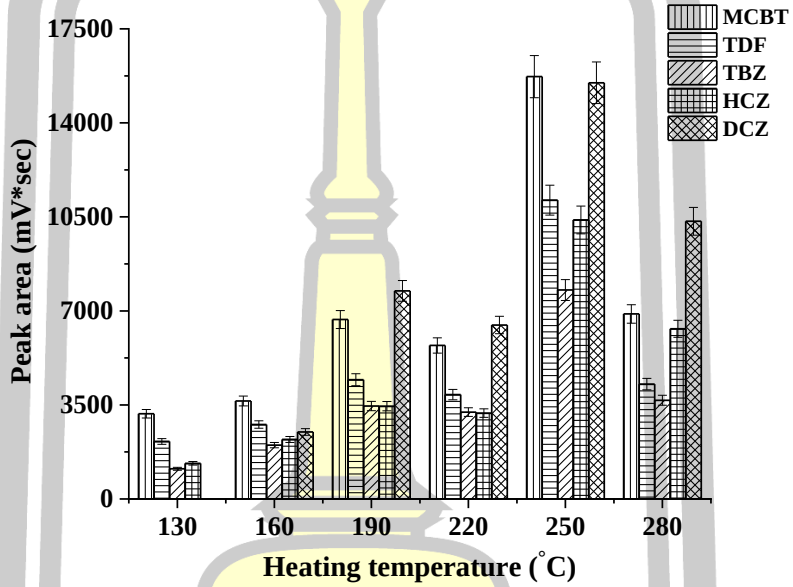

Figure 46 Effect of heating temperature (°C).

Conditions: 1×1×1 cm^3 of melamine sponge material; MeS was immersed in an ethanolic solution containing citric acid 0.04 mol L^{-1} (as a precursor) overnight; heat at 250 °C for 5 h.; SPE-condition with 5 mL of n-hexane and eluted with 200 µL of acetonitrile (sample volume 10 mL, 100 µg L^{-1} of each triazole fungicide).

4.3.4 Optimization of SPE conditions

To ensure the extraction efficiency of the investigated procedure for the analysis of triazole fungicides, various parameters were studied such as the kind and volume of elution solvent. The optimization process was carried out using the univariate method as a one-factor-at-a-time approach with three replicates for each factor. All experiments were examined in triplicate using standard solutions of

triazoles 100 µg L^{-1}. Relative standard deviation (%RSD) was utilized to assess experimental precision.

4.3.4.1 Effect of kind and volume of elution solvent

The kinds of elution solvent are an essential parameter for micro-SPE since it determines the accomplish of the analytes elution and therefore will consequence the sensitivity [231]. Due to the polarity of the target analytes, polar solvents were investigated including methanol, acetonitrile (ACN), and deionization water. The result was shown in Figure 47. It was found that the high extraction efficiency of all analytes was obtained when acetonitrile was used due to a wide polarity range. Therefore, acetonitrile was selected as the desorption solvent, studied triazole fungicides obtained an increased extraction efficiency.

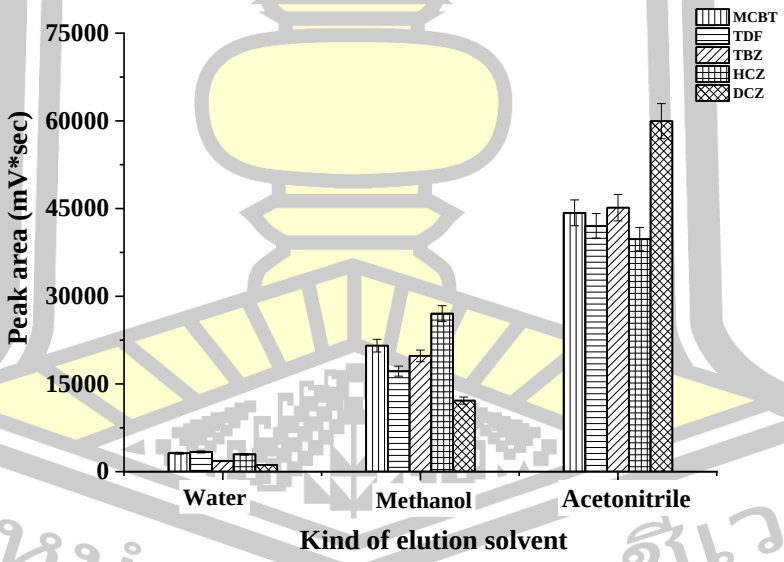

Figure 47 Effect of kind of elution solvent.

Conditions: 1×1×1 cm^3 of melamine sponge material; MeS was immersed in an ethanolic solution containing citric acid 0.04 mol L^{-1}(as a precursor) overnight; heat at

250 °C for 5 h.; SPE-condition with 5 mL of n-hexane and eluted with 200 µL of acetonitrile (sample volume 10 mL, 100 µg L^{-1} of each triazole fungicide).

The effect of volume of the acetonitrile (as elution solvent) was also studied in the range of 100-250 µL. As shown in Figure 48 illustrate that the maximum recoveries of all TFs were achieved when the volume was 200 µL and then decreased due to dilution effect. Therefore, volume of the acetonitrile of 200 µL was chosen.

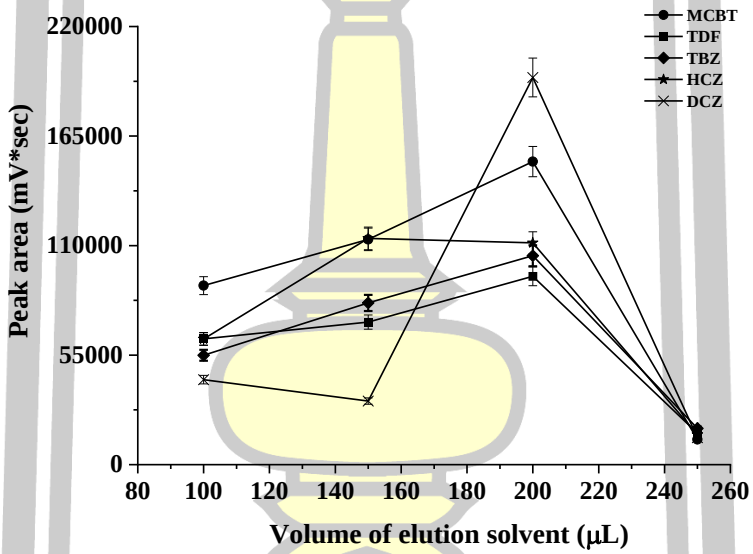

Figure 48 Effect of volume of elution solvent.

Conditions: 1×1×1 cm^3 of melamine sponge material; MeS was immersed in an ethanolic solution containing citric acid 0.04 mol L^{-1} (as a precursor) overnight; heat at 250 °C for 5 h.; SPE-condition with 5 mL of n-hexane and eluted with 200 µL of acetonitrile (sample volume 10 mL, 100 µg L^{-1} of each triazole fungicide).

4.3.5 Reusability and selectivity of the sorbent

Reusability experiments of the sorbent were studied after desorbing the target analytes. Between the cycles, the sorbent was washed using acetonitrile and then dried for the next micro-SPE cycle. The result was shown in Figure 49. It was found that the peak area of five TFs had a significant decrease after 3 micro-SPE cycles, indicating that the as-prepared CA-CD-MeS could be reused at least 3 times. The extraction efficiency decreased thereafter because the CA-CD-MeS was destroyed. Consequently, this alternative sorbent was cost-effective for the determination of triazoles.

To estimate the selectivity of CA-CD-MeS to the tested analytes, the extraction efficiency of carbamate pesticides (methomyl, carbofuran, carbaryl, isoprocarb, fenobucarb), and neonicotinoid insecticides (clotianidin, imidacloprid, dinotefuran, thiacloprid) were examined. The extraction was performed in fungi samples. The results showed that only five triazoles studied were extracted from CA-CD-MeS from the studied samples. The total extraction recovery of the five triazoles studied were in the range of 80.6-120.5%. Therefore, the developed sorbent material exhibited some selectivity over some commonly used pesticides, whereas we see a prospect of it being used as a sorbent for some of them.

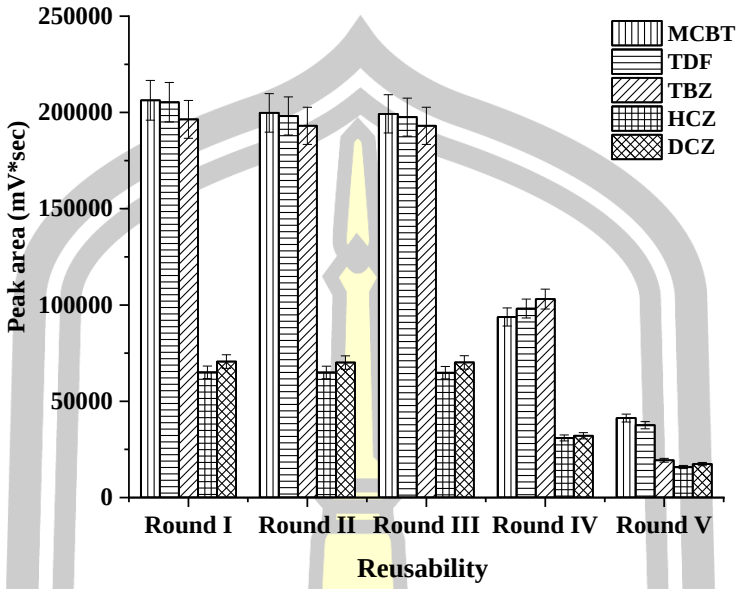

Figure 49 Reusability of the CA-CD-MeS sorbent**.**

4.3.6 Analytical figure of merit

Under the optimum experimental conditions, the analytical figure of merit of the proposed method were evaluated by assessing the linearity, correlation coefficients, limit of detection (LOD), limit of quantification (LOQ), enrichment factor (EF), and extraction recovery (ER). The analytical figure of merit of the developed method are summarized in Table 20. The method exhibited good linearity in concentration ranges of 9-500 µg L^{-1} with the correlation coefficients (R^2) of 0.99. The LODs and LOQs, which are calculated based on signal-to-noise ratios of 3 and 10, respectively, were in the range of 3-10 µg L^{-1} and 9-30 µg L^{-1}, respectively. The RSDs of the intra-day (n=5) and inter-day (n =3×5) at three concentration levels (30, 50, and 100 µg L^{-1}) were used to evaluate the reproducibility of the proposed methodology. All targets exhibited satisfactory intra-day and inter-day precision, with %RSDs less than 8. The enrichment factor (EF) were found to be in the range of 19.87-64.60 folds when computed as the concentration ratio of the analytes in the

settled phase (C_{set}) later the sedimented phase is diluted with 150 µL of acetonitrile and in the aqueous sample (C_o). The extraction recovery (ER) were calculated using Equation (1):

$$ER\ \% = \frac{C_f V_f}{C_i V_i} \times 100 \qquad (1)$$

Where V_i and V_f are the initial and final volumes, C_i is the initial sample solution concentration and C_f is the final concentration of analyte in the desorption solvent [232]. %ER were in the range of 39.74-129.20. Figure 50 demonstrates the chromatograms of the triazole fungicides generated by direct HPLC and after extraction by the investigated micro-SPE-HPLC procedure. The signal was increased after extraction using the proposed micro-SPE-HPLC method.

The robustness of investigated method becomes evaluated to decide their ability to face up to minor changes in access states. The %RSD of peak area and retention time were studied after samples had been injected with some minor change of flow rate (± 0.1 mL min^{-1}), detection wavelength (± 2 nm), and mobile phase composition (± 2 %). The results received from each parameter (n=9) were also determined by a one-way ANOVA test at a 95% confidence level ($p < 0.05$) (data not shown). The result is considered acceptable with %RSDs lower than 8.2 and 1.5 for peak area and retention time, respectively. It was found that, no effect on the resolution of all analytes by adjustment of some separation factors (data not shown). Thus, the proposed method was robustness.

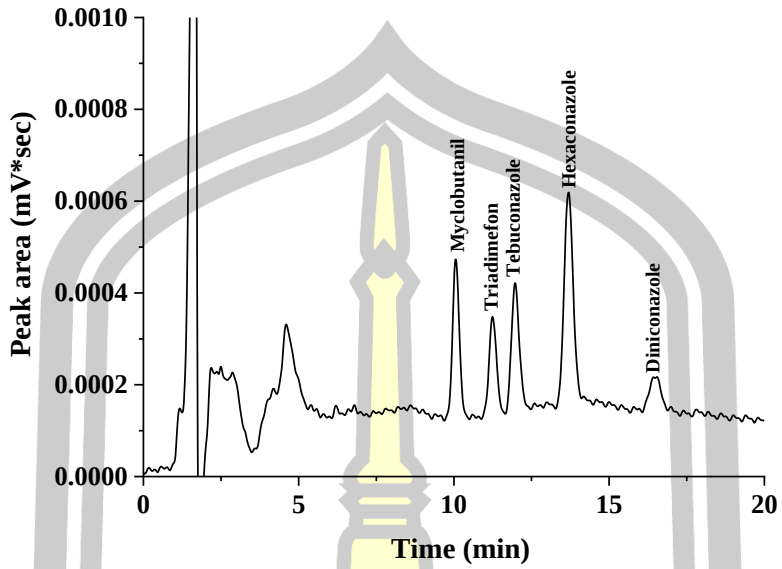

(a)

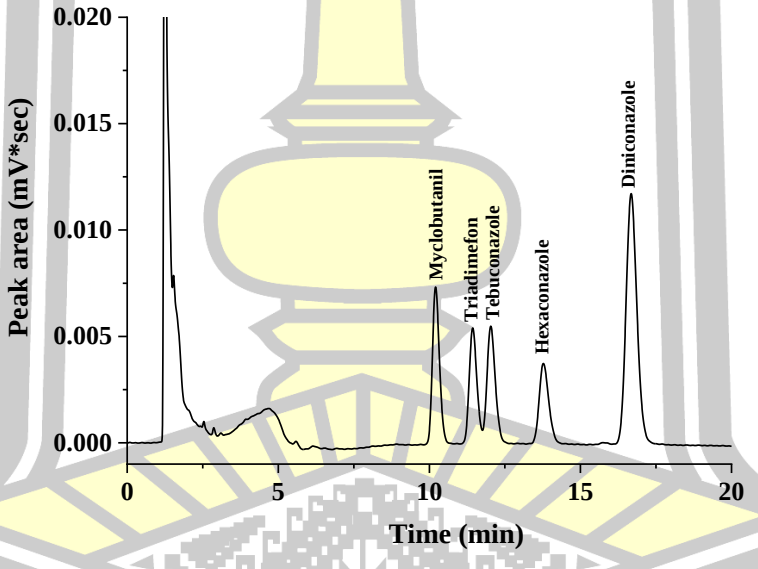

(b)

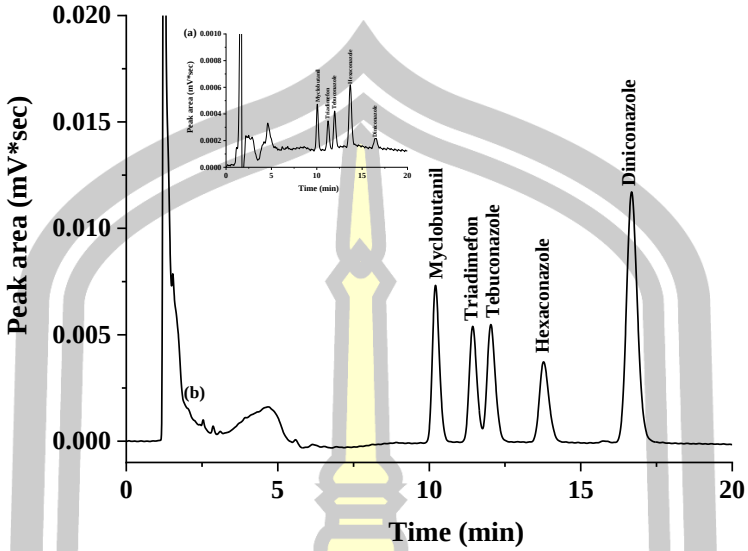

(c)

Figure 50 Chromatograms of the studied triazole fungicides obtained from direct HPLC (a), preconcentrated by the proposed microextraction method (b), and the overlaid chromatograms of standard triazole fungicides were obtained from the proposed microextraction method (c).

Analyte	Linear range ($\mu g\ L^{-1}$)	Linear equation	R^2	LOD ($\mu g\ L^{-1}$)	LOQ ($\mu g\ L^{-1}$)	RSD (%, 100 $\mu g\ L^{-1}$ of each triazole)				EF	ER
						Intra-day precision (n=5)		Inter-day precision (n=5)			
						t_R	Peak area	t_R	Peak area		
Myclobutanil	9-500	y = 455674x + 7590.5	0.9976	3	9	0.12	2.61	0.37	6.11	28.34	56.68
Triadimefon	9-500	y = 277671x + 8070.3	0.9975	3	9	0.20	3.99	0.42	7.54	19.87	39.74
Tebuconazole	9-500	y = 468699x + 12111	0.9962	3	9	0.11	3.87	0.23	5.11	35.95	71.90
Hexaconazole	30-500	y = 388409x - 1860.6	0.9982	10	30	0.33	4.28	0.24	7.89	23.63	47.26
Diniconazole	30-500	y = 534944x + 958.14	0.9965	10	30	0.24	2.67	1.09	4.79	64.60	129.20

Table 20 Analytical figure of merit.

4.3.7 Application to real samples

The extraction of triazole residues in fungi samples was accomplished according to the developed micro-SPE-HPLC method. A matrix-matched calibration approach was used to evaluate the matrix effect in real samples. A set of matrix-matched calibration curves was prepared by extracting representative fungi samples spiked with 50-500 µg kg^{-1} of each target analyte. Most triazoles exhibit wide calibration capability and excellent linearity, with R^2 greater than 0.99 for all samples. The matrix effect (ME) was calculated by comparing the ratio of the slopes of the matrix-matched curve to that of the solvent as the following equation:

$$ME\ (\%) = (S_m/S_S) \times 100$$

where S_m and S_s are the slopes of the calibration curve in the matrix and solvent, respectively. In general, there are no matrix effects in case of ME between 80 and 120 %, minor matrix effects in case of a ME between 50 and 80 % or 120-150 %, and major matrix effects in case of a ME less than 50 % or greater than 150 % [233], [234]. As seen in Table 21, minor and major MEs were found in fungi sample studies. To verify the applicability of the proposed method, six edible fungi samples spiked at two concentrations (30 µg kg^{-1} and 50 µg kg^{-1}) were analyzed. Results showed that none of the triazoles were found in the studied edible fungi samples. The typical chromatograms of studied edible fungi samples II, III, and IV are demonstrated in Figure 51, Figure 52, and Figure 53, respectively. The extraction recoveries of all TFs in the spiked fungi samples extracted under the selected conditions were in a range of 70.45-110.38 %, with RSDs below 5 %. The obtained results were shown in Table 22.

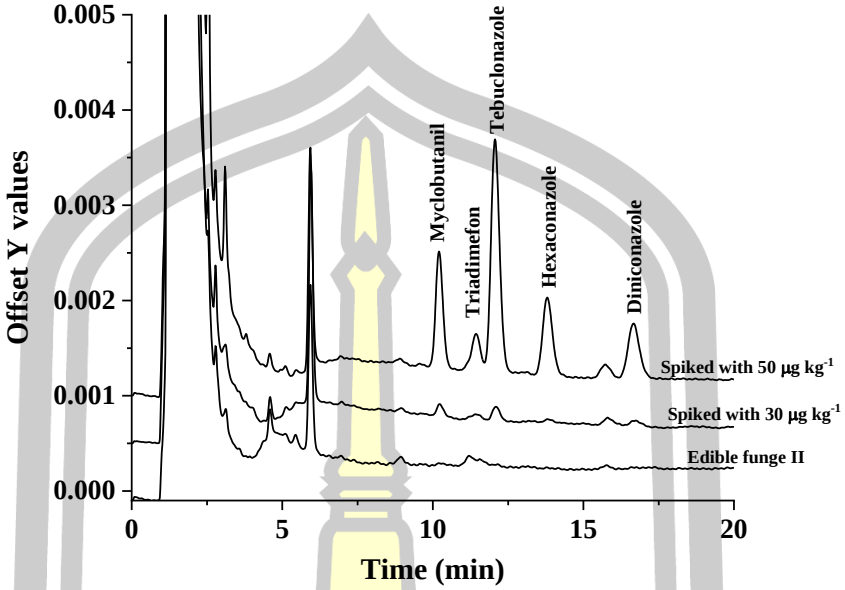

Figure 51 The overlaid chromatograms of studied edible fungi samples II.

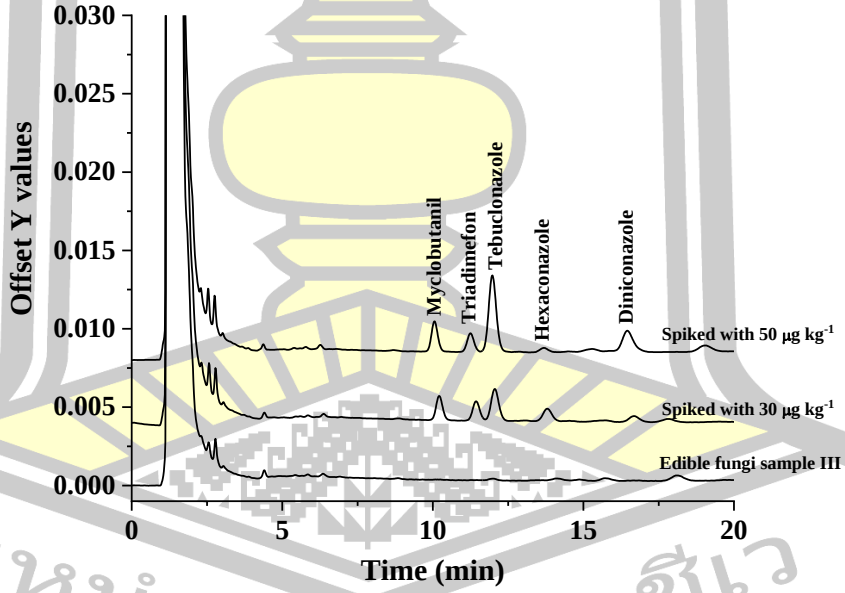

Figure 52 The overlaid chromatograms of studied edible fungi samples III.

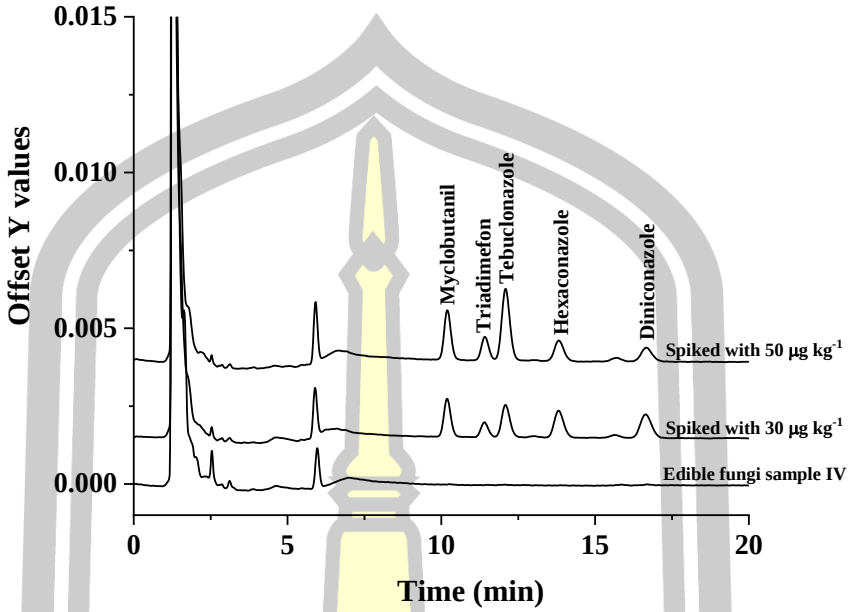

Figure 53 The overlaid chromatograms of edible fungi sample IV.

Table 21 Matrix effect (ME).

Sample	%ME				
	MCBT	**TDF**	**TBZ**	**HCZ**	**DCZ**
Edible fungi I	25.15	33.90	31.25	25.95	23.57
Edible fungi II	50.81	33.43	69.81	40.56	31.17
Edible fungi III	44.83	24.70	52.20	30.08	21.62
Edible fungi IV	42.14	36.56	53.39	37.52	31.71
Edible fungi V	29.07	30.07	25.36	19.95	25.67
Edible fungi VI	12.88	24.85	19.61	24.39	12.57

Table 22 Recovery obtained from the determination of studied triazoles in studied samples (n = 3).

Analyte	Spiked	Edible fungi sample I			Edible fungi sample II			Edible fungi sample III			Edible fungi sample IV			Edible fungi sample V			Edible fungi sample VI		
	(μg kg^{-1})	Found (μg kg^{-1})	%RR	%RSD	Found (μg kg^{-1})	%RR	%RSD	Found (μg kg^{-1})	%RR	%RSD	Found (μg kg^{-1})	%RR	%RSD	Found (μg kg^{-1})	%RR	%RSD	Found (μg kg^{-1})	%RR	%RSD
MCBT	0	ND[a]	-	-	ND	-	-	ND	-	-	ND	-	-	ND	-	-	ND	-	-
	30	27.84	92.81	1.98	24.32	81.08	2.34	24.83	82.76	1.24	31.17	103.93	1.89	28.32	94.42	1.54	23.26	77.56	1.10
	50	50.07	101.52	1.52	35.65	71.31	1.26	39.56	79.12	3.80	47.91	95.82	3.86	53.39	106.78	2.12	35.51	71.02	1.50
TDF	0	ND	-	-	ND	-	-	ND*	-	-	ND*	-	-	ND*	-	-	ND	-	-
	30	31.20	104.00	1.05	21.11	70.48	1.81	23.28	77.62	2.03	22.60	75.36	2.27	22.02	73.42	1.77	22.37	74.58	1.96
	50	50.02	100.06	1.25	39.97	79.94	2.10	37.16	74.32	1.88	46.79	93.79	1.75	38.72	77.45	1.24	35.22	70.45	1.22
TBZ	0	ND	-	-	ND	-	-	ND*	-	-	ND*	-	-	ND*	-	-	ND*	-	-
	30	29.27	97.82	1.54	21.36	71.23	1.58	33.11	110.38	2.93	23.78	79.29	3.08	23.60	78.69	3.20	21.93	73.11	2.82
	50	43.71	87.42	2.55	49.47	98.95	3.58	41.52	83.05	1.80	47.20	94.40	3.91	47.54	95.09	2.30	39.90	79.80	2.73
HCZ	0	ND	-	-	ND	-	-	ND	-	-	ND*	-	-	ND*	-	-	ND	-	-
	30	29.86	99.54	2.40	25.48	84.95	3.52	32.54	108.47	1.40	31.48	104.96	1.62	33.10	110.34	1.80	22.59	75.30	1.89
	50	52.84	105.69	1.28	44.05	88.12	4.16	52.29	104.59	1.82	46.02	92.04	1.39	35.43	70.86	1.39	51.05	102.11	1.73
DCZ	0	ND	-	-	ND	-	-	ND	-	-	ND*	-	-	ND*	-	-	ND	-	-
	30	29.10	97.02	1.49	26.98	89.94	1.61	31.49	104.98	1.47	25.76	85.89	4.05	31.65	105.51	1.81	21.97	73.24	1.56
	50	54.30	108.61	2.22	35.59	71.19	1.40	37.94	75.89	2.55	38.24	76.48	1.92	52.81	105.63	2.19	35.42	70.85	1.84

4.3.8 Evaluation of method greenness

Two metric tools were performed to confirm the greenness of the proposed approach via Analytical Eco-scale [235] and Analytical GREEnness metric (AGREE)[236]. The ideal green analysis according to the Analytical Eco-Scale has a value of 100. Penalty points are assigned for each of the parameters of the analytical procedure that deviate from the ideal green analysis (reagent use, risk, energy and waste). A set of penalty points (PPs) are used to assign the departure from ideal greenness. The PPs for hazardous chemicals can be assessed by multiplying the sub-total PPs for a given quantity and the hazard. The ultimate AEC value can be calculated from "AEC =100 - total PPs". If the score is more than 75, the method is expressed as an "excellent green" procedure, while values in the range 75 <x <50 are considered "acceptable green analysis" and values below 50 indicate insufficient green method [237]. The final score for this method is 73 (as shown in Table 22) and it can be acceptable as a green method.

The AGREE metric, assessed via The Analytical Greenness Calculator software, evaluates adherence to the 12 principles of Green Analytical Chemistry, assigning scores from 0 to 1 for each criterion [234]. Results are depicted through a pictogram, indicating a final score from 0 to 1 and color-coded from green to red. The width of the segment corresponding to each individual GAC principle shows its impact on the final score for the method. As depicted in Figure 54, the AGREE evaluation resulted in a final score of 0.47 which shown that the present method can be acceptable as a green. An overall score greater than 0.6 [235]indicates a high level of adherence to green analytical chemistry principles, such as reducing or eliminating hazardous compounds, reducing waste creation, optimizing energy use, and increasing

health and safety. It displays a strong commitment to environmental stewardship and sustainability [238], [239]. The lowest performing subsectors was obtained in sectors 3 (device positioning) and 10 (source of reagents). The evaluation, assessed by Analytical Eco-scale and Analytical GREEnness metric (AGREE), confirmed its superior environmental friendliness.

Table 23 The penalty points (PPs) for the analytical procedure for the determination of TFs in edible fungi samples.

Parameter	**Penalty points**
Amount of sample (10 mL)	2
Decoration procedure	
Citric acid	1
Ethanol (F)	5
Room temperature, 24 h	1
Heating >1 h	2
Removal of solvent with bp < 150°C	0
Hazard (physical, environment, health)	1
Energy (≤ 1.5 kWh per sample)	1
Occupational hazard	0
Waste (1-10 mL)	3
n-Hexane (SPE procedure)	8
Acetonitrile (SPE procedure)	2
FTIR (≤ 0.1 kWh per sample)	0
UV-Vis spectrometry (≤ 0.1 kWh per sample)	0
LC (≤ 1.5 kWh per sample)	1
Penalty points total:	27
Eco Scale	**73**

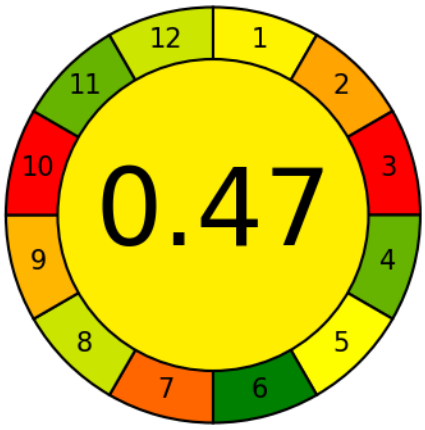

1. Sample treatment
2. Sample amount
3. Device positioning
4. Sample prep. Stages
5. Automation, miniaturization
6. Derivatization
7. Waste
8. Analysis throughput
9. Energy consumption
10. Source of reagents
11. Toxicity
12. Operator's safety

Figure 54 Result of the green evaluation of the proposed analytical methodology obtained by the Analytical GREEnness metric (AGREE) tool.

4.3.9 Comparison with other reported methods

Table 23 exhibits the analytical performance of the established carbon dot embedded melamine sponge method compared with other microextraction methods [214], [240], [241], [242], [243], [244]. With a brief comparison among the methods, it can be seen that the proposed method shows an extraction method, analytical technique, and relative recovery percentage. Also, LODs values are comparable with the other methods. The important point of this method is introducing an alternative sorbent which is based on the carbon dot embedded melamine sponge method, easy and quick operation. Compared with the traditional SPE, the present extraction method is considerably simpler as it does not need additional centrifugation steps or external magnets, and the carbon dot embedded melamine sponge method used in the present method can be quickly separated from the sample solution. In addition, the volumes of the organic solvents and the operating times required for the carbon dot embedded melamine sponge method as a sorbent in the micro-SPE method were significantly

lower than those required for other reported methods. It was found that a simple and efficient propose method could be determined trace triazole in edible fungi samples. Moreover, the favorable analytical figures of merit and cost effective, not only its potential for reuse, but also renders it a better alternative for matrix purification.

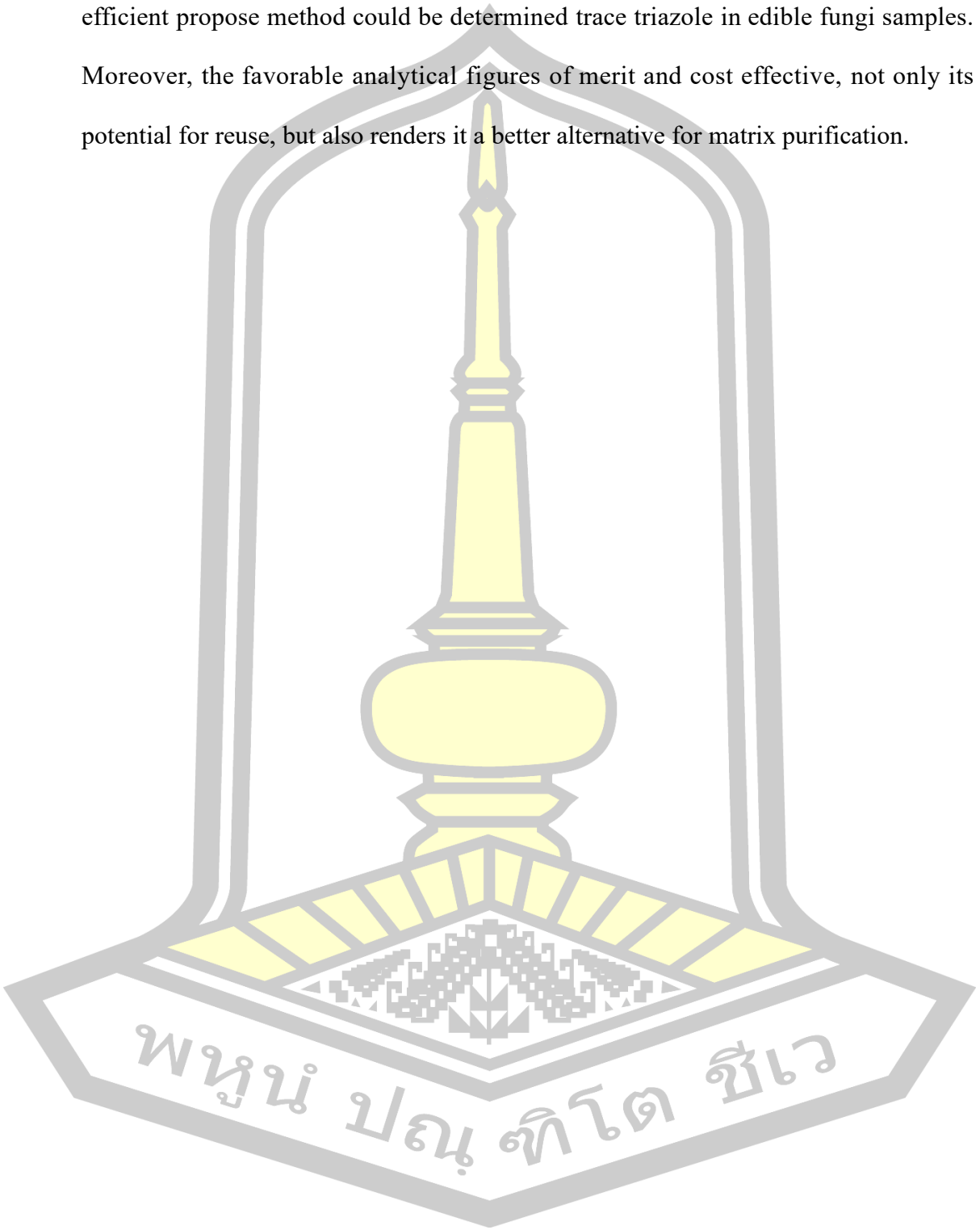

Table 24 Comparisons of the proposed method with other sample preparation methods for the quantitation of triazole fungicides.

Sample	Sorbent	Extraction method	Analytical technique	Linear range	LODs	RSD (%)	%RR	Ref.
Environmental water, soybean milk, fruit juice and alcoholic beverage samples	Coconut husk fiber (CHF)	µ-SPE	HPLC-UV	9-300 µg L^{-1}	3 µg L^{-1}	1.96–4.38	67–105	[245]
Waters and fruit juices	GO-PmAP	SPE	HPLC-UV	0.5–100 µg L^{-1}	0.2-0.4 µg L^{-1}	2.6–6.1	95.2-98.0	[241]
Environmental waters and soils	Azo-PP/PDMS	SBSE	HPLC-DAD	0.5–100 µg L^{-1}	0.12-0.33 µg L^{-1}	2.5–6.4	88.2-119.0	[242]
Waters	In situ SMMH-Fe_3O_4@SiO_2	dSPE	HPLC-DAD	2.5–50 µg L^{-1}	1.0-2.5 µg L^{-1}	less than 8%	90.0-104.0	[243]
Tomato, apple and pare	CAs	PT-SPE	GC-FID	0.96–200.0 mg kg^{-1} and 0.24-200.0 mg kg^{-1}	0.08-0.32 mg kg^{-1}	0.4–1.8% and 7.4–8.5%	81.0-119.0	[214]
Environmental water, honey and fruit juice samples	*Moringa oleifera* seed powder	µ-SPE	HPLC-DAD	10 –500 µg L^{-1}	30-50 µg L^{-1}	76.9–113.9%	70–116	[244]
Edible fungi samples	CD- MeS	Micro-SPE	HPLC-DAD	9-500 µg L^{-1}	3-10 µg L^{-1}	70.45–110.38%	70.45-110.38	**This work**

4.4 In situ formation of ionic liquid for enrichment of triazole fungicides in food applications followed by HPLC determination

This chapter present the result obtained section describes a development of then extraction method and then prior to high performance liquid chromatography (HPLC). The triazole fungicides such as myclobutanil, triadimefon, tebuconazole, and hexaconazole were selected as model compounds. The second section present the analytical performance of the proposed method. Finally, the proposed method was applied to analyze triazole fungicide residues in honey, fruit juice, and egg samples. The results were discussed.

4.4.1 Characterization of in situ ionic liquid

The halide anion of tributylhexadecylphosphonium bromide ($[P_{44412}]Br$) and potassium hexafluorophosphate (KPF_6) was the main force for the formation of the hydrophobic ionic liquid. FT-IR spectra were used to confirm the formation of hydrogen bonding, as shown in Figure 55. In the FT-IR spectra, the characteristic peaks presented at 2850, 2920, and 2960 cm^{-1} were assigned to the C-H stretching or CH_3 stretching, while those at 1410 and 1465 cm^{-1} were attributed to the C-H bending and CH_3 bending vibrations of pure $[P_{44412}]Br$ [246]. Moreover, the FT-IR spectra of the characteristic peaks showed the halogen compound vibrations at 577 and 795 cm^{-1}. This may have been due to a transfer of the bromide ion cloud electron to hydrogen bonding, and consequently, a decrease in the force constant [247]. Thus, the shift of the hexafluorophosphate counter-ion vibrations suggested the existence of hydrogen bonding between $[P_{44412}]Br$ and KPF_6 when the hydrophobic ionic liquid was formed.

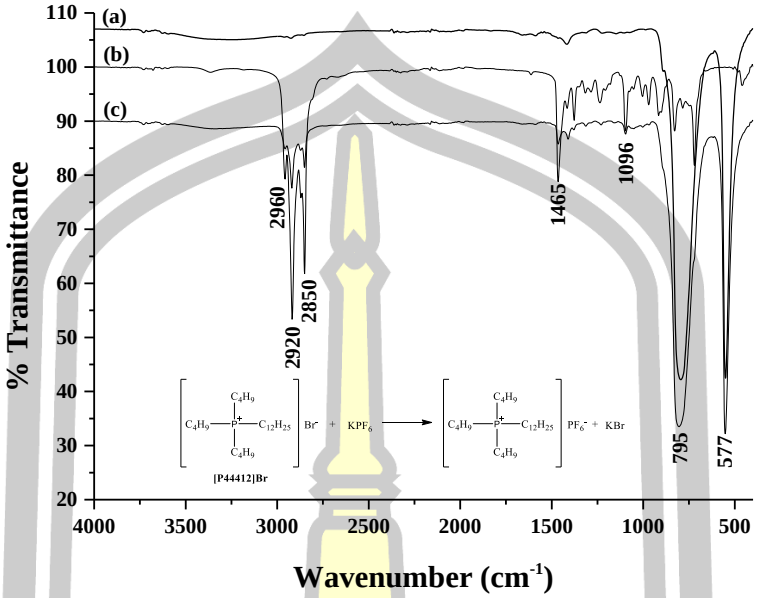

Figure 55 FT-IR spectra of (a) KPF_6, (b) $[P_{44412}]Br$, and (c) ionic liquid ($[P_{44412}][PF_6]$).

4.4.2 Optimization of in situ metathesis reaction generated ionic liquid combined with liquid-liquid microextraction

Due to their low concentrations and matrix interferences in real samples, it is difficult to directly analyze triazole fungicides. Therefore, a sample-preparation method is necessary before analysis. In this work, an in-situ metathesis reaction that generated the ionic liquid was combined with a liquid-liquid microextraction in the triazole fungicide analysis. In order to obtain a high extraction efficiency, various parameters had to be investigated. The optimization was carried out using the aqueous solution (10 mL) containing 100 μg L^{-1} of each triazole fungicides. All experiments were performed at least in triplicate.

4.4.2.1 Effect of the amount of IL components

In order to form the ionic liquid ($[P_{44412}][PF_6]$), $[P_{44412}]Br$ and KPF_6 were selected because the starting extraction solvent could be completely

dissolved in the aqueous solution, which promoted the analyte extraction in the absence of a dispersion solvent; the melting of this IL ($[P_{44412}][PF_6]$) was between 10 and 30 °C, and it could solidify at low temperatures [248]. Moreover, $[P_{44412}][PF_6]$ is denser than water, therefore it was easy to collect as the bottom layer after centrifugation. The amount of $[P_{44412}]Br$ was studied in the range of 0.01-0.10 g. The results are shown in Figure 56. The results showed that the maximum peak area was obtained at 0.01 g of $[P_{44412}]Br$. Therefore, 0.01 g of $[P_{44412}]Br$ was chosen.

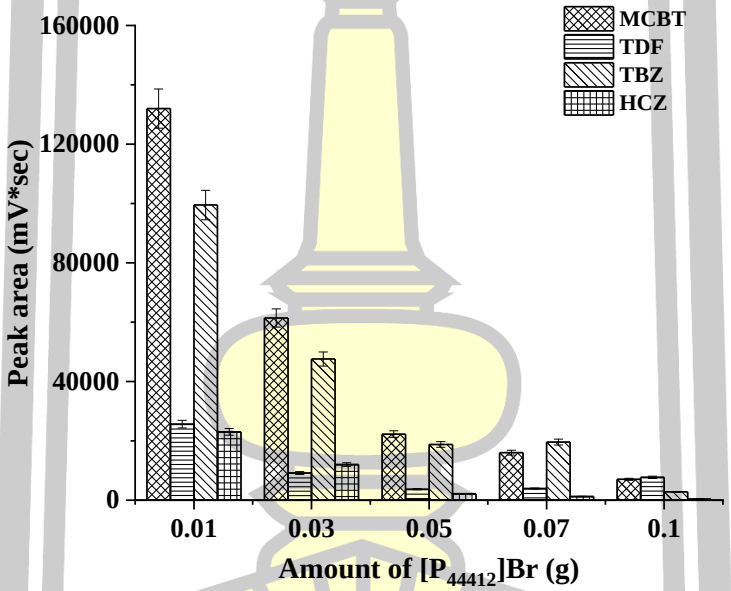

Figure 56 Effect of the amount of $[P_{44412}]Br$ on the extraction efficiency. Conditions: 0.01 g of $[P_{44412}]Br$; 0.01 g of KPF_6; centrifuge at 4500 rpm for 10 min; 200 µL of acetonitrile (sample volume 10 mL, 300 µg L^{-1} of each triazole fungicide).

The amount of KPF_6 varied in a range of 0.01-0.10 g. The results are shown in Figure 57. The results showed that the maximum peak area was obtained at 0.01 g of KPF_6. Then, the signal decreased at a higher amount of KPF_6. Thus, 0.01 g of KPF_6 was selected. The molar ratio of $[P_{44412}]Br$ to KPF_6 was selected as 1:2.5

because the excess KPF_6 ensured 100% completion of the in-situ metathesis reaction [248].

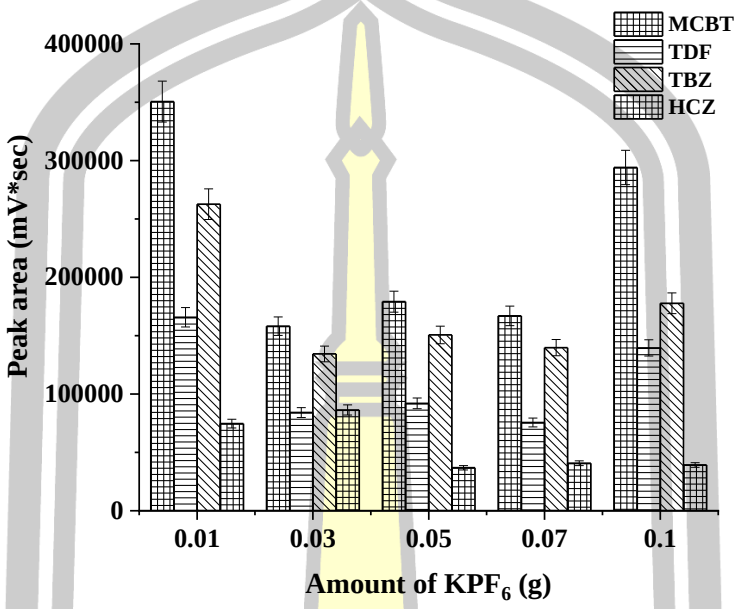

Figure 57 Effect of the amount of KPF_6 on the extraction efficiency. Conditions: 0.01 g of $[P_{44412}]Br$; 0.01 g of KPF_6; centrifuge at 4500 rpm for 10 min; 200 µL of acetonitrile (sample volume 10 mL, 300 µg L^{-1} of each triazole fungicide).

4.4.2.2 Effect of extraction speed and time

Because the process of mass transfer and completely phase separation in an extraction procedure should be time-dependent, the effects of extraction speed and time on the peak area was studied [249]. The effect of centrifugation speed was evaluated in the range of 1500-5000 rpm (as show in Figure 58). It was found that the peak areas of all the analytes increased up to a 4500-rpm centrifugation speed, above which the peak areas slightly decreased due to disintegration of the phase of target analytes. Therefore, a centrifugation speed of 4500 rpm was selected. The extraction times studied ranged from 3 to 15 min, while other experimental conditions were kept constant (data not shown). The peak areas of

most of the triazoles increased with increases in the extraction time and reached the highest at 10 min. Therefore, 10 min was chosen to ensure an efficient extraction.

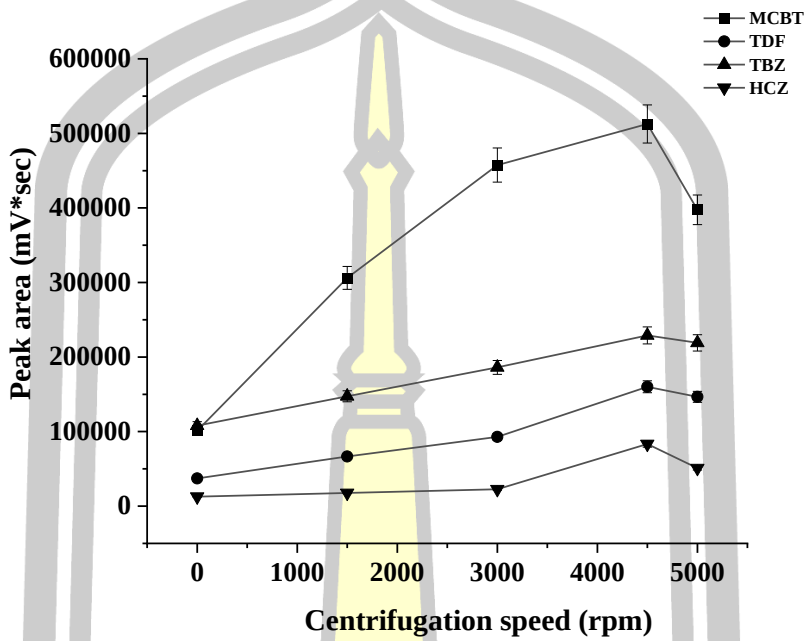

Figure 58 Effect of centrifugation speed (rpm) on extraction efficiency. Conditions: 0.01 g of $[P_{44412}]Br$; 0.01 g of KPF_6; centrifuge at 4500 rpm for 10 min; 200 µL of acetonitrile (sample volume 10 mL, 300 µg L^{-1} of each triazole fungicide).

4.4.2.3 Effect of dissolving solvent

Before HPLC analysis, acetonitrile (ACN) was added to dissolve the RTIL-rich phase due to its solubility property in the $[P_{44412}]PF_6$ phase and the compatibility with the mobile phase being used. The ACN volume was investigated in the range of 30-250 µL (as shown in Figure 59). It was found that ACN 200 µL provided the highest peak areas of all analytes. After that, the peak area decreased due to the dilution effect. When using ACN at less than 30 µL, the phase could not be completely dissolved. Thus, 200 µL of ACN was chosen.

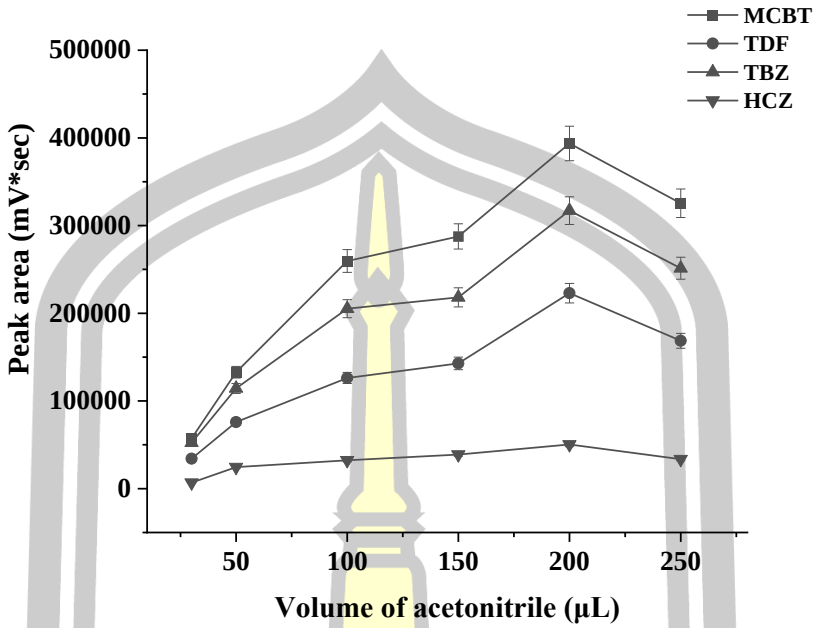

Figure 59 Effect of dissolving solvent (acetonitrile, µL) on extraction efficiency. Conditions: 0.01 g of $[P_{44412}]Br$; 0.01 g of KPF_6; centrifuge at 4500 rpm for 10 min; 200 µL of acetonitrile (sample volume 10 mL, 300 µg L^{-1} of each triazole fungicide).

4.4.3 Analytical performance of the proposed method

Under the chosen extraction condition, a series of experiment were conducted to study the enrichment factors (EFs), extraction recoveries (ERs), linear ranges, limits of detection (LODs), limits of quantitation (LOQs), and precisions (intra-day and inter-day). The results are shown in Table 1. The calibration graphs were linear over concentration ranges of 90-1000 µg L^{-1} for myclobutanil, triadimefon, and tebuconazole, and 90-1000 µg L^{-1} for hexaconazole, with a coefficient of determination in the range of 0.9988-0.9991. The LODs were evaluated as the concentrations giving a signal-to-noise ratio of 3 (S/N = 3) and were in the range of 30-50 µg L^{-1}. The LOQs (S/N = 10) were in the range of 90-150 µg L^{-1}.

The relative standard deviation (RSD) was determined using five solutions of 150 µg L^{-1} of each triazole fungicide. The RSD values of the retention times and peak areas were in the ranges of 0.40-0.80% and 4.84-6.23%, respectively. The EFs were in the range of 8.53-12.26. The ERs were in the range of 59.71-85.82. The chromatograms obtained from the proposed preconcentration method and direct analysis (without preconcentration) are shown in Figure 60. It was found that the developed method showed high chromatographic signals when compared to the direct analysis.

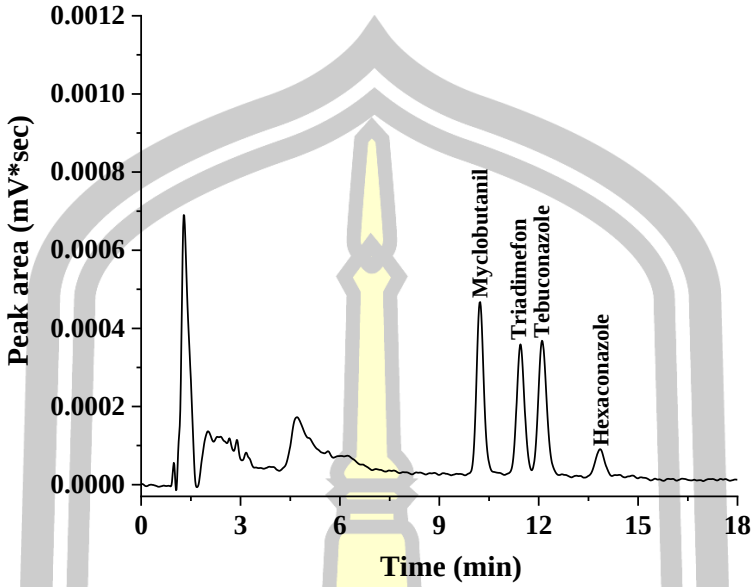
0.0012
0.0010
0.0008
0.0006
0.0004
0.0002
0.0000
Peak area (mV*sec)
Myclobutanil
Triadimefon
Tebuconazole
Hexaconazole
0
3
6
9
12
15
18
Time (min)

(a)

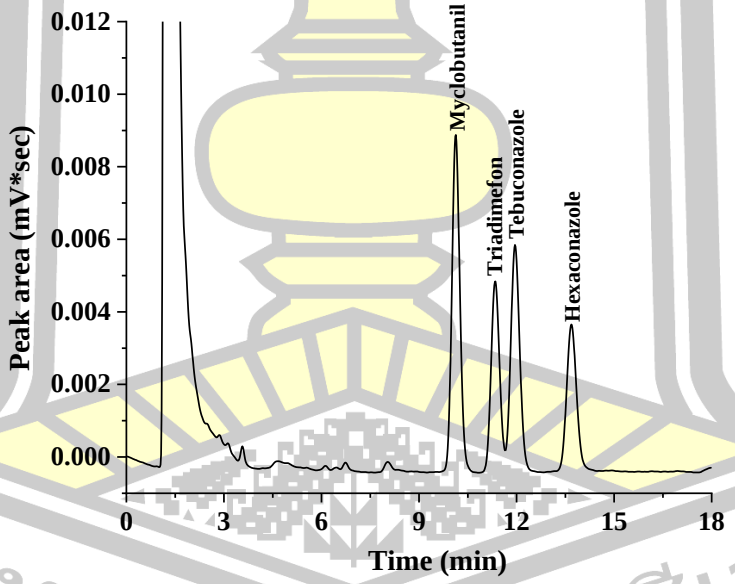
0.012
0.010
0.008
0.006
0.004
0.002
0.000
Peak area (mV*sec)
Myclobutanil
Triadimefon
Tebuconazole
Hexaconazole
0
3
6
9
12
15
18
Time (min)

(b)

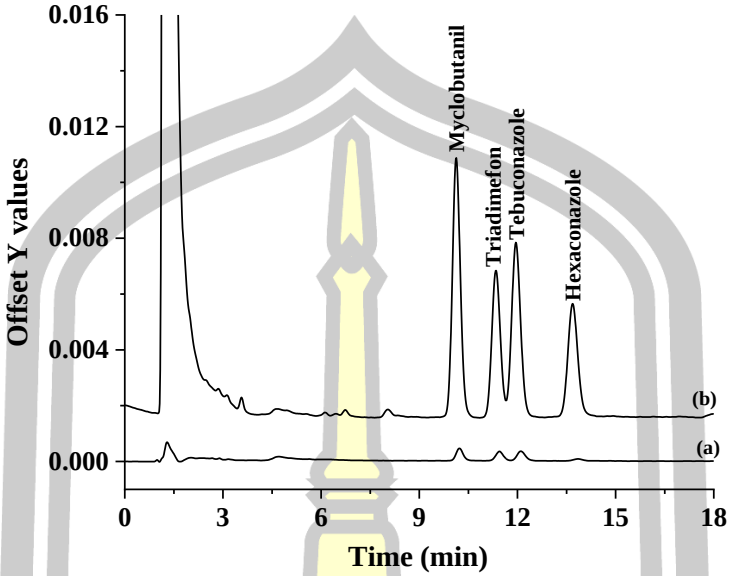

(c)

Figure 60 Chromatograms of standard triazole fungicides were obtained by (a) without preconcentration, (b) with preconcentration using the proposed microextraction method, and (c) the overlaid chromatograms of standard triazole fungicides were obtained from the proposed microextraction method; the concentration of all standards was 300 µg L^{-1}.

Table 25 Analytical characteristics of the standards triazole fungicides.

Analyte	Linear range (µg L^{-1})	Linear equation	R^2	LOD (µg L^{-1})	LOQ (µg L^{-1})	Intra-day precision[a] (n=5), RSD (%)		Inter-day precision[a] (n=5), RSD (%)		EF	ER
						t_R	Peak area	t_R	Peak area		
Myclobutanil	90-500	$y = 1\times10^6x + 9995.5$	0.9994	30	90	0.61	2.48	0.77	2.70	12.26	85.82
Triadimefon	90-500	$y = 907260x + 11705$	0.9989	30	90	0.51	2.92	0.80	3.50	8.53	59.71
Tebuconazole	90-500	$y = 484103x + 4328.4$	0.9991	30	90	0.40	2.60	0.46	2.72	11.01	77.07
Hexzaconazole	90-500	$y = 689281x + 3751.6$	0.9988	50	150	0.70	2.55	0.77	2.60	11.34	79.38

[a]Precision were calculated at the concentration of 100 µg L^{-1} of each triazole.
[b] Ratio of the concentration of the target analytes in extraction phase to the initial concentration in the original sample solutions.

4.4.4 Analysis of real samples

To study the applicability of the proposed method, an in-situ formation and preconcentration method using the ionic liquid was applied in the determination of triazole fungicides in honey, fruit juice, and egg samples. A standard addition method was applied to study the matrix effect (ME). ME(%) is expressed as the ratio of the slopes obtained from calibration curves of each analyte spiked into the samples to those obtained after extraction using the proposed method, as followed equation [250]:

ME(%) = slope of spiked real sample/slope of standard solution × 100

In the absence of the ME, the slope of the calibration curves from both the standard solution and spiked real samples should be similar (ME (%) ≈ 100%). However, in the presence of ME, the signal intensity for the analytes can decrease or increase. Generally, ME values between 80 and 120% indicate no ME, ME values between 50 and 80% or 120 and 150% indicate minor MEs, and ME values less than 50% or greater than 150% indicate major MEs [192]. It was found that the MEs (%) were in the range of 76.9-113.9%. In order to confirm the accuracy of the proposed method, the relative recoveries (RRs) were investigated using an analysis of five real samples spiked with five triazole fungicides at a concentration of 300 μg L^{-1} within one day. Table 25 shows acceptable recoveries (62-112%) with relative standard deviations (RSDs) of less than 7.9% were obtained. The results showed no triazole fungicide residues were detected in all samples. These results confirmed that the proposed microextraction method could successfully be utilized to estimate triazole fungicide residues at trace levels in real samples with high accuracy and validity. The chromatograms of blank and spiked samples are shown in Figure 61-Figure 64.

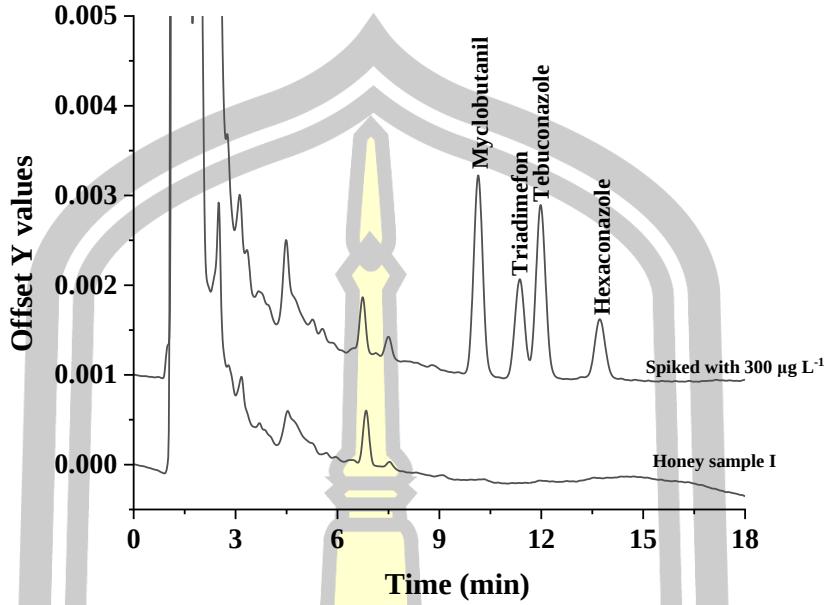

Figure 61 The overlaid chromatograms of honey I and spiked honey I sample.

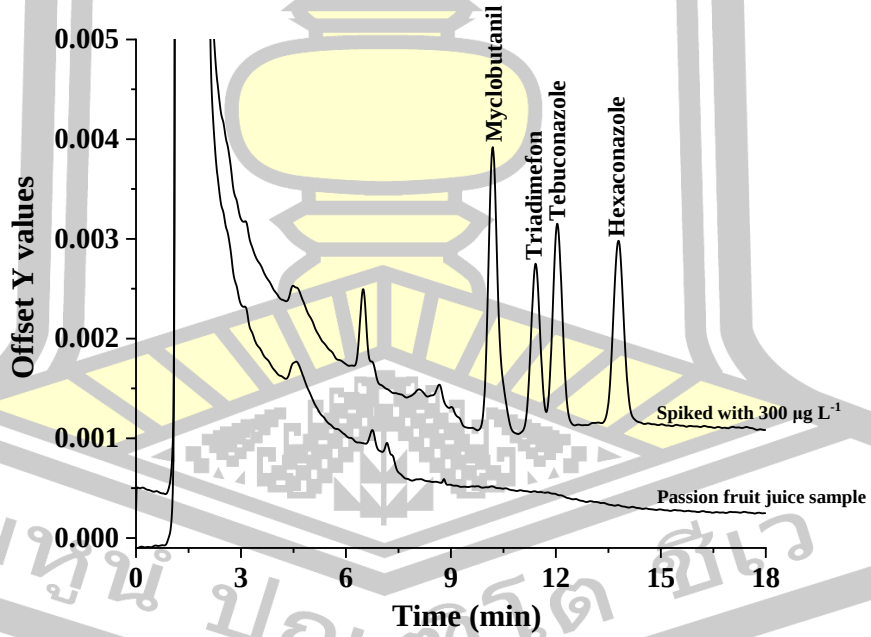

Figure 62 The overlaid chromatograms of passion fruit juice and spiked passion fruit juice sample.

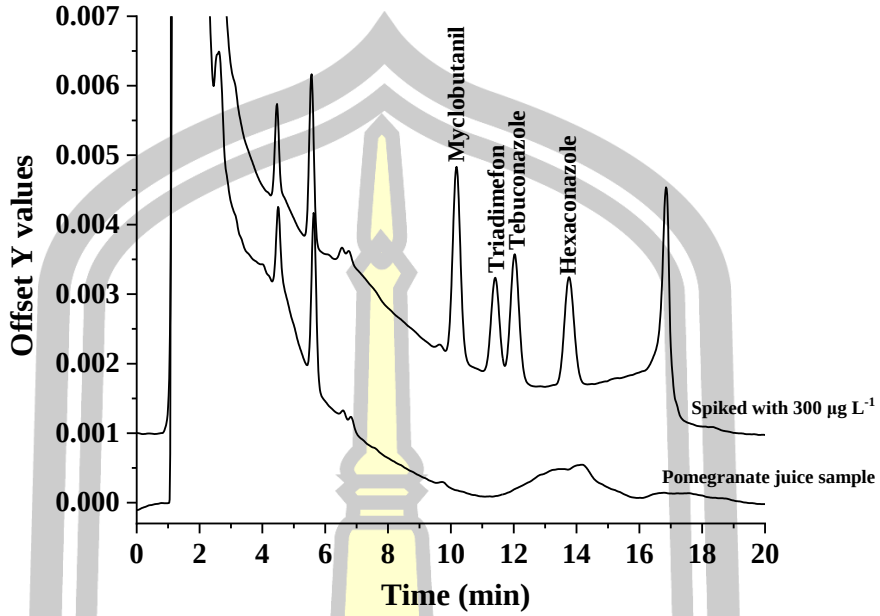

Figure 63 The overlaid chromatograms of pomegranate juice and spiked pomegranate juice sample.

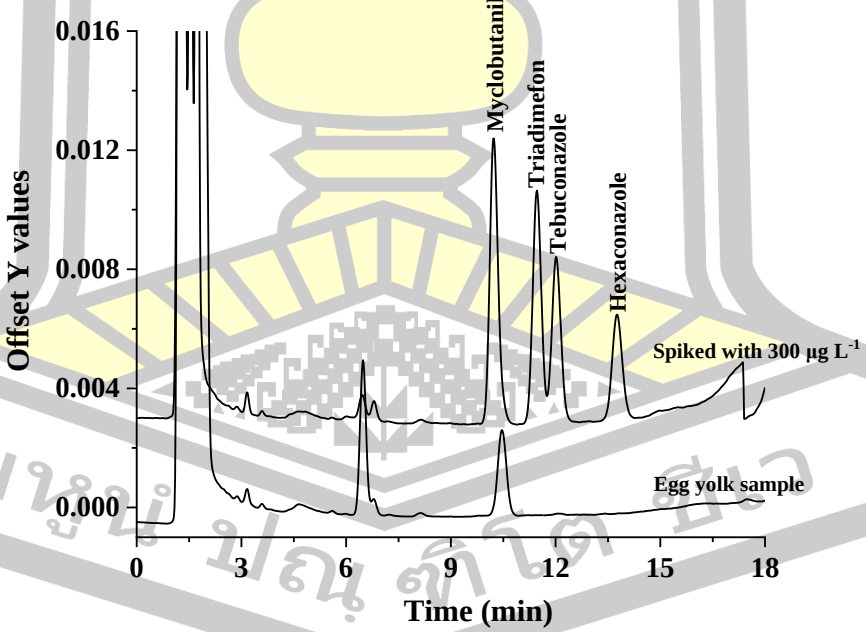

Figure 64 The overlaid chromatograms of egg yolk and spiked egg yolk sample.

Table 26 Recoveries obtained from the analysis of triazole fungicides in real samples (n=3).

Sample	Spiked	MTBC			TDF			TBZ			HCZ		
	(µg L^{-1})	Found (µg L^{-1})	%RR*	%RSD**	Found (µg L^{-1})	%RR*	%RSD**	Found (µg L^{-1})	%RR*	%RSD**	Found (µg L-1)	%RR*	%RSD**
Honey I	0	ND	-	-	ND	-	-	ND	-	-	ND	-	-
	300	198.57	66.17	1.04	275.00	92.41	2.82	297.25	99.72	1.99	285.32	94.12	1.06
Honey II	0	ND	-	-	ND	-	-	ND	-	-	ND	-	-
	300	260.01	86.98	2.47	218.47	72.03	3.12	182.59	60.26	2.60	186.63	62.22	2.57
Passion fruit juice	0	ND	-	-	ND	-	-	ND	-	-	ND	-	-
	300	228.92	76.14	0.84	231.55	77.87	1.80	243.44	81.50	1.82	262.61	87.63	1.20
Pomegranate juice	0	ND	-	-	ND	-	-	ND	-	-	ND	-	-
	300	218.42	72.14	0.71	183.24	61.77	1.78	209.58	69.19	0.20	18	62.98	1.53
Grape juice	0	ND	-	-	ND	-	-	ND	-	-	ND	-	-
	300	218.64	72.50	1.82	188.11	62.65	1.39	200.21	66.16	0.87	191.88	63.59	2.87
Egg yolk	0	ND	-	-	ND	-	-	ND	-	-	ND	-	-
	300	252.02	84.19	0.31	216.22	72.72	0.47	208.60	69.41	1.69	207.88	69.05	1.08

*RR: relative recovery; **RSD: relative standard deviation, ND: not detected.

4.4.5 Comparison of the proposed microextraction method with other sample-preparation methods

Table 26 shows a comparison of the developed microextraction in this work with other published methods [152], [162], [239], [241]. The ionic liquid could be prepared under facile conditions, which simplified the experimental operation, and no complicated instrument was required. Compared to the other sample-preparation methods, the proposed method provided a wide linear calibration range (150-1000 μg L^{-1}), a high precision (less than 5), and acceptable recoveries (61-112) within shorter extraction times for simultaneous extraction determinations for various samples. In conclusion, the proposed microextraction method was demonstrated as a simple, fast, effective, and environmentally friendly technique.

Table 27 Comparisons of the proposed method with other methods for the quantitation of triazole fungicides.

Extraction method	Analytical method	Samples	Adsorbent/Desorbed	Linear Range (μgL^{-1})	Recovery (%)	LOD ($\mu g\ L^{-1}$ or $\mu g\ kg^{-1}$)	EF	%RSD	Ref.
SMMH-d-SPME	HPLC-UV	Water	Fe_3O_4@SiO_2/ACN	5-100 and 2.5-50	90-104	1.0-2.5	40-237	Less than 8%	[243]
MSPE	HPLC-UV	River water	BCDP/ACN-0.1% (v/v) HCOOH	1-1200	82.8-113.2	0.2-0.3	281-283	1.2-4.6	[251]
SBSE	HPLC-DAD	Grape and cabbage	HC-POF/ACN-water	0.1-500	80.7-111	0.022-0.071	49-57	6.4-12.4	[193]
MSPE	LC-MS/MS	Water and fruit juices	GO-PmAP/ACN-water in NaOH	0.001-0.5	80.3-106.3	0.08-2.04 ng g^{-1}	0.45-0.60	2.1-13.4	[241]
Ionic liquid combined with liquid-liquid microextraction	HPLC-DAD	Honey, fruit juices, and egg yolk	IL-ACN	90-500	61-112	30-50	8-11	≤5	This work

** MSPE-HPLC-UV: magnetic solid-phase extraction–high-performance liquid chromatography–ultraviolet detector; SBSE-HPLC-DAD: stir bar sorption extraction–high-performance liquid chromatography–diode array detector; SPME-HPLC-DAD: solid-phase microextraction–high-performance liquid chromatography–diode array detector; MSPE-LC-MS/MS: magnetic solid-phase extraction–liquid chromatography–tandem mass spectrometry; MSPE-HPLC-PDA: micro solid-phase extraction–high-performance liquid chromatography–photodiode array; SMMH-d-SPME: in situ surfactant-mixed metal hydroxide (SMMH); d-SPME: dispersive solid-phase microextraction; *** Fe_3O_4@SiO_2: magnetic nanoparticle; ACN: acetonitrile; BCDP: bridged bisCD-bonded chiral column; HCOOH: formic acid; HC-POF: hydroxyl-containing porous organic framework; GO-PmAP: graphene oxide-poly-3-aminophenol.

4.5 Trace-level determination of triazole fungicides using effervescence-assisted liquid-liquid microextraction based ternary deep eutectic solvent prior to high-performance liquid chromatography

This chapter present the result obtained section describes a development of then extraction method and then prior to high performance liquid chromatography (HPLC). The studied triazole fungicides such as myclobutanil, triadimefon, tebuconazole, and hexaconazole were studied. The second section presents the analytical performance of the proposed method. Finally, apply the proposed method for the analysis of triazole fungicide residues in environmental water (near agricultural area), honey, and bean samples. The results were discussed.

4.5.1 Characterization of Ternary DES (TDES)

FTIR spectra (as shown in Figure 65) were used for characterization of the synthesized TDES. The spectra were obtained in the range of 500-4500 cm^{-1}. In the spectrum in Figure 65(a), the bands located at 3031.03, 2955.81, 2925.13, 2856.54, and 2671.11 cm^{-1} correspond to the vibration bonds of the broad peak due to the O−H stretch superimposed on the sharp band due to the C−H stretch, that at 1705.74 cm^{-1} corresponds to the vibration bonds of the CO stretch, those 1460.74, 1412.72, and 1378.99 cm^{-1} correspond to the vibration bonds of the C−O stretch and O−H bend, and that at 932.79 cm^{-1} corresponds to the vibration bonds of the C−H bend, which are indicators of octanoic acid. In the spectrum in Figure 65(b), the bands located in the areas of 3017.23, 2953.32, 2916.47, 2849.11, 2767.87, 2669.98, and 2636.34 cm^{-1} correspond to the vibration bonds of the O−H and C−H stretch, that at 1692.33 cm^{-1} corresponds to the vibration bonds of the C=O stretch, those at 1467.38, 1429.19, 1410.98, 1352.41, 1326.51, and 1295.60 cm^{-1} correspond to the vibration bonds of the

C−O stretch and O−H bend, and that at 930.11 cm^{-1} corresponds to the vibrations of the O−H bend, which are the indicators of decanoic acid. In the spectrum in Figure 65(c), the bands located at 3031.90, 2953.45, 2911.72, 2847.81, 2666.02, and 2640.71 cm^{-1} correspond to the vibration bonds of the O−H and C−H stretches, that at 1694.50 cm^{-1} corresponds to the vibration bonds of the CO stretch, those at 1470.02, 1431.06, 1302.50, 1275.79, 1247.84, 1219.17, and 1193.30 cm^{-1} correspond to the vibration bonds of the C−O stretch and O−H bend, and that at 915.94 cm^{-1} corresponds to the vibrations of the O−H bend, which are the indicators of dodecanoic acid; these wavenumbers of the three components show the unique FTIR spectra of carboxylic acids. The FTIR spectra in Figure 65(d) shows the spectrum of solvent synthesized TDES. One of the significant changes was a decrease in the vibration signal found in the 2955.57−2670.75 cm^{-1} region, possibly related to the displacement of the O−H and C−H bands in forming hydrogen bonds between octanoic acid, decanoic acid, and dodecanoic acid. This combination can be accredited to the slight modification in the force constant generated by the reduced electron cloud density, which strongly indicates hydrogen binding in the TDES. Moreover, the FTIR spectrum of TDES was obtained after the extraction (Figure 66). The results showed that the structure of TDES did not change after extraction.

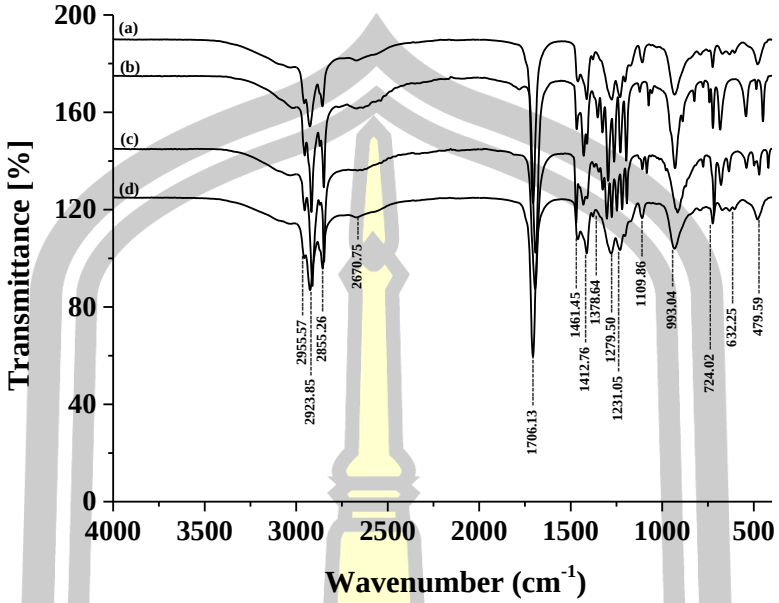

Figure 65 FT-IR spectra of (a) octanoic acid, (b) decanoic acid, (c) dodecanoic acid, and (d) ternary deep eutectic solvent when was formed.

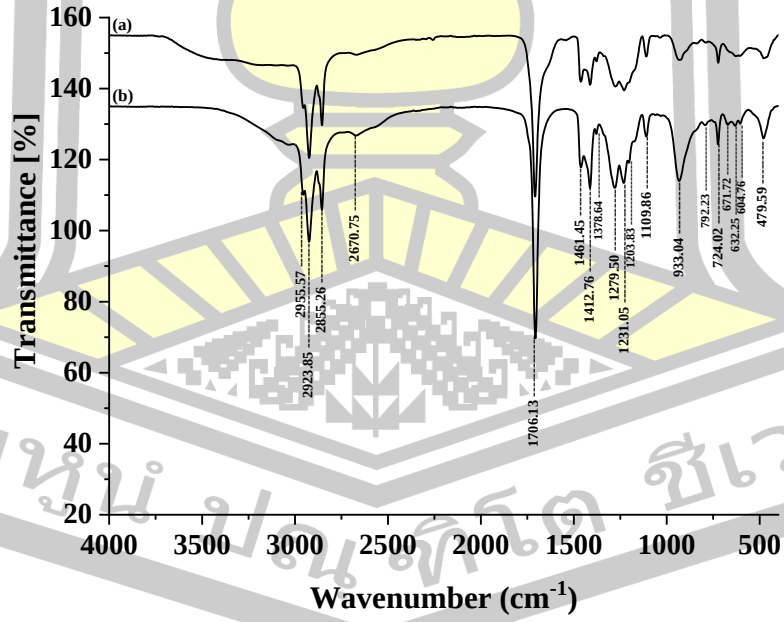

Figure 66 FT-IR spectra of (a) standard with TDES and (b) solvent synthesized TDES.

4.5.2 Optimization of effervescence-assisted liquid-liquid microextraction based on TDES (EA-LLME-TDES) conditions

To obtain high extraction efficiencies of studied triazoles, several experimental parameters were investigated and optimized via the univariate method. A mixed standard solution containing 100 μg L^{-1} of each standard was used to examine the extraction performance of the proposed microextraction method under different experimental conditions. All optimization experiments were carried out in triplicate (n = 3). Peak areas were used to evaluate the extraction efficiency of the developed procedure.

4.5.2.1 Effect of mole ratio and volume of TDESs

The appropriate extracting solvent is important because this is a significant parameter in the proposed method. Extracting solvents should have low viscosity, high hydrophobicity, and melting point below room temperature [250]. TDESs as extracting solvent were synthesized through mixing various molar ratios of the hydrogen bond donor (HBD) and hydrogen bond acceptor (HBA). The fatty acids with a shorter alkyl chain (octanoic acid or decanoic acid) act as HBA, while those with the longest one (dodecanoic acid) act as HBD. It is worth noting that use of acids smaller than octanoic acid (hydrophilic acids) was not considered due to the chemical instability of the formed DES upon contacting with water (acids leach to water) [250]. The results are shown in Figures 67-69. As a conclusion, TDES with the mole ratio of 4:1:1 (octanoic acid : decanoic acid : dodecanoic acid) gave the highest extraction efficiency. All the eutectic solvents gave a recovery higher than that of their own constituents (octanoic acid and decanoic acid) owing to the higher affinity of the analytes to the hydrophobic TDES. Finally, TDES with the mole ratio of 4:1:1

(octanoic acid : decanoic acid : dodecanoic acid) was selected as the best extracting solvent for separation of the studied compounds. Moreover, volumes of TDES were studied (50, 100, 150, and 200 µL). The results in Figure 70 demonstrate that the extraction efficiency increased with the volume of TDES from 50 to 100 µL and then decreased due to the dilution effect. As a result, 100 µL of TDES was found to be sufficient for successful extraction of the analytes at the concentration test and it was used for the subsequent experiment.

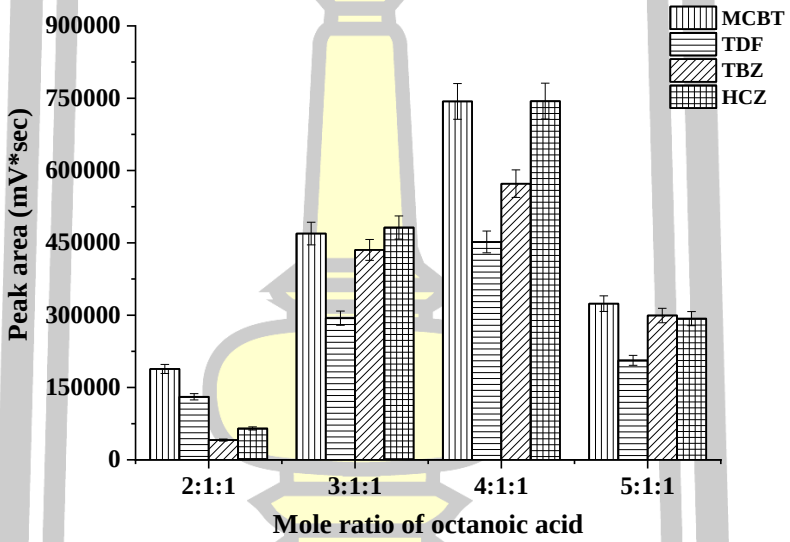

Figure 67 Effect of mole ratio of octanoic acid (octanoic acid: decanoic acid: dodecanoic acid).

Conditions: 100 µL of TDES (mole ratio 4:1:1); 0.5 %w/v of $NaHCO_3$; 50 µL of acetonitrile (dissolving solvent) (sample volume 10 mL, 100 µg L^{-1} of each triazole fungicide).

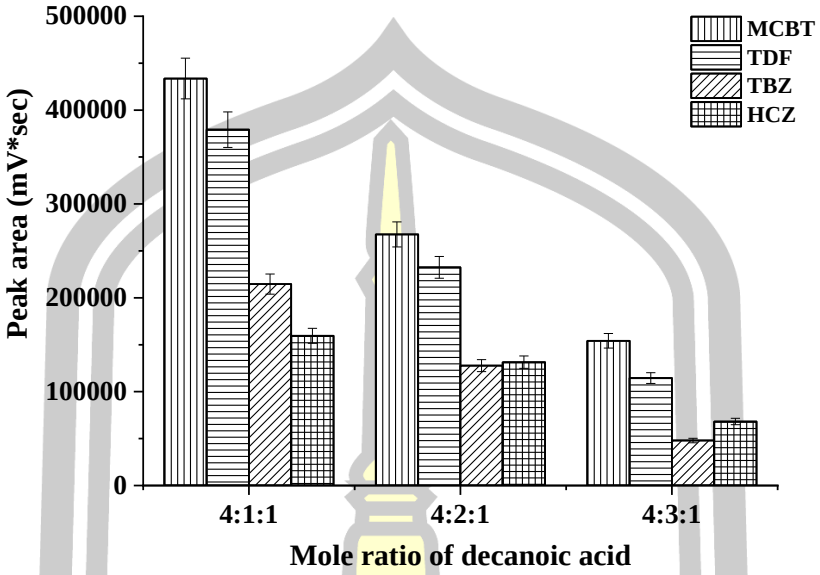

Figure 68 Effect of mole ratio of decanoic acid (octanoic acid: decanoic acid: dodecanoic acid).

Conditions: 100 µL of TDES (mole ratio 4:1:1); 0.5 %w/v of $NaHCO_3$; 50 µL of acetonitrile (dissolving solvent) (sample volume 10 mL, 100 µg L^{-1} of each triazole fungicide).

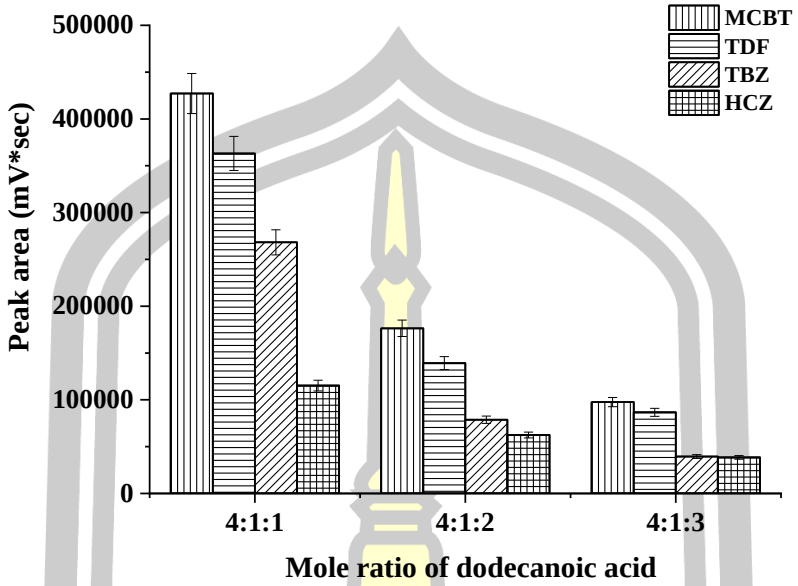

Figure 69 Effect of mole ratio of dodecanoic acid (octanoic acid: decanoic acid: dodecanoic acid).

Conditions: 100 µL of TDES (mole ratio 4:1:1); 0.5 %w/v of $NaHCO_3$; 50 µL of acetonitrile (dissolving solvent) (sample volume 10 mL, 100 µg L^{-1} of each triazole fungicide).

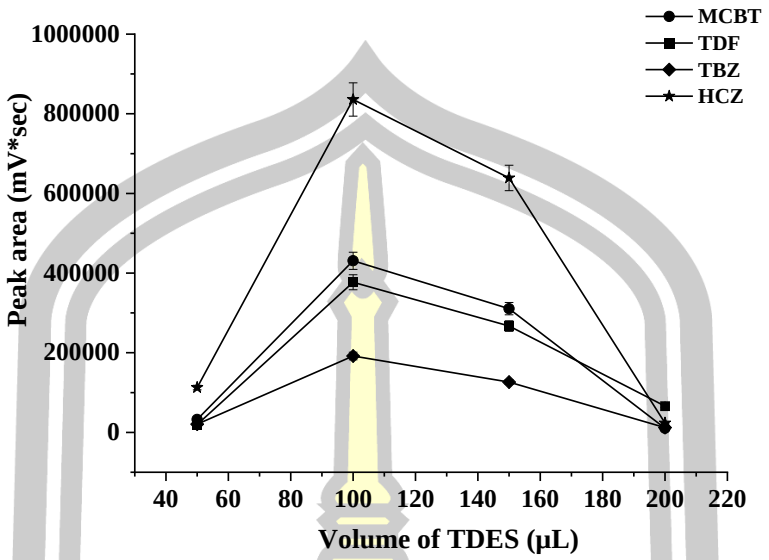

Figure 70 Effect of volume of TDES (µL)

Conditions: 100 µL of TDES (mole ratio 4:1:1); 0.5 %w/v of $NaHCO_3$; 50 µL of acetonitrile (dissolving solvent) (sample volume 10 mL, 100 µg L^{-1} of each triazole fungicide).

4.5.2.2 Concentration of effervescent agent

To induce the mass transfer (without another agitator), the main necessities of an effective effervescent process are an effervescency agent (CO_2 source) and a proton donor agent, which can be less-alkali compounds (sodium carbonate, sodium bicarbonate, etc.) [252]. In this work, sodium bicarbonate ($NaHCO_3$) was used. The concentration of $NaHCO_3$ was investigated (0.2, 0.5, 1.0, 3.0 %w/v); the results are shown in Figure 71. When 0.2 %w/v of $NaHCO_3$ was added, the final phase was not obtained. A high extraction efficiency for all analytes was obtained when 0.5 %w/v of $NaHCO_3$ was added. Therefore, further studies were done using 0.5 %w/v of $NaHCO_3$.

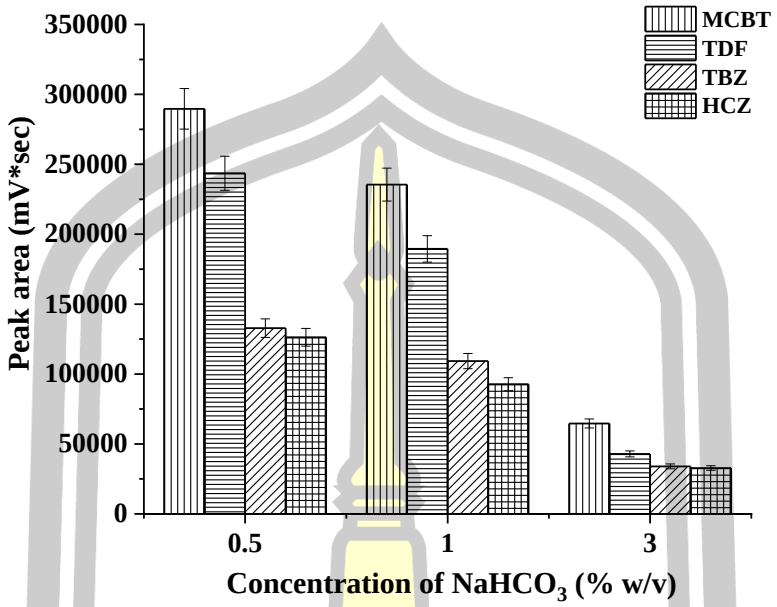

Figure 71 Effect of concentration of $NaHCO_3$ (%w/v) on extraction efficiency. Conditions: 100 µL of TDES (mole ratio 4:1:1); 0.5 %w/v of $NaHCO_3$; 50 µL of acetonitrile (dissolving solvent) (sample volume 10 mL, 100 µg L^{-1} of each triazole fungicide).

4.5.2.3 Kind and volume of dissolving solvent

In order to reduce the viscosity of the extract before injecting it to the chromatographic system, different dissolving solvents were studied including methanol, ethanol, isopropanol, and acetonitrile (shown in Figure 72). It was found that acetonitrile gave a high extraction efficiency in terms of peak area. Therefore, acetonitrile was used, and the volume of acetonitrile was evaluated in the range of 25, 50, 75, 100, 150, and 200 µL (shown in Figure 73). It was found that 25 µL of acetonitrile could not dissolve the TDES phase. The highest response was obtained when 50 µL of acetonitrile was added. Therefore, 50 µL of acetonitrile was used.

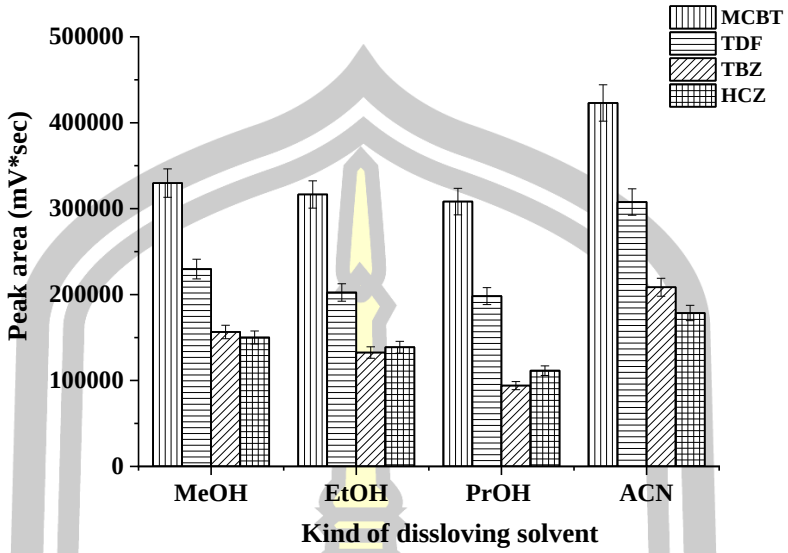

Figure 72 Effect of kind of dissolving solvent on extraction efficiency. Conditions: 100 µL of TDES (mole ratio 4:1:1); 0.5 %w/v of $NaHCO_3$; 50 µL of acetonitrile (dissolving solvent) (sample volume 10 mL, 100 µg L^{-1} of each triazole fungicide).

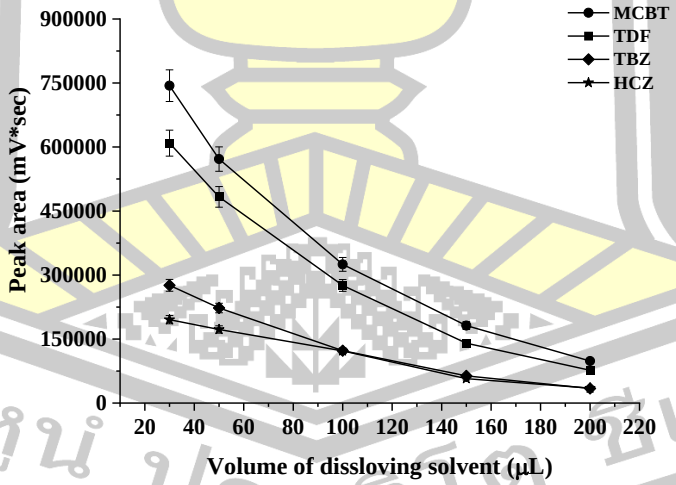

Figure 73 Effect of kind of dissolving solvent on extraction efficiency. Conditions: 100 µL of TDES (mole ratio 4:1:1); 0.5 %w/v of $NaHCO_3$; 50 µL of acetonitrile (dissolving solvent) (sample volume 10 mL, 100 µg L^{-1} of each triazole fungicide).

4.5.3. Analytical performance and method validation

In order to evaluate the proposed method, some analytical parameters such as linearity, limit of detection (LOD), limit of quantitation (LOQ), recovery, and precision were determined under optimal conditions. The analytical performances of the proposed method are summarized in Table 27. After preconcentration by the proposed microextraction method, the linearity ranged from 3 to 1000 μg L^{-1} for all triazoles, with the coefficient of determination (R^2) greater than 0.99. The LODs and LOQs were evaluated based on the signal-to-noise ratios of 3 and 10, respectively. The LODs and LOQs were in the range of 0.3-1.0 and 3-10 μg L^{-1}, respectively. The precisions were calculated from the relative standard deviations (RSDs) of retention time and peak area obtained from intra- (n = 3) and inter-day (n = 3 × 5) experiments, which were greater than 1.66 and 13.52%, respectively. Moreover, enrichment factors (EFs) were calculated from the analyte concentration in the final phase (C_{sed}) and the initial concentration in the analyte in the aqueous sample solution (C_0), which ranged from 112 to 142 folds. Chromatograms of the studied triazoles obtained by direct HPLC and the proposed microextraction method are shown in Figure 74-76. After the microextraction process, the chromatographic signals were increased.

A matrix-match calibration method was used to study the matrix effect of real-sample analysis. The matrix-match calibration was investigated by spiking each target compound in real samples in the range of 50-500 μg L^{-1}. All compounds showed good linearity with R^2 greater than 0.9. In addition, the matrix effect (ME, %) of each calibration graph in the soil sample was calculated as follows the equation:

$$ME\ (\%) = [(S_m/S_s) - 1] \times 100$$

where S_m and S_s are the slopes of the calibration curve in the matrix and solvent, respectively. Generally, an ME between 80 and 120% shows no matrix effects, an ME between 50 and 80% or between 120 and 150% shows minor matrix effects and an ME <50 or >150% indicates major matrix effects. ME values ranged from -65.1 to -75.6% in water samples, -68.1 to -78.6% in honey samples, and -41.1 to -70.6% in bean samples. The results indicate that the honey and bean samples showed major effects while the water samples showed minor effects for triazole analysis.

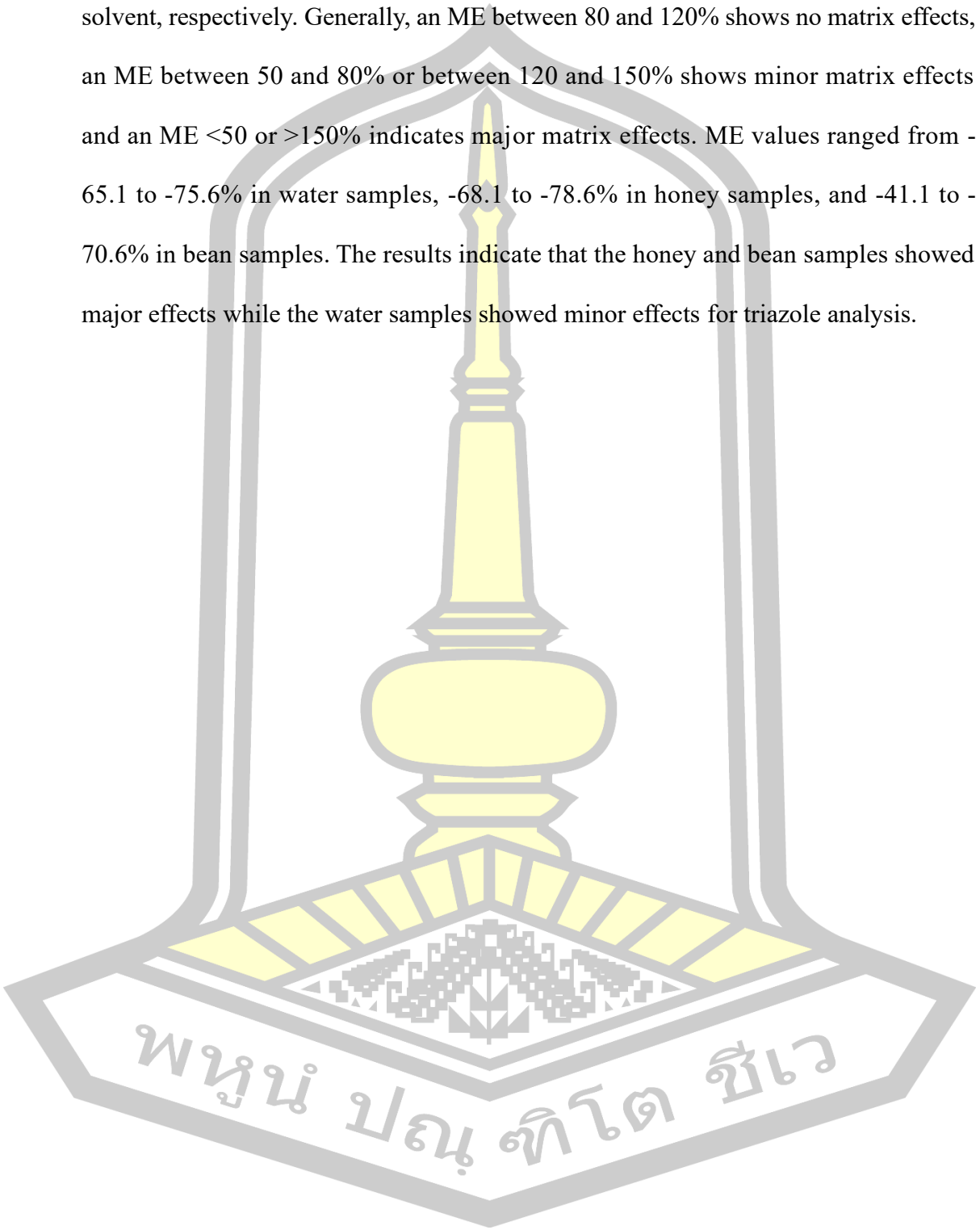

Analyte	Linear range (µg L^{-1})	Linear equation	R^2	LOD (µg L^{-1})	LOQ (µg L^{-1})	Intraday Precision (n = 5), RSD (%)		Intraday Precision (n = 5), RSD (%)		EF
						t_R	Peak area	t_R	Peak area	
Myclobutanil	3-1000	y = 1E+06x + 56742	0.9979	0.3	3.0	1.06	4.35	1.21	4.08	142.04
Triadimefon	3-1000	y = 2E+06x + 59918	0.9989	0.3	3.0	0.84	2.65	0.95	4.02	139.13
Tebuconazole	3-1000	y = 2E+06x + 5323.4	0.9979	0.3	3.0	0.39	4.02	0.43	4.79	112.60
Hexzaconazole	3-1000	y = 924257x + 5964.9	0.9988	1.0	10.0	0.15	4.70	0.31	4.69	134.70

Table 28 Analytical performance of the proposed method for four different triazole fungicides (n=3).

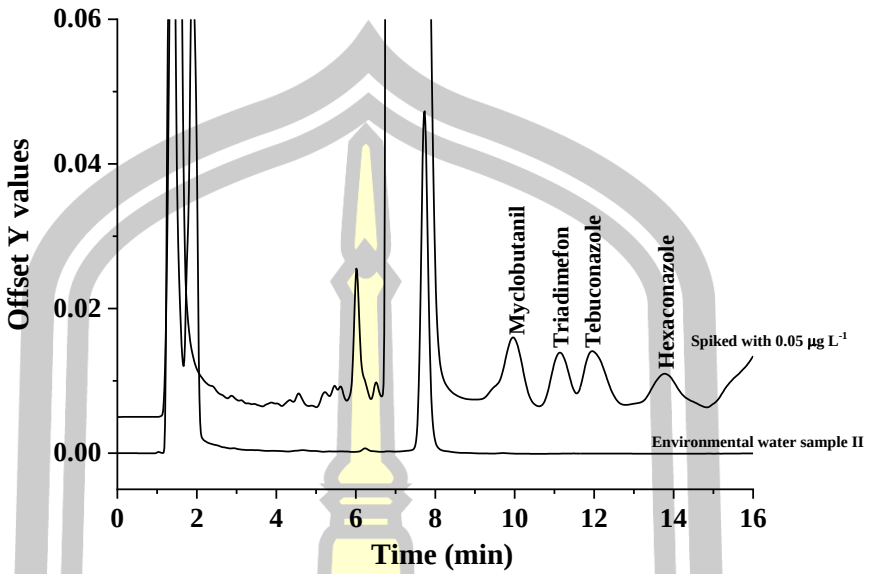

Figure 74 The overlaid chromatogram of environmental water sample II.

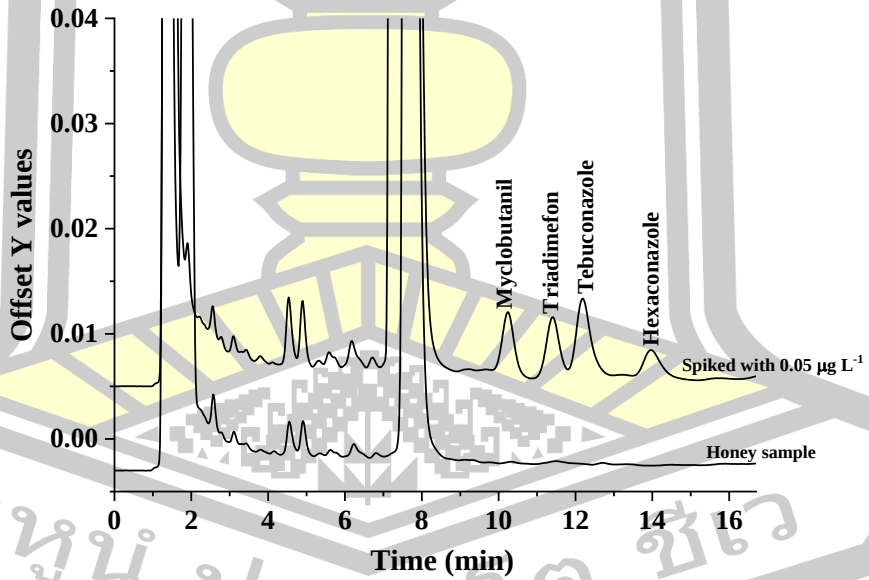

Figure 75 The overlaid chromatogram of honey sample.

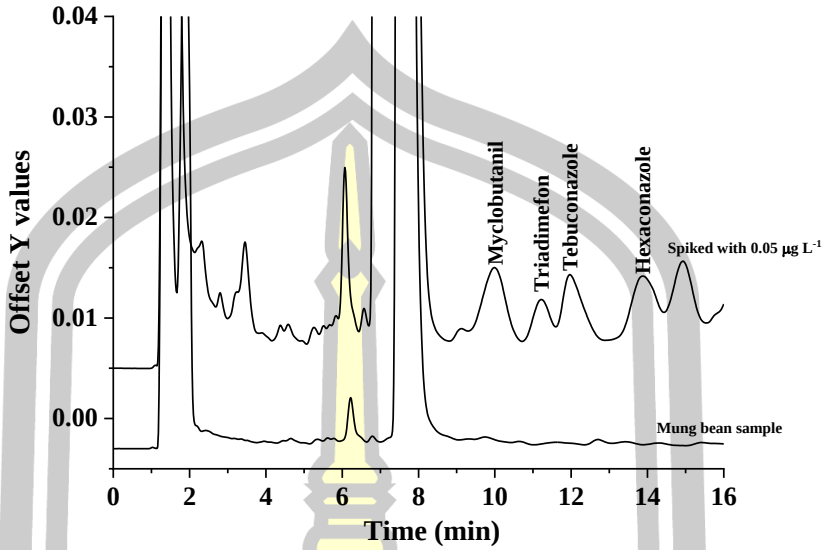

Figure 76 The overlaid chromatogram of mung bean sample.

4.5.4 Application to real samples.

The proposed microextraction procedure was then applied for analysis of TF in water, honey, and bean samples. Prior to their analysis, each sample was prepared and extracted by the proposed microextraction. On the other hand, matrix-match calibration was used for determination of the studied compounds in real samples to compensate for the matrix effect. It was found that no residues of the investigated TFs were detected in all studied samples (as shown in Table 28). In order to investigate the accuracy of the proposed method, the water, honey, and bean samples were spiked with 50 µg L^{-1} of each triazole before applying the proposed microextraction procedure. The recoveries of the studied triazoles (as shown in Table 28) were obtained in the range of 82-106% with an RSD less than 4.89.

Table 29 The determination of triazole fungicides and recovery in studied various samples (n = 3).

Analyte	Spiked ($\mu g\ L^{-1}$)	Environmental water sample I			Environmental water sample II			Soy bean sample			Mung bean sample			Red bean sample			Honey sample		
		Found ($\mu g\ L^{-1}$)	%R	%RSD	Found ($\mu g\ L^{-1}$)	%R	%RSD	Found ($\mu g\ L^{-1}$)	%R	%RSD	Found ($\mu g\ L^{-1}$)	%R	%RSD	Found ($\mu g\ L^{-1}$)	%R	%RSD	Found ($\mu g\ L^{-1}$)	%R	%RSD
MCBT	0	ND*	-	-	ND*	-	-	ND*	-	-	ND*	-	-	ND*	-	-	ND*	-	-
	50	43.7	87.4	1.05	51.8	103.7	1.89	47.6	103.7	1.97	47.9	95.8	1.39	44.1	88.2	0.11	47.7	95.4	0.99
TDF	0	ND*	-	-	ND*	-	-	ND*	-	-	ND*	-	-	ND*	-	-	ND*	-	-
	50	41.32	82.7	0.88	44.4	88.8	2.36	46.2	92.3	1.71	45.8	91.6	0.59	42.6	85.1	0.67	41.7	83.5	0.78
TBZ	0	ND*	-	-	ND*	-	-	ND*	-	-	ND*	-	-	ND*	-	-	ND*	-	-
	50	53.25	106.5	1.35	49.4	98.8	2.07	48.9	97.8	1.92	50.8	101.6	1.36	48.9	97.7	1.70	47.5	94.9	1.58
HCZ	0	ND*	-	-	ND*	-	-	ND*	-	-	ND*	-	-	ND*	-	-	ND*	-	-
	50	41.5	82.9	4.89	49.1	98.2	4.13	49.3	98.5	2.01	47.5	95.0	0.78	46.4	92.8	4.58	47.5	95.1	2.70

*ND: Not detect.

4.5.5 Comparison of the proposed method with other previously reported methods

To highlight the emphasizing purposes of the developed method, some major characteristics were compared with those obtained from other reported methods [253], [254], [255], [256], [257]as listed in Table 29. In comparison with other methods, the investigated method has various advantages, such as the use of a green extraction solvent (TDES), less amount of solvent (100 μL), and avoidance of the use of a disperser solvent. The sensitivity of the present method is greater than that of previous approaches with a short extraction time (<1 min). Additionally, the dispersion of extractant and extraction of analytes was performed by using the proposed technique without the need for extraction equipment. Moreover, the proposed method exhibits a favorable linear range, a low LOD, acceptable recovery, and a high EF, demonstrating that the sample preparation in this work is substantially more efficient and selective, followed by the relatively simple and inexpensive HPLC-DAD technique. In addition, the precision and accuracy of the proposed method fit for purpose adhered to the AOAC acceptability criteria. The comparison clearly highlights the advantages of the proposed microextraction method.

Table 30 Comparisons of the proposed method with other methods for the quantitation of triazole fungicides.

Method	Linear range	Extraction solvents	Solvent usage	Extraction time	LOD	%Recovery	Ref.
SDES-HLLME-HPLC-DAD	0.001–10 μg mL^{-1}	SDES	110 μL	3.45 min	0.089–0.351 ng mL^{-1}	90.6-110.9	[257]
DES-UALPME-UHPLC-QTOF-MS	5-1000 ng mL^{-1}	DES	800 μL	15 min	0.5–4.0 ng mL^{-1}	65-107	[256]
DES-DLLME-liquid polymer-GC-μECD	0.004-100 μg L^{-1}	DES	450 μL	4 min	0.001-100 μg L^{-1}	60.5-105.0	[255]
DES-HS-SDME-GC-FID	0.01–100 mgL^{-1}	DES	2 μL	30 min	0.08-1.0 μg L^{-1}	93-97	[254]
DES-UAE-MSPE-HPLC-DAD	0.1–50 μg mL^{-1}	DES	2 mL	11 min	0.02–0.05 μg mL^{-1}	76.09-97.96	[253]
TDES-DLLME-HPLC-DAD	3-1000 μg L^{-1}	TDES	100 μL	< 1 min	0.3-1.0 μg L^{-1}	70.3-106.5	This work

* SDES-HLLME-HPLC-DAD : Switchable deep eutectic solvents-homogeneous liquid-liquid microextraction-high performance liquid chromatography-diode array detector, DES-UALPME-UHPLC-QTOF-MS : Deep eutectic solvent-ultrasound-assisted liquid-phase microextraction-quadrupole time-of-flight mass spectrometry, DES-DLLME-liquid polymer-GC-μECD : Deep eutectic solvent-dispersive liquid-liquid microextraction based liquid polymer-gas chromatography-micro-electron capture detector, DES-HS-SDME-GC-FID : Deep eutectic solvent-head-space single-drop microextraction- gas chromatography-flame ionization detector, DES-UAE-MSPE-HPLC-DAD : Deep eutectic solvent-ultrasound-assisted extraction-magnetic solid-phase extraction-high performance liquid chromatography-diode array detector, TDES-DLLME-HPLC-DAD : Ternary deep eutectic solvent- dispersive liquid-liquid microextraction- high performance liquid chromatography-diode array detector.

CHAPTER 5

CONCLUSION

A simple, fast and inexpensive micro-solid phase extraction (μSPE) and solid phase extraction (SPE) procedure coupled with high performance liquid chromatography was proposed to determine five triazole fungicides (TFs), including myclobutanil, triadimefon, tebuconazole, hexaconazole, and diniconazole in several real samples. An eco-friendly and selective sorbent was prepared using many sources of sorbent via modification and functionalization of bio- and synthesis sorbent such as *Moringa Oleifera* (MO) seed, Coconut husk fiber (CHF), and carbon dot (CD). In the first part, *Moringa oleifera* seeds was modified as efficient bio-sorbent for preconcentration and determination of TFs prior to HPLC analysis. Since *Moringa oleifera* seed as a sorbent could be applied to other samples, it represents an excellent alternative cation exchange medium, due to its facility of operation and obtainment. The *Moringa oleifera* seeds were shown to be an efficient adsorbent material of natural origin, thereby contributing to the development of low-cost analytical methodologies which fall within the current concept of clean chemistry. The μSPE procedure, the optimum conditions were 10 mL sample, 0.1 g biosorbent, 30 μL formic acid (HCOOH), adsorption step: vortex 30 sec and centrifugation at 3000 rpm for 5 min, 200 μL of acetonitrile and desorption step: vortex 15 sec and centrifugation at 1500 rpm for 5 min. The extraction was then analyzed by Purospher® STAR RP-18 endcapped (4.6 × 150 mm, 5 μm) as an analytical column at room temperature. The injection volume was 20 μL. For data processing, Empowers 3 software was used. Chromatographic analysis using isocratic elution with 50 %v/v acetonitrile in water as the mobile phase at a flow rate of 1.0 mL min^{-1} was used to separate the

studied TF residues. Separation of five TF residues was achieved less than 20 min. Under the optimum conditions, this method showed satisfactory low method detection limit (MDL) were 30-50 μg L^{-1} for all target analytes which below the acceptable maximum residue limits (MRLs) for triazole fungicides and good accuracy was obtained. This method provided wide linear range between 10 and 500 μg L^{-1} (coefficient of determination greater than 0.99), and good precisions with relative standard deviations greater than 5.0%. The developed method was successfully applied for analysis of triazole fungicides in environmental water, honey and fruit juice samples. Acceptable relative recovery ranging from 70.00 to 112.00%. This method could be used for comprehensive use of Moringa oleifera seed. Moreover, to our knowledge, this is the first time for applicability of *Moringa oleifera* seed in the preconcentration of triazole fungicides analysis.

In the second part, surfactant modified coconut husk fiber as a green sorbent for trace determination of triazole fungicides was developed. The surface of modified CHF will become hydrophobic, which favors the adsorption of non-ionic organic compounds onto the sorbents. CHF modification also enhanced the mechanical properties of cellulose and lignocellulosic while enhancing the extraction performance of the biosorbent materials. Meanwhile, the CHF as the biosorbent in μSPE method not only reduced the agricultural waste device but also resolved the use of expensive commercial adsorbents in the extraction process, The CHF-μSPE assessment was established for analyzing some trace triazole fungicides in various samples followed by HPLC. This method showed good relative recoveries, high sensitivity, and satisfied repeatability. Furthermore, this method indicated several benefits including simplicity, the use of a small amount of sample and organic solvent, relatively low cost, easy

elution of analytes, and short time analysis. Ultimately, the analytical method can be applied to the determination of trace triazole fungicides from other complex samples. The green analytical way of μ-SPE using CHF is demonstrated to be more tested and employed in the advancement of biosorbent materials in different fields.

In the third part, the Fabrication of superhydrophobic melamine sponge functionalized with carbon dots was investigated and used as an effective adsorbent for the extraction of triazole fungicides. Carbon dot (CD) embedded melamine sponge method was successfully prepared by a simple and facile method by using citric acid (CA) as a precursor. CA-CD was used not only as an adsorption assistant but also as an adhesive in the preparation of functionalized sponge materials. Melamine sponge was selected as an adsorbed base material in the micro-SPE to simplify the separation procedures with superficial one-step infiltration, excellent mechanical stability, and low cost. This study provides a new avenue for exploring other functionalized coating adsorbent materials using CA-CD as a coater and for preparing new functionalized sponges to detect other contaminants in different complex matrix samples. The carbon dot embedded melamine sponge method as a sorbent in micro-SPE assessment was established for analysis of trace level contamination of triazole fungicides in fungi samples followed by HPLC detection. It is conceivable that CA-CD can be operative not only in case of triazoles but also for other analytes which can interact with carbon dots. This developed approach, with its green procedure, could be enhanced by performing in-situ strategy, eradicating the utilization of hazardous reagents, and replacing them with their green alternatives.

The developed sample pretreatment procedure based on liquid phase microextraction (LPME) of triazole fungicides from various samples prior to their

determination by HPLC analysis is simple, fast, and meets most of the green principles since it is a multianalyte method and it includes the application of a reduced volume of a sample, reagent, and non-hazardous extractant solvent (i.e., ionic liquid and deep eutectic solvent), among other. In the first part, the present study, an in-situ extraction and preconcentration method using an ionic liquid for separation and preconcentration of triazole fungicides in honey, fruit juice, and egg samples was performed prior to high-performance liquid chromatographic analysis. The halide anion of tributylhexadecylphosphonium bromide ($[P_{44412}]Br$) and potassium hexafluorophosphate (KPF_6) was used for the formation of the hydrophobic ionic liquid. In the proposed microextraction method, forming the immiscible IL extraction phase and the transfer of analytes occurred simultaneously. The metathesis reaction and extraction were accomplished in single step, making the transfer of the analytes into the extracting phase very quick and efficient. In-situ metathesis of hydrophobic IL and liquid-liquid microextraction procedure, the optimum conditions were 0.01 g of $[P_{44412}]Br$, 0.01 g of KPF_6, centrifugation at 4500 rpm for 10 min, 200 µL acetonitrile. The extraction was then analyzed by Purospher® STAR RP-18 endcapped (4.6 × 150 mm, 5 µm) as an analytical column carried out at room temperature. The injection volume was 20 µL. For data processing, Empowers 3 software was used. Chromatographic analysis using isocratic elution with 50 %v/v acetonitrile in water as the mobile phase at a flow rate of 1.0 mL min^{-1} was used for separation of the studied TFs. Separation of five TFs was achieved less than 20 min. Under the optimum conditions, this method provided a good linear range in the range of 90-1000µg L^{-1} with correlation coefficient higher than 0.99. Low limit of detection was in the range of 30-50µg L^{-1} and limit of quantification was in the range of 90-150 µg L^{-1} with RSD

below 3.5%. The enrichment factors ranged from 8.53 to 12.26. The extraction recoveries of all TFs in the spiked samples extracted under the same conditions were in a range of 59.71-85.82 % with RSDs less than 5 %. The proposed method provided good repeatability, a wide linearity range, and an acceptable extraction recovery for each compound, and matrix effects did not interfere with the quantification process. Therefore, the proposed method is recommended as a fast, simple, sensitive, and environmentally friendly sample-preparation technique.

In second part, a simple and sensitive preconcentration method, namely, effervescence assisted liquid-liquid microextraction based on the ternary deep eutectic solvent method, was developed for enrichment of triazole fungicide residues prior to their determination by high-performance liquid chromatography coupled with UV detection. TDESs (as extractant) were prepared by combination of octanoic acid, decanoic acid, and decanoic acid in mole ratio of 4:1:1 at 65 $^{\circ}$C. The effervescence-assisted LLME based TDES procedure, the optimum conditions were 10 mL sample, 100 µL of TDES (extracting solvent), 0.05 g of sodium hydrogen carbonate (effervescence precursors), extraction time 20 sec, 30 µL of acetonitrile (dissolving solvent). The extraction was then analyzed by Purospher® STAR RP-18 endcapped (4.6 × 150 mm, 5 µm) was used as an analytical column carried out at room temperature. The injection volume was 20 µL. For data processing, Empowers 3 software was used. Chromatographic analysis using isocratic elution with 50 %v/v acetonitrile in water as the mobile phase at a flow rate of 1.0 mL min^{-1} was used for separation of the studied TFs. Separation of five TFs was achieved less than 20 min. Under the optimum conditions, the proposed method showed good linearity within the range of 1-1000 µg L^{-1}with a coefficient for determination (R^2) greater than 0.997. The

low limits of detection (LODs)were in the range of 0.3-1.0 μg L^{-1}. The precisions were assessed from the relative standard deviations (RSDs) of retention time and peak area obtained from intra- (n=3) and inter-day (n=5 ×5) experiments, which were greater than 1.21 and 4.79%, respectively. Moreover, the proposed method provided high enrichment factors ranging from 112 to 142 folds. A matrix-match calibration method was used for analysis of real samples. Finally, the developed method exhibited good linearity, high sensitivity, and satisfactory accuracy and precision. And this method was successfully applied for determination of the triazole fungicide in environmental water (near agricultural area), honey, and bean samples, and it represents a promising alternative method for analysis of triazoles. The recoveries of the studied triazoles were obtained in the range of 82−106% with an RSD less than 4.89.

Appendix

Research aboard

Project: Analysis of PFAS in drinking water and fish samples

Under the cooperation of Assoc. Prof. Dr. Jitlada Vichapong (Mahasarakham University) and Prof. Dr. Diana S. Aga (University at Buffalo, New York)

Between 29 Nov 2023 to 29 July 2024

1. Analysis of PFAS in drinking water and fish samples

Per- and poly-fluoroalkyl substances (PFAS) are synthetic fluorinated compounds produced since the 1940s [258]. PFAS comprises a fully fluorinated carbon chain of typically four to sixteen carbon atoms and an acidic functional group, such as carboxylic acid and sulfonic acid [259] toward new fluorinated compounds possessing one or more perfluoroalkyl ($-C_nF_{2n}-$) moieties. The extraordinary stability of carbon-fluorine bonds is of significant importance due to their unique chemical and physical properties, such as resistance to temperature, chemicals, oil, stains, grease, water, and surfactant characteristics [260]. These substances have been widely used in various industrial and commercial applications, including food packaging, adhesive, fire-fighting foams, paints, cleaners, textiles, cosmetics, clothing, raincoats, non-stick cooking surfaces, insulation of electrical wire materials, and so on [261], [262], [263]. PFAS can be entered into the environment during production and application procedures. As a result, PFAS have been found to contaminate environments such as soil and water and the bioaccumulation of these compounds in humans and animals such as birds, fish, and seafood [264]. The two most studied PFAS, perfluorooctanoic acid (PFOA) and perfluorooctane sulfonic acid (PFOS) were voluntarily phased out of manufacturing in the U.S. starting in 2000–2002 [265]. These compounds are

associated with the nervous, reproductive, metabolic, and hormonal systems and are carcinogenic to humans. For humans, drinking water, fresh food, and dietary exposure have been recognized as the main entrance pathways for the general population even if occupational exposure has been also pinpointed. Once an individual is exposed to these chemicals, they are able to bind to blood proteins and accumulate in blood-rich tissues such as the liver and kidney[266].

In the early stages of PFAS research, analytical methods were developed to detect the original PFAS classes, such as perfluorooctane sulfonic acid (PFOS) and perfluorooctanoic acid (PFOA), in various matrices including air, water, solids, human samples, wildlife, food, and consumer products [267]. As manufacturing has shifted toward alternative compounds, recent research has focused on identifying new PFAS and developing methods to detect, capture, and characterize these emerging molecules. However, creating cost-effective and environmentally sustainable analytical techniques capable of covering a broad range of PFAS species remains a significant challenge [268]. Attention was also paid to the significance of inter-laboratory comparisons and quality assurance using certified reference materials, as these methods must address a diverse range of compounds in complex matrices. Numerous studies have highlighted advancements in high-resolution mass spectrometry (HRMS) techniques and their effective application in PFAS identification and analysis [268], [269]. Emerging PFAS have been discovered through the suspected and non-targeted screening of environmental [270], water [271], sediments, and biological samples [272].

This work is focused on drinking water and fish samples, In the United States, the 1996 amendments to the Safe Drinking Water Act [273] mandate the US

Environmental Protection Agency (USEPA) to safeguard public health by setting drinking water standards. As part of this responsibility, the USEPA compiles a Contaminant Candidate List (CCL) every five years to identify unregulated chemicals and microorganisms of potential health concern that are known or expected to occur in public water systems. The fourth list (CCL4), finalized in 2016 [274], includes 97 chemicals, among which are perfluorooctanoic acid (PFOA) and perfluorooctane sulfonic acid (PFOS). One of the key criteria for determining whether a substance should be regulated is its frequent detection in drinking water at levels that pose a risk to public health. Similarly, in the U.S., short-chain PFAS are defined as perfluorosulfonic acids with less than six carbons and perfluorocarboxylic acids with less than eight carbons [275]. Contrastingly, long-chain PFAS refers to compounds with greater carbon chain lengths including PFOA and PFOS. In some locations, the highest PFOS concentrations have been found in prey species, such as aquatic and insects, potentially due to differential contamination source signatures between trophic levels [276]. Polyfluoroalkyl substances are less stable or persistent relative to perfluoroalkyl substances; many polyfluoroalkyl substances can degrade and are precursors to perfluoroalkyl substances. Higher biotransformation is assumed to be more likely relative to lower trophic levels, which can confound bioaccumulation patterns[277]. Biotransformation, along with recently increased use of short chain PFAS in industry, may also be responsible for the wide distribution of these compounds, such as PFBS and perfluorobutanoic acid (PFBA), in the environment. PFAS biomagnification and biotransformation are not only important to examine at the community-level, but also inform how organisms may be exposed and affected [276]. The toxic effects of various PFAS have been documented, primarily in fish.

However, the fate, transport, accumulation, and full spectrum of toxicity of these compounds remain poorly understood. In addition, PFAS contamination can adversely affect fish tissue health, leading to increased liver lesions and potentially reduced liver function [278]. Among long-chain PFAS, perfluorooctane sulfonate (PFOS) and perfluorooctanoic acid (PFOA) have received significant research attention because of their hepatotoxic, carcinogenic, developmental, reproductive, and neurotoxic effects in animals [276], [278]. Toxicity also varies with PFAS chain length. For example, acute toxicity values decrease with shorter carbon chains when comparing short-chain PFAS including perfluorobutanoic acid and perfluorohexanoic acid to PFOA. Furthermore, long-chain perfluoroalkyl acids can inhibit the bioconcentration of short-chain compounds in aquatic organisms such as zebrafish, Bluegill (*Lepomis macrochirus*), Common Carp (*Cyprinus carpio*), Smallmouth Bass (*Micropterus dolomieu*), Walleye (*Sander vitreus*), and Channel Catfish (*Ictalurus punctatus*)[275], [276], [277], [278], [279].

Sample preparation is a crucial step in any analytical methodology. In the case of PFAS analysis, numerous factors must be considered, which accounts for the wide range of successful approaches that have been developed. Due to the significant potential negative effects of PFAS, these compounds have been analyzed across a broad spectrum of matrices, including environmental and drinking water [280], wastewater [281], soils [280], food products (i.e. fish, carp, shrimp etc.) [277], milk, and dairy items [282]. The diverse nature of these matrices highlights widespread concern about the presence of PFAS in various environmental compartments and living organisms. Consequently, the wide variability in sample types has necessitated the application of different extraction techniques during PFAS determination. Such

techniques must achieve a high degree of preconcentration, as PFAS are often present at trace levels. For example, solid-phase extraction (SPE) [283], [284], [285], [286] has been extensively employed for the analysis of PFAS in water and food samples. This method utilizes a variety of sorbents, with polymeric weak anion exchange sorbents being the most commonly used [283]. However, natural sorbents [287] and combinations of different sorbents have also been reported in the previous works. The widespread application of SPE techniques using anion exchange sorbents can be attributed to the inherent chemical properties of PFAS, which favor this method. Several key factors must be considered when developing a weak anion exchange (WAX) SPE cartridge for PFAS analysis. Primarily, the resin should function as a mixed-mode sorbent, combining ion-exchange retention from the WAX ligand with hydrophobic retention from the polymer substrate. Ion exchange is the dominant retention mechanism for shorter-chain hydrophilic carboxylic acids ($< C_8$) and sulfonic acids ($< C_6$). As the alkyl chain length increased, the hydrophobic interactions contributed more significantly to retention. For neutral PFAS lacking acidic functional groups, such as sulfonamides, sulfonamide ethanol, and fluorotelomer alcohols, the retention relies exclusively on hydrophobic interactions. As PFAS research expands, the number of target compounds has grown including EPA method 537 (2009) focused on 14 compounds in drinking water, EPA method 533 (2019) targets 25 compounds in drinking water, while EPA draft method 1633 (2021) targets 40 compounds across aqueous, solid, and tissue samples [288]. This increase highlights the need to consider extraction performance for a broader range of targets and target classes.

The analysis of PFAS is typically conducted using liquid chromatography coupled with tandem mass spectrometry (LC-MS/MS) employing electrospray ionization. However, this technique is recognized for its limitations and considerable uncertainties, particularly in multitarget approaches at trace concentrations [289]. Recent advancements in high-resolution mass spectrometry (HRMS) have introduced greater mass spectral resolving power, minimized interferences and uncovered subtle features. This capability enables the annotation and identification of numerous unknown compounds alongside targeted analytes [290]. Among the HRMS instruments available, Orbitrap and Time-of-Flight (q-TOF) systems stand out as promising tools for the trace-level analysis of compounds in complex matrices such as plasma. Compared to the triple quadrupole mass spectrometry method in Multiple Reaction Monitoring (MRM) mode, HRMS analyzers offer not only precise mass measurements for both precursor and product ions but also deliver enhanced confidence in analyte identification without compromising analytical performance [291].High-resolution mass spectrometry (HRMS) confidently provides accurate mass, isotopic distribution, and fragmentation spectra of organics, allowing for the precise discovery of contaminants without a reference standard. The HRMS-based screening method for suspect and non-target analysis is indispensable in confidently discovering known and unknown PFAS [292]. The ion mobility spectrometry (IMS) coupled with the HRMS instrument may offer a new solution to enhance the performance of the data-independent acquisition (DIA) full scan mode. Ion mobility spectrometry is an emerging separation technique that characterizes ions based on their size, shape, and charge state in the gas phase [293].

This study successfully introduced a rapid, straightforward, and highly adaptable method for quantifying target PFAS in drinking water and fish samples from Lake Erie, Buffalo, New York. The analysis utilized LC-MS/MS following a solid-phase extraction (SPE) procedure, while UHPLC-IMS-QTOF-MS was employed to separate and identify PFAS isomers confidently.

1. **Objectives**

2.1 To adapt the EPA 533 method in Aga's lab.

2.2 To develop the extraction method for PFAS in fish samples.

2.3 To analysis of PFOS isomer in fish samples using IMS

2. **Results**

Table 31 The details of EPA method 533 for drinking water samples and EPA method 1633 for aqueous, solid, biosolids, and tissue samples.

	Method 533 (Nov 2019)	**Method 1633 (update Jan 2024)**	
Sample	Drinking water	Aqueous, solid, biosolids, and tissue	
SPE	WAX cartridge (500 mg)	WAX cartridge (150 mg)	
Sample volume	100-250 mL	Aqueous: 500 mL Solid: 50 mg Biosolids: 50 mg Tissue: 50 mg	Method 1633 is used in the Clean Water Act Leachate samples: 100 mL Solid: soil, sediment, biosolid excluding tissue Tissue: fish tissue

Table 30 The details of EPA method 533 for drinking water samples and EPA method 1633 for aqueous, solid, biosolids, and tissue samples (cont.).

	Method 533 (Nov 2019)	**Method 1633 (update Jan 2024)**
Conditioning solvent	10 mL of methanol 10 mL of 0.1 M phosphate buffer	15 mL of 1% methanolic ammonium hydroxide 5 mL of 0.3 M formic acid
Washing solvent	10 mL 1 g L^{-1} ammonium acetate in reagent water 1 mL of methanol (rinse and clean line)	5 mL of reagent water (×2) 5 mL of 1:1 of 0.1 M formic acid: methanol
Eluting solvent	5 mL of methanol with 2% ammonium hydroxide (v/v) (twice)	5 mL of methanolic ammonium hydroxide

Table 32 The details of target PFAS used in EPA methods 533 and 1633.

Analyte		**^{13}C mass label PFAS**	
Method 533 (Nov 2019)	Method 1633 (update Jan 2024)	Method 533 (Nov 2019)	Method 1633 (update Jan 2024)
PFBA	PFBA	$^{13}C_4$-PFBA	$^{13}C_4$-PFBA
PFMPA	PFMPA	$^{13}C_4$-PFBA	$^{13}C_5$-PFPeA
PFPeA	PFPeA	$^{13}C_5$-PFPeA	$^{13}C_5$-PFPeA
PFBS	PFBS	$^{13}C_3$-PFBS	$^{13}C_3$-PFBS
PFMBA	PFMBA	$^{13}C_5$-PFPeA	$^{13}C_5$-PFPeA
PFEESA	PFEESA	$^{13}C_3$-PFBS	$^{13}C_5$-PFHxA
NFDHA	NFDHA	$^{13}C_5$-PFHxA	$^{13}C_5$-PFHxA
4:2 FTS	4:2 FTS	$^{13}C_2$-4:2FTS	$^{13}C_2$-4:2FTS
PFHxA	PFHxA	$^{13}C_5$-PFHxA	$^{13}C_5$-PFHxA
PFPeS	PFPeS	$^{13}C_3$-PFHxS	$^{13}C_3$-PFHxS
HFPO-DA	HFPO-DA	$^{13}C_3$-HFPO-DA	$^{13}C_3$-HFPO-DA
PFHpA	PFHpA	$^{13}C_4$-PFHpA	$^{13}C_4$-PFHpA
PFHxS	PFHxS	$^{13}C_3$-PFHxS	$^{13}C_3$-PFHxS
ADONA	ADONA	$^{13}C_4$-PFHpA	$^{13}C_3$-HFPO-DA
6:2 FTS	6:2 FTS	$^{13}C_2$-6:2FTS	$^{13}C_2$-6:2FTS
PFOA	PFOA	$^{13}C_8$-PFOA	$^{13}C_8$-PFOA
PFHpS	PFHpS	$^{13}C_8$-PFOS	$^{13}C_8$-PFOS
PFNA	PFNA	$^{13}C_9$-PFNA	$^{13}C_9$-PFNA
PFOS	PFOS	$^{13}C_8$-PFOS	$^{13}C_8$-PFOS
9Cl-PF3ONS	9Cl-PF3ONS	$^{13}C_8$-PFOS	$^{13}C_3$-HFPO-DA
8:2 FTS	8:2 FTS	$^{13}C_2$-8:2FTS	$^{13}C_2$-8:2FTS

Table 31 The details of target PFAS used in EPA methods 533 and 1633 (cont.).

Analyte		**^{13}C mass label PFAS**	
Method 533 (Nov 2019)	Method 1633 (update Jan 2024)	Method 533 (Nov 2019)	Method 1633 (update Jan 2024)
PFDA	PFDA	$^{13}C_6$-PFDA	$^{13}C_6$-PFDA
PFUnA	PFUnA	$^{13}C_7$-PFUnA	$^{13}C_7$-PFUnA
11Cl-PF3OUdS	11Cl-PF3OUdS	$^{13}C_8$-PFOS	$^{13}C_3$-HFPO-DA
PFDoA	PFDoA	$^{13}C_2$-PFDoA	$^{13}C_2$-PFDoA
N/A	PFTrDA	N/A	avg.$^{13}C_2$-PFTeDA and$^{13}C_2$-PFDoA
N/A	PFTeDA	N/A	$^{13}C_2$-PFTeDA
N/A	PFNS	N/A	$^{13}C_8$-PFOS
N/A	PFDS	N/A	$^{13}C_8$-PFOS
N/A	PFDoS	N/A	$^{13}C_8$-PFOS
N/A	FOSA	N/A	$^{13}C_8$-PFOSA
N/A	NMeFOSA	N/A	D_3-NMeFOSA
N/A	NEtFOSA	N/A	D_5-NEtFOSA
N/A	NMeFOSAA	N/A	D_3-NMeFOSAA
N/A	NEtFOSAA	N/A	D_5-N-EtFOSAA
N/A	NMeFOSE	N/A	D_7-NMeFOSE
N/A	NEtFOSE	N/A	D_9-NEtFOSE
N/A	3:3 FTCA	N/A	$^{13}C_5$-PFPeA
N/A	5:3 FTCA	N/A	$^{13}C_5$-PFHxA
N/A	7:3 FTCA	N/A	$^{13}C_5$-PFHxA

2.1 Analysis of PFAS in water samples using the EPA 533 method.

2.1.1 Recovery study of 40 mixes PFAS in water sample using WAX cartridge

1. A 100 mL of drinking water sample is spiked with 20 µL of 1 ppm 40 mixed PFAS
2. Adjusted pH of sample solution to be in the range of 6-8 using acetic acid.
3. SPE step
   - Conditioning:
     - 10 mL methanol
     - 10 mL 0.1M phosphate buffer
   - Loading
   - Washing:
     - 10 mL of 1 g/L ammonium acetate
     - 1 mL of methanol (rinse bottle and line)
     - Dry under high vacuum for 5 min
   - Eluting
     - 5 mL 2% NH_4OH (v/v) in methanol (twice)
     - Dry under stream N_2
4. Spike with 20 µL of 1 mg L^{-1} of nineteen ^{13}C mass label PFAS into the SPE extract (in step 3.)
5. Reconstitute to 200 µL using the starting mobile phase before LC-MS/MS analysis

2.1.2 Chromatographic conditions

Parameters	Conditions
Analytical column	Raptor C18, 2.7 µm × 100 × 3.0 mm (Restek, USA)
Mobile phase A	5 mM ammonium acetate in 95 % nanopure™ water : 5 % acetonitrile
Mobile phase B	50 % acetonitrile: 50 % methanol
Flow rate	0.37 mL min^{-1}
Injection volume	10.0 µL

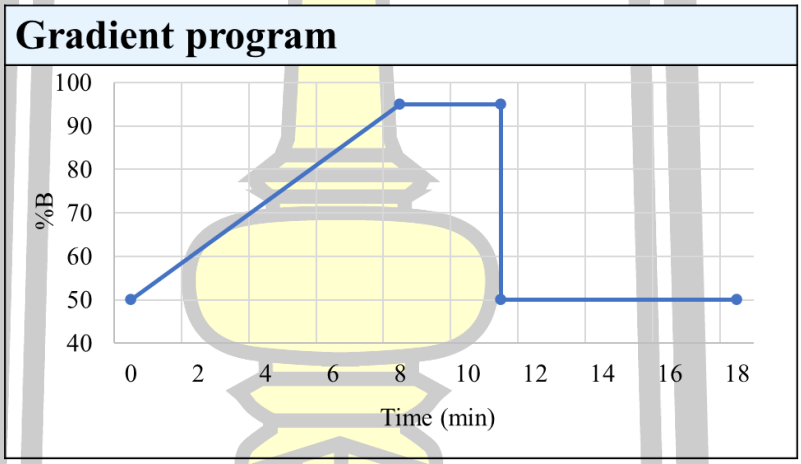

Reference: Restek_Dino method

2.1.3 Results of LC-MS/MS analysis

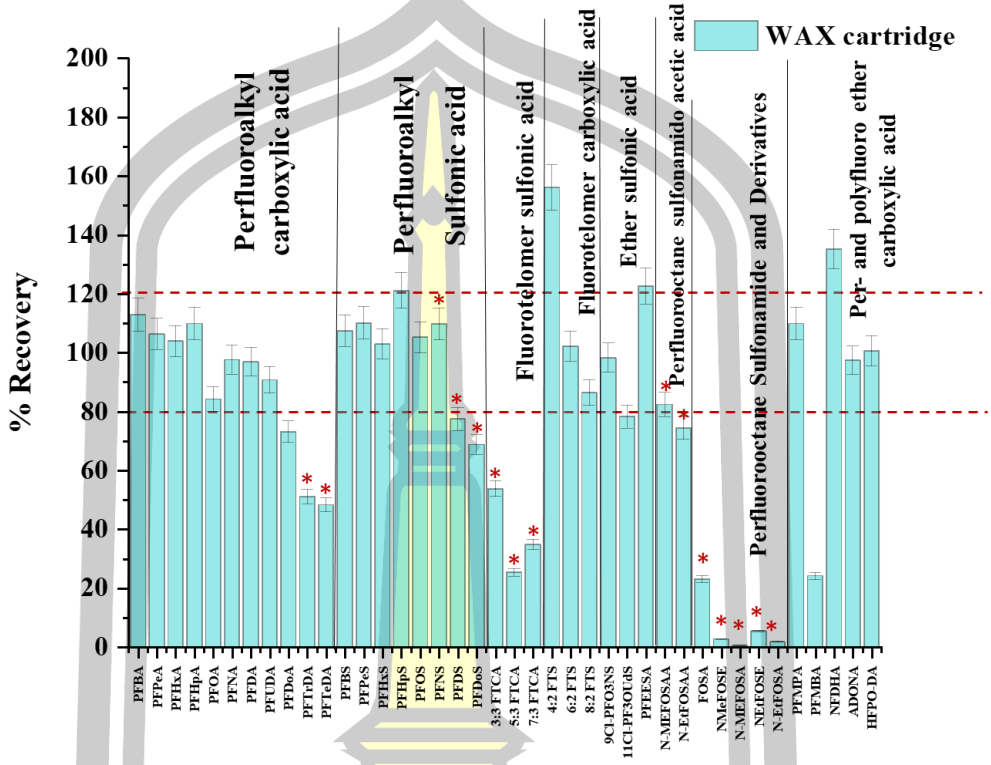

***: PFAS that are not present in the EPA 533 method**

2.1.4 Recovery study of 40 mixes PFAS in water sample using HLB-WAX cartridge

1. A 100 mL of drinking water sample is spiked with 20 µL of 1 mg L^{-1} of 40 mixed PFAS
2. Adjusted pH of sample solution to be in the range of 6-8 using acetic acid.
3. SPE step
   - Conditioning:
     - 10 mL methanol
     - 10 mL 0.1M phosphate buffer

- Loading
- Washing:
  - 10 mL of 1 g L^{-1} ammonium acetate
  - 1 mL of methanol (rinse bottle and line)
  - Dry under high vacuum for 5 min
- Eluting
  - 5 mL 2% NH_4OH (v/v) in methanol (twice)
  - Dry under stream N_2

4. Spike with 20 µL of 1 ppm of nineteen ^{13}C mass label PFAS into the SPE extract (in step 3.)

5. Reconstitute to 200 µL using the starting mobile phase before LC-MS/MS analysis

2.1.5 Chromatographic conditions

Parameters	**Conditions**
Analytical column	Raptor C18, 2.7 µm × 100 × 3.0 mm (Restek, USA)
Mobile phase A	5 mM ammonium acetate in 95 % nanopure™ water : 5 % acetonitrile
Mobile phase B	50 % acetonitrile: 50 % methanol
Flow rate	0.37 mL min^{-1}
Injection volume	10.0 µL

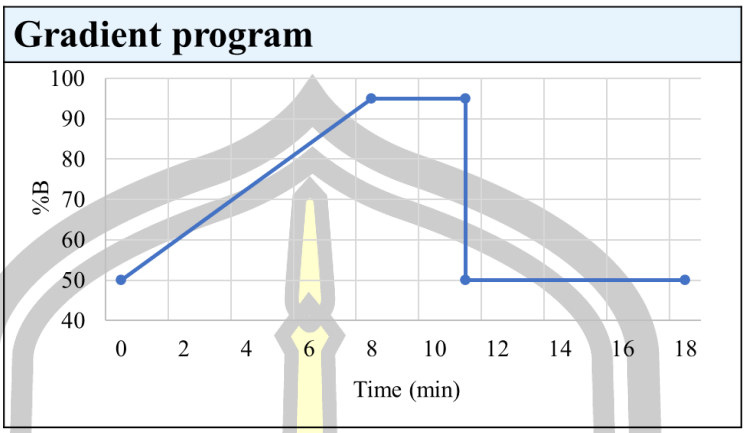

Reference: Restek_Dino method

2.1.6 Result of LC-MS/MS analysis

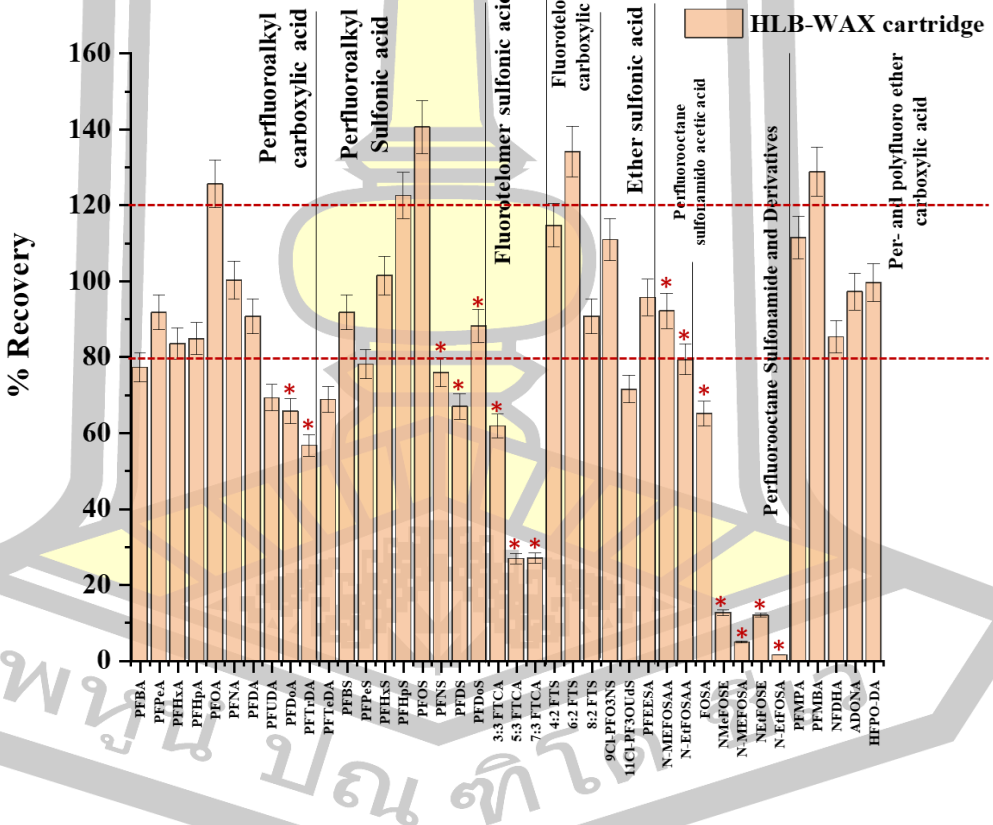

***: PFAS that are not present in the EPA 533 method**

2.1.7 Comparison of %Recovery using WAX and HLB-WAX cartridges prior to LC-MS/MS analysis

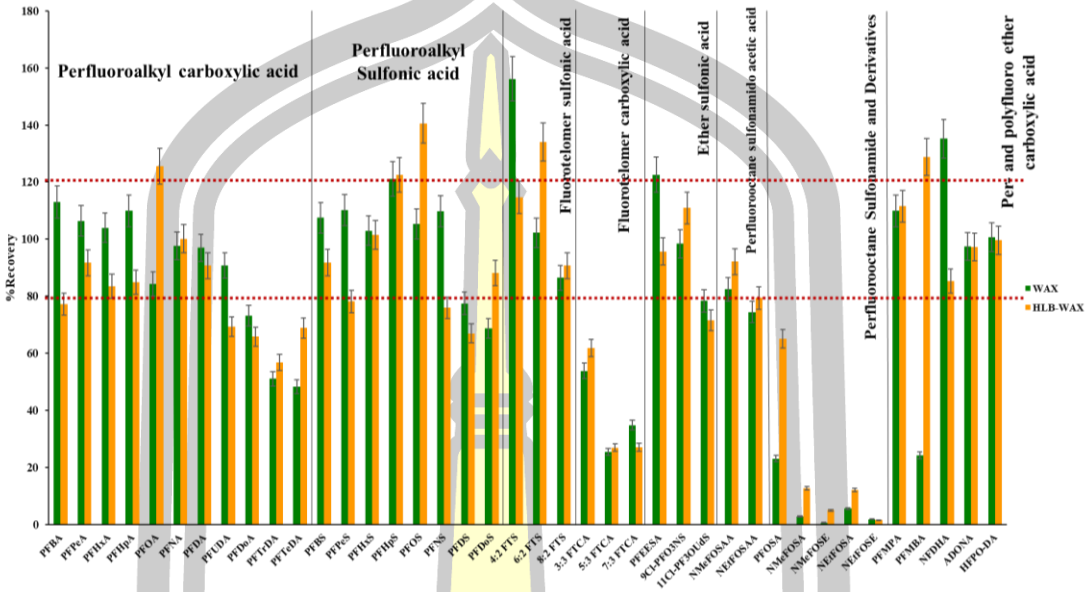

2.1.8 Concentration of PFAS in water

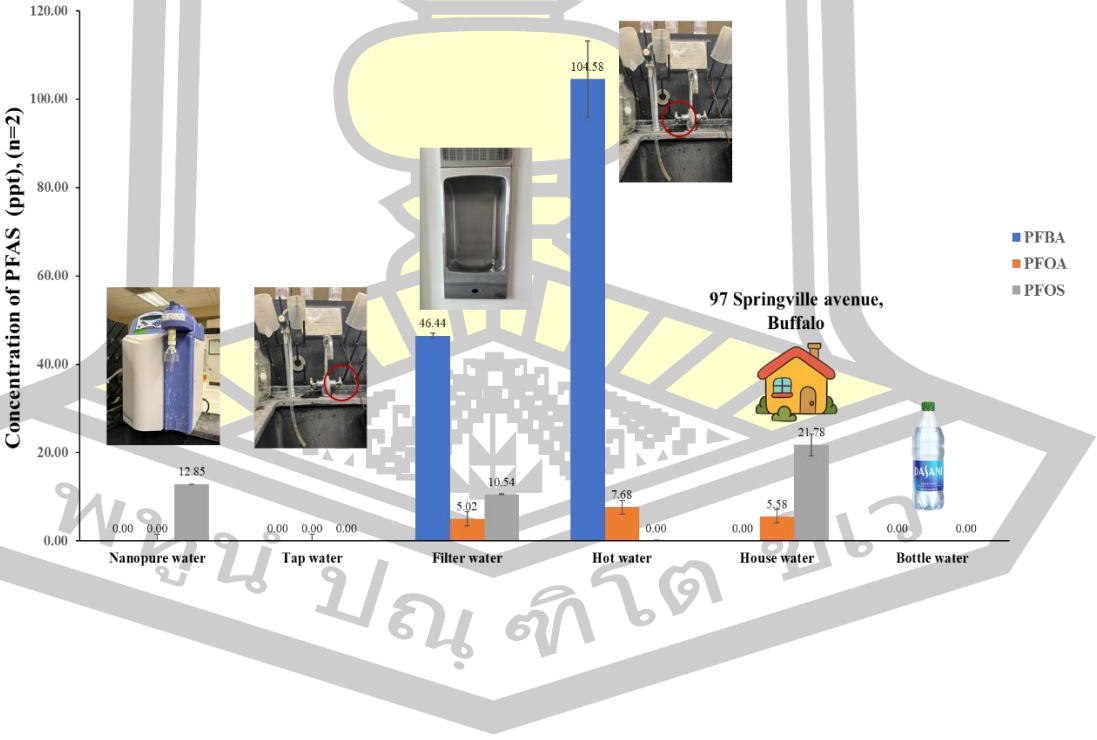

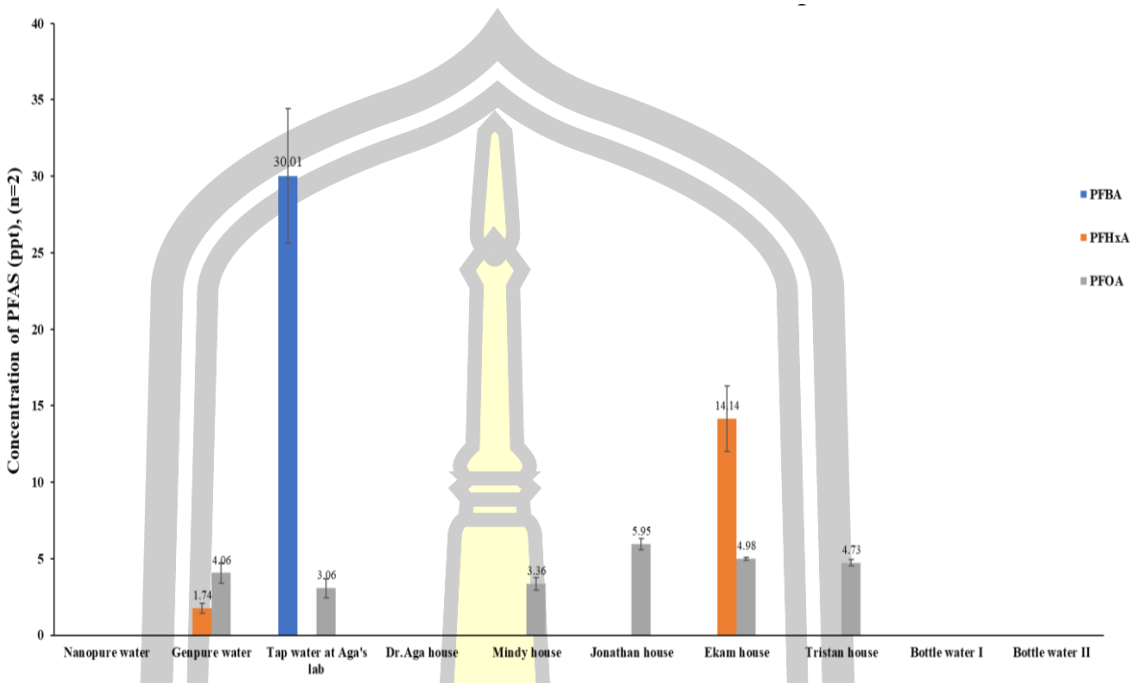

2.2 Analysis of PFAS in fish samples.

2.2.1 Solid-liquid extraction (Zach's method)

2.2.2 Solid phase microextraction (SPME), collaboration with Dr. Emanuela laboratory

2.2.3 Solid-liquid extraction combined with solid phase extraction based on EPA 1633 method

3.2.3.1 Development of solid phase extraction for fish samples analysis (Based on the EPA 1633 method)

1. Weigh 1 g of sample into a 15 mL centrifuge tube.
2. Spiked with ^{13}C mass label PFAS and vortex 30 minutes.
3. Add 10 mL of 0.05 M KOH (Potassium hydroxide) in methanol.
    a. Vortex.
    b. Low-speed shake on the mixing table for 16 hours.
    c. Centrifuge at 2800 rpm for 10 minutes.

d. Transfer supernatant to a clean 50 mL centrifuge tube.

4. Add 10 mL of acetonitrile.

a. Vortex.

b. Sonicate for 30 minutes.

c. Centrifuge at 2800 rpm for 10 minutes.

d. Transfer supernatant and combine with supernatant from step 3d.

5. Add 5 mL of 0.05 KOH in methanol.

a. Shake by hand to disperse.

b. Centrifuge at 2800 rpm for 10 minutes.

c. Transfer supernatant and combine with supernatant from steps 3d and 4d.

6. Add 1 mL of water.

7. Concentrate under nitrogen (55 °C) to 2.5 mL.

8. Dilute the sample to 50 mL with water.

9. Check pH and adjust to 6.5 ± 0.5 using 50% formic acid or ammonium hydroxide if needed.

10. Pack glass wool into half the height of the SPE barrel.

11. SPE step

a. Conditioning step: 15 mL of 1% (v/v) ammonium hydroxide methanol and 5 mL of 0.3 M formic acid

b. Loading step: Load sample at 5 mL min^{-1}

c. Washing step: wash the cartridge with 10 mL of reagent water, ensuring to rinse the reservoir with this solution, and wash with 5 mL of

1:1 0.1 M formic acid: methanol, ensuring to rinse the reservoir with this solution, and dry the cartridge under high vacuum.

d. Elution steps: 5 mL 1% NH4OH (v/v) in methanol and 5 mL of ACN.

12. After SEP the extracts were centrifuged (4°C) at 2800 rpm for 10 minutes and decant the supernatant into a clean tube (tube 1)

13. Dry under nitrogen to 500 µL.

a. Centrifuge.

b. Decant the supernatant to a clean tube (tube 2).

14. Add 250 µL of methanol

a. Vortex.

b. Centrifuge.

c. Decant the supernatant to tube 2 (in step 13b.) and dry under nitrogen to 100 µL.

15. Centrifuge and decant the supernatant to tube 3

16. Add 100 µL of methanol

a. Vortex.

b. Centrifuge at 4000 rpm for 15 minutes and decant supernatant to tube 3 (in step 15).

17. Centrifuge at 4000 rpm for 10 minutes and decant supernatant to tube 4.

18. Dry under nitrogen to 100 µL.

19. Spiked with 25 µL of 0.5 mg L^{-1} of mixture M4PFOA and M4PFOS (internal standard).

20. Dilute to 250 µL using the starting mobile phase (mobile phase A: 5 mM ammonium acetate in 95 % nanopure^{TM} water: 5 % acetonitrile, mobile B: 50 % acetonitrile: 50 % methanol) (final concentration 50 ppb)

21. Centrifuge at 4200 rpm for 10 min before LC-MS/MS analysis.

3.2.3.2 Chromatographic conditions

Parameters	Conditions
Analytical column	Raptor C18, 2.7 µm × 100 × 3.0 mm (Restek, USA)
Mobile phase A	5 mM ammonium acetate in 95 % nanopure^{TM} water : 5 % acetonitrile
Mobile phase B	50 % acetonitrile: 50 % methanol
Flow rate	0.37 mL min^{-1}
Injection volume	10.0 µL

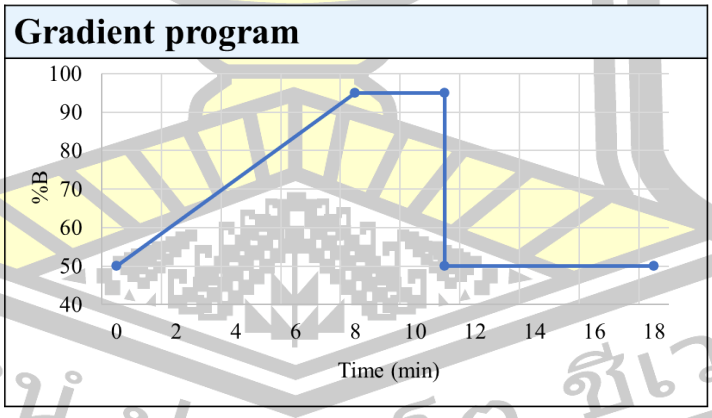

Reference: Restek_Dino method

3.2.3.3 Result of LC-MS/MS analysis

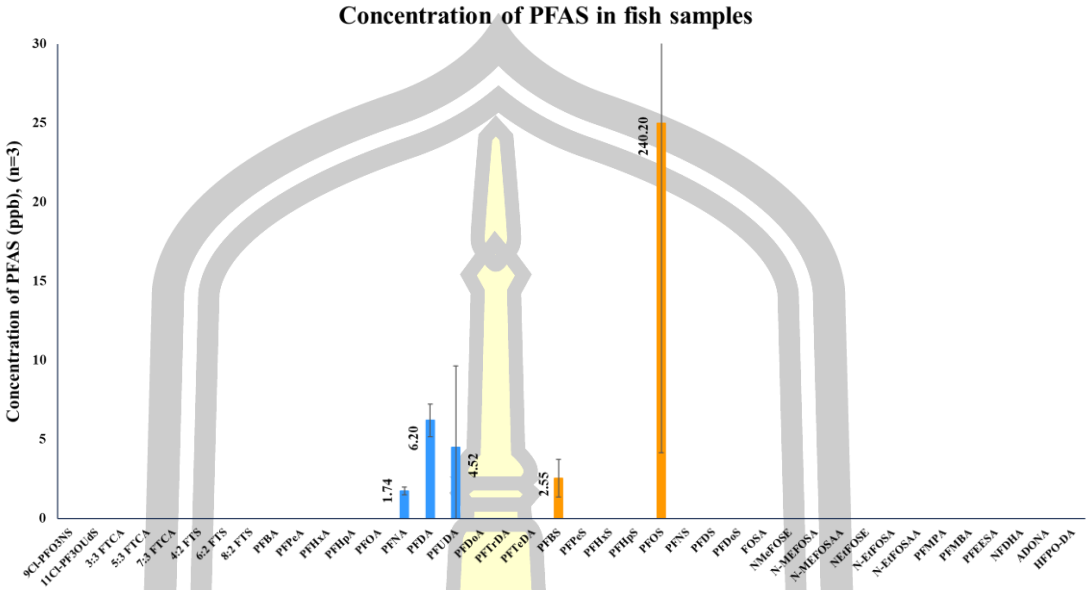

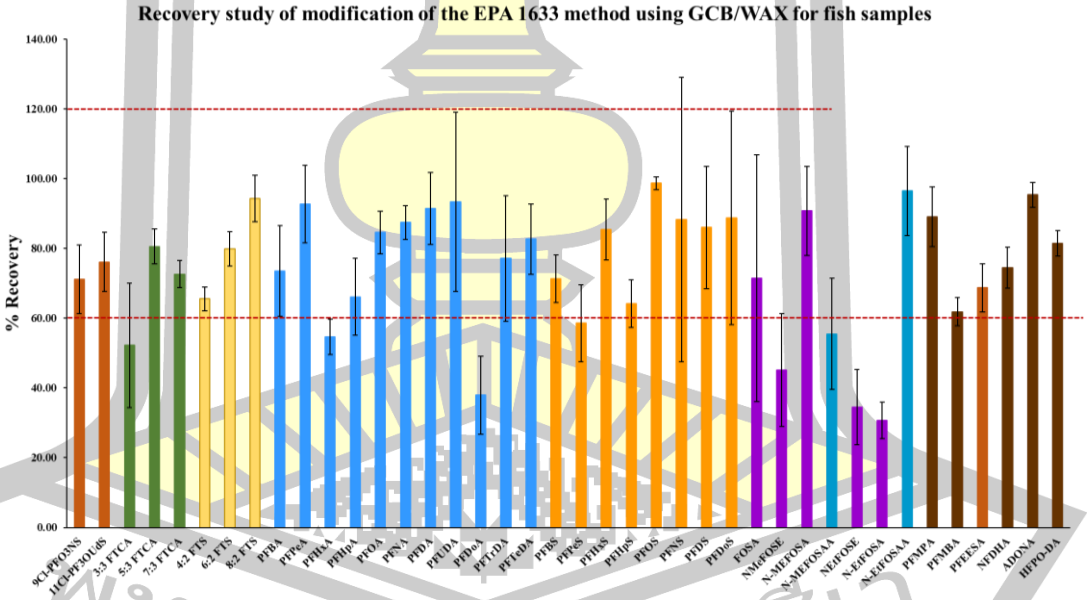

---Ether sulfonic acid

---Fluorotelomer carboxylic acid

---Fluorotelomer sulfonic acid

---Perfluoroalkyl carboxylic acid

---Perfluoroalkyl sulfuric acid

---Perfluorooctane sulfonamide and derivatives

---Perfluorooctane sulfonamido acetic acid

3.2.3.4 Method limit of detection and method limits of quantification

Analyte	Calibration curve	R^2	LOD (ppb)	LOQ (ppb)
PFBA	y = 0.503x + 0.3154	0.9948	2.93	9.78
PFPeA	y = 0.032x + 0.3679	0.9909	3.54	11.79
PFHxA	y = 0.0623x + 0.1345	0.9977	1.64	5.46
PFHpA	y = 0.0475x - 0.0345	0.9995	3.01	10.02
PFOA	y = 0.0346x + 0.0144	0.9996	3.25	10.84
PFNA	y = 0.0743x + 0.0620	0.9992	3.23	10.76
PFDA	y = 0.1253x - 0.7458	0.9976	6.70	22.32
PFUDA	y = 0.1676x - 0.8874	0.9946	8.10	27.00
PFDoA	y = 0.1694x - 0.0410	0.9987	5.56	18.52
PFTrDA	y = 0.0967x + 0.2822	0.9959	1.88	6.27
PFTeDA	y = 0.0967x + 0.2822	0.9959	1.88	6.27
PFBS	y = 0.0424x - 0.0972	0.9993	2.19	7.28
PFPeS	y = 0.0256x - 0.0308	0.9994	3.28	10.94
PFHxS	y = 0.0256x - 0.0308	0.9994	3.28	10.94
PFHpS	y = 0.0472x - 0.1026	0.9992	5.14	17.12
PFOS	y = 0.0472x - 0.1026	0.9992	5.14	17.12
PFNS	M8PFOS			
PFDS	M8PFOS			
PFDoS	M8PFOS			
4:2 FTS	y = 0.0294x + 0.0130	0.9999	1.98	6.59
6:2 FTS	y = 0.0337x - 0.0527	0.9990	3.73	12.45

Analyte	Calibration curve	R^2	LOD (ppb)	LOQ (ppb)
8:2 FTS	y = 0.0535x - 0.1339	0.9995	2.93	9.78
3:3 FTCA	M5PFPeA			
5:3 FTCA	M6PFHxA			
7:2 FTCA	M6PFHxA			
PFEESA	M3PFBS			
9Cl-PFO3NS	M8PFOS			
11Cl-PF3OUdS	M8PFOS			
NMeFOSAA	M8FOSA			
NEtFOSAA	M8FOSA			
PFOSA	y = 0.1358x - 0.1233	0.9988	2.78	9.27
NMeFOSA	M8FOSA			
NMeFOSE	M8FOSA			
NEtFOSA	M8FOSA			
NEtFOSE	M8FOSA			
PFMPA	MPFBA			
PFMBA	M5PFPeA			
NFDHA	M5PFPeA			
ADONA	M4PFHpA			
HFPO-DA	M6PFDA			

2.2.4 Separation and identification of PFOS isomers using Ion Mobility High-Resolution Mass Spectrometry (IMS)

2.2.4.1 Chromatographic conditions

Parameters	Conditions
Analytical column	Atlantis Premier BEH C18 AX, 1.7µm; 2.1mm x 100mm
Mobile phase A	Water with 2mM Ammonium Acetate
Mobile phase B	Methanol + 0.1% Ammonium Hydroxide
Flow rate	0.30 mL min^{-1}
Injection volume	10.0 µL

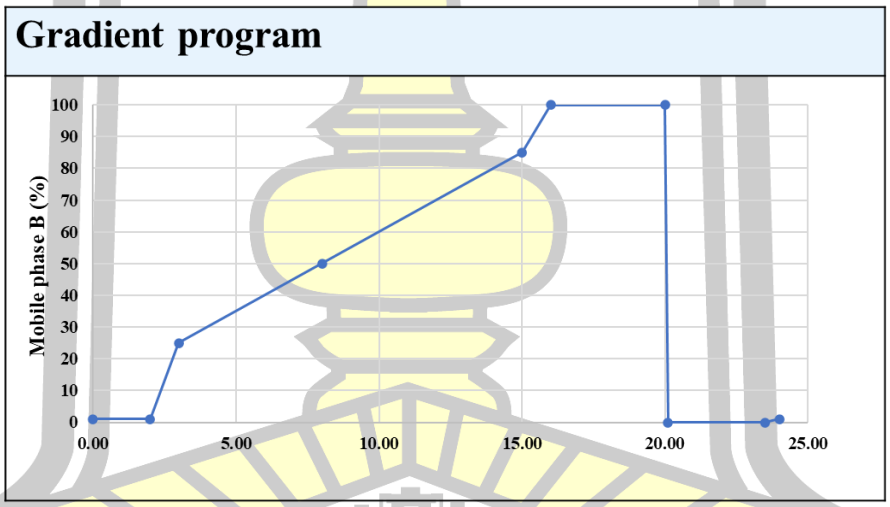

Reference: Sara's method

2.2.4.2 FPOS isomers

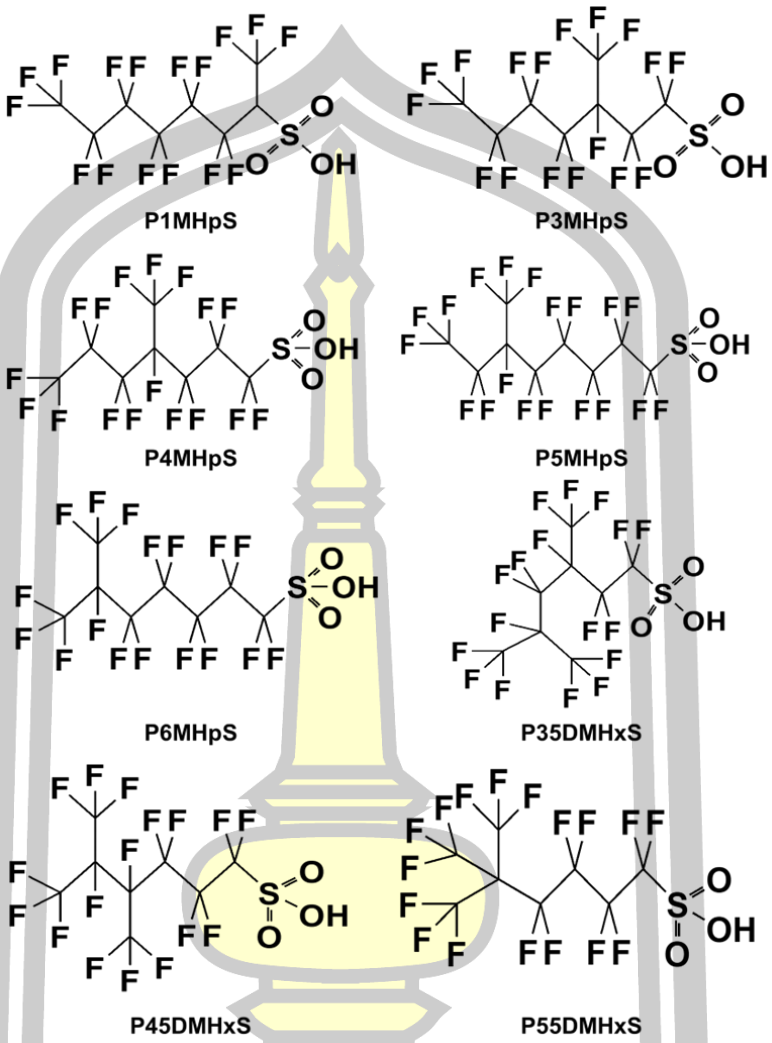

PFOS isomers	
L-PFOS	$CF_3CF_2CF_2CF_2CF_2CF_2CF_2SO_3^-$
P1MHpS	$CF_3CF_2CF_2CF_2CF_2CF_2CF(CF_3)\ SO_3^-$
P2MHpS	$CF_3CF_2CF_2CF_2CF_2CF(CF_3)CF_2SO_3^-$
P3MHpS	$CF_3CF_2CF_2CF_2CF(CF_3)CF_2CF_2SO_3^-$
P4MHpS	$CF_3CF_2CF_2CF(CF_3)CF_2CF_2CF_2SO_3^-$
P5MHpS	$CF_3CF_2CF(CF_3)CF_2CF_2CF_2CF_2SO_3^-$
P6MHpS	$CF_3CF(CF_3)CF_2CF_2CF_2CF_2CF_2SO_3^-$

PFOS isomers

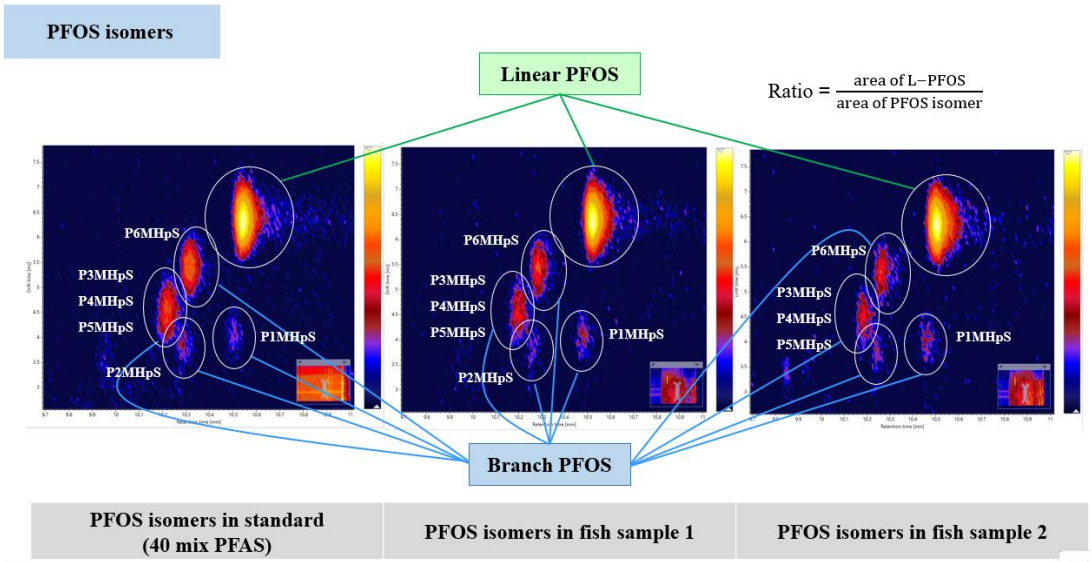

Ratio of area L-PFOS/area of PFOS isomer

PFOS isomers	Standard (40 mix PFAS)	Fish sample 1	Fish sample 2
P1MHpS	186.09	169.37	158.41
P2MHpS	268.47	306.83	61.11
P3MHpS, P4MHpS			
P5MHpS	21.28	45.58	60.39
P6MHpS	12.38	26.77	41.98

REFERENCES

[1] L. P. A. Marciano, N. Kleinstreuer, X. Chang, L. F. Costa, A. C. P. Silvério, and I. Martins, "A novel approach to triazole fungicides risk characterization: Bridging human biomonitoring and computational toxicology," *Science of the Total Environment*, vol. 953, Nov. 2024, doi: 10.1016/j.scitotenv.2024.176003.

[2] J. Pang, M. Mei, D. Yuan, and X. Huang, "Development of on-line monolith-based in-tube solid phase microextraction for the sensitive determination of triazoles in environmental waters," *Talanta*, vol. 184, pp. 411–417, Jul. 2018, doi: 10.1016/j.talanta.2018.03.005.

[3] X. Han, J. Chen, Z. Li, K. Quan, and H. Qiu, "Magnetic solid-phase extraction of triazole fungicides based on magnetic porous carbon prepared by combustion combined with solvothermal method," *Anal Chim Acta*, vol. 1129, pp. 85–97, Sep. 2020, doi: 10.1016/j.aca.2020.06.077.

[4] M. Rutkowska, J. Płotka-Wasylka, M. Sajid, and V. Andruch, "Liquid–phase microextraction: A review of reviews," Sep. 01, 2019, *Elsevier Inc.* doi: 10.1016/j.microc.2019.103989.

[5] A. Abdi Hassan, M. Sajid, H. Al Ghafly, and K. Alhooshani, "Ionic liquid-based membrane-protected micro-solid-phase extraction of organochlorine pesticides in environmental water samples," *Microchemical Journal*, vol. 158, Nov. 2020, doi: 10.1016/j.microc.2020.105295.

[6] M. Oehme, U. Berger, S. Brombacher, F. Kuhn, and S. Kölliker, "Trace analysis by HPLC-MS: contamination problems and systematic errors." *TrAC*

Trends in Analytical Chemistry, vol. 21(5), pp. 322-331, 2002, doi: https://doi.org/10.1016/S0165-9936(02)00503-4.

[7] "4 Analysis of Pesticides by HPLC-UV, HPLC-DAD (HPLC-PDA), and other detection methods, Tomasz Tuzimski 14.1 Properties of analytes determined by high-performance liquid chromatography coupled with spectrophotometric determination."

[8] L. Fu *et al.*, "Determination of two pesticides in soils by dispersive liquid-liquid microextraction combined with LC-fluorescence detection," *Chromatographia*, vol. 70, no. 11–12, pp. 1697–1701, Dec. 2009, doi: 10.1365/s10337-009-1356-9.

[9] L. Gámiz-Gracia, A. M. García-Campaña, J. J. Soto-Chinchilla, J. F. Huertas-Pérez, and A. González-Casado, "Analysis of pesticides by chemiluminescence detection in the liquid phase," *TrAC - Trends in Analytical Chemistry*, vol. 24, no. 11, pp. 927–942, 2005, doi: 10.1016/j.trac.2005.05.009.

[10] Y. Picó, C. Blasco, and G. Font, "Environmental and food applications of LC-tandem mass spectrometry in pesticide-residue analysis: An overview," Jan. 2004. doi: 10.1002/mas.10071.

[11] L. Wang, X. Zang, Q. Chang, G. Zhang, C. Wang, and Z. Wang, "Determination of Triazole Fungicides in Vegetable Samples by Magnetic Solid-Phase Extraction with Graphene-Coated Magnetic Nanocomposite as Adsorbent Followed by Gas Chromatography-Mass Spectrometry Detection," *Food Anal Methods*, vol. 7, no. 2, pp. 318–325, Jan. 2014, doi: 10.1007/s12161-013-9629-1.

[12] R. Konášová, J. J. Dytrtová, and V. Kašička, “Determination of acid dissociation constants of triazole fungicides by pressure assisted capillary electrophoresis,” *J Chromatogr A*, vol. 1408, pp. 243–249, 2015, doi: 10.1016/j.chroma.2015.07.005.

[13] R. J. Ekiert, J. Krzek, and P. Talik, “Chromatographic and electrophoretic techniques used in the analysis of triazole antifungal agents - A review,” Sep. 15, 2010, *Elsevier B.V.* doi: 10.1016/j.talanta.2010.06.056.

[14] H. Y. Liu, S. L. Lin, and M. R. Fuh, “Determination of chloramphenicol, thiamphenicol and florfenicol in milk and honey using modified QuEChERS extraction coupled with polymeric monolith-based capillary liquid chromatography tandem mass spectrometry,” *Talanta*, vol. 150, pp. 233–239, Apr. 2016, doi: 10.1016/j.talanta.2015.12.045.

[15] J. Namieśnik, “Trends in environmental analytics and monitoring,” *Crit Rev Anal Chem*, vol. 30, no. 2–3, pp. 221–269, 2000, doi: 10.1080/10408340091164243.

[16] A. Gałuszka, Z. Migaszewski, and J. Namieśnik, “The 12 principles of green analytical chemistry and the SIGNIFICANCE mnemonic of green analytical practices,” 2013, *Elsevier B.V.* doi: 10.1016/j.trac.2013.04.010.

[17] Á. Santana-Mayor, R. Rodríguez-Ramos, A. V. Herrera-Herrera, B. Socas-Rodríguez, and M. Á. Rodríguez-Delgado, “Deep eutectic solvents. The new generation of green solvents in analytical chemistry,” Jan. 01, 2021, *Elsevier B.V.* doi: 10.1016/j.trac.2020.116108.

[18] M. Vian, C. Breil, L. Vernes, E. Chaabani, and F. Chemat, “Green solvents for sample preparation in analytical chemistry,” Jun. 01, 2017, *Elsevier B.V.* doi: 10.1016/j.cogsc.2017.03.010.

[19] J. Pang, M. Mei, D. Yuan, and X. Huang, “Development of on-line monolith-based in-tube solid phase microextraction for the sensitive determination of triazoles in environmental waters,” *Talanta*, vol. 184, pp. 411–417, Jul. 2018, doi: 10.1016/j.talanta.2018.03.005.

[20] Á. Santana-Mayor, R. Rodríguez-Ramos, A. V. Herrera-Herrera, B. Socas-Rodríguez, and M. Á. Rodríguez-Delgado, “Deep eutectic solvents. The new generation of green solvents in analytical chemistry,” Jan. 01, 2021, *Elsevier B.V.* doi: 10.1016/j.trac.2020.116108.

[21] E. L. Smith, A. P. Abbott, and K. S. Ryder, “Deep Eutectic Solvents (DESs) and Their Applications,” Nov. 12, 2014, *American Chemical Society*. doi: 10.1021/cr300162p.

[22] D. Mueller, “50-Integrated Crop Management-Fungicides: Triazoles,” 2006.

[23] J. Pang, M. Mei, D. Yuan, and X. Huang, “Development of on-line monolith-based in-tube solid phase microextraction for the sensitive determination of triazoles in environmental waters,” *Talanta*, vol. 184, pp. 411–417, Jul. 2018, doi: 10.1016/j.talanta.2018.03.005.

[24] M. O’Malley, “The Regulatory Evaluation of the Skin Effects of Pesticides,” in *Hayes’ Handbook of Pesticide Toxicology, Third Edition: Volume 1*, vol. 1, Elsevier, 2010, pp. 701–787. doi: 10.1016/B978-0-12-374367-1.00028-8.

[25] R. Poulsen, X. Luong, M. Hansen, B. Styrishave, and T. Hayes, "Tebuconazole disrupts steroidogenesis in Xenopus laevis," *Aquatic Toxicology*, vol. 168, pp. 28–37, Nov. 2015, doi: 10.1016/j.aquatox.2015.09.008.

[26] G. Hellinghausen *et al.*, "Mass Spectrometry-Compatible Enantiomeric Separations of 100 Pesticides Using Core–Shell Chiral Stationary Phases and Evaluation of Iterative Curve Fitting Models for Overlapping Peaks," *Chromatographia*, vol. 82, no. 1, pp. 221–233, Jan. 2019, doi: 10.1007/s10337-018-3604-3.

[27] R. Kachangoon, J. Vichapong, Y. Santaladchaiyakit, and S. Srijaranai, "Green fabrication of Moringa oleifera seed as efficient biosorbent for selective enrichment of triazole fungicides in environmental water, honey and fruit juice samples," *Microchemical Journal*, vol. 175, Apr. 2022, doi: 10.1016/j.microc.2022.107194.

[28] C. K. Jain, D. S. Malik, and A. K. Yadav, "Applicability of plant based biosorbents in the removal of heavy metals: a review," Jun. 01, 2016, *Springer Basel*. doi: 10.1007/s40710-016-0143-5.

[29] O. Abdelwahab, A. El Sikaily, A. Khaled, and A. El Nemr, "Mass-transfer processes of chromium(VI) adsorption onto guava seeds," *Chemistry and Ecology*, vol. 23, no. 1, pp. 73–85, Feb. 2007, doi: 10.1080/02757540601083922.

[30] B. V. Babu and S. Gupta, "Adsorption of Cr(VI) using activated neem leaves: Kinetic studies," *Adsorption*, vol. 14, no. 1, pp. 85–92, Feb. 2008, doi: 10.1007/s10450-007-9057-x.

[31] V. Sarin and K. K. Pant, “Removal of chromium from industrial waste by using eucalyptus bark,” *Bioresour Technol*, vol. 97, no. 1, pp. 15–20, Jan. 2006, doi: 10.1016/j.biortech.2005.02.010.

[32] J. Soares da Silva Burato, D. A. Vargas Medina, A. L. de Toffoli, E. Vasconcelos Soares Maciel, and F. Mauro Lanças, “Recent advances and trends in miniaturized sample preparation techniques,” Jan. 01, 2020, *Wiley-VCH Verlag*. doi: 10.1002/jssc.201900776.

[33] S. Moldoveanu and V. David, “Solid-Phase Extraction,” in *Modern Sample Preparation for Chromatography*, Elsevier, 2015, pp. 191–286. doi: 10.1016/B978-0-444-54319-6.00007-4.

[34] Y. Liu, X. Liu, and J. Wang, “Molecularly imprinted solid-phase extraction sorbent for removal of nicotine from tobacco smoke,” *Anal Lett*, vol. 36, no. 8, pp. 1631–1645, 2003, doi: 10.1081/AL-120021554.

[35] K. Zoroufchi Benis, M. Shakouri, K. McPhedran, and J. Soltan, “Enhanced arsenate removal by Fe-impregnated canola straw: assessment of XANES solid-phase speciation, impacts of solution properties, sorption mechanisms, and evolutionary polynomial regression (EPR) models,” *Environmental Science and Pollution Research*, vol. 28, no. 10, pp. 12659–12676, Mar. 2021, doi: 10.1007/s11356-020-11140-0.

[36] I. Brás, L. T. Lemos, A. Alves, and M. F. R. Pereira, “Application of pine bark as a sorbent for organic pollutants in effluents,” *Management of Environmental Quality: An International Journal*, vol. 15, no. 5, pp. 491–501, 2004, doi: 10.1108/14777830410553933.

[37] D. Mohan, H. Kumar, A. Sarswat, M. Alexandre-Franco, and C. U. Pittman, "Cadmium and lead remediation using magnetic oak wood and oak bark fast pyrolysis bio-chars," *Chemical Engineering Journal*, vol. 236, pp. 513–528, Jan. 2014, doi: 10.1016/j.cej.2013.09.057.

[38] V. Halysh *et al.*, "Sugarcane bagasse and straw as low-cost lignocellulosic sorbents for the removal of dyes and metal ions from water," *Cellulose*, vol. 27, no. 14, pp. 8181–8197, Sep. 2020, doi: 10.1007/s10570-020-03339-8.

[39] A. Keikavousi Behbahan, V. Mahdavi, Z. Roustaei, and H. Bagheri, "Preparation and evaluation of various banana-based biochars together with ultra-high performance liquid chromatography-tandem mass spectrometry for determination of diverse pesticides in fruiting vegetables," *Food Chem*, vol. 360, Oct. 2021, doi: 10.1016/j.foodchem.2021.130085.

[40] A. El Barnossi, F. Moussaid, and A. Iraqi Housseini, "Tangerine, banana and pomegranate peels valorisation for sustainable environment: A review," Mar. 01, 2021, *Elsevier B.V.* doi: 10.1016/j.btre.2020.e00574.

[41] A. M. E. Gomaa, "CHARACTERIZATION OF BOTH BANANA PEEL AND WATERMELON PEEL AS NATURAL BIOSORBENT AGENTS OF IRON IN AQUEOUS SOLUTION." [Online]. Available: www.journals.zu.edu.eg/journalDisplay.aspx?JournalId=1&queryType=Master

[42] E. N. Ali, S. R. Alfarra, M. M. Yusoff, and M. L. Rahman, "Environmentally Friendly Biosorbent from Moringa Oleifera Leaves for Water Treatment," *International Journal of Environmental Science and Development*, vol. 6, no. 3, pp. 165–169, 2015, doi: 10.7763/IJESD.2015.V6.582.

[43] C. C. Chien, Y. P. Huang, W. C. Wang, J. H. Chao, and Y. Y. Wei, “Efficiency of Moso Bamboo Charcoal and Activated Carbon for Adsorbing Radioactive Iodine,” *Clean (Weinh)*, vol. 39, no. 2, pp. 103–108, Feb. 2011, doi: 10.1002/clen.201000012.

[44] A. Bagheri, E. Abu-Danso, J. Iqbal, and A. Bhatnagar, “Modified biochar from Moringa seed powder for the removal of diclofenac from aqueous solution,” *Environmental Science and Pollution Research*, vol. 27, no. 7, pp. 7318–7327, Mar. 2020, doi: 10.1007/s11356-019-06844-x.

[45] S. Shrestha, G. Son, S. H. Lee, and T. G. Lee, “Isotherm and thermodynamic studies of Zn (II) adsorption on lignite and coconut shell-based activated carbon fiber,” *Chemosphere*, vol. 92, no. 8, pp. 1053–1061, 2013, doi: 10.1016/j.chemosphere.2013.02.068.

[46] P. Rodsamran and R. Sothornvit, “Bioactive coconut protein concentrate films incorporated with antioxidant extract of mature coconut water,” *Food Hydrocoll*, vol. 79, pp. 243–252, Jun. 2018, doi: 10.1016/j.foodhyd.2017.12.037.

[47] G. Basu, L. Mishra, S. Jose, and A. K. Samanta, “Accelerated retting cum softening of coconut fibre,” *Ind Crops Prod*, vol. 77, pp. 66–73, Dec. 2015, doi: 10.1016/j.indcrop.2015.08.012.

[48] E. B. C. Lima *et al.*, “Cocos nucifera (L.) (arecaceae): A phytochemical and pharmacological review,” Nov. 01, 2015, *Associacao Brasileira de Divulgacao Cientifica*. doi: 10.1590/1414-431X20154773.

[49] M. A. S. Azizi Samir, F. Alloin, and A. Dufresne, “Review of recent research into cellulosic whiskers, their properties and their application in nanocomposite field,” Mar. 2005. doi: 10.1021/bm0493685.

[50] S. Abedini and V. Alipour, “Cadmium removal from synthetic wastewater by using Moringa oleifera seed powder,” 2015.

[51] P. T. Parmar, A. K. Singh, and S. G. Borad, “Coconut (Cocos nucifera),” in *Oilseeds: Health Attributes and Food Applications*, Springer Singapore, 2020, pp. 163–189. doi: 10.1007/978-981-15-4194-0_7.

[52] K. Thinkohkaew, N. Rodthongkum, and S. Ummartyotin, “Coconut husk (Cocos nucifera) cellulose reinforced poly vinyl alcohol-based hydrogel composite with control-release behavior of methylene blue,” *Journal of Materials Research and Technology*, vol. 9, no. 3, pp. 6602–6611, 2020, doi: 10.1016/j.jmrt.2020.04.051.

[53] L. A. Araujo *et al.*, “Moringa oleifera biomass residue for the removal of pharmaceuticals from water,” *J Environ Chem Eng*, vol. 6, no. 6, pp. 7192–7199, Dec. 2018, doi: 10.1016/j.jece.2018.11.016.

[54] G. S. Tomasin, W. R. Silva, B. E. dos Santos Costa, and N. M. M. Coelho, “Highly sensitive determination of Cu(II) ions in hemodialysis water by F AAS after disposable pipette extraction (DPX) using Moringa oleifera as solid phase,” *Microchemical Journal*, vol. 161, Feb. 2021, doi: 10.1016/j.microc.2020.105749.

[55] P. Sirajudheen, P. Karthikeyan, and S. Meenakshi, “Mechanistic performance of organic pollutants removal from water using Zn/Al layered double hydroxides

imprinted carbon composite," *Surfaces and Interfaces*, vol. 20, Sep. 2020, doi: 10.1016/j.surfin.2020.100581.

[56] R. K. Aldakheel, M. A. Gondal, M. M. Nasr, M. A. Almessiere, and N. Idris, "Spectral analysis of Miracle Moringa tree leaves using X-ray photoelectron, laser induced breakdown and inductively coupled plasma -optical emission spectroscopic techniques," *Talanta*, vol. 217, Sep. 2020, doi: 10.1016/j.talanta.2020.121062.

[57] A. A. Adenuga, O. Ayinuola, E. A. Adejuyigbe, and A. O. Ogunfowokan, "Biomonitoring of phthalate esters in breast-milk and urine samples as biomarkers for neonates' exposure, using modified quechers method with agricultural biochar as dispersive solid-phase extraction absorbent," *Microchemical Journal*, vol. 152, Jan. 2020, doi: 10.1016/j.microc.2019.104277.

[58] A. Çelekli, A. I. Al-Nuaimi, and H. Bozkurt, "Adsorption kinetic and isotherms of Reactive Red 120 on Moringa oleifera seed as an eco-friendly process," *J Mol Struct*, vol. 1195, pp. 168–178, Nov. 2019, doi: 10.1016/j.molstruc.2019.05.106.

[59] M. M. Kgatitsoe, S. Ncube, H. Tutu, I. A. Nyambe, and L. Chimuka, "Synthesis and characterization of a magnetic nanosorbent modified with Moringa oleifera leaf extracts for removal of nitroaromatic explosive compounds in water samples," *J Environ Chem Eng*, vol. 7, no. 3, Jun. 2019, doi: 10.1016/j.jece.2019.103128.

[60] Z. Shirani, C. Santhosh, J. Iqbal, and A. Bhatnagar, "Waste Moringa oleifera seed pods as green sorbent for efficient removal of toxic aquatic pollutants," *J*

Environ Manage, vol. 227, pp. 95–106, Dec. 2018, doi: 10.1016/j.jenvman.2018.08.077.

[61] L. A. Araujo *et al.*, "Moringa oleifera biomass residue for the removal of pharmaceuticals from water," *J Environ Chem Eng*, vol. 6, no. 6, pp. 7192–7199, Dec. 2018, doi: 10.1016/j.jece.2018.11.016.

[62] M. Ma *et al.*, "Coconut shell biochar application in liquid-solid microextraction of triazine herbicides from multi-media environmental samples," *Anal Chim Acta*, vol. 1261, p. 341225, Jun. 2023, doi: 10.1016/j.aca.2023.341225.

[63] K. Xiao *et al.*, "Distribution of eight organophosphorus pesticides and their oxides in surface water of the East China Sea based on high volume solid phase extraction method," *Environmental Pollution*, vol. 279, Jun. 2021, doi: 10.1016/j.envpol.2021.116886.

[64] N. A. Baharum, H. M. Nasir, M. Y. Ishak, N. M. Isa, M. A. Hassan, and A. Z. Aris, "Highly efficient removal of diazinon pesticide from aqueous solutions by using coconut shell-modified biochar," *Arabian Journal of Chemistry*, vol. 13, no. 7, pp. 6106–6121, Jul. 2020, doi: 10.1016/j.arabjc.2020.05.011.

[65] T. R. de Aguiar Jr, J. A. Osmar Guimar, aes Neto, and H. Pereira, "Study of two cork species as natural biosorbents for five selected pesticides in water," 2019, doi: 10.1016/j.heliyon.2019.

[66] K. Kumrić, R. Vujasin, M. Egerić, Đ. Petrović, A. Devečerski, and L. Matović, "Coconut Shell Activated Carbon as Solid-Phase Extraction Adsorbent for Preconcentration of Selected Pesticides from Water Samples," *Water Air Soil Pollut*, vol. 230, no. 12, Dec. 2019, doi: 10.1007/s11270-019-4359-7.

[67] W. Liang, J. Wang, X. Zang, W. Dong, C. Wang, and Z. Wang, “Barley husk carbon as the fiber coating for the solid-phase microextraction of twelve pesticides in vegetables prior to gas chromatography–mass spectrometric detection,” *J Chromatogr A*, vol. 1491, pp. 9–15, Mar. 2017, doi: 10.1016/j.chroma.2017.02.034.

[68] F. Augusto, L. W. Hantao, N. G. S. Mogollón, and S. C. G. N. Braga, “New materials and trends in sorbents for solid-phase extraction,” 2013, *Elsevier B.V.* doi: 10.1016/j.trac.2012.08.012.

[69] C. F. Poole, “New trends in solid-phase extraction,” Jun. 01, 2003, *Elsevier*. doi: 10.1016/S0165-9936(03)00605-8.

[70] Y. Miao, F. Han, B. Pan, Y. Niu, G. Nie, and L. Lv, “Antimony(V) removal from water by hydrated ferric oxides supported by calcite sand and polymeric anion exchanger,” *J Environ Sci (China)*, vol. 26, no. 2, pp. 307–314, Feb. 2014, doi: 10.1016/S1001-0742(13)60418-0.

[71] S. E. Bailey, T. J. Olin, R. Mark Bricka, and D. Dean Adrian, “and 2 USAE Waterways Experiment Station, 3909 Halls Ferry Rd.”

[72] A. H. Berger and A. S. Bhown, “Comparing physisorption and chemisorption solid sorbents for use separating CO2 from flue gas using temperature swing adsorption,” in *Energy Procedia*, Elsevier Ltd, 2011, pp. 562–567. doi: 10.1016/j.egypro.2011.01.089.

[73] C. F. Poole, “New trends in solid-phase extraction,” Jun. 01, 2003, *Elsevier*. doi: 10.1016/S0165-9936(03)00605-8.

[74] B. Saad, M. F. Bari, M. I. Saleh, K. Ahmad, and M. K. M. Talib, “Simultaneous determination of preservatives (benzoic acid, sorbic acid,

methylparaben and propylparaben) in foodstuffs using high-performance liquid chromatography," in *Journal of Chromatography A*, Elsevier, May 2005, pp. 393–397. doi: 10.1016/j.chroma.2004.10.105.

[75] V. Pichon, L. Chen, and M.-C. Hennion, "ANALYTIcA On-line preconcentration and liquid chromatographic analysis of phenylurea pesticides in environmental water using a silica-based immunosorbent," 1995.

[76] S. K. Poole, T. A. Dean, J. W. Oudsema, and C. F. Poole, "Sample preparation for chromatographic separations: an overview," 1990.

[77] L. F. De Oliveira, K. Bouchmella, K. D. A. Gonçalves, J. Bettini, J. Kobarg, and M. B. Cardoso, "Functionalized Silica Nanoparticles As an Alternative Platform for Targeted Drug-Delivery of Water Insoluble Drugs," *Langmuir*, vol. 32, no. 13, pp. 3217–3225, Apr. 2016, doi: 10.1021/acs.langmuir.6b00214.

[78] Q. Zhao, F. Wei, Y. B. Luo, J. Ding, N. Xiao, and Y. Q. Feng, "Rapid magnetic solid-phase extraction based on magnetic multiwalled carbon nanotubes for the determination of polycyclic aromatic hydrocarbons in edible oils," *J Agric Food Chem*, vol. 59, no. 24, pp. 12794–12800, Dec. 2011, doi: 10.1021/jf203973s.

[79] S. Kochmann, T. Hirsch, and O. S. Wolfbeis, "Graphenes in chemical sensors and biosensors," Oct. 2012. doi: 10.1016/j.trac.2012.06.004.

[80] Y. P. Sun *et al.*, "Quantum-sized carbon dots for bright and colorful photoluminescence," *J Am Chem Soc*, vol. 128, no. 24, pp. 7756–7757, Jun. 2006, doi: 10.1021/ja062677d.

[81] Q. L. Zhao, Z. L. Zhang, B. H. Huang, J. Peng, M. Zhang, and D. W. Pang, "Facile preparation of low cytotoxicity fluorescent carbon nanocrystals by

electrooxidation of graphite," *Chemical Communications*, no. 41, pp. 5116–5118, 2008, doi: 10.1039/b812420e.

[82] K. L. Aillon, Y. Xie, N. El-Gendy, C. J. Berkland, and M. L. Forrest, "Effects of nanomaterial physicochemical properties on in vivo toxicity," Jun. 21, 2009. doi: 10.1016/j.addr.2009.03.010.

[83] Y. P. Sun *et al.*, "Quantum-sized carbon dots for bright and colorful photoluminescence," *J Am Chem Soc*, vol. 128, no. 24, pp. 7756–7757, Jun. 2006, doi: 10.1021/ja062677d.

[84] J. Reignier, P. Alcouffe, F. Méchin, and F. Fenouillot, "The morphology of rigid polyurethane foam matrix and its evolution with time during foaming-New Insight by cryogenic scanning electron microscopy," 2019. [Online]. Available: https://www.elsevier.com/open-access/userlicense/1.0/

[85] M. T. García-Valverde, T. Chatzimitakos, R. Lucena, S. Cárdenas, and C. D. Stalikas, "Melamine sponge functionalized with urea-formaldehyde co-oligomers as a sorbent for the solid-phase extraction of hydrophobic analytes," *Molecules*, vol. 23, no. 10, Oct. 2018, doi: 10.3390/molecules23102595.

[86] Y. Yang, Y. Deng, Z. Tong, and C. Wang, "Multifunctional foams derived from poly(melamine formaldehyde) as recyclable oil absorbents," *J Mater Chem A Mater*, vol. 2, no. 26, pp. 9994–9999, Jul. 2014, doi: 10.1039/c4ta00939h.

[87] C. S. Dourado *et al.*, "Optimization of a saccharin molecularly imprinted solid-phase extraction procedure and evaluation by MIR hyperspectral imaging for analysis of diet tea by HPLC," *Food Chem*, vol. 367, Jan. 2022, doi: 10.1016/j.foodchem.2021.130732.

[88] M. Shirani, E. Parandi, H. R. Nodeh, B. Akbari-adergani, and F. Shahdadi, "Development of a rapid efficient solid-phase microextraction: An overhead rotating flat surface sorbent based 3-D graphene oxide/ lanthanum nanoparticles @ Ni foam for separation and determination of sulfonamides in animal-based food products," *Food Chem*, vol. 373, Mar. 2022, doi: 10.1016/j.foodchem.2021.131421.

[89] P. Huang, H. Kou, X. Wang, Z. Zhou, X. Du, and X. Lu, "Porous cage-like hollow magnetic carbon-doped CoO nanocomposite as an advanced sorbent for magnetic solid-phase extraction of nine polycyclic aromatic hydrocarbons," *Talanta*, vol. 227, May 2021, doi: 10.1016/j.talanta.2021.122149.

[90] A. Yadeghari and M. A. Farajzadeh, "Synthesis of a magnetic sorbent and its application in extraction of different pesticides from water, fruit, and vegetable samples prior to their determination by gas chromatography-tandem mass spectrometry," *J Chromatogr A*, vol. 1635, Jan. 2021, doi: 10.1016/j.chroma.2020.461718.

[91] J. Yang *et al.*, "Metal organic framework assisted in situ complexation for miniaturized solid phase extraction of organic mercury in fish and Dendrobium officinale," *Talanta*, vol. 209, Mar. 2020, doi: 10.1016/j.talanta.2019.120598.

[92] Y. A. Ghorbani, S. M. Ghoreishi, and M. Ghani, "Derived N-doped carbon through core-shell structured metal-organic frameworks as a novel sorbent for dispersive solid phase extraction of Cr(III) and Pb(II) from water samples followed

by quantitation through flame atomic absorption spectrometry," *Microchemical Journal*, vol. 155, Jun. 2020, doi: 10.1016/j.microc.2020.104786.

[93] R. M. Toudeshki, S. Dadfarnia, and A. M. Haji Shabani, "Surface molecularly imprinted polymer on magnetic multi-walled carbon nanotubes for selective recognition and preconcentration of metformin in biological fluids prior to its sensitive chemiluminescence determination: Central composite design optimization," *Anal Chim Acta*, vol. 1089, pp. 78–89, Dec. 2019, doi: 10.1016/j.aca.2019.08.070.

[94] F. J. Ruiz, L. Ripoll, M. Hidalgo, and A. Canals, "Dispersive micro solid-phase extraction (DμSPE) with graphene oxide as adsorbent for sensitive elemental analysis of aqueous samples by laser induced breakdown spectroscopy (LIBS)," *Talanta*, vol. 191, pp. 162–170, Jan. 2019, doi: 10.1016/j.talanta.2018.08.044.

[95] T. Wang, "Polyethyleneimine-modified hybrid silica sorbent for hydrophilic solid-phase extraction of thyreostats in animal tissues," *J Chromatogr A*, vol. 1581–1582, pp. 16–24, Dec. 2018, doi: 10.1016/j.chroma.2018.11.006.

[96] M. A. Farajzadeh and A. Mohebbi, "Development of magnetic dispersive solid phase extraction using toner powder as an efficient and economic sorbent in combination with dispersive liquid–liquid microextraction for extraction of some widely used pesticides in fruit juices," *J Chromatogr A*, vol. 1532, pp. 10–19, Jan. 2018, doi: 10.1016/j.chroma.2017.11.048.

[97] P. Anastas and N. Eghbali, "Green Chemistry: Principles and Practice," *Chem Soc Rev*, vol. 39, no. 1, pp. 301–312, Dec. 2010, doi: 10.1039/b918763b.

[98] J. Płotka-Wasylka, M. Rutkowska, K. Owczarek, M. Tobiszewski, and J. Namieśnik, “Extraction with environmentally friendly solvents,” Jun. 01, 2017, *Elsevier B.V.* doi: 10.1016/j.trac.2017.03.006.

[99] M. J. Trujillo-Rodríguez, H. Nan, M. Varona, M. N. Emaus, I. D. Souza, and J. L. Anderson, “Advances of Ionic Liquids in Analytical Chemistry,” Jan. 02, 2019, *American Chemical Society*. doi: 10.1021/acs.analchem.8b04710.

[100] K. N. Marsh, J. A. Boxall, and R. Lichtenthaler, “Room temperature ionic liquids and their mixtures - A review,” in *Fluid Phase Equilibria*, May 2004, pp. 93–98. doi: 10.1016/j.fluid.2004.02.003.

[101] B. Herce-Sesa, J. A. López-López, and C. Moreno, “Advances in ionic liquids and deep eutectic solvents-based liquid phase microextraction of metals for sample preparation in Environmental Analytical Chemistry,” Oct. 01, 2021, *Elsevier B.V.* doi: 10.1016/j.trac.2021.116398.

[102] B. Herce-Sesa, P. Pirkwieser, J. A. López-López, F. Jirsa, and C. Moreno, “Selective liquid phase micro-extraction of metal chloro-complexes from saline waters using ionic liquids,” *J Clean Prod*, vol. 262, Jul. 2020, doi: 10.1016/j.jclepro.2020.121415.

[103] M. Karimi, S. Dadfarnia, A. M. H. Shabani, F. Tamaddon, and D. Azadi, “Deep eutectic liquid organic salt as a new solvent for liquid-phase microextraction and its application in ligandless extraction and preconcentraion of lead and cadmium in edible oils,” *Talanta*, vol. 144, pp. 648–654, Jul. 2015, doi: 10.1016/j.talanta.2015.07.021.

[104] E. L. Smith, A. P. Abbott, and K. S. Ryder, “Deep Eutectic Solvents (DESs) and Their Applications,” Nov. 12, 2014, *American Chemical Society*. doi: 10.1021/cr300162p.

[105] J. Płotka-Wasylka, M. de la Guardia, V. Andruch, and M. Vilková, “Deep eutectic solvents vs ionic liquids: Similarities and differences,” Dec. 01, 2020, *Elsevier Inc.* doi: 10.1016/j.microc.2020.105539.

[106] Á. Santana-Mayor, R. Rodríguez-Ramos, A. V. Herrera-Herrera, B. Socas-Rodríguez, and M. Á. Rodríguez-Delgado, “Deep eutectic solvents. The new generation of green solvents in analytical chemistry,” Jan. 01, 2021, *Elsevier B.V.* doi: 10.1016/j.trac.2020.116108.

[107] Y. Dai, J. van Spronsen, G.-J. Witkamp, R. Verpoorte, and Y. H. Choi, “Natural deep eutectic solvents as new potential media for green technology,” *Anal Chim Acta*, vol. 766, pp. 61–68, Mar. 2013, doi: 10.1016/j.aca.2012.12.019.

[108] C. Florindo, F. Lima, B. D. Ribeiro, and I. M. Marrucho, “Deep eutectic solvents: overcoming 21st century challenges,” *Curr Opin Green Sustain Chem*, vol. 18, pp. 31–36, Aug. 2019, doi: 10.1016/j.cogsc.2018.12.003.

[109] A. Paiva, R. Craveiro, I. Aroso, M. Martins, R. L. Reis, and A. R. C. Duarte, “Natural deep eutectic solvents - Solvents for the 21st century,” May 05, 2014, *American Chemical Society*. doi: 10.1021/sc500096j.

[110] X. Xu, J. Gao, M. Ran, Y. Guo, D. Feng, and L. Zhang, “Nanoconfinement of functionalized ionic liquid for enhanced adsorption and rapid sensitive detection of phenylurea herbicides in food and environmental samples,” *Food Chem*, vol. 431, Jan. 2024, doi: 10.1016/j.foodchem.2023.137149.

[111] L. Wang, Y. Wang, Y. Qin, and Y. Zhou, “Room-temperature synthesis of ionic liquid@covalent organic frameworks for the solid phase extraction and analysis of six herbicides from water samples,” *Microchemical Journal*, vol. 195, p. 109497, Dec. 2023, doi: 10.1016/j.microc.2023.109497.

[112] V. R. Zeger, D. S. Bell, J. S. Herrington, and J. L. Anderson, “Selective isolation of pesticides and cannabinoids using polymeric ionic liquid-based sorbent coatings in solid-phase microextraction coupled to high-performance liquid chromatography,” *J Chromatogr A*, vol. 1680, p. 463416, Sep. 2022, doi: 10.1016/j.chroma.2022.463416.

[113] W. Xu, J. Li, J. Feng, Z. Wang, and H. Zhang, “In-syringe temperature-controlled liquid–liquid microextraction based on solidified floating ionic liquid for the simultaneous determination of triazine and phenylurea pesticide in vegetable protein drinks,” *Journal of Chromatography B*, vol. 1174, p. 122721, Jun. 2021, doi: 10.1016/j.jchromb.2021.122721.

[114] H. Sereshti, G. Abdolhosseini, S. Soltani, H. Sadatfaraji, S. Karami, and H. Rashidi Nodeh, “A green ternary polymeric deep eutectic solvent used in dispersive liquid-liquid microextraction technique for isolation of multiclass pesticides in fruit juice samples,” *Journal of Food Composition and Analysis*, vol. 124, p. 105663, Dec. 2023, doi: 10.1016/j.jfca.2023.105663.

[115] X. Jing, H. Xue, X. Sang, X. Wang, and L. Jia, “Magnetic deep eutectic solvent-based dispersive liquid–liquid microextraction for enantioselectively determining chiral mefentrifluconazole in cereal samples via ultra-high-performance

liquid chromatography," *Food Chem*, vol. 391, p. 133220, Oct. 2022, doi: 10.1016/j.foodchem.2022.133220.

[116] F. Monajemzadeh, A. Mohebbi, M. A. Farajzadeh, M. Nemati, and M. R. Afshar Mogaddam, "Dispersive solid phase extraction combined with in syringe deep eutectic solvent based dispersive liquid-liquid microextraction for determination of some pesticides and their metabolite in egg samples," *Journal of Food Composition and Analysis*, vol. 96, p. 103696, Mar. 2021, doi: 10.1016/j.jfca.2020.103696.

[117] X. Li *et al.*, "Magnetic nanoparticle-assisted in situ ionic liquid dispersive liquid-liquid microextraction of pyrethroid pesticides in urine samples," *Microchemical Journal*, vol. 159, p. 105350, Dec. 2020, doi: 10.1016/j.microc.2020.105350.

[118] H. Heidari, S. Ghanbari-Rad, and E. Habibi, "Optimization deep eutectic solvent-based ultrasound-assisted liquid-liquid microextraction by using the desirability function approach for extraction and preconcentration of organophosphorus pesticides from fruit juice samples," *Journal of Food Composition and Analysis*, vol. 87, p. 103389, Apr. 2020, doi: 10.1016/j.jfca.2019.103389.

[119] Y. Yamini, M. Rezazadeh, and S. Seidi, "Liquid-phase microextraction – The different principles and configurations," Mar. 01, 2019, *Elsevier B.V.* doi: 10.1016/j.trac.2018.06.010.

[120] J. R. Broich, D. 13 Hoixxan, S. J. Goldner, S. Andryauskas, and C. J. Um3erger, “liquid-solid extraction of lyophilized biological material for forensic analysis I. application to urine samples for detection of drugs of abuse.”

[121] N. Fontanals, R. M. Marcé, and F. Borrull, “Porous polymer sorbents,” in *Solid-Phase Extraction*, Elsevier, 2019, pp. 55–82. doi: 10.1016/B978-0-12-816906-3.00003-0.

[122] M. E. I. Badawy, M. A. M. El-Nouby, P. K. Kimani, L. W. Lim, and E. I. Rabea, “A review of the modern principles and applications of solid-phase extraction techniques in chromatographic analysis,” Dec. 01, 2022, *Springer*. doi: 10.1007/s44211-022-00190-8.

[123] S. Moldoveanu and V. David, “Solid-Phase Extraction,” in *Modern Sample Preparation for Chromatography*, Elsevier, 2015, pp. 191–286. doi: 10.1016/B978-0-444-54319-6.00007-4.

[124] C. F. Poole, “New trends in solid-phase extraction,” Jun. 01, 2003, *Elsevier*. doi: 10.1016/S0165-9936(03)00605-8.

[125] S. Seidi, M. Tajik, M. Baharfar, and M. Rezazadeh, “Micro solid-phase extraction (pipette tip and spin column) and thin film solid-phase microextraction: Miniaturized concepts for chromatographic analysis,” Sep. 01, 2019, *Elsevier B.V.* doi: 10.1016/j.trac.2019.06.036.

[126] E. N. Ali, S. R. Alfarra, M. M. Yusoff, and M. L. Rahman, “Environmentally Friendly Biosorbent from Moringa Oleifera Leaves for Water Treatment,” *International Journal of Environmental Science and Development*, vol. 6, no. 3, pp. 165–169, 2015, doi: 10.7763/IJESD.2015.V6.582.

[127] A. Bagheri, E. Abu-Danso, J. Iqbal, and A. Bhatnagar, “Modified biochar from Moringa seed powder for the removal of diclofenac from aqueous solution,” *Environmental Science and Pollution Research*, vol. 27, no. 7, pp. 7318–7327, Mar. 2020, doi: 10.1007/s11356-019-06844-x.

[128] Z. Shirani, C. Santhosh, J. Iqbal, and A. Bhatnagar, “Waste Moringa oleifera seed pods as green sorbent for efficient removal of toxic aquatic pollutants,” *J Environ Manage*, vol. 227, pp. 95–106, Dec. 2018, doi: 10.1016/j.jenvman.2018.08.077.

[129] J. Chen, B. Zhang, D. Zheng, X. Dang, Y. Ai, and H. Chen, “A novel needle trap device coupled with gas chromatography for determination of five fatty alcohols in tea samples,” *Analytical Methods*, vol. 10, no. 48, pp. 5783–5789, Dec. 2018, doi: 10.1039/c8ay01894d.

[130] M.-C. Hennion´laboratoire, “Graphitized carbons for solid-phase extraction,” 2000. [Online]. Available: www.elsevier.com/locate/chroma

[131] S. Amini, H. Ebrahimzadeh, S. Seidi, and N. Jalilian, “Application of electrospun polyacrylonitrile/Zn-MOF-74@GO nanocomposite as the sorbent for online micro solid-phase extraction of chlorobenzenes in water, soil, and food samples prior to liquid chromatography analysis,” *Food Chem*, vol. 363, p. 130330, Nov. 2021, doi: 10.1016/j.foodchem.2021.130330.

[132] M. N. H. Rozaini *et al.*, “Green adsorption–desorption of mixed triclosan, triclocarban, 2-phenylphenol, bisphenol A and 4-tert-octylphenol using MXene encapsulated polypropylene membrane protected micro-solid-phase extraction

device in amplifying the HPLC analysis," *Microchemical Journal*, vol. 170, p. 106695, Nov. 2021, doi: 10.1016/j.microc.2021.106695.

[133] P.-C. Tsai, A. Pundi, K. Brindhadevi, and V. K. Ponnusamy, "Novel semi-automated graphene nanosheets based pipette-tip assisted micro-solid phase extraction as eco-friendly technique for the rapid detection of emerging environmental pollutant in waters," *Chemosphere*, vol. 276, p. 130031, Aug. 2021, doi: 10.1016/j.chemosphere.2021.130031.

[134] N. Atirah Mohd Nazir, M. Raoov, and S. Mohamad, "Spent tea leaves as an adsorbent for micro-solid-phase extraction of polycyclic aromatic hydrocarbons (PAHs) from water and food samples prior to GC-FID analysis," *Microchemical Journal*, vol. 159, p. 105581, Dec. 2020, doi: 10.1016/j.microc.2020.105581.

[135] M. Manouchehri, S. Seidi, A. Rouhollahi, H. Noormohammadi, and M. Shanehsaz, "Micro solid phase extraction of parabens from breast milk samples using Mg-Al layered double hydroxide functionalized partially reduced graphene oxide nanocomposite," *Food Chem*, vol. 314, p. 126223, Jun. 2020, doi: 10.1016/j.foodchem.2020.126223.

[136] T. Sun, M. M. Ali, D. Wang, and Z. Du, "On-site rapid screening of benzodiazepines in dietary supplements using pipette-tip micro-solid phase extraction coupled to ion mobility spectrometry," *J Chromatogr A*, vol. 1610, p. 460547, Jan. 2020, doi: 10.1016/j.chroma.2019.460547.

[137] L. Xia, Y. Du, X. Xiao, and G. Li, "One-step membrane protected micro-solid-phase extraction and derivatization coupling to high-performance liquid

chromatography for selective determination of aliphatic aldehydes in cosmetics and food," *Talanta*, vol. 202, pp. 580–590, Sep. 2019, doi: 10.1016/j.talanta.2019.05.035.

[138] K. Alhooshani, "Determination of N-nitrosamines in water resources using Al-AC sorbent for stir-bar supported micro-solid-phase extraction coupled with gas chromatography mass-spectrometry," *Microchemical Journal*, vol. 146, pp. 622–629, May 2019, doi: 10.1016/j.microc.2019.01.061.

[139] M. S. Sammani, S. Clavijo, A. González, and V. Cerdà, "Development of an on-line lab-on-valve micro-solid phase extraction system coupled to liquid chromatography for the determination of flavonoids in citrus juices," *Anal Chim Acta*, vol. 1082, pp. 56–65, Nov. 2019, doi: 10.1016/j.aca.2019.06.032.

[140] B. Arabsorkhi and H. Sereshti, "Determination of tetracycline and cefotaxime residues in honey by micro-solid phase extraction based on electrospun nanofibers coupled with HPLC," *Microchemical Journal*, vol. 140, pp. 241–247, Jul. 2018, doi: 10.1016/j.microc.2018.04.030.

[141] G.-T. Zhu, X.-L. Hu, S. He, X.-M. He, S.-K. Zhu, and Y.-Q. Feng, "Hydrothermally tailor-made chitosan fiber for micro-solid phase extraction of petroleum acids in crude oils," *J Chromatogr A*, vol. 1564, pp. 42–50, Aug. 2018, doi: 10.1016/j.chroma.2018.06.006.

[142] L. H. Keith, L. U. Gron, and J. L. Young, "Green Analytical Methodologies," *Chem Rev*, vol. 107, no. 6, pp. 2695–2708, Jun. 2007, doi: 10.1021/cr068359e.

[143] A. Aly and T. Górecki, "Green Approaches to Sample Preparation Based on Extraction Techniques," *Molecules*, vol. 25, no. 7, p. 1719, Apr. 2020, doi: 10.3390/molecules25071719.

[144] J. Salafranca, D. Pezo, and C. Nerín, “Assessment of specific migration to aqueous simulants of a new active food packaging containing essential oils by means of an automatic multiple dynamic hollow fibre liquid phase microextraction system,” *J Chromatogr A*, vol. 1216, no. 18, pp. 3731–3739, May 2009, doi: 10.1016/j.chroma.2009.03.001.

[145] R. Rodríguez-Ramos, A. V. Herrera-Herrera, C. Díaz-Romero, B. Socas-Rodríguez, and M. Á. Rodríguez-Delgado, “Eco-friendly approach developed for the microextraction of xenobiotic contaminants from tropical beverages using a camphor-based natural hydrophobic deep eutectic solvent,” *Talanta*, vol. 266, p. 124932, Jan. 2024, doi: 10.1016/j.talanta.2023.124932.

[146] K. A. Ago, S. A. Kitte, G. Chirfa, and A. Gure, “Effervescent powder-assisted floating organic solvent-based dispersive liquid-liquid microextraction for determination of organochlorine pesticides in water by GC–MS,” *Heliyon*, vol. 9, no. 1, p. e12954, Jan. 2023, doi: 10.1016/j.heliyon.2023.e12954.

[147] P. Yadav *et al.*, “Modified DLLME-SFO approach for evaluation of multiclass agrochemicals and its associated risk assessment: Soil, Saccharum officinarum and Jaggery,” *Food Chemistry Advances*, vol. 1, p. 100032, Oct. 2022, doi: 10.1016/j.focha.2022.100032.

[148] V. Gallo *et al.*, “Dispersive liquid-liquid microextraction using a low transition temperature mixture and liquid chromatography-mass spectrometry analysis of pesticides in urine samples,” *J Chromatogr A*, vol. 1642, p. 462036, Apr. 2021, doi: 10.1016/j.chroma.2021.462036.

[149] S. C. Machado, B. M. Souza, L. P. de Aguiar Marciano, A. F. Souza Pereira, D. T. de Carvalho, and I. Martins, "A sensitive and accurate vortex-assisted liquid-liquid microextraction-gas chromatography-mass spectrometry method for urinary triazoles," *J Chromatogr A*, vol. 1586, pp. 9–17, Feb. 2019, doi: 10.1016/j.chroma.2018.11.082.

[150] T. Tang, K. Qian, T. Shi, F. Wang, J. Li, and Y. Cao, "Determination of triazole fungicides in environmental water samples by high performance liquid chromatography with cloud point extraction using polyethylene glycol 600 monooleate," *Anal Chim Acta*, vol. 680, no. 1–2, pp. 26–31, Nov. 2010, doi: 10.1016/j.aca.2010.09.034.

[151] D. Li, M. He, B. Chen, and B. Hu, "Magnetic porous organic polymers for magnetic solid-phase extraction of triazole fungicides in vegetables prior to their determination by gas chromatography-flame ionization detection," *J Chromatogr A*, vol. 1601, pp. 1–8, Sep. 2019, doi: 10.1016/j.chroma.2019.04.062.

[152] Y. Wang, M. He, B. Chen, and B. Hu, "Hydroxyl-containing porous organic framework coated stir bar sorption extraction combined with high performance liquid chromatography-diode array detector for analysis of triazole fungicides in grape and cabbage samples," *J Chromatogr A*, vol. 1633, Dec. 2020, doi: 10.1016/j.chroma.2020.461628.

[153] M. Rutkowska, J. Płotka-Wasylka, M. Sajid, and V. Andruch, "Liquid–phase microextraction: A review of reviews," Sep. 01, 2019, *Elsevier Inc.* doi: 10.1016/j.microc.2019.103989.

[154] X. Han, J. Chen, Z. Li, K. Quan, and H. Qiu, “Magnetic solid-phase extraction of triazole fungicides based on magnetic porous carbon prepared by combustion combined with solvothermal method,” *Anal Chim Acta*, vol. 1129, pp. 85–97, Sep. 2020, doi: 10.1016/j.aca.2020.06.077.

[155] X. Han, J. Chen, Z. Li, K. Quan, and H. Qiu, “Magnetic solid-phase extraction of triazole fungicides based on magnetic porous carbon prepared by combustion combined with solvothermal method,” *Anal Chim Acta*, vol. 1129, pp. 85–97, Sep. 2020, doi: 10.1016/j.aca.2020.06.077.

[156] J. Płotka-Wasylka, M. Rutkowska, K. Owczarek, M. Tobiszewski, and J. Namieśnik, “Extraction with environmentally friendly solvents,” *TrAC Trends in Analytical Chemistry*, vol. 91, pp. 12–25, Jun. 2017, doi: 10.1016/j.trac.2017.03.006.

[157] P. Zhao, Z. Wang, K. Li, X. Guo, and L. Zhao, “Multi-residue enantiomeric analysis of 18 chiral pesticides in water, soil and river sediment using magnetic solid-phase extraction based on amino modified multiwalled carbon nanotubes and chiral liquid chromatography coupled with tandem mass spectrometry,” *J Chromatogr A*, vol. 1568, pp. 8–21, Sep. 2018, doi: 10.1016/j.chroma.2018.07.022.

[158] J. A. Ocaña-González, N. Aranda-Merino, J. L. Pérez-Bernal, and M. Ramos-Payán, “Solid supports and supported liquid membranes for different liquid phase microextraction and electromembrane extraction configurations. A review,” *J Chromatogr A*, vol. 1691, p. 463825, Feb. 2023, doi: 10.1016/j.chroma.2023.463825.

[159] M. E. Hergueta-Castillo, E. López-Rodríguez, R. López-Ruiz, R. Romero-González, and A. Garrido Frenich, “Targeted and untargeted analysis of triazole

fungicides and their metabolites in fruits and vegetables by UHPLC-orbitrap-MS2," *Food Chem*, vol. 368, p. 130860, Jan. 2022, doi: 10.1016/j.foodchem.2021.130860.

[160] B. Gao *et al.*, "Development of an analytical method based on solid-phase extraction and LC-MS/MS for the monitoring of current-use pesticides and their metabolites in human urine," *Journal of Environmental Sciences*, vol. 111, pp. 153–163, Jan. 2022, doi: 10.1016/j.jes.2021.03.029.

[161] F. Yang *et al.*, "A rapid method for the simultaneous stereoselective determination of the triazole fungicides in tobacco by supercritical fluid chromatography-tandem mass spectrometry combined with pass-through cleanup," *J Chromatogr A*, vol. 1642, p. 462040, Apr. 2021, doi: 10.1016/j.chroma.2021.462040.

[162] K. Seebunrueng, S. Tamuang, S. Ruangchai, S. Sansuk, and S. Srijaranai, "In situ self-assembled coating of surfactant-mixed metal hydroxide on Fe3O4@SiO2 magnetic composite for dispersive solid phase microextraction prior to HPLC analysis of triazole fungicides," *Microchemical Journal*, vol. 168, p. 106396, Sep. 2021, doi: 10.1016/j.microc.2021.106396.

[163] S. Belarbi, M. Vivier, W. Zaghouani, A. De Sloovere, V. Agasse-Peulon, and P. Cardinael, "Comparison of new approach of GC-HRMS (Q-Orbitrap) to GC–MS/MS (triple-quadrupole) in analyzing the pesticide residues and contaminants in complex food matrices," *Food Chem*, vol. 359, p. 129932, Oct. 2021, doi: 10.1016/j.foodchem.2021.129932.

[164] X. Han, J. Chen, Z. Li, K. Quan, and H. Qiu, “Magnetic solid-phase extraction of triazole fungicides based on magnetic porous carbon prepared by combustion combined with solvothermal method,” *Anal Chim Acta*, vol. 1129, pp. 85–97, Sep. 2020, doi: 10.1016/j.aca.2020.06.077.

[165] M. M. Abolghasemi, M. Piryaei, and R. M. Imani, “Deep eutectic solvents as extraction phase in head-space single-drop microextraction for determination of pesticides in fruit juice and vegetable samples,” *Microchemical Journal*, vol. 158, p. 105041, Nov. 2020, doi: 10.1016/j.microc.2020.105041.

[166] I. A. Senosy, H.-M. Guo, M.-N. Ouyang, Z.-H. Lu, Z.-H. Yang, and J.-H. Li, “Magnetic solid-phase extraction based on nano-zeolite imidazolate framework-8-functionalized magnetic graphene oxide for the quantification of residual fungicides in water, honey and fruit juices,” *Food Chem*, vol. 325, p. 126944, Sep. 2020, doi: 10.1016/j.foodchem.2020.126944.

[167] H. Zeng *et al.*, “Enantioseparation and determination of triazole fungicides in vegetables and fruits by aqueous two-phase extraction coupled with online heart-cutting two-dimensional liquid chromatography,” *Food Chem*, vol. 301, p. 125265, Dec. 2019, doi: 10.1016/j.foodchem.2019.125265.

[168] Y. Jabali, M. Millet, and M. El-Hoz, “Optimization of a DI-SPME-GC–MS/MS method for multi-residue analysis of pesticides in waters,” *Microchemical Journal*, vol. 147, pp. 83–92, Jun. 2019, doi: 10.1016/j.microc.2019.03.004.

[169] X. Ye *et al.*, “Trace enantioselective determination of triazole fungicides in honey by a sensitive and efficient method,” *Journal of Food Composition and Analysis*, vol. 74, pp. 62–70, Dec. 2018, doi: 10.1016/j.jfca.2018.09.005.

[170] I. A. Senosy, H.-M. Guo, M.-N. Ouyang, Z.-H. Lu, Z.-H. Yang, and J.-H. Li, "Magnetic solid-phase extraction based on nano-zeolite imidazolate framework-8-functionalized magnetic graphene oxide for the quantification of residual fungicides in water, honey and fruit juices," *Food Chem*, vol. 325, p. 126944, Sep. 2020, doi: 10.1016/j.foodchem.2020.126944.

[171] X.-Z. Hu, J.-X. Wang, and Y.-Q. Feng, "Determination of Benzimidazole Residues in Edible Animal Food by Polymer Monolith Microextraction Combined with Liquid Chromatography−Mass Spectrometry," *J Agric Food Chem*, vol. 58, no. 1, pp. 112–119, Jan. 2010, doi: 10.1021/jf902888a.

[172] J. Vichapong, Y. Santaladchaiyakit, R. Burakham, and S. Srijaranai, "Determination of Benzimidazole Anthelminthics in Eggs by Advanced Microextraction with High-Performance Liquid Chromatography," *Anal Lett*, vol. 48, no. 4, pp. 617–631, Mar. 2015, doi: 10.1080/00032719.2014.952371.

[173] J. Domínguez-Álvarez, M. Mateos-Vivas, D. García-Gómez, E. Rodríguez-Gonzalo, and R. Carabias-Martínez, "Capillary electrophoresis coupled to mass spectrometry for the determination of anthelmintic benzimidazoles in eggs using a QuEChERS with preconcentration as sample treatment," *J Chromatogr A*, vol. 1278, pp. 166–174, Feb. 2013, doi: 10.1016/j.chroma.2012.12.064.

[174] Y. Huang, Q. Zhou, and G. Xie, "Development of micro-solid phase extraction with titanate nanotube array modified by cetyltrimethylammonium bromide for sensitive determination of polycyclic aromatic hydrocarbons from environmental water samples," *J Hazard Mater*, vol. 193, pp. 82–89, Oct. 2011, doi: 10.1016/j.jhazmat.2011.07.025.

[175] Q. Zhao, F. Wei, Y. B. Luo, J. Ding, N. Xiao, and Y. Q. Feng, “Rapid magnetic solid-phase extraction based on magnetic multiwalled carbon nanotubes for the determination of polycyclic aromatic hydrocarbons in edible oils,” *J Agric Food Chem*, vol. 59, no. 24, pp. 12794–12800, Dec. 2011, doi: 10.1021/jf203973s.

[176] R. Konášová, J. J. Dytrtová, and V. Kašička, “Determination of acid dissociation constants of triazole fungicides by pressure assisted capillary electrophoresis,” *J Chromatogr A*, vol. 1408, pp. 243–249, 2015, doi: 10.1016/j.chroma.2015.07.005.

[177] N. Hendrasarie and S. H. Maria, “Combining grease trap and Moringa Oleifera as adsorbent to treat wastewater restaurant,” *S Afr J Chem Eng*, vol. 37, pp. 196–205, Jul. 2021, doi: 10.1016/j.sajce.2021.05.004.

[178] Z. U. Zango *et al.*, “An Overview and Evaluation of Highly Porous Adsorbent Materials for Polycyclic Aromatic Hydrocarbons and Phenols Removal from Wastewater,” *Water (Basel)*, vol. 12, no. 10, p. 2921, Oct. 2020, doi: 10.3390/w12102921.

[179] W. Boulaiche, B. Hamdi, and M. Trari, “Removal of heavy metals by chitin: equilibrium, kinetic and thermodynamic studies,” *Appl Water Sci*, vol. 9, no. 2, p. 39, Mar. 2019, doi: 10.1007/s13201-019-0926-8.

[180] A. De Olivera, C. Kreutz, and R. Martins, “Physicochemical characterization of Moringa oleífera’s shells as biosorbent for pharmaceuticals biosorption,” *The Academic Society Journal*, pp. 99–103, Jun. 2020, doi: 10.32640/tasj.2020.2.99.

[181] A. De Olivera, C. Kreutz, and R. Martins, “Physicochemical characterization of Moringa oleífera’s shells as biosorbent for pharmaceuticals biosorption,” *The Academic Society Journal*, pp. 99–103, Jun. 2020, doi: 10.32640/tasj.2020.2.99.

[182] C. S. T. Araújo, E. I. Melo, V. N. Alves, and N. M. M. Coelho, “Moringa oleifera Lam. seeds as a natural solid adsorbent for removal of AgI in aqueous solutions,” *J Braz Chem Soc*, vol. 21, no. 9, pp. 1727–1732, 2010, doi: 10.1590/S0103-50532010000900019.

[183] E. N. Ali, S. R. Alfarra, M. M. Yusoff, and M. L. Rahman, “Environmentally Friendly Biosorbent from Moringa Oleifera Leaves for Water Treatment,” *International Journal of Environmental Science and Development*, vol. 6, no. 3, pp. 165–169, 2015, doi: 10.7763/IJESD.2015.V6.582.

[184] Y. H. Boon, N. N. Mohamad Zain, S. Mohamad, H. Osman, and M. Raoov, “Magnetic poly(β-cyclodextrin-ionic liquid) nanocomposites for micro-solid phase extraction of selected polycyclic aromatic hydrocarbons in rice samples prior to GC-FID analysis,” *Food Chem*, vol. 278, pp. 322–332, Apr. 2019, doi: 10.1016/j.foodchem.2018.10.145.

[185] J. de A. N. Oliveira, L. M. Cândido Siqueira, J. A. de Sousa Neto, N. M. M. Coelho, and V. N. Alves, “Preconcentration system for determination of lead in chicken feed using Moringa oleifera husks as a biosorbent,” *Microchemical Journal*, vol. 133, pp. 327–332, Jul. 2017, doi: 10.1016/j.microc.2017.04.001.

[186] Y. ALDEGS, M. ELBARGHOUTHI, A. ELSHEIKH, and G. WALKER, “Effect of solution pH, ionic strength, and temperature on adsorption behavior of

reactive dyes on activated carbon," *Dyes and Pigments*, vol. 77, no. 1, pp. 16–23, 2008, doi: 10.1016/j.dyepig.2007.03.001.

[187] F. B. Scheufele *et al.*, "Biosorption of direct black dye by cassava root husks: Kinetics, equilibrium, thermodynamics and mechanism assessment," *J Environ Chem Eng*, vol. 8, no. 2, p. 103533, Apr. 2020, doi: 10.1016/j.jece.2019.103533.

[188] M. Sulyok, F. Berthiller, R. Krska, and R. Schuhmacher, "Development and validation of a liquid chromatography/tandem mass spectrometric method for the determination of 39 mycotoxins in wheat and maize," *Rapid Communications in Mass Spectrometry*, vol. 20, no. 18, pp. 2649–2659, Sep. 2006, doi: 10.1002/rcm.2640.

[189] T. Khezeli, A. Daneshfar, and R. Sahraei, "A green ultrasonic-assisted liquid–liquid microextraction based on deep eutectic solvent for the HPLC-UV determination of ferulic, caffeic and cinnamic acid from olive, almond, sesame and cinnamon oil," *Talanta*, vol. 150, pp. 577–585, Apr. 2016, doi: 10.1016/j.talanta.2015.12.077.

[190] M. Becerra-Herrera, M. Sánchez-Astudillo, R. Beltrán, and A. Sayago, "Determination of phenolic compounds in olive oil: New method based on liquid–liquid micro extraction and ultra high performance liquid chromatography-triple–quadrupole mass spectrometry," *LWT - Food Science and Technology*, vol. 57, no. 1, pp. 49–57, Jun. 2014, doi: 10.1016/j.lwt.2014.01.016.

[191] X. Han, J. Chen, Z. Li, K. Quan, and H. Qiu, "Magnetic solid-phase extraction of triazole fungicides based on magnetic porous carbon prepared by

combustion combined with solvothermal method," *Anal Chim Acta*, vol. 1129, pp. 85–97, Sep. 2020, doi: 10.1016/j.aca.2020.06.077.

[192] Y. Shuang, T. Zhang, H. Zhong, and L. Li, "Simultaneous enantiomeric determination of multiple triazole fungicides in fruits and vegetables by chiral liquid chromatography/tandem mass spectrometry on a bridged bis(β-cyclodextrin)-bonded chiral stationary phase," *Food Chem*, vol. 345, p. 128842, May 2021, doi: 10.1016/j.foodchem.2020.128842.

[193] Y. Wang, M. He, B. Chen, and B. Hu, "Hydroxyl-containing porous organic framework coated stir bar sorption extraction combined with high performance liquid chromatography-diode array detector for analysis of triazole fungicides in grape and cabbage samples," *J Chromatogr A*, vol. 1633, p. 461628, Dec. 2020, doi: 10.1016/j.chroma.2020.461628.

[194] D. Orazbayeva, J. A. Koziel, M. J. Trujillo-Rodríguez, J. L. Anderson, and B. Kenessov, "Polymeric ionic liquid sorbent coatings in headspace solid-phase microextraction: A green sample preparation technique for the determination of pesticides in soil," *Microchemical Journal*, vol. 157, p. 104996, Sep. 2020, doi: 10.1016/j.microc.2020.104996.

[195] P. Zhao, Z. Wang, K. Li, X. Guo, and L. Zhao, "Multi-residue enantiomeric analysis of 18 chiral pesticides in water, soil and river sediment using magnetic solid-phase extraction based on amino modified multiwalled carbon nanotubes and chiral liquid chromatography coupled with tandem mass spectrometry," *J Chromatogr A*, vol. 1568, pp. 8–21, Sep. 2018, doi: 10.1016/j.chroma.2018.07.022.

[196] D. Li, M. He, B. Chen, and B. Hu, “Magnetic porous organic polymers for magnetic solid-phase extraction of triazole fungicides in vegetables prior to their determination by gas chromatography-flame ionization detection,” *J Chromatogr A*, vol. 1601, pp. 1–8, Sep. 2019, doi: 10.1016/j.chroma.2019.04.062.

[197] A. Tanimu, S. M. S. Jillani, A. A. Alluhaidan, S. A. Ganiyu, and K. Alhooshani, “4-phenyl-1,2,3-triazole functionalized mesoporous silica SBA-15 as sorbent in an efficient stir bar-supported micro-solid-phase extraction strategy for highly to moderately polar phenols,” *Talanta*, vol. 194, pp. 377–384, Mar. 2019, doi: 10.1016/j.talanta.2018.10.012.

[198] M. Poletto, V. Pistor, M. Zeni, and A. J. Zattera, “Crystalline properties and decomposition kinetics of cellulose fibers in wood pulp obtained by two pulping processes,” *Polym Degrad Stab*, vol. 96, no. 4, pp. 679–685, Apr. 2011, doi: 10.1016/j.polymdegradstab.2010.12.007.

[199] M.-C. Popescu, C.-M. Popescu, G. Lisa, and Y. Sakata, “Evaluation of morphological and chemical aspects of different wood species by spectroscopy and thermal methods,” *J Mol Struct*, vol. 988, no. 1–3, pp. 65–72, Mar. 2011, doi: 10.1016/j.molstruc.2010.12.004.

[200] M. F. Rosa *et al.*, “Cellulose nanowhiskers from coconut husk fibers: Effect of preparation conditions on their thermal and morphological behavior,” *Carbohydr Polym*, vol. 81, no. 1, pp. 83–92, May 2010, doi: 10.1016/j.carbpol.2010.01.059.

[201] F. Xu, J. Yu, T. Tesso, F. Dowell, and D. Wang, “Qualitative and quantitative analysis of lignocellulosic biomass using infrared techniques: A mini-review,” *Appl Energy*, vol. 104, pp. 801–809, Apr. 2013, doi: 10.1016/j.apenergy.2012.12.019.

[202] M. Poletto, H. Ornaghi, and A. Zattera, “Native Cellulose: Structure, Characterization and Thermal Properties,” *Materials*, vol. 7, no. 9, pp. 6105–6119, Aug. 2014, doi: 10.3390/ma7096105.

[203] C. Richard, F. Balavoine, P. Schultz, T. W. Ebbesen, and C. Mioskowski, “Supramolecular Self-Assembly of Lipid Derivatives on Carbon Nanotubes,” *Science (1979)*, vol. 300, no. 5620, pp. 775–778, May 2003, doi: 10.1126/science.1080848.

[204] K. Press-Kristensen, E. Lindblom, J. E. Schmidt, and M. Henze, “Examining the biodegradation of endocrine disrupting bisphenol A and nonylphenol in WWTPs,” *Water Science and Technology*, vol. 57, no. 8, pp. 1253–1256, Apr. 2008, doi: 10.2166/wst.2008.229.

[205] F. de S. Dias *et al.*, “Lignocellulosic materials as adsorbents in solid phase extraction for trace elements preconcentration,” *TrAC Trends in Analytical Chemistry*, vol. 158, p. 116891, Jan. 2023, doi: 10.1016/j.trac.2022.116891.

[206] S. Iftekhar, D. L. Ramasamy, V. Srivastava, M. B. Asif, and M. Sillanpää, “Understanding the factors affecting the adsorption of Lanthanum using different adsorbents: A critical review,” *Chemosphere*, vol. 204, pp. 413–430, Aug. 2018, doi: 10.1016/j.chemosphere.2018.04.053.

[207] M. Chen, Q. Yi, J. Hong, L. Zhang, K. Lin, and D. Yuan, “Simultaneous determination of 32 antibiotics and 12 pesticides in sediment using ultrasonic-assisted extraction and high performance liquid chromatography-tandem mass spectrometry,” *Analytical Methods*, vol. 7, no. 5, pp. 1896–1905, 2015, doi: 10.1039/C4AY02895C.

[208] M. N. Sahmoune, “Evaluation of thermodynamic parameters for adsorption of heavy metals by green adsorbents,” *Environ Chem Lett*, vol. 17, no. 2, pp. 697–704, Jun. 2019, doi: 10.1007/s10311-018-00819-z.

[209] K. Molaei, A. A. Asgharinezhad, H. Ebrahimzadeh, N. Shekari, N. Jalilian, and Z. Dehghani, “Surfactant-assisted dispersive liquid-liquid microextraction of nitrazepam and lorazepam from plasma and urine samples followed by high-performance liquid chromatography with UV analysis,” *J Sep Sci*, vol. 38, no. 22, pp. 3905–3913, Nov. 2015, doi: 10.1002/jssc.201500586.

[210] A. Gałuszka, Z. M. Migaszewski, P. Konieczka, and J. Namieśnik, “Analytical Eco-Scale for assessing the greenness of analytical procedures,” *TrAC Trends in Analytical Chemistry*, vol. 37, pp. 61–72, Jul. 2012, doi: 10.1016/j.trac.2012.03.013.

[211] H. Sereshti, M. Zarei-Hosseinabadi, S. Soltani, and M. Taghizadeh, “Green vortex-assisted emulsification microextraction using a ternary deep eutectic solvent for extraction of tetracyclines in infant formulas,” *Food Chem*, vol. 396, p. 133743, Dec. 2022, doi: 10.1016/j.foodchem.2022.133743.

[212] D. Li, M. He, B. Chen, and B. Hu, “Magnetic porous organic polymers for magnetic solid-phase extraction of triazole fungicides in vegetables prior to their determination by gas chromatography-flame ionization detection,” *J Chromatogr A*, vol. 1601, pp. 1–8, Sep. 2019, doi: 10.1016/j.chroma.2019.04.062.

[213] Z. Aladaghlo, S. Javanbakht, A. Sahragard, A. Reza Fakhari, and A. Shaabani, “Cellulose-based nanocomposite for ultrasonic assisted dispersive solid phase microextraction of triazole fungicides from water, fruits, and vegetables

samples," *Food Chem*, vol. 403, p. 134273, Mar. 2023, doi: 10.1016/j.foodchem.2022.134273.

[214] H. Sun, J. Feng, J. Feng, M. Sun, Y. Feng, and M. Sun, "Carbon aerogels derived from waste paper for pipette-tip solid-phase extraction of triazole fungicides in tomato, apple and pear," *Food Chem*, vol. 395, p. 133633, Nov. 2022, doi: 10.1016/j.foodchem.2022.133633.

[215] G. Liu *et al.*, "Preparation of magnetic MOFs for use as a solid-phase extraction absorbent for rapid adsorption of triazole pesticide residues in fruits juices and vegetables," *Journal of Chromatography B*, vol. 1166, p. 122500, Mar. 2021, doi: 10.1016/j.jchromb.2020.122500.

[216] Y. Shuang, T. Zhang, H. Zhong, and L. Li, "Simultaneous enantiomeric determination of multiple triazole fungicides in fruits and vegetables by chiral liquid chromatography/tandem mass spectrometry on a bridged bis(β-cyclodextrin)-bonded chiral stationary phase," *Food Chem*, vol. 345, p. 128842, May 2021, doi: 10.1016/j.foodchem.2020.128842.

[217] M. Kadivar and A. Aliakbar, "A new composite based on graphene oxide-poly 3-aminophenol for solid-phase microextraction of four triazole fungicides in water and fruit juices prior to high-performance liquid chromatography analysis," *Food Chem*, vol. 299, p. 125127, Nov. 2019, doi: 10.1016/j.foodchem.2019.125127.

[218] M. Kadivar and A. Aliakbar, "A new composite based on graphene oxide-poly 3-aminophenol for solid-phase microextraction of four triazole fungicides in water and fruit juices prior to high-performance liquid chromatography analysis," *Food Chem*, vol. 299, Nov. 2019, doi: 10.1016/j.foodchem.2019.125127.

[219] Z. Gao *et al.*, "Functionalized melamine sponge based on β-cyclodextrin-graphene oxide as solid-phase extraction material for rapidly pre-enrichment of malachite green in seafood," *Microchemical Journal*, vol. 150, p. 104167, Nov. 2019, doi: 10.1016/j.microc.2019.104167.

[220] A. F. Shaikh, M. S. Tamboli, R. H. Patil, A. Bhan, J. D. Ambekar, and B. B. Kale, "Bioinspired Carbon Quantum Dots: An Antibiofilm Agents," *J Nanosci Nanotechnol*, vol. 19, no. 4, pp. 2339–2345, Apr. 2019, doi: 10.1166/jnn.2019.16537.

[221] S. Parvate, P. Dixit, and S. Chattopadhyay, "Superhydrophobic Surfaces: Insights from Theory and Experiment," *J Phys Chem B*, vol. 124, no. 8, pp. 1323–1360, Feb. 2020, doi: 10.1021/acs.jpcb.9b08567.

[222] S. Dua, P. Kumar, B. Pani, A. Kaur, M. Khanna, and G. Bhatt, "Stability of carbon quantum dots: a critical review," *RSC Adv*, vol. 13, no. 20, pp. 13845–13861, 2023, doi: 10.1039/D2RA07180K.

[223] P. Makoś-Chełstowska, E. Słupek, and A. Małachowska, "Superhydrophobic sponges based on green deep eutectic solvents for spill oil removal from water," *J Hazard Mater*, vol. 425, p. 127972, Mar. 2022, doi: 10.1016/j.jhazmat.2021.127972.

[224] Y. Tang, D. Li, D. Ao, S. Li, and X. Zu, "Ultralight, highly flexible and conductive carbon foams for high performance electromagnetic shielding application," *Journal of Materials Science: Materials in Electronics*, vol. 29, no. 16, pp. 13643–13652, Aug. 2018, doi: 10.1007/s10854-018-9493-2.

[225] B. Merillas, A. Lamy-Mendes, F. Villafañe, L. Durães, and M. Á. Rodríguez-Pérez, "Polyurethane foam scaffold for silica aerogels: effect of cell size on the

mechanical properties and thermal insulation," *Mater Today Chem*, vol. 26, p. 101257, Dec. 2022, doi: 10.1016/j.mtchem.2022.101257.

[226] F. A. Permatasari *et al.*, "Solid-state nitrogen-doped carbon nanoparticles with tunable emission prepared by a microwave-assisted method," *RSC Adv*, vol. 11, no. 63, pp. 39917–39923, 2021, doi: 10.1039/D1RA07290K.

[227] C. Peng, A. H. L. Chow, and C. K. Chan, "Hygroscopic Study of Glucose, Citric Acid, and Sorbitol Using an Electrodynamic Balance: Comparison with UNIFAC Predictions," *Aerosol Science and Technology*, vol. 35, no. 3, pp. 753–758, Jan. 2001, doi: 10.1080/02786820152546798.

[228] H. Alhassan, Y. W. Soon, A. Usman, and V. N. Yoong, "Ultrahydrophobic melamine sponge via interfacial modification with reduced graphene oxide/titanium dioxide nanocomposite and polydimethylsiloxane for oily wastewater treatment," *Water Science and Engineering*, vol. 17, no. 2, pp. 139–149, Jun. 2024, doi: 10.1016/j.wse.2023.09.003.

[229] Y. Dong *et al.*, "Blue luminescent graphene quantum dots and graphene oxide prepared by tuning the carbonization degree of citric acid," *Carbon N Y*, vol. 50, no. 12, pp. 4738–4743, Oct. 2012, doi: 10.1016/j.carbon.2012.06.002.

[230] Z.-A. Qiao *et al.*, "Commercially activated carbon as the source for producing multicolor photoluminescent carbon dots by chemical oxidation," *Chemical Communications*, vol. 46, no. 46, p. 8812, 2010, doi: 10.1039/c0cc02724c.

[231] Y. Guo, J. Wang, L. Hao, Q. Wu, C. Wang, and Z. Wang, "Triazine-triphenylphosphine based porous organic polymer as sorbent for solid phase

extraction of nitroimidazoles from honey and water," *J Chromatogr A*, vol. 1649, p. 462238, Jul. 2021, doi: 10.1016/j.chroma.2021.462238.

[232] M. Rezazadeh, Y. Yamini, S. Seidi, and A. Esrafili, "One-way and two-way pulsed electromembrane extraction for trace analysis of amino acids in foods and biological samples," *Anal Chim Acta*, vol. 773, pp. 52–59, Apr. 2013, doi: 10.1016/j.aca.2013.02.030.

[233] W. Khiaophong and J. Vichapong, "Green application of surfactant modified silica as effective sorbent for extraction and preconcentration of sulfonamide residues in environmental water and honey samples," *J Chromatogr A*, vol. 1718, p. 464720, Mar. 2024, doi: 10.1016/j.chroma.2024.464720.

[234] T. Boontongto and R. Burakham, "Eco-friendly fabrication of a magnetic dual-template molecularly imprinted polymer for the selective enrichment of organophosphorus pesticides for fruits and vegetables," *Anal Chim Acta*, vol. 1186, p. 339128, Nov. 2021, doi: 10.1016/j.aca.2021.339128.

[235] A. Gałuszka, Z. M. Migaszewski, P. Konieczka, and J. Namieśnik, "Analytical Eco-Scale for assessing the greenness of analytical procedures," *TrAC Trends in Analytical Chemistry*, vol. 37, pp. 61–72, Jul. 2012, doi: 10.1016/j.trac.2012.03.013.

[236] F. Pena-Pereira, W. Wojnowski, and M. Tobiszewski, "AGREE—Analytical GREEnness Metric Approach and Software," *Anal Chem*, vol. 92, no. 14, pp. 10076–10082, Jul. 2020, doi: 10.1021/acs.analchem.0c01887.

[237] H. Sereshti, M. Zarei-Hosseinabadi, S. Soltani, and M. Taghizadeh, "Green vortex-assisted emulsification microextraction using a ternary deep eutectic solvent

for extraction of tetracyclines in infant formulas," *Food Chem*, vol. 396, p. 133743, Dec. 2022, doi: 10.1016/j.foodchem.2022.133743.

[238] S. K. Muchakayala *et al.*, "Implementation of analytical quality by design and green chemistry principles to develop an ultra-high performance liquid chromatography method for the determination of Fluocinolone Acetonide impurities from its drug substance and topical oil formulations," *J Chromatogr A*, vol. 1679, p. 463380, Aug. 2022, doi: 10.1016/j.chroma.2022.463380.

[239] A. H. Akabari, P. Mistry, S. K. Patel, J. Surati, S. P. Patel, and U. Shah, "Simultaneous Estimation of Fimasartan potassium trihydrate and Atorvastatin calcium with Greenness Assessment using HPLC and UV Spectrophotometric Methods," *Green Analytical Chemistry*, vol. 6, p. 100067, Sep. 2023, doi: 10.1016/j.greeac.2023.100067.

[240] R. Kachangoon, J. Vichapong, and Y. Santaladchaiyakit, "Surfactant modified coconut husk fiber as a green alternative sorbent for micro-solid phase extraction of triazole fungicides at trace level in environmental water, soybean milk, fruit juice and alcoholic beverage samples," *RSC Adv*, vol. 14, no. 11, pp. 7290–7302, 2024, doi: 10.1039/D3RA07506K.

[241] M. Kadivar and A. Aliakbar, "A new composite based on graphene oxide-poly 3-aminophenol for solid-phase microextraction of four triazole fungicides in water and fruit juices prior to high-performance liquid chromatography analysis," *Food Chem*, vol. 299, p. 125127, Nov. 2019, doi: 10.1016/j.foodchem.2019.125127.

[242] Z. Wang, M. He, B. Chen, and B. Hu, "Azo-linked porous organic polymers/polydimethylsiloxane coated stir bar for extraction of benzotriazole

ultraviolet absorbers from environmental water and soil samples followed by high performance liquid chromatography-diode array detection," *J Chromatogr A*, vol. 1616, p. 460793, Apr. 2020, doi: 10.1016/j.chroma.2019.460793.

[243] K. Seebunrueng, S. Tamuang, S. Ruangchai, S. Sansuk, and S. Srijaranai, "In situ self-assembled coating of surfactant-mixed metal hydroxide on Fe3O4@SiO2 magnetic composite for dispersive solid phase microextraction prior to HPLC analysis of triazole fungicides," *Microchemical Journal*, vol. 168, p. 106396, Sep. 2021, doi: 10.1016/j.microc.2021.106396.

[244] R. Kachangoon, J. Vichapong, Y. Santaladchaiyakit, and S. Srijaranai, "Green fabrication of Moringa oleifera seed as efficient biosorbent for selective enrichment of triazole fungicides in environmental water, honey and fruit juice samples," *Microchemical Journal*, vol. 175, p. 107194, Apr. 2022, doi: 10.1016/j.microc.2022.107194.

[245] R. Kachangoon, J. Vichapong, and Y. Santaladchaiyakit, "Surfactant modified coconut husk fiber as a green alternative sorbent for micro-solid phase extraction of triazole fungicides at trace level in environmental water, soybean milk, fruit juice and alcoholic beverage samples," *RSC Adv*, vol. 14, no. 11, pp. 7290–7302, 2024, doi: 10.1039/D3RA07506K.

[246] Z. Ullah, M. A. Bustam, Z. Man, and A. S. Khan, "PHOSPHONIUM-BASED IONIC LIQUIDS AND THEIR APPLICATION IN SEPARATION OF DYE FROM AQUEOUS SOLUTION," vol. 11, no. 3, 2016, [Online]. Available: www.arpnjournals.com

[247] W. Guo, Y. Hou, W. Wu, S. Ren, S. Tian, and K. N. Marsh, "Separation of phenol from model oils with quaternary ammonium saltsvia forming deep eutectic solvents," *Green Chem.*, vol. 15, no. 1, pp. 226–229, 2013, doi: 10.1039/C2GC36602A.

[248] C. Yao and J. L. Anderson, "Dispersive liquid–liquid microextraction using an in situ metathesis reaction to form an ionic liquid extraction phase for the preconcentration of aromatic compounds from water," *Anal Bioanal Chem*, vol. 395, no. 5, pp. 1491–1502, Nov. 2009, doi: 10.1007/s00216-009-3078-0.

[249] J. Liu, Y. Chi, G. Jiang, C. Tai, J. Peng, and J.-T. Hu, "Ionic liquid-based liquid-phase microextraction, a new sample enrichment procedure for liquid chromatography," *J Chromatogr A*, vol. 1026, no. 1–2, pp. 143–147, Feb. 2004, doi: 10.1016/j.chroma.2003.11.005.

[250] T. Khezeli, A. Daneshfar, and R. Sahraei, "A green ultrasonic-assisted liquid–liquid microextraction based on deep eutectic solvent for the HPLC-UV determination of ferulic, caffeic and cinnamic acid from olive, almond, sesame and cinnamon oil," *Talanta*, vol. 150, pp. 577–585, Apr. 2016, doi: 10.1016/j.talanta.2015.12.077.

[251] Y. Shuang, T. Zhang, H. Zhong, and L. Li, "Simultaneous enantiomeric determination of multiple triazole fungicides in fruits and vegetables by chiral liquid chromatography/tandem mass spectrometry on a bridged bis(β-cyclodextrin)-bonded chiral stationary phase," *Food Chem*, vol. 345, p. 128842, May 2021, doi: 10.1016/j.foodchem.2020.128842.

[252] M. Hemmati and M. Rajabi, “Switchable fatty acid based CO2-effervescence ameliorated emulsification microextraction prior to high performance liquid chromatography for efficient analyses of toxic azo dyes in foodstuffs,” *Food Chem*, vol. 286, pp. 185–190, Jul. 2019, doi: 10.1016/j.foodchem.2019.01.197.

[253] J. Zhao, Z. Meng, Z. Zhao, and L. Zhao, “Ultrasound-assisted deep eutectic solvent as green and efficient media combined with functionalized magnetic multi-walled carbon nanotubes as solid-phase extraction to determine pesticide residues in food products,” *Food Chem*, vol. 310, p. 125863, Apr. 2020, doi: 10.1016/j.foodchem.2019.125863.

[254] M. M. Abolghasemi, M. Piryaei, and R. M. Imani, “Deep eutectic solvents as extraction phase in head-space single-drop microextraction for determination of pesticides in fruit juice and vegetable samples,” *Microchemical Journal*, vol. 158, p. 105041, Nov. 2020, doi: 10.1016/j.microc.2020.105041.

[255] H. Sereshti, M. Zarei-Hosseinabadi, S. Soltani, F. Jamshidi, and M. H. Shojaee AliAbadi, “Hydrophobic liquid-polymer-based deep eutectic solvent for extraction and multi-residue analysis of pesticides in water samples,” *Microchemical Journal*, vol. 167, p. 106314, Aug. 2021, doi: 10.1016/j.microc.2021.106314.

[256] C.-J. Hsu and W.-H. Ding, “Determination of benzotriazole and benzothiazole derivatives in tea beverages by deep eutectic solvent-based ultrasound-assisted liquid-phase microextraction and ultrahigh-performance liquid chromatography-high resolution mass spectrometry,” *Food Chem*, vol. 368, p. 130798, Jan. 2022, doi: 10.1016/j.foodchem.2021.130798.

[257] J. Zhang *et al.*, “pH-responsive switchable deep eutectic solvents to mediate pretreatment method for trace analysis of triazole fungicides in peel wastes,” *Food Chem*, vol. 411, p. 135486, Jun. 2023, doi: 10.1016/j.foodchem.2023.135486.

[258] Z. Wang, J. C. DeWitt, C. P. Higgins, and I. T. Cousins, “A Never-Ending Story of Per- and Polyfluoroalkyl Substances (PFASs)?,” *Environ Sci Technol*, vol. 51, no. 5, pp. 2508–2518, Mar. 2017, doi: 10.1021/acs.est.6b04806.

[259] S. Ullah, T. Alsberg, and U. Berger, “Simultaneous determination of perfluoroalkyl phosphonates, carboxylates, and sulfonates in drinking water,” *J Chromatogr A*, vol. 1218, no. 37, pp. 6388–6395, Sep. 2011, doi: 10.1016/j.chroma.2011.07.005.

[260] R. Dhore and G. S. Murthy, “Per/polyfluoroalkyl substances production, applications and environmental impacts,” *Bioresour Technol*, vol. 341, p. 125808, Dec. 2021, doi: 10.1016/j.biortech.2021.125808.

[261] R. Gonzalez de Vega, A. Cameron, D. Clases, T. M. Dodgen, P. A. Doble, and D. P. Bishop, “‘Simultaneous targeted and non-targeted analysis of per- and polyfluoroalkyl substances in environmental samples by liquid chromatography-ion mobility-quadrupole time of flight-mass spectrometry and mass defect analysis,’” *J Chromatogr A*, vol. 1653, p. 462423, Sep. 2021, doi: 10.1016/j.chroma.2021.462423.

[262] R. A. Dickman and D. S. Aga, “A review of recent studies on toxicity, sequestration, and degradation of per- and polyfluoroalkyl substances (PFAS),” *J Hazard Mater*, vol. 436, p. 129120, Aug. 2022, doi: 10.1016/j.jhazmat.2022.129120.

[263] Y. Shen *et al.*, “Trends in the Analysis and Exploration of per- and Polyfluoroalkyl Substances (PFAS) in Environmental Matrices: A Review,” *Crit Rev*

Anal Chem, vol. 54, no. 8, pp. 3171–3195, Nov. 2024, doi: 10.1080/10408347.2023.2231535.

[264] E. Piva, P. Fais, G. Cecchetto, M. Montisci, G. Viel, and J. P. Pascali, "Determination of perfluoroalkyl substances (PFAS) in human hair by liquid chromatography-high accurate mass spectrometry (LC-QTOF)," *Journal of Chromatography B*, vol. 1172, p. 122651, May 2021, doi: 10.1016/j.jchromb.2021.122651.

[265] U. Environmental Protection Agency Federal Facilities Restoration and R. Office, "Technical Fact Sheet – Perfluorooctane Sulfonate (PFOS) and Perfluorooctanoic Acid (PFOA)," 2017.

[266] A. San Román, E. Abilleira, A. Irizar, L. Santa-Marina, B. Gonzalez-Gaya, and N. Etxebarria, "Optimization for the analysis of 42 per- and polyfluorinated substances in human plasma: A high-throughput method for epidemiological studies," *J Chromatogr A*, vol. 1712, p. 464481, Dec. 2023, doi: 10.1016/j.chroma.2023.464481.

[267] S. P. J. van Leeuwen and J. de Boer, "Extraction and clean-up strategies for the analysis of poly- and perfluoroalkyl substances in environmental and human matrices," *J Chromatogr A*, vol. 1153, no. 1–2, pp. 172–185, Jun. 2007, doi: 10.1016/j.chroma.2007.02.069.

[268] M. Lorenzo, J. Campo, and Y. Picó, "Analytical challenges to determine emerging persistent organic pollutants in aquatic ecosystems," *TrAC Trends in Analytical Chemistry*, vol. 103, pp. 137–155, Jun. 2018, doi: 10.1016/j.trac.2018.04.003.

[269] E. Concha-Graña, G. Fernández-Martínez, P. López-Mahía, D. Prada-Rodríguez, and S. Muniategui-Lorenzo, "Fast and sensitive determination of per- and polyfluoroalkyl substances in seawater," *J Chromatogr A*, vol. 1555, pp. 62–73, Jun. 2018, doi: 10.1016/j.chroma.2018.04.049.

[270] S. F. Nakayama *et al.*, "Worldwide trends in tracing poly- and perfluoroalkyl substances (PFAS) in the environment," *TrAC Trends in Analytical Chemistry*, vol. 121, p. 115410, Dec. 2019, doi: 10.1016/j.trac.2019.02.011.

[271] T. Sanan and M. Magnuson, "Analysis of per- and polyfluorinated alkyl substances in sub-sampled water matrices with online solid phase extraction/isotope dilution tandem mass spectrometry," *J Chromatogr A*, vol. 1626, p. 461324, Aug. 2020, doi: 10.1016/j.chroma.2020.461324.

[272] Md. Al Amin *et al.*, "Recent advances in the analysis of per- and polyfluoroalkyl substances (PFAS)—A review," *Environ Technol Innov*, vol. 19, p. 100879, Aug. 2020, doi: 10.1016/j.eti.2020.100879.

[273] "PLAW-104publ182".

[274] "2016-27667".

[275] F. Li *et al.*, "Short-chain per- and polyfluoroalkyl substances in aquatic systems: Occurrence, impacts and treatment," *Chemical Engineering Journal*, vol. 380, p. 122506, Jan. 2020, doi: 10.1016/j.cej.2019.122506.

[276] C. O. Coy *et al.*, "Differing behavioral changes in crayfish and bluegill under short- and long-chain PFAS exposures: Field study in Northern Michigan, USA," *Ecotoxicol Environ Saf*, vol. 247, p. 114212, Dec. 2022, doi: 10.1016/j.ecoenv.2022.114212.

[277] G. T. Tomy *et al.*, “Fluorinated Organic Compounds in an Eastern Arctic Marine Food Web,” *Environ Sci Technol*, vol. 38, no. 24, pp. 6475–6481, Dec. 2004, doi: 10.1021/es049620g.

[278] Y. Du, X. Shi, C. Liu, K. Yu, and B. Zhou, “Chronic effects of water-borne PFOS exposure on growth, survival and hepatotoxicity in zebrafish: A partial life-cycle test,” *Chemosphere*, vol. 74, no. 5, pp. 723–729, Feb. 2009, doi: 10.1016/j.chemosphere.2008.09.075.

[279] M. Sands, X. Zhang, T. Jensen, M. La Frano, M. Lin, and J. Irudayaraj, “PFAS assessment in fish – Samples from Illinois waters,” *Science of The Total Environment*, vol. 927, p. 172357, Jun. 2024, doi: 10.1016/j.scitotenv.2024.172357.

[280] H. A. Kaboré *et al.*, “Worldwide drinking water occurrence and levels of newly-identified perfluoroalkyl and polyfluoroalkyl substances,” *Science of The Total Environment*, vol. 616–617, pp. 1089–1100, Mar. 2018, doi: 10.1016/j.scitotenv.2017.10.210.

[281] Y. Xian *et al.*, “Fluorine and nitrogen functionalized magnetic graphene as a novel adsorbent for extraction of perfluoroalkyl and polyfluoroalkyl substances from water and functional beverages followed by HPLC-Orbitrap HRMS determination,” *Science of The Total Environment*, vol. 723, p. 138103, Jun. 2020, doi: 10.1016/j.scitotenv.2020.138103.

[282] B. Morris, “The components of the wired spanning forest are recurrent,” *Probab Theory Relat Fields*, vol. 125, no. 2, pp. 259–265, Feb. 2003, doi: 10.1007/s00440-002-0236-0.

[283] A. Vavrouš, V. Ševčík, M. Dvořáková, R. Čabala, A. Moulisová, and K. Vrbík, “Easy and Inexpensive Method for Multiclass Analysis of 41 Food Contact Related Contaminants in Fatty Food by Liquid Chromatography–Tandem Mass Spectrometry,” *J Agric Food Chem*, vol. 67, no. 39, pp. 10968–10976, Oct. 2019, doi: 10.1021/acs.jafc.9b02544.

[284] P. Meng, N. J. DeStefano, and D. R. U. Knappe, “Extraction and Matrix Cleanup Method for Analyzing Novel Per- and Polyfluoroalkyl Ether Acids and Other Per- and Polyfluoroalkyl Substances in Fruits and Vegetables,” *J Agric Food Chem*, vol. 70, no. 16, pp. 4792–4804, Apr. 2022, doi: 10.1021/acs.jafc.1c07665.

[285] G. Munoz *et al.*, “Optimization of extraction methods for comprehensive profiling of perfluoroalkyl and polyfluoroalkyl substances in firefighting foam impacted soils,” *Anal Chim Acta*, vol. 1034, pp. 74–84, Nov. 2018, doi: 10.1016/j.aca.2018.06.046.

[286] S. Liu, M. Junaid, W. Zhong, Y. Zhu, and N. Xu, “A sensitive method for simultaneous determination of 12 classes of per- and polyfluoroalkyl substances (PFASs) in groundwater by ultrahigh performance liquid chromatography coupled with quadrupole orbitrap high resolution mass spectrometry,” *Chemosphere*, vol. 251, p. 126327, Jul. 2020, doi: 10.1016/j.chemosphere.2020.126327.

[287] Z.-H. Deng, C.-G. Cheng, X.-L. Wang, S.-H. Shi, M.-L. Wang, and R.-S. Zhao, “Preconcentration and Determination of Perfluoroalkyl Substances (PFASs) in Water Samples by Bamboo Charcoal-Based Solid-Phase Extraction Prior to Liquid Chromatography–Tandem Mass Spectrometry,” *Molecules*, vol. 23, no. 4, p. 902, Apr. 2018, doi: 10.3390/molecules23040902.

[288] M. Giardina, “Application Note Environmental Author Determination of Per and Polyfluoroalkyl Substances in Drinking Water Using Agilent Bond Elut PFAS WAX SPE and LC/MS/MS 2.”

[289] M. Liang *et al.*, “High throughput analysis of 21 perfluorinated compounds in drinking water, tap water, river water and plant effluent from southern China by supramolecular solvents-based microextraction coupled with HPLC-Orbitrap HRMS,” *Environmental Pollution*, vol. 263, p. 114389, Aug. 2020, doi: 10.1016/j.envpol.2020.114389.

[290] N. Yu *et al.*, “Non-Target and Suspect Screening of Per- and Polyfluoroalkyl Substances in Airborne Particulate Matter in China,” *Environ Sci Technol*, vol. 52, no. 15, pp. 8205–8214, Aug. 2018, doi: 10.1021/acs.est.8b02492.

[291] Y. Liu, L. A. D’Agostino, G. Qu, G. Jiang, and J. W. Martin, “High-resolution mass spectrometry (HRMS) methods for nontarget discovery and characterization of poly- and per-fluoroalkyl substances (PFASs) in environmental and human samples,” *TrAC Trends in Analytical Chemistry*, vol. 121, p. 115420, Dec. 2019, doi: 10.1016/j.trac.2019.02.021.

REFERENCES

พหุน ปณฺ ฑิโต ชีเว

BIOGRAPHY

NAME	Miss Rawikan Kachangoon
DATE OF BIRTH	08/01/1995
PLACE OF BIRTH	Nakhon Ratchasima Province
ADDRESS	12 Moo 5 Sadao, Nangrong District, Buriram 31110
EDUCATION	2013 - High School, Nangrong School, Nangrong, Buriram, Thailand 2017 - Bachelor of Science (Chemistry), B.Sc. Mahasarakham University, Maha Sarakham, Thailand 2020 - Master of Science (Chemistry), M.Sc., Mahasarakham University, Maha Sarakham, Thailand 2025 - Doctor of Philosophy (Chemistry), Ph.D., Mahasarakham University, Maha Sarakham, Thailand
Research grants & awards	Royal Golden Jubilee Ph.D. Program (N41A640218)
Research output	R.Kachangoon, Y. Santaladchaiyakit, O. Prasitnok, and J. Vichapong, "Hydrophobic melamine sponge incorporated with carbon dots as a green sorbent for micro-solid phase extraction of triazole fungicide residues in edible fungi samples," Microchemical Journal, Vol. 207 (2024), p. 111901, doi: https://doi.org/10.1016/j.microc.2024.111901. P. Rattanaphonsaen, S. Rakkote, R. Kachangoon, W. Khiaophong, O. Prasitnok, K. Ponhong, Y. Santaladchaiyakit, N. Teshima, and J. Vichapong, "A facile and green alternative method for preconcentration of triazole fungicides using fabrication of melamine sponge anchoring with Ni/Al-LDH adsorbent followed by HPLC analysis" Microchemical Journal, Vol. 203 (2024), p. 110928, doi: https://doi.org/10.1016/j.microc.2024.110928 R. Kachangoon, J. Vichapong, and Y. Santaladchaiyakit, "Surfactant modified coconut husk fiber as a green alternative sorbent for micro-solid phase extraction of triazole fungicides at trace level in environmental water, soybean milk, fruit juice, and alcoholic beverage samples," RSC Advances, Vol. 14(11) (2024), p. 7290-7302, doi: 10.1039/d3ra07506k. K. Katthanet, S. Supo, J. Jaroensan, W. Khiaophong, R. Kachangoon, K. Ponhong, P. Pramual, I. Thanee, and J. Vichapong, "Preconcentration of Heterocyclic Aromatic

Amines in Edible Fried Insects Using Surfactant-Assisted Hydrophobic Deep Eutectic Solvent for Homogeneous Liquid–Liquid Microextraction prior to HPLC," ACS Omega (2024), Vol. 9(3), p. 3962-3970, doi: 10.1021/acsomega.3c08365.

R. Kachangoon, J. Vichapong, Y. Santaladchaiyakit, and N. Teshima, "Trace-Level Determination of Triazole Fungicides Using Effervescence-Assisted Liquid–Liquid Microextraction Based on Ternary Deep Eutectic Solvent Prior to High-Performance Liquid Chromatography," ACS Omega (2023), Vol. 8(23), p. 21332-21340, doi: 10.1021/acsomega.3c02919.

J. Jaroensan, W. Khiaophong, R. Kachangoon, and J. Vichapong, "Efficient analyses of triazole fungicides in water, honey and soymilk samples by popping candy-generated CO2 and sugaring-out-assisted supramolecular solvent-based microextraction prior to HPLC determinations," RSC Advances (2023), Vol. 13(7), p. 4195-4201, doi: https://doi.org/10.1039/D2RA06560F.

R. Kachangoon, J. Vichapong, Y. Santaladchaiyakit, R. Burakham, and S. Srijaranai, "Sample Preparation Approach by In Situ Formation of Supramolecular Solvent Microextraction for Enrichment of Neonicotinoid Insecticide Residues," Food Analytical Methods (2023), Vol. 16, p. 330-339, https://doi.org/10.1007/s12161-022-02417-w.

R. Buppasang, J. Palasak, R. Kachangoon, K. Ponhong, N. Teshima, R. Burakham, S. Srijaranai, and J. Vichapong, "Simultaneous Preconcentration of Triazole Fungicide Residues Using In-Situ Coacervative Extraction Based on a Double-Solvent Supramolecular System Prior to High Performance Liquid Chromatographic Analysis," Molecules (2022), Vol. 27(19), p. 6273, doi: 10.3390/molecules27196273.

W. Khiaophong, J. Jaroensan, R. Kachangoon, J. Vichapong, R. Burakham, Y. Santaladchaiyakit, and S. Srijaranai,"Modified Peanut Shell as an Eco-Friendly Biosorbent for Effective Extraction of Triazole Fungicide Residues in Surface Water and Honey Samples before Their Determination by High-Performance Liquid Chromatography," ACS Omega (2022), Vol. 7(39, p. 34877-34887, doi: 10.1021/acsomega.2c03410.

J. Palasak, R. Buppasang, R. Kachangoon, J. Vichapong, R.Burakham, Y. Santaladchaiyakit, and S. Srijaranai, "Preconcentration of triazole fungicides using effervescent assisted switchable hydrophilicity solvent-based microextraction prior to high-performance liquid chromatographic analysis," Microchemical Journal (2022), Vol. 182, p. 107882, doi: https://doi.org/10.1016/j.microc.2022.107882.

R. Kachangoon, J. Vichapong, Y. Santaladchaiyakit, and S. Srijaranai, “An In Situ Formation of Ionic Liquid for Enrichment of Triazole Fungicides in Food Applications Followed by HPLC Determination,” Molecules (2022), Vol. 27(11), p. 3416, doi: 10.3390/molecules27113416.

J. Vichapong, R. Kachangoon, R. Burakham, Y. Santaladchaiyakit, and S. Srijaranai, “Ringer Tablet-Based Micelle-Mediated Extraction-Solvent Back Extraction Coupled with High-Performance Liquid Chromatography for Preconcentration and Determination of Neonicotinoid Pesticides”. Food Anal. Methods (2022), Vol. 15, p. 970–980, doi: https://doi.org/10.1007/s12161-021-02067-4.

R. Kachangoon, J. Vichapong, Y. Santaladchaiyakit, and S. Srijaranai, "Green fabrication of Moringa oleifera seed as efficient biosorbent for selective enrichment of triazole fungicides in environmental water, honey and fruit juice samples," Microchemical Journal (2022), Vol. 175, p. 107194, doi: https://doi.org/10.1016/j.microc.2022.107194.

J. Vichapong, R. Kachangoon, R. Burakham, Y. Santaladchaiyakit, and S. Srijaranai, “In-Situ Formation of Modified Nickel–Zinc-Layered Double Hydroxide Followed by HPLC Determination of Neonicotinoid Insecticide Residues,” Molecules (2021), Vol. 27(1), p. 43, doi: 10.3390/molecules27010043.

R. Kachangoon, J. Vichapong, Y. Santaladchaiyakit, R. Burakham, and S. Srijaranai, “An Eco-Friendly Hydrophobic Deep Eutectic Solvent-Based Dispersive Liquid-Liquid Microextraction for the Determination of Neonicotinoid Insecticide Residues in Water, Soil and Egg Yolk Samples,” Molecules (2020), Vol. 25(12), p. 2785, doi: 10.3390/molecules25122785.

R. Kachangoon, J. Vichapong, Y. Santaladchaiyakit, and S. Srijaranai, "Cloud-point extraction coupled to in-situ metathesis reaction of deep eutectic solvents for preconcentration and liquid chromatographic analysis of neonicotinoid insecticide residues in water, soil and urine samples," Microchemical Journal (2020), Vol. 152, p. 104377, doi: https://doi.org/10.1016/j.microc.2019.104377.

J. Vichapong, K, Moyakao, R. Kachangoon, R. Burakham, Y. Santaladchaiyakit, and S. Srijaranai, “β-Cyclodextrin Assisted Liquid-Liquid Microextraction Based on Solidification of the Floating Organic Droplets Method for Determination of Neonicotinoid Residues,” Molecules (2019), Vol. 24(21), p. 3954, doi: 10.3390/molecules24213954.

R. Kachangoon, J. Vichapong, R. Burakham, Y. Santaladchaiyakit, and S. Srijaranai, “Ultrasonically Modified Amended-Cloud Point Extraction for Simultaneous Pre-Concentration of Neonicotinoid Insecticide Residues,” Molecules (2018), Vol. 23(5), p. 1165, doi: 10.3390/molecules23051165.